Platelet recruitment to lungs following inhalation of bacterial lipopolysaccharides

Cleary, Simon John

Awarding institution:
King's College London

Platelet recruitment to lungs following inhalation of bacterial lipopolysaccharides

Simon Cleary

A thesis submitted in fulfilment
of the requirements for the degree of
Doctor of Philosophy

Supervisors:
Dr. Simon Pitchford and Prof. Clive Page

Sackler Institute of Pulmonary Pharmacology
Institute of Pharmaceutical Science
Faculty of Life Sciences & Medicine
King's College London
2017

Abstract

Background

Platelets contribute to disease-relevant inflammatory processes, and research indicates that platelet recruitment to inflamed lungs might be important in the platelet-dependence of inflammatory responses. Compared to platelet recruitment to lesions in blood vessel walls or to thrombi, the mechanisms of platelet recruitment to lungs following inflammatory responses in lung airpaces are poorly understood, so methods were sought to enable the characterisation of this response in mouse and human models.

Methods

Bright field and fluorescence microscopy for quantifying immunostained platelets, non-invasive radiolabelled platelet tracking, radiolabelled platelet biodistribution, lung intravital multiphoton microscopy with genetic platelet labelling, and blood microsample platelet counts were assessed as methods for measuring and describing lung platelet recruitment in a mouse model of lung inflammation induced by intranasal challenge with bacterial lipopolysaccharides (LPS). Platelets were also immunostained in human lung samples exposed to LPS *via* intrabronchial installation during *ex vivo* blood-perfused lung experiments. The effects of neutrophil depletion, blockade of the adhesion molecules P-selectin or PSGL-1, and treatment with the anti-platelet drugs MRS2500, AR-C 66096 or aspirin on LPS-induced lung platelet recruitment were then investigated in mice.

Results

Immunostaining and radiolabelled platelet tracking methods showed that LPS inhalation caused platelet recruitment to lungs of mice, and intravital microscopy revealed that LPS

inhalation increased platelet adhesion without causing thrombosis. Radiolabelled and immunostained platelets were also found in airspaces of LPS-challenged mice and human lungs. The lung platelet recruitment response was preceded by a decrease in blood platelet counts associated with recruitment of platelets to the liver and spleen. Platelet recruitment to mouse lungs was not detectably altered by neutrophil depletion, blockade of PSGL-1 or P-selectin, or treatment with MRS2500, AR-C 66096, or aspirin. In this model, lung neutrophil recruitment was reduced with neutrophil depletion or PSGL-1 blockade but not with other interventions tested. Platelet depletion did not significantly alter neutrophil counts in bronchoalveolar lavage in the mouse model used but did reduce the quantity of neutrophil extracellular traps detected in lung airspaces.

Conclusions

Platelet recruitment to mouse lungs following LPS inhalation showed no clear evidence of dependence on neutrophils or PSGL-1, suggestive that platelet recruitment occurs through mechanisms distinct from those driving lung neutrophil recruitment. Platelet recruitment to lungs inflamed by LPS inhalation involved increased platelet adhesion not extending to thrombosis, and migration of platelets into lung airspaces in mice and in human lungs, with interactions of platelets with the release of neutrophil extracellular traps in lung airspaces identified. The immunostaining, radiolabelling and intravital microscopy methods described in this thesis allow for further investigation into the molecular mediators and physiological consequences of platelet recruitment to inflamed lungs.

Acknowledgements

To my supervisors, Dr. Simon Pitchford and Prof. Clive Page, thank you for always supporting my development as a researcher, and for an enjoyable time spent working on my PhD.

I am indebted to fellow Sackler Institute students Dr. Richard Amison, Dr. Francis Man, Mr. Sajeel Shah, Ms. Stephanie Arnold and Ms. Blaze O'Shaughnessy, as well as all of our brilliant colleagues in the Institute of Pharmaceutical Science for some great times at King's. I am also grateful for the input of project students, animal unit staff, technicians (particularly Mr. Dan Asker) and administrators (particularly Mrs. Paola Thatcher).

This project, and my growth as a scientist, also benefited greatly from insights from the late Dr. Domenico Spina into the design, analysis, and interpretation of experiments.

I would like to thank Prof. Mark Looney, UCSF, for welcoming me into his laboratory and for the support and friendship of everyone I worked with at UCSF, particularly Dr. Emma Lefrançais and Dr. Beñat Mallavia who always made time to help me.

I am also thankful to Dr. Michael Emerson, Imperial College London, as well as Dr. Erica Smyth and Dr. Francesca Rauzi for helping me set up and run radiation experiments, to Mr. Carl Hobbs for making time to help me become proficient in histological techniques and for always being enthusiastic about helping out with my project, to Prof. Lea-Ann Dailey and Dr. Abhinav Kumar for help providing access to state-of-the-art microscopy technology, and to Dr. Cecilia O'Kane, Queen's University Belfast, for trusting me with valuable tissue samples.

I am grateful to British taxpayers, the MRC and King's College London for funding my PhD scholarship, and to the British Pharmacological Society and the King's College London departments of Physiology and Pharmacology for supporting me with travelling fellowships and grants for setting up research collaborations.

Lastly, I would like to thank my parents for their huge amounts of support and patience during my studies, and Trusha for always being there for me, no matter where.

"it is not inconceivable that platelets, along with many cells of the body, play an important part in resisting infection. The difficulty comes when one attempts to analyse and define their exact mode and sphere of activity in this respect"

Leandro M. Tocantins (1938)

Publications and conference proceedings

Publications

Amison, R.T., Arnold, S., O'Shaughnessy, B.G., Cleary, S.J., Ofoedu, J., Idzko, M., et al. (2017). Lipopolysaccharide (LPS) induced pulmonary neutrophil recruitment and platelet activation is mediated via the $P2Y_1$ and $P2Y_{14}$ receptors in mice. Pulm. Pharmacol. Ther. 45: 62–68.

Inacio, R., Poland, S., Cai, X.J., Cleary, S.J., Ameer-Beg, S., Keeble, J., et al. (2016). The application of local hypobaric pressure — A novel means to enhance macromolecule entry into the skin. J. Control. Release 226: 66–76.

Pan, D., Amison, R.T., Riffo-Vasquez, Y., Spina, D., Cleary, S.J., Wakelam, M.J., et al. (2015). P-Rex and Vav Rac-GEFs in platelets control leukocyte recruitment to sites of inflammation. Blood 125: 1146–1159.

Cleary, S.J., and Page, C.P. (2015). Exploring dual PDE3/4 inhibition in the treatment of airway diseases. Drugs Future 40: 301–310.

Conference proceedings

"Antibody, radionuclide and genetic platelet labelling reveal LPS-induced lung platelet recruitment in mice" (poster presentation) Platelet Society 1st UK-Italian Platelet Meeting, Bath, UK, 2017

"Neither P-selectin nor PSGL-1 are critical for lung platelet recruitment following LPS inhalation in mice" (poster presentation) European Respiratory Society Congress, Milan, Italy, 2017

"Visualising LPS-induced platelet adhesion and activation in lungs using immunohistochemistry and intravital microscopy" (oral communication) International Society on Thrombosis and Haemostasis Congress, Berlin, Germany, 2017

"Investigating the neutrophil dependence of platelet recruitment to lungs inflamed by lipopolysaccharides" (poster presentation) British Pharmacological Society Winter Meeting, London, UK, 2016

"Platelets are recruited to lipopolysaccharide-challenged lungs of neutrophil replete and depleted mice" (poster presentation) American Thoracic Society Congress, San Francisco, USA, 2016

Table of contents

List of abbreviations

^{111}In	Indium-111 radionuclide
ABC	Avidin-biotinylated HRP complex (reporter construct)
ACD	Acid-citrate-dextrose anti-coagulant solution
ANCOVA	Analysis of covariance
ANOVA	Analysis of variance
ARDS	Acute respiratory distress syndrome
BAL	Bronchoalveolar lavage
CD	Cluster of differentiation (nomenclature system)
CFTS	Ca^{2+}-free Tyrode's solution
COPD	Chronic obstructive pulmonary disease
DAB	3,3'-Diaminobenzidine
DMSO	Dimethyl sulphoxide
ELISA	Enzyme-linked immunosorbent assay
fMLP	Formyl-methionyl-leucyl-phenylalanine
GFP	Green fluorescent protein
GP	Glycoprotein
GPCR	G-protein coupled receptor
h	Hour(s)
HEPES	4-(2-hydroxyethyl)-1-piperazineethanesulfonic acid
HRP	Horseradish peroxidase (reporter enzyme)
i.n.	Intranasal
i.p.	Intraperitoneal
i.t.	Intratracheal
i.v.	Intravenous
IgG	Immunoglobulin G
IHC	Immunohistochemistry
LPS	Lipopolysaccharides
MHCI	Major histocompatibility complex I

mTmG	*Gt(ROSA)26Sortm4(ACTB-tdTomato,-EGFP)Luo*/J mouse
NETs	Neutrophil extracellular traps
OD	Optical density
PAMP	Pathogen-associated molecular pattern
PBS	Phosphate-buffered saline
PF4	Platelet factor 4 (CXCL4)
PGE_1	Prostaglandin E1
PRP	Platelet-rich plasma
PSGL-1	P-selectin glycoprotein ligand-1
rcf	Relative centrifugal force
SDF-1α	Stromal cell-derived factor 1α (CXCL12)
SEM	Standard error of the mean
TAP (buffer)	Micture of CFTS, ACD and PGE_1
vWF	von Willebrand factor

List of figures

List of tables

1 Introduction

1.1 The need for research into lung health, disease and platelets

1.1.1 The global burden of lung diseases

Diseases affecting the lungs result in around 12% of the world's total suffering from death and disability, with particularly large global disease burdens of lung infections, chronic obstructive pulmonary disease (COPD), lung cancers and asthma (Figure 1.1). In pathophysiological terms, the majority of this global lung disease burden comes from a failure of the immune system to defend against infection or the growth of cancerous cells, or from excessive inflammatory responses against inappropriate stimuli.

The most urgent and obvious interventions required for improving global lung health are reducing the major COPD, cancer and infection risk factors of exposure to tobacco smoke and other air pollutants, but tobacco use is projected to continue contributing to the deaths at the present rate or higher, and the world continues to become increasingly urbanised with cities across the world struggling to control air pollution (Mathers and Loncar, 2006). Adding the burden of disease on these sufferers to that on those whose disease is due to chance, genetics or other environmental factors, leaves a huge unmet need for drugs for lung diseases.

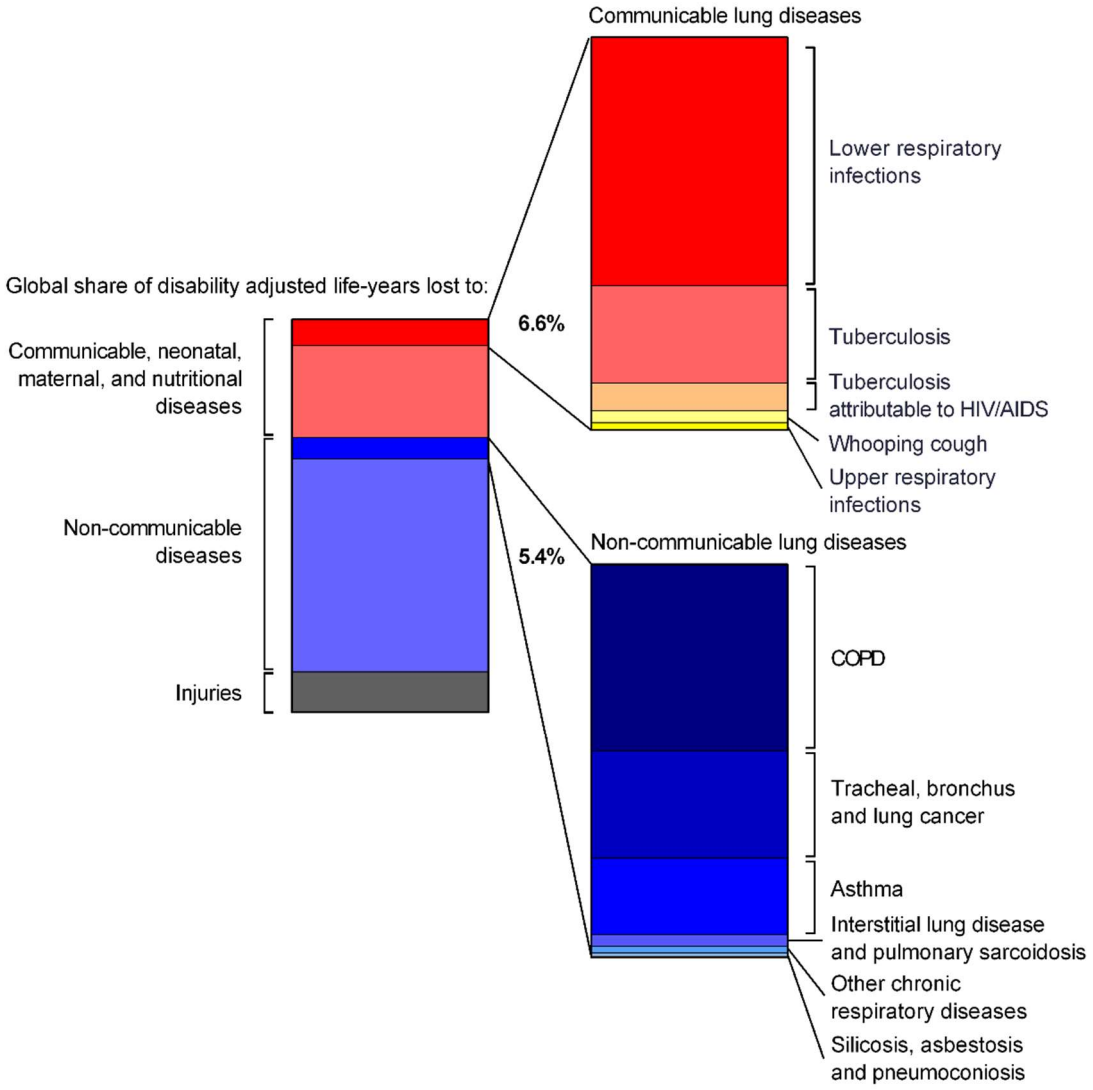

Figure 1.1. Contribution of lung diseases to global suffering and death. Expressed as disability adjusted life years (DALYs, years of life lost + years of life lived with disability), the global disease burden in 2015 was 30% communicable, neonatal, maternal and nutritional diseases, 60% non-communicable diseases and 10% injuries. Around 6.6% of global loss of DALYs was due to communicable diseases affecting the lungs, and 5.4% was due to non-communicable diseases affecting the lungs. Data are from Global Burden of Disease, Institute for Health Metrics and Evaluation.[1]

[1] Institute for Health Metrics and Evaluation, Global Burden of Disease project: http://healthdata.org/gbd

Lung diseases have been particularly challenging for drug discovery and development programmes and make up a large and growing proportion of the global unmet need for new treatments (Barnes et al., 2015). There has been a stagnation in discovery of new antimicrobial drugs for treating infectious diseases together with an increase in microbial resistance to existing drugs, with tuberculosis, for example, escaping eradication and increasing in morbidity due to multi drug resistance, and to immunocompromisation of hosts with concomitant human immunodeficiency virus infection (Silver, 2011).

Despite some advances in cancer treatment, amongst cancer types those affecting the lungs have some of the lowest survival rates and highest contributions to the total mortality from cancers (Siegel et al., 2015).

Asthma and Chronic Obstructive Pulmonary Disease (COPD) lack cures, no drugs have been successful in preventing the progression of COPD, and a subpopulation of asthmatic patients are resistant to current preventative treatment and suffer from a disproportionate share of the asthma disease burden (Barnes, 2010; Mushtaq, 2014).

Prognosis of acute respiratory distress syndrome (ARDS) has been improved with ventilation strategies, but drug interventions have been without success and chances of survival are still around 50% lower in patients with injured lungs compared to other critically ill intensive care patients (Summers et al., 2016).

Many, or all of the diseases mentioned can have a characteristically large inflammatory component, with pulmonary recruitment and activation of inflammatory cells, or cancer cells in the case of secondary lung cancers. In inflammatory lung diseases and some lung infections, the inflammation component of the disease has been causally associated with progression of

symptoms, and has therefore been the subject of many drug discovery programmes (Barnes et al., 2015).

1.1.2 Platelets as targets for therapeutic interventions

Research has enabled the production of drugs targeting platelets which have proven clinical success in treating patients presenting with unstable angina, and the in the secondary prevention of further morbidity and mortality in patients who have survived a myocardial infarction or a cerebrovascular ischaemic event (Antithrombotic Trialists' Collaboration, 2002; Jackson and Schoenwaelder, 2003). Platelets have proven to be particularly useful targets for drugs, as many functionally important proteins have expression relatively restricted to the megakaryocyte-platelet lineage, and platelets are relatively easy to isolate and study in pharmacological and proteomic studies compared to other cell types.

There is also a growing body of evidence that platelets contribute to pathological processes underlying infectious and inflammatory diseases as well as related functions in the growth and metastasis of cancers across the body (reviewed in Pitchford and Page, 2006; Pitchford, 2007; Zarbock and Ley, 2009; Semple et al., 2011; Menter et al., 2014; Yeaman, 2014; Middleton et al., 2016).

A better understanding of these roles for platelets in processes other than haemostasis and thrombosis could lead to development of new antiplatelet drugs for novel indications. In particular, these drugs could find use in inflammatory diseases affecting the lungs, as the lung diseases with inflammatory compenents such as asthma, COPD, ARDS and cystic fibrosis

are all under investigation as diseases in which platelets might have key roles (Pitchford, 2009; Zarbock and Ley, 2009; Sin, 2014; Toner et al., 2015; Middleton et al., 2016).

The sections of this thesis introduction that follow review current understanding of platelet contributions to inflammatory processes and the phenomenon of platelet recruitment in lung inflammation, in order to set the scene for the broad experimental aim of the present doctoral research project: to develop methods for imaging, measuring and characterising the cellular and molecular basis of lung platelet recruitment in models of lung inflammation, which can also be used for investigating lung platelet recruitment in other disease contexts.

1.2 Platelets as mediators of haemostasis, thrombosis and inflammation

1.2.1 Mechanisms of platelet function in haemostasis, thrombosis and repair

Platelets, are small, anucleate cells[2] ~2-3 µm in diameter in humans at their widest point (Paulus, 1975), formed by the fragmentation of large, polyploid megakaryocyte cells originating from hematopoetic precursor cells (Wright, 1906; Schmitt et al., 2001). Platelets circulate in the blood as the second most numerous endogenous single cell type after erythrocytes – a 70 Kg human male has around 1.4 $\times 10^{12}$ platelets and 24.9 $\times 10^{12}$ red blood cells (Sender et al., 2016). The human blood platelet pool is maintained by the estimated daily production of around 10^{11} platelets which stay in the circulation for an average of 8-9 days (Leeksma and Cohen, 1955), before entering programmed cell death and clearance from the blood by the mononuclear phagocyte system in the liver or the spleen (Kile, 2014).

The classical and best-understood role of platelets comes following traumatic breaching of the blood vessel wall, a role particulary important in the high-pressure, high-shear arterial system where blood rheology particularly favours platelet adhesion and blood clots are most platelet-rich (Watts et al., 2013). The mediators that are employed by platelets to prevent bleeding following trauma to blood vessels have been well characterised in experiments *in vitro*, in preclinical animal models, and in many cases have been clinically proven by the

[2] Platelets are referred to here as cells – there is a strong case that has been made that they are at least as qualified as anucleate red blood cells for this title – but there is some controversy about whether to do so (Garraud and Cognasse, 2015).

increased bleeding risk in patients treated with antiplatelet drugs targeting relevant pathways, and in patients with relevant hereditary bleeding disorders (Jackson and Schoenwaelder, 2003).

In healthy conditions, circulating platelets are actively prevented from sticking to the endothelial wall through the release of substances from healthy endothelial cells such as prostacyclin (PGI_2), nitric oxide and ectoadenosine 5'-diphosphatase, which act respectively to promote platelet quiescence mediated through elevation of platelet cyclic adenodine monophosphate (cAMP), or cyclic guanosine monophosphate (cGMP) signalling; or to prevent platelet activation by metabolising the platelet agonist adenosine diphosphate (ADP) (Davì and Patrono, 2007). Platelets may also assist in maintenance of resting endothelial integrity, although the mechanisms underlying this function of platelets are relatively poorly understood compared with haemostasis following trauma (Nachman and Rafii, 2008; Ho-Tin-Noé et al., 2011).

When the endothelial lining is damaged, the anti-adhesion effects of endothelial cells are absent or overcome, and surface receptors constitutively expressed by platelets engage in tethering interactions on exposed subendothelial matrix components including von Willebrand Factor (vWF), collagen, fibronectin, vitronectin and laminin (Figure 1.2B), or on activated endothelial cells which have released vWF through exocytosis of their Weibel Palade bodies (Figure 1.2A). Tethering is mediated by platelets expressing a variety of adhesion molecules, for example the glycoprotein (GP) receptors, the GPIb-V-IX complex (which binds vWF) and GPVI (a receptor for collagen), and integrins including $\alpha_2\beta_1$ (GPIa-IIa, also a collagen receptor), $\alpha_{IIb}\beta_3$ (GPIIb-IIIa, a receptor for fibrinogen), $\alpha_5\beta_1$ (receptor for fibronectin)

and $\alpha_6\beta_1$ (binding partner of laminins) (Jackson and Schoenwaelder, 2003; Varga-Szabo et al., 2008).

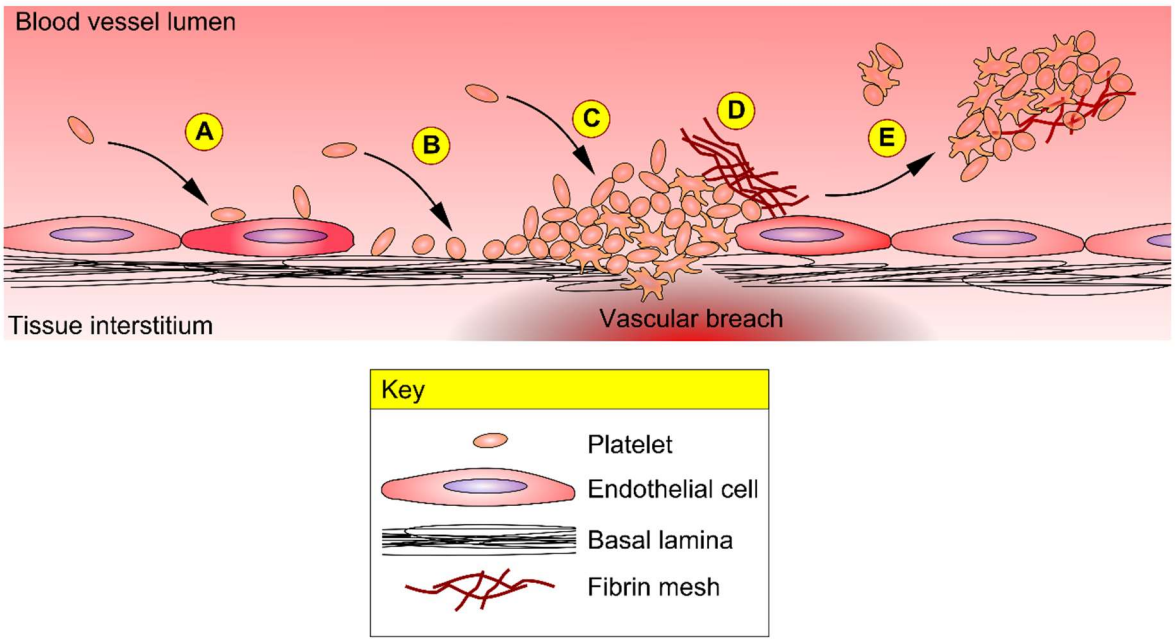

Figure 1.2: Overview of roles of platelets in haemostasis and thrombosis. Schematic of a blood vessel with damaged endothelial lining showing platelet adhesion to (A) activated endothelial cells, (B) subendothelial matrix components, (C) development of platelet thrombus covering the site of injury, (D) fibrin mesh formation around the platelet thrombus, and (E) tearing away of platelet emboli into the bloodstream.

Continued engagement of adhesion molecules triggers signalling that promotes a series of changes in platelets referred to as 'activation'. When platelet activation is initiated by adhesion molecule engagement, it involves PLC-γ-driven increases in cytoplasmic Ca^{2+} flux leading to shape change, increases in avidity of integrin engagement, and exocytosis of platelet granules (Varga-Szabo et al., 2008). The activated platelets increase the local concentration of soluble platelet agonists such as ADP released through exocytosis of dense granules, thromboxane A_2 (TXA_2) generated through increased production from phospholipase A_2-mediated

arachidonic acid generation from platelet membranes, and thrombin produced in greatly increased amounts from plasma prothrombin by the assembly of the intrinsic factor Xase complex on phospholipid surfaces of activated platelet membranes (Mann et al., 2003).

ADP, TXA_2 and thrombin all act through autocrine or paracrine signalling involving G-protein coupled receptors and PLC-β induction, leading to a positive feedback loop which further promotes platelet activation, and recruitment of more platelets from the blood to the already adherent platelets (Varga-Szabo et al., 2008). A critical mechanism for platelet-platelet interactions leading is the increased expression and conformational change of integrin $\alpha_{IIb}\beta_3$, allowing fibrinogen to bivalently bind to adjacent platelets to form a permament platelet aggregate, although other mechanisms can also promote platelet aggregation (Jackson and Schoenwaelder, 2003). These mechanisms lead the the rapid, local formation of a platelet thrombus which can temporarily cover the lesion in the vessel wall and prevent blood leakage (Figure 1.2C). Serotonin (5-hydroxytryptamine, 5-HT) is also released from platelet dense granules, and causes local vasoconstriction, therefore diverting blood away from the site of a potential breach in the circulation (Versteeg et al., 2013).

Platelet aggregates are continually torn away from the vessel wall by the shear force of passing blood, forming emboli (Figure 1.2E). In the healthy state, most of these thromboemboli are small, and as pro-thrombotic stimuli are diluted in the bloodstream in the absence of endothelial damage, will dissipate. If thromboemboli fail to disaggregate they can occlude vessels and cause downstream ischaemia. Depending on the site of generation and size of the embolus, this process can cause acute thrombotic diseases such as a myocardial infarction or

a thrombotic cerebrovascular incident (Jackson and Schoenwaelder, 2003). Excessive thrombosis can also cause vascular disease if the growth of the primary thrombus causes unresolving or unwarranted occlusion (Dicuio et al., 2003; Jackson and Schoenwaelder, 2003).

Platelets in the primary adherent thrombus greatly promote the activation of the coagulation cascade. Platelet phospholipids support the coagulant factor Xase activating complex (Factor IXa, platelet bound factor VIIIa, and calcium), and prothrombinase complex formation (factor Xa, platelet bound factor Va, and calcium). As mentioned above, thrombin generation, granule release of platelet agonists, and the synthesis of TXA_2 are boosted, activating and recruiting additional platelets, provides a greater surface for the development of a fibrin mesh, the synthesis of which is a product of the coagulation cascade, which strengthens the haemostatic plug on the vessel wall (Versteeg et al., 2013).

The contractile apparatus in platelets will then contribute to clot retraction, further strengthening the clot and assisting in wound closure (Bettex-Galland and Luescher, 1959), and factors released by platelets contribute to the eventual dissolution of the clot through promotion of fibrinolysis (Whyte et al., 2015), and to wound healing and tissue regeneration through release of substances including stromal cell-derived factor-1α (SDF-1α: CXCL12), vascular endothelial growth factor (VEGF), platelet derived growth factor (PDGF) and hepatocyte growth factor (HGF), which can promote angiogenesis, and the recruitment, activation and proliferation of both stromal and inflammatory cells, leading to resolution of the injury (Gawaz and Vogel, 2013).

1.2.2 Platelet function in inflammatory responses

Overlapping platelet roles in haemostasis, thrombosis and inflammation

In a non-sterile world, haemostasis and host defence against invading pathogens are often required simultaneously, and interplay has therefore evolved between the haemostatic processes of coagulation, platelet adhesion and activation, and the immune responses of complement cascade activation and cell-mediated inflammation (Semple et al., 2011; Li et al., 2017).

In inflammatory responses where thrombosis occurs, thrombosis itself can be viewed as a host defence response to block the entry of pathogens to the bloodstream and their dissemination throughout the body, as in some cases immune cell activation can promote the formation of thrombi which are thought to act as scaffolds for pathogen immobilisation in 'immunothrombosis' (Engelmann and Massberg, 2013).

Conversely, thrombi can recruit leukocytes from the blood as the haemostatic plug grows, develops and resolves, but this ability of platelets to recruit and activate leukocytes has potential for causing pathological 'thromboinflammation', where thrombi promote inflammation that may cause tissue damage (Maugeri et al., 2014).

Alterations in platelet function in inflammatory lung diseases

There are also mechanisms of platelet function in inflammation, which are discussed further below, which have no clear overlap with haemostatic or thrombotic function (Nachman and Weksler, 1972; Page, 1988, 1989; Li et al., 2017). In clinical studies, evidence has been found of altered platelet function in a variety of inflammatory diseases, but these alterations

are often subtle and can occur without any major alterations in haemostatic or thrombotic function.

For example, patients with asthma show no overt changes in haemostasis, with a small increase in risk of cardiovascular disease (Iribarren et al., 2012). Platelets from asthmatics exhibit either a reduced lifespan (Taytard et al., 1986), or a similar lifespan to healthy control platelets, with reduced evidence of clearance in the spleen and liver (Plaza et al., 1992). Platelet responsiveness to collagen or platelet activating factor (PAF) was reduced in asthmatics (Gresele et al., 1993), whilst blood platelet counts are decreased after allergen challenge (Sullivan et al., 2000; Kowal et al., 2006) and blood platelet-leukocyte conjugates (Pitchford et al., 2003), and platelet activation markers such as soluble P-selectin are increased (Kowal et al., 2006). Platelets from patients with asthma may also be metabolically altered as they show less reliance on glycolysis than platelets from healthy controls, despite evidence of similar mitochondrial mass (Xu et al., 2015).

COPD and ARDS patients may have altered haemostatic and thrombotic responses due to cardiovascular comorbidities (Barnes, 2008; Yadav and Kor, 2015), but nonetheless COPD patients have increased blood platelet-monocyte conjugates which increase further during exacerbations (Maclay et al., 2011), ARDS incidence and mortality is associated with decreased blood platelet counts (Wang et al., 2014), whilst platelet-derived platelet factor 4 (PF4, CXCL4)-CCL5 complexes correlate positively with extent of pulmonary leukocyte recruitment (Grommes et al., 2012). In sepsis, a major risk factor for ARDS, blood platelet-neutrophil conjugates are increased in the context of septicaemia without organ failure, and

then decreased if sepsis progresses to multiple organ failure, which may reflect increased platelet-neutrophil or platelet recruitment to failing organs (Gawaz et al., 1995, 1997).

When innate immune inflammatory responses are studied through intravenous administration of healthy volunteers with bacterial lipopolysaccharides (LPS), LPS exposure has been shown to cause small decreases in blood platelet counts with increases in blood platelet-neutrophil and platelet-monocyte conjugates in the absence of increases in platelet P-selectin (Thomas et al., 2015), small decreases in blood platelet count with evidence of platelet activation through increased surface CD40L expression, elevated plasma CXCL4 and increased endothelial cell adhesion *ex vivo*, all occurring in the absence of increases in the traditional thrombotic platelet activation markers, increased surface P-selectin or $\alpha_{IIb}\beta_3$ expression (Schrottmaier et al., 2016), or no effect on blood platelet counts with increases in platelet-neutrophil conjugates and decreases in platelet-monocyte conjugates (Schoergenhofer et al., 2016).

Platelets are functionally important in lung inflammation

Interestingly, although the effects of inflammation on haemostatic and thrombotic platelet responses can be minor compared to those of classical platelet agonists, experiments where platelets are depleted in animal models of inflammatory lung disease mechanisms have shown that removal of platelets can have major effects on the inflammatory response. These studies provide evidence that alterations in platelet function are causal in, rather than the sequelae of, inflammatory disease progression, with a particularly extensive number of studies carried

out in lung inflammation models involving lung neutrophil recruitment, especially those involving LPS exposure (overview in Table 1.1), and in allergic airway inflammation models (overview in Table 1.2).

Table 1.1: Effects of platelet depletion in lung inflammation models involving pulmonary neutrophil recruitment. Summary of studies in which lung inflammation outcomes have been measured in control animals and animals depleted of platelets in models where pulmonary neutrophil recruitment occurs. Effects or otherwise on primary outcomes of platelet depletion are given, and results are shaded according to outcome of platelet depletion with regards to health status of experimental animal: orange=positive outcome of platelet depletion, no shading=no detected effect of platelet depletion, blue shading=negative outcome of platelet depletion. Results are loosely chronologically sorted within categories of inflammation model. *Different results were obtained with different routes of depleting antibody administration (Table overleaf).

Model	Effect of platelet depletion	Reference
Dog, LPS i.v.	↓lung resistance	(Stein and Thomas, 1967)
Dog, LPS i.v.	↓Pulmonary arterial pressure ↓Pulmonary microvascular slowing	(Bredenberg et al., 1980)
Sheep, LPS i.v.	–haemodynamics, –gas exchange	(Snapper et al., 1984)
Guinea pig, LPS inhalation	↓pulmonary inflatory pressure	(Vincent et al., 1993)
Mouse, LPS inhalation	↓BAL neutrophils	(Kornerup et al., 2010)
Mouse, LPS inhalation	↓BAL neutrophils, ↓BAL protein	(Grommes et al., 2012)
Mouse, LPS inhalation	↓lung histological injury score	(Kornerup et al., 2010)
Mouse, LPS inhalation	↓BAL neutrophils	(Pan et al., 2015)
Mouse, LPS inhalation	↑lung haemmorhage	(Goerge et al., 2008)
Mouse, LPS inhalation	↑lung haemmorhage	(Boulaftali et al., 2013)
Mouse, LPS inhalation	↑lung haemmorhage	(Deppermann et al., 2017)
Mouse, LPS i.p.	–/↑ lung haemmorhage*, ↓survival	(Xiang et al., 2013)
Mouse, LPS i.p.	–lung MPO	(Andonegui et al., 2005)
Mouse, anti-MHCI antibody i.v.	↓BAL protein	(Hidalgo et al., 2009)
Mouse, LPS inhalation, anti-MHCI antibody i.v.	↑survival, ↓oedema	(Looney et al., 2009)
Mouse, LPS i.p.	↑lung MPO	(Andonegui et al., 2005)
Mouse, LPS i.p., anti-MHCI antibody i.p.	↑survival	(Sreeramkumar et al., 2014)
Mouse, acid inhalation	↑gas exchange	(Zarbock et al., 2006)
Mouse, LPS i.v. and human UVB-treated platelets i.v.	↓BAL protein, ↓human UVB-treated platelet recruitment	(Chi et al., 2012)
Mouse, mesenteric ischaemia reperfusion	↓histological lung injury score	(Lapchak et al., 2012)
Mouse, caecal ligation and puncture	↓BAL neutrophils ↓oedema	(Asaduzzaman et al., 2009a)
Mouse, caecal ligation and puncture*	↓BAL neutrophils*	(Asaduzzaman et al., 2009b)
Mouse, caecal ligation and puncture*	–lung Ly-6G or MPO*	(Asaduzzaman et al., 2009b)
Mouse, *K. pneumoniae* inhalation	↑lung haemmorhage, ↓survival	(de Stoppelaar et al., 2014)
Mouse, colon carcinoma cells i.v.	↓neutrophils in lung metastatic niches	(Labelle et al., 2014)
Sheep, complement i.v.	–haemodynamics, –gas exchange	(McDonald et al., 1983)
Sheep, phorbol myristate acetate i.v.	↓Pulmonary arterial pressure	(Nakano et al., 1995)
Mouse, NY1DD sickle cell crisis model	↓pulmonary vascular permeability	(Polanowska-Grabowska et al., 2010)

Table 1.2: Effects of platelet depletion in models of allergic lung inflammation. Summary of studies in which lung inflammation outcomes have been measured in control animals and animals depleted of platelets in models of allergic airway inflammation. Effects or otherwise on primary outcomes of platelet depletion are given, and results are shaded according to outcome of platelet depletion with regards to health status of experimental animal: orange=positive outcome of platelet depletion, no shading=no detected effect of platelet depletion. Results are loosely chronologically sorted within categories of inflammation model.

Model	Effect of platelet depletion	Reference
Guinea pig, ovalbumin allergen challnege	↓Bronchial wall eosinophils	(Lellouch-Tubiana et al., 1988)
Rabbit, ragweed allergen challenge	↓BAL eosinophils	(Coyle et al., 1990)
Guinea pig, ovalbumin allergen challnege	↓airway reactivity to histamine	(Lellouch-Tubiana et al., 1988)
Guinea pig, ovalbumin allergen challenge	–BAL eosinophils –airway reactivity to histamine	(Sanjar et al., 1990)
Mouse, ovalbumin allergen challenge	↓BAL eosinophils, lymphocytes –airway responsiveness to methacholine	(Pitchford et al., 2003)
Mouse, ovalbumin allergen challenge (chronic)	↓airway remodelling	(Pitchford et al., 2004)
Mouse, ovalbumin allergen challenge	↓BAL eosinophils, lymphocytes	(Pitchford et al., 2005)
Mouse, ovalbumin allergen challenge	↓BAL eosinophils, lymphocytes	(Tian et al., 2014)
Mouse, ovalbumin allergen challenge	↓BAL eosinophils, lymphocytes	(Amison et al., 2015)
Mouse, ovalbumin allergen challenge	↓BAL eosinophils, lymphocytes	(Pan et al., 2015)
Mouse, dust mite allergy, ptges$^{-/-}$, lysine-aspirin inhalation	↓lung resistance	(Liu et al., 2013)
Mouse, papain-induced airway inflammation	↓BAL eosinophils	(Takeda et al., 2016)

Moving away from the lung, platelet depletion studies also indicate that platelets are important for inflammation occurring elsewhere in the body, in ischaemia and reperfusion injuries in the gut (Salter et al., 2001), in synovial inflammation occurring in arthritis models (Boilard et al., 2010), in autoimmune encephalitis (Langer et al., 2012), in the eyes when inflammation is induced by corneal abrasion (Lam et al., 2011), and in various skin inflammation models (Tamagawa-Mineoka et al., 2007, 2009; Hara et al., 2010).

Platelets may also contribute to pathophysiological inflammatory responses in influenza virus infections (Lê et al., 2015) and in some phases of infection with the parasite *P. berghei* (van der Heyde et al., 2005; Gramaglia et al., 2017). However platelet depletion experiments in infection models have also shown that platelets are integrated into protective host defence responses, as platelet-depleted animals respond poorly relative to platelet-replete controls following infection with a variety of bacteria including *S. sanguis* (Dall et al., 1998), *E. coli* (Xiang et al., 2013), *S. aureus* (Wuescher et al., 2015), *K. pneumoniae* (de Stoppelaar et al., 2014) and *S. pneumoniae* (van den Boogaard et al., 2015), as well the parasites *T. cruzi* (Fernandes et al., 1992) and *P. falciparum* (Polack et al., 1997).

Another cautionary observation from some platelet depletion studies is that of inflammatory bleeding in the context of both thrombocytopaenia and inflammation (Table 1.1). Although bleeding does not normally accompany leukocyte transendothelial migration and plasma extravasation in inflammation, a minority of experimental thrombocytopaenia studies have produced data which suggest that pathological bleeding occurs in platelet-depleted mice following inflammatory challenge, indicating roles for platelets in maintaining haemostasis in some inflammatory contexts (Goerge et al., 2008; Boulaftali et al., 2013; Gros et al., 2015; Deppermann et al., 2017).

Together these clinical and experimental studies indicate that platelets, like other immune cells that have been effectively targeted in inflammatory diseases, are effectors in both pathological inflammation and in protective host defence across a variety of tissue and inflammatory contexts.

Studies in human volunteer LPS challenge models using drugs with anti-platelet activity are also suggestive that it may be possible to reduce inflammation in the human context, including in lungs, by targeting platelets. Drugs used in these studies include the dual PDE3/4 inhibitor RPL-544 which possesses anti-platelet, anti-inflammatory and bronchodilatory activity and reduces lung leukocyte recruitment following LPS inhalation (Franciosi et al., 2013), the $P2Y_{12}$ antagonists ticagrelor and clopidogrel which reduce systemic inflammation following intravenous LPS (Thomas et al., 2015), although the $P2Y_{12}$ antagonist prasugrel had no effect in a similar study (Schoergenhofer et al., 2016), and aspirin, which reduced lung leukocyte recruitment following inhaled LPS challenge (Hamid et al., 2017).

However, in the more complex setting of clinical trials, the $P2Y_{12}$ antagonist prasugrel had no detected effect on lung function in asthmatics (Lussana et al., 2015), and aspirin did not prevent the development of ARDS in a trial in at-risk intensive care patients (Kor et al., 2016a). These unsuccessful trials indicate a need for better understanding of platelet contributions to inflammatory responses, and a need for new drugs that can inhibit inflammatory platelet responses.

Recent studies in mouse models have also shown that disruption of the function of the signalling pathways in platelets that control lung leukocyte recruitment can be achieved without prevention of haemostatic functions. These reports have identified platelet $P2Y_1$ antagonism at doses insufficient to increase bleeding time (Amison et al., 2015, 2017), deletion of guanine nucleotide exchange factors (GEFs) P-Rex1 and either Vav1 or Vav3 in platelets (Pan et al., 2015) and the treatment of platelets with non-anticoagulant fragments of heparin (Riffo-Vasquez et al., 2016) as potential mechanisms through which platelets promote lung

leukocyte recruitment in inflammation through pathways that are not integral for haemostasis. These observations open up the possibility of targeting platelets in inflammation without causing bleeding-related side effects (Page, 1988; Pitchford, 2007), an aim which mirrors research in the thrombosis field, where processes key to thrombosis, but not haemostasis, are sought as targets for anti-thrombotic drugs (Jackson and Schoenwaelder, 2003). The following sections provide an overview of mechanisms through which platelets exert their functions in inflammation.

1.2.3 Mechanisms involved in inflammatory platelet responses

Platelet sensing of the presence of pathogens

As well as acting as early sensors of damage to the endothelial barrier when conventional haemostatic responses are required, platelets also express pathogen-associated molecular pattern (PAMP) recognition receptors, the initial host sensors of invading microbes in innate immunity (Janeway and Medzhitov, 2002).

Receptors for PAMPs are more classically associated with immunity than haemostasis, but a wide variety are expressed by platelets. These include the toll-like receptors (TLRs): TLR1, a receptor for bacterial peptidoglycan and lipoproteins; TLR2, which recognises a variety of bacterial, viral, fungal, parasite and endogenous ligands; TLR4, which is the most-studied PAMP recognition receptor which binds the LPS which coat Gram-negative bacteria, to which the platelet adhesion molecule P-selectin can also bind (Malhotra et al., 1998); and TLR9, which detects unmethylated CpG dinucleotides in bacterial DNA, as well as functional receptors for detection of bacterial N-formyl peptides (Czapiga et al., 2005).

Bacteria use receptors for, or mimicry of, endogenous proteins to operate within hosts. This has led to the evolution of the expression of bacterial proteins with similar structural motifs to host extracellular matrix or adhesion molecule proteins resulting in the ability of platelet receptors including $\alpha_{IIb}\beta_3$ and GP1bα to recognise a variety of bacterial surface proteins through, or independently of, their binding by fibrinogen, fibronectin or vWF (Verschoor et al., 2011; Wong et al., 2013; Hamzeh-Cognasse et al., 2015). The platelet collagen and thrombin receptors GPIV and PAR1 can also mediate activation signals following exposure of platelets to bacterial toxins (Cox et al., 2011). This homology of bacterial toxins with platelet agonists may promote pathological thrombosis in infection, but may also enable platelets to assist in host defence (Hamzeh-Cognasse et al., 2015).

Platelets also sense the presence of pathogens through detection of inflammation resulting from PAMP recognition by other parts of the immune system. Platelets sense activation of the complement cascade through expression of gC1q-R, and other unidentified receptors, for C1q and C3b (Peerschke et al., 2003; Hamad et al., 2010; Cox et al., 2011), antigen-antibody binding through functional expression of the receptor FcγRIIA for immunoglobulin Fc as well as other Fc receptors (Joseph et al., 1997). Functional expression on platelets of receptors for various inflammatory chemokines and cytokines has been demonstrated, including the CCR4 receptor for the chemokines CCL17 (TARC) and CCL22 (MDC), the CCR3 receptor which binds CCL11 (eotaxin) and CCL5 (RANTES), the CCR1 receptor which has ligands including CCL3 (MIP-1α), as well as the IL1R1 and IL1R8 receptors for IL-1 cytokines (Clemetson et al., 2000; Abi-Younes et al., 2001; Brown et al., 2013; Anselmo et al., 2016).

Direct platelet responses to the presence of pathogens

Experiments *in vitro* with isolated platelets have shown that platelets are capable of independently mounting responses against pathogens. Platelet expression of PAMP recognition receptors and adhesion molecules means that platelets can bind pathogens directly, as first observed over a century ago with the observation of platelet adhesion on *V. cholerae* (Levaditi, 1901), and platelet adhesion to wide variety of other bacteria, as well as other pathogens including viruses, plasmodia, funghi and parasites has since been observed (Fitzgerald et al., 2006; Semple et al., 2011; Yeaman, 2014).

The suggested consequences of platelet-pathogen interactions range from trapping of pathogens in the platelet open canalicular system (White, 2005, 2006), more broadly to trapping of pathogens in circulatory beds of the lung and the liver in order to prevent dissemination throughout the circulation (Tocantins, 1938; Wong et al., 2013), as well as to the direct killing of a range of bacteria by platelets through the release of a variety of platelet microbicidal proteins including β defensin-1, platelet factor 4 (PF4, CXCL4), and platelet microbicidal proteins (PmPs) -1 and -2 (Kraemer et al., 2011a; Drago et al., 2013; Hamzeh-Cognasse et al., 2015).

Platelets may also act as 'sentinel cells', acting as the primary sensors of PAMPs *in vivo*, as TLR4 expressed on platelets is important for mounting lung platelet recruitment responses to intraperitoneal LPS in mice (Andonegui et al., 2005), although in the context of Gram-negative infection, deletion of MyD88, a critical mediator of signalling downstream of TLR4, exclusively in platelets of mice had no detected effect on responses to systemic or lung infection with *K. pneumoniae* (de Stoppelaar et al., 2015).

The nature of platelet activation responses following interaction with pathogenic stimuli are highly context-dependent even when isolated platelets are exposed to a purified pathogen component such as bacterial lipopolysaccharide (LPS) (Tocantins, 1938; Walker and Casey, 1985; Middleton et al., 2016). A great number of studies have looked at isolated platelet responses to LPS and the variation in responses of platelets has been recently summarised (see Table 2 in Middleton et al., 2016). With the example of platelet aggregation as a readout, LPS can induce (Nocella et al., 2017), enhance (Montrucchio et al., 2003), inhibit (Matera et al., 1992; Lopes-Pires et al., 2012), or have no detected effect (Nystrom et al., 1993) on platelet aggregation depending on the experimental set-up and origin of LPS.

Measurements of platelet activation response to LPS stimulation have also produced complex results, with a wide range of activation responses reported (Middleton et al., 2016). Some of this variation in platelet responses to LPS preparations may be explained by the ability of platelets to mount different responses to different serotypes of LPS, suggestive of TLR4-independent mechanisms through which LPS alters platelet function (Berthet et al., 2012). It is of note that despite their lack of a nucleus, platelets retain mRNA and transcriptional apparatus and isolated platelets can produce new proteins *in vitro*, as revealed in experiments exposing platelets to LPS. One example of a protein produced *de novo* by platelets is the inflammatory cytokine interleukin-1β (IL-1β), the mRNA of which is spliced, transcribed into protein and released, and responsed to by further platelets as part of an autocrine feedback loop induced by exposure to LPS (Shashkin et al., 2008; Brown et al., 2013).

1.2.4 Platelet interactions with leukocytes and endothelium in inflammation

Adhesion molecules mediating platelet-cell interactions

As well as independently mounting responses to pathogens, the presence of inflammatory stimuli can also promote the interaction of platelets and leukocytes, leading to the formation of platelet-leukocyte conjugates which have been found free flowing in blood, on the endothelial wall, extravascularly in inflamed tissue, and can be induced to form *in vitro* (Page and Pitchford, 2013; Middleton et al., 2016; Pitchford et al., 2017). Platelet leukocyte conjugates are increased in the blood following a variety of inflammatory stimuli, including following LPS inhalation (Kornerup et al., 2010; Ortiz-Muñoz et al., 2014), or allergen challenge in mice (Pitchford et al., 2003; 2005), as well as in human volunteers exposed to LPS (Thomas et al., 2015) and patients with sepsis (Gawaz et al., 1995), COPD (Maclay et al., 2011), or with asthma (Pitchford et al., 2003; Kowal et al., 2006).

Platelet-endothelial cell interactions may also be upregulated in inflammation, as platelets from human volunteers exposed to LPS show increased endothelial cell adhesion ex vivo (Schrottmaier et al., 2016), and in mice platelet-endothelium adhesion is increased in ischaemia-reperfusion injury in the mesenteric circulation (Massberg et al., 1998; Cooper et al., 2004), in the mouse mesenteric circulation inflamed by TNFα (Frenette et al., 1998), and in the cremaster muscle circulation inflamed by LPS (Rumbaut et al., 2006; Riffo-Vasquez et al., 2016).

Several key adhesion molecule pairings mediating platelet-leukocyte interactions have been identified. P-selectin glycoprotein ligand-1 (PSGL-1, CD162) is a membrane receptor expressed by leukocytes but also by platelets and endothelial cells (Carlow et al., 2009). The

classical binding partner of PSGL-1 is P-selectin (CD62P, GMP-140) released to the surface of platelets and endothelial cells from their respective α-granules and Weibel-Palade bodies during activation (Page and Pitchford, 2013), but E-selectin (CD62E), synthesised *de novo* by endothelial cells during inflammation, and L-selectin (CD62L), expressed most strongly in leukocytes and downregulated following activation of neutrophils, can also interact with PSGL-1 (Page and Pitchford, 2013). As platelets also express functional PSGL-1, so it is possible that platelet PSGL-1 and endothelial P or E-selectins could mediate platelet-endothelium interactions in inflammation (Frenette et al., 2000).

Interactions mediated through PSGL-1-selectin binding are thought to be mainly transient, but if activation signals are sustained, platelets and leukocytes can also be held together through stronger interactions involving the integrin $\alpha_L\beta_2$ (CD11a/CD18, LFA-1) on leukocytes, and platelet ICAM-2 (CD102) (Diacovo et al., 1994), or the integrin $\alpha_M\beta_2$ (CD11b/CD18, Mac-1, complement receptor 3) on leukocytes and platelet GPIbα (Diacovo et al., 1996b), or junctional adhesion molecule (JAM)-C (Santoso et al., 2002). Interactions between endothelial vWF and platelet $\alpha_{IIb}\beta_3$ or GP1b may also mediate platelet-endothelial cell interactions when endothelial cells are activated by inflammation (Bombeli et al., 1998; André et al., 2000).

Platelet-cell interactions can alter function of platelets and cells

There is strong evidence that platelet-leukocyte, as well as possibly platelet-endothelium, interactions are functionally important for leukocyte recruitment in inflammation, as this process can be impaired in a variety of contexts with disruption of the function of P-selectin (Mulligan et al., 1992; Singbartl et al., 2001; Pitchford et al., 2005; Pan et al., 2015), PSGL-

1 (Asaduzzaman et al., 2009b; Hara et al., 2010; Kornerup et al., 2010; Lam et al., 2011; Stadtmann et al., 2013)[3], ICAM-2 (Diacovo et al., 1994; Weber et al., 2004; Basit et al., 2006), $\alpha_L\beta_2$ (Diacovo et al., 1996b; Basit et al., 2006; Asaduzzaman et al., 2008; Stadtmann et al., 2013) and JAMs (Ostermann et al., 2002; Bradfield et al., 2007).

Many of these adhesion molecules directly regulate signalling that can enhance platelet, leukocyte or endothelial activation state, but platelet-cell interactions also enable interaction of other platelet and cell surface receptors. These surface receptors include platelet CD40L (CD40 ligand, CD154) (Inwald et al., 2003), which is typically associated with expression on CD4+ T cells, as well as mast cells, basophils, eosinophils and natural killer T-cells, where it classically mediates binding of these cells with CD40 expressed by antigen-presenting cells to help guide the induction of an antigen-appropriate appropriate immune response. CD40L expression can be upregulated on the surface of platelets activated by stimuli which include exposure to LPS (Rahman et al., 2009; Schrottmaier et al., 2016), and interactions between platelet CD40L with endothelial CD40 alters endothelial cell function with the end result of increasing leukocyte recruitment (Henn et al., 1998). Platelet CD40L is important for neutrophil recruitment to lungs and for allergic airway inflammation in mouse models (Rahman et al., 2009; Tian et al., 2014).

[3] As well as binding with selectins, PSGL-1 also mediates signalling both through, and independently of, selectins interactions, and has a recently-discovered role in checkpoint regulation in T-lymphocytes, decreasing T-cell proliferation through promoting exhaustion (Hicks et al., 2003; Asaduzzaman et al., 2009b; Tinoco et al., 2016).

Also expressed on the surface of platelets is an unknown ligand for the triggering receptor expressed on myeloid cells 1 (TREM-1), which enables platelets to promote activation of TREM-1-expressing neutrophils with functional outcomes for neutrophil recruitment to lungs (Haselmayer et al., 2007).

Platelets can also release soluble mediators which influence the function of nearby lecukocytes and endothelial cells in inflammation. Platelets are the major store of serotonin, (5-hydroxytryptamine, 5-HT) in the body outside of the nervous system, and studies in mouse inflammation models suggest that release of platelet serotonin is important for neutrophil recruitment, including in LPS-inflamed lungs (Duerschmied et al., 2013).

Studies where apyrase was used to metabolise ADP, and P2Y receptor antagonists have been used to block ADP responses, suggest that platelet ADP release is important for both neutrophil and eosinophil recruitment to lungs (Amison et al., 2015, 2017). Platelet-derived PF4-CCL5 chemokine heteromers are also important for the development of lung inflammation following LPS inhalation (Grommes et al., 2012)

Platelet-leukocyte and platelet-endothelial cell interactions also allow the transfer of arachidonic acid metabolites between platelets and cells, enabling the production of different bioactive end-products than those that can be produced by individual cell types alone (Folco and Murphy, 2006). In a similar manner to how endothelial cells can use platelet-derived arachidonic acid metabolites to produce prostacyclin, a potential mechanism through which intact endothelial cells limit platelet adhesion (Bunting et al., 1976; Nowak and FitzGerald, 1989; Karim et al., 1996), neutrophils and monocytes produce leukotriene (LT)A_4, which can be shuttled to platelets which express LTC_4 synthase and so can produce bioactive LTC_4

(Edenius et al., 1988; Maclouf and Murphy, 1988; Bigby and Meslier, 1989). Platelets can also use arachidonic acid metabolites produced by monocytes to synthesis lipoxin A_4 (Bigby and Meslier, 1989). Bioactive leukotrienes are important in inflammatory reactions, particularly in asthma (Busse, 1998; Montuschi and Peters-Golden, 2010), and lipoxins may be protective in resolving inflammation in the lung (Serhan et al., 2014).

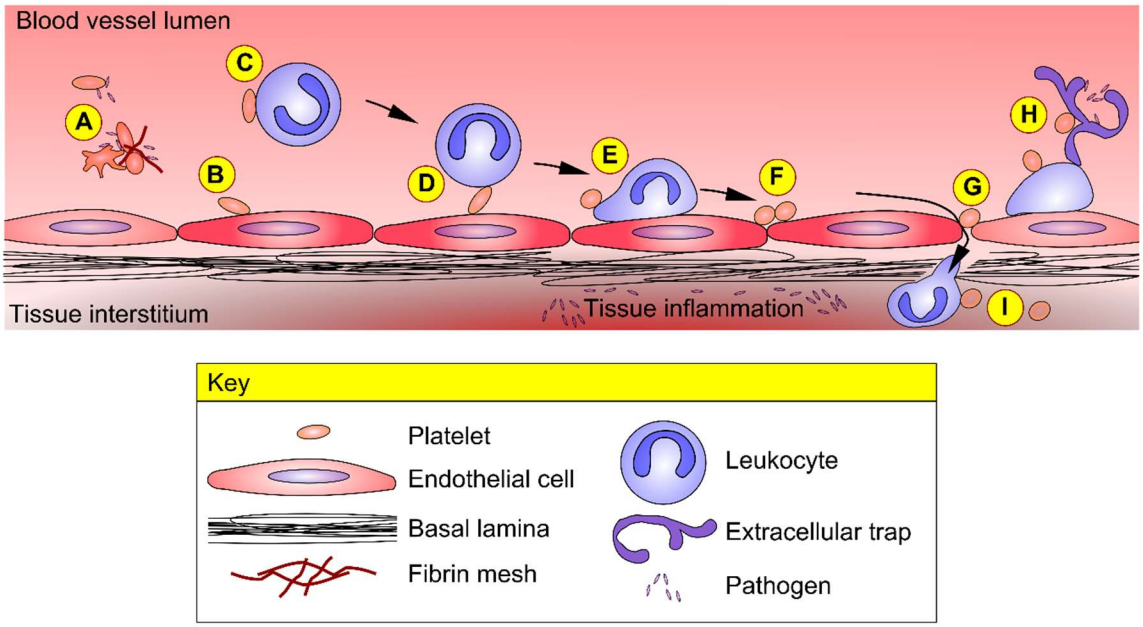

Figure 1.3: Overview of platelet interactions with pathogens, endothelium and leukocytes in inflammation. (A) Platelets directly interact with a variety of pathogens in blood and *in vitro*, with some pathogens triggering aggregation and coagulation and some not. (B) Inflammatory stimuli and danger signals can promote tethering of individual platelets on endothelial cells. (C) Inflammatory and thrombotic stimuli can cause platelet-leukocyte conjugates form in blood and *in vitro*. (D) In some situations, platelets may act as bridges to tether leukocytes to vessel walls. (E) Platelets interact with vessel-adherent leukocytes and (F) guide leukocytes to sites for transendothelial migration. (G) Platelets may be important for preventing bleeding following transendothelial migration of leukocytes. (H) Platelets are important for neutrophil extracellular trap formation. (I) Platelets can also migrate across the endothelium, but the influence of leukocytes on this event is unknown.

Platelet-cell interactions in the leukocyte (and platelet) recruitment cascade

Advances in imaging technology have revealed interactions of platelets with leukocytes and endothelial cells at every step required in the leukocyte recruitment cascade, a set of adhesion stages required for the movement of leukocytes from the bloodstream to the endothelial wall and then out into tissue, an integral process in host defence and immune surveillance (Ley et al., 2007).

In order to leave the bloodstream and become arrested on the endothelial wall, leukocytes must overcome the inflammatory shear from passing blood and tether to endothelial cells. In several tissue contexts, the rolling of leukocytes along the endothelium is the first step in this process. In several models, leukocyte rolling has shown dependence upon platelets, with interactions between P- and E- selectin adhesion molecules expressed by activated endothelial cells and platelets, and PSGL-1 on leukocytes have been implicated in this process (Diacovo et al., 1996a; Carvalho-Tavares et al., 2000; Salter et al., 2001; Ludwig et al., 2004; Kuckleburg et al., 2011).

However, in other preparations, such as in the capillaries of the lung and kidney glomeruli, selectin-mediated rolling is dispensible for leukocyte recruitment, but platelets, and in some cases, P-selectin, are still required (Singbartl et al., 2001; Hickey et al., 2006; Kuligowski et al., 2006; Zarbock et al., 2006; Kornerup et al., 2010). This may be because platelet-leukocyte interactions in free-flowing blood in inflamed tissues that current imaging technologies cannot resolve are important, but recent studies have also indicated that platelet interactions with endothelium-adhesive leukocytes may also be important in the platelet-dependence of leukocyte recruitment. In inflamed cremaster venules for example, platelets interact with PSGL-1-

rich uropods of endothelium-adhesive neutrophils, with intravascular crawling greatly diminished in the absence of platelets, suggesting a requirement for platelet interactions with endothelium-adherent neutrophils for promoting intravascular crawling to sites of neutrophil endothelial transmigration (Sreeramkumar et al., 2014). *In vitro* assays have further revealed that platelets can promote neutrophil migration through interactions requiring P-selectin (Bengtsson et al., 1999; Kornerup et al., 2010; Amison et al., 2015).

As well as platelet-leukocyte interactions, platelet-endothelium interactions may also be important for intravascular crawling towards sites for leukocyte extravasation, as in another study in the mouse cremaster preparation, platelets have been proposed to act as guides which lead leukocytes to appropriate sites for endothelial transmigration, as platelet adhesion can be seen at sites on the endothelium which later become 'hotspots' of leukocyte transendothelial migration (Zuchtriegel et al., 2016).

Furthermore, platelet adhesion has also been observed at sites where leukoytes have previously emigrated from the bloodstream, a response which has been associated with the prevention of inflammatory bleeding, but contrasts with classical haemostatic plug formation in that platelet adhesion appears to be limited to single platelets (Gros et al., 2015).

Platelet migration beyond the endothelial barrier

Platelets may also pass through the endothelium and have been found extravascularly with leukocytes, or alone, with consequences that are poorly understood. Extravascular platelets have also been observed in pathological samples from human patients with inflammatory bowel disease (Weissmüller et al., 2008), tumours (Miyashita et al., 2015), aspirin exacerbated respiratory disease (Laidlaw et al., 2012), ARDS (Miyashita et al., 2016), and asthma

(Metzger et al., 1987). Furthermore, platelets have been found outside of blood vessels without evidence of bleeding in models of skin inflammation in guinea pigs (Feng et al., 1998), in lungs following intravenous platelet activating factor challenge in guinea pigs (Lellouch-Tubiana et al., 1985), in allergic mouse airways (Pitchford et al., 2008), in LPS-inflamed mouse lung airspaces (Ortiz-Muñoz et al., 2014), and in healthy mouse high endothelial venules (Herzog et al., 2013). Platelet microparticles have also been found in increased numbers in the inflamed synovia of mice with inflammatory arthritis (Boilard et al., 2010).

This accumulating evidence of the extravascular presence of platelets in response to inflammatory signals, and the intimate involvement of platelets with the process of the leukocyte recruitment cascade, suggests the presence of platelets extravascularly might be as a secondary consequence of leukocyte migration. However, platelets display motility that suggests they might independently be able to achieve transendothelial migration, as *in vitro* human platelets can exhibit random motility (Valone et al., 1974), and directed motility towards a chemotactic gradient (Lowenhaupt, 1978; Lowenhaupt et al., 1982; Czapiga et al., 2005; Kraemer et al., 2010, 2011b). Platelets from mice have also been shown to achieve directed migration towards chemotactic gradients (Pitchford et al., 2008; Schmidt et al., 2012).

Signalling through phosphoinositol 3-kinase, serum and glucocorticoid-regulated kinase 1 (SGK1) signalling, and elevated cytoplasmic Ca^{2+}, actin polymerisation and focal adhesion formation, and the chemotactic stimuli fMLP, stromal cell-derived factor 1α (SDF-1α) and antigen-antibody-Fc receptor interactions have been implicated in these *in vitro* studies (Pitchford et al., 2008; Kraemer et al., 2010, 2011b; Schmidt et al., 2012), and provide further

evidence that platelets have the capacity to migrate across the endothelial barrier into inflamed tissue. Recently-developed microfluidic models have also demonstrated that migrating neutrophils can 'pick up' and 'drop' platelets as the neutrophils move towards a source of chemokine, providing another way in which platelets may migrate from blood into inflamed tissues (Frydman et al., 2017).

Methods are required for enabling the imaging and quantification of platelet transendothelial migration in inflammation *in vivo* for further investigation into mechanisms of platelet migration in inflamed tissues and establishing what roles extravascular platelets in play in health and disease.

1.2.5 Lung platelet recruitment in inflammation

Platelet recruitment to lungs in inflammation

As many of the functions of platelets reviewed above require spatio-temporally limited juxtacrine and paracrine signalling it is conceivable that, like platelet adhesion in haemostatic responses and leukocyte recruitment in inflammation responses, the platelet responses that mediate the platelet-dependence of inflammation depend on local platelet recruitment.

Lung platelet recruitment has previously been demonstrated across a range of non-human animal models showing that platelet recruitment to the lung is an evolutionarily conserved response elicited by a wide range of stimuli (See overview in Table 1.3). There is evidence that some of this recruitment may be because platelets are slowed by interactions with cells in the lung as they travel through the pulmonary circulation (Bierman et al., 1951; Kien et al., 1971; Doerschuk et al., 1990; Eichhorn et al., 2002).

Platelets may also be deposited in the lung in inflammatory states as a result of microvascular thrombosis, or disseminated intravascular coagulation, responses to interplay between inflammation responses with processes involved in regulating thrombosis, coagulation and fibrinolysis (Vesconi et al., 1988; Davis et al., 2016).

It is also of note that the platelet content of the lungs can be influenced by local production, as lungs contain 'embolised' megakaryocytes which produce proplatelets and platelets locally, as well as progenitor stem cells capable of differentiating into megakaryocytes (Aschoff, 1893; Howell and Donahue, 1937; Trowbridge et al., 1984; Lefrançais et al., 2017). Little is known of the effects of lung inflammation on the quantity and duration of pulmonary thrombopoiesis, although megakaryocytes in mice produce functionally altered platelets after LPS exposure through a TLR4-independent mechanisms (Jayachandran et al., 2007).

Further to studies in non-human animal models, increased quantities of platelets have also been found inside and outside of blood vessels in autopsy samples of lungs from human sufferers of ARDS (Bone et al., 1976; Miyashita et al., 2016), activated platelets have been found in arterial blood samples of patients with COPD and pulmonary hypertension (Rostagno et al., 1991), and platelets have been detected in the bronchoalveolar spaces of asthmatic patients (Metzger et al., 1987), indicative of involvement of lung platelet recruitment, activation and transendothelial migration in human inflammatory lung disease pathology.

Table 1.3: *In vivo* inflammation studies showing platelet recruitment to lungs. Model organism, inflammatory stimulus and references to studies where lung platelet recruitment has been measured in the context of inflammation.

Animal	Stimulus	Reference
Dogs	Systemic trauma	(Ljungqvist et al., 1971)
Dogs	Disintegrated Pseudomonas i.v.	(Myrvold and Brandberg, 1977; Myrvold and Lewis, 1977)
Dogs	Oleic acid i.v. or *E. coli* i.v.	(Hechtman et al., 1978)
Dogs	LPS i.v.	(Almqvist et al., 1983)
Rabbits	fMLP i.v.	(Issekutz et al., 1983)
Rats	Hyperoxia	(Barry and Crapo, 1985)
Guinea pigs	LPS aerosol	(Beijer et al., 1987)
Rabbits	Ragweed allergen aerosol	(Metzger et al., 1987)
Sheep	LPS i.v.	(Al-Sarraf et al., 1988, 1989)
Baboons	Paf-acether i.t.	(Arnoux et al., 1988)
Aged rats	LPS i.v.	(Durham et al., 1989)
Guinea Pigs	fMLP i.v. or PAF-acether i.v.	(Bureau et al., 1989)
Mice	LPS i.v.	(Shibazaki et al., 1996, 1999)
Rats	LPS i.v.	(Itoh et al., 1996)
Mice	Ovalbumin allergen i.v.	(Yoshida et al., 2002)
Mice	LPS i.p.	(Andonegui et al., 2005)
Rabbits	LPS i.v.	(Kiefmann et al., 2006)
Mice	Ovalbumin allergen aerosol	(Pitchford et al., 2008)
Mice	LPS i.t. + anti-MHCI i.v.	(Looney et al., 2009)
Mice	LPS i.t.	(Ortiz-Muñoz et al., 2014)

Lung platelet recruitment following intravenous versus inhaled inflammatory stimuli

Interestingly, these previous studies show that lung platelet recruitment can be elicited following intravenous administration of inflammatory stimuli (Table 1.3), which may result in lung platelet recruitment due to systemic platelet aggregation and embolism in the lung microvasculature, but lung platelet recruitment can also be provoked when lung inflammation is induced by hyperoxia (Barry and Crapo, 1985), challenge with inhaled allergen (Metzger et al., 1987; Pitchford et al., 2008), or LPS inhalation (Beijer et al., 1987; Ortiz-Muñoz et al., 2014). In these models the lung is the focus of inflammation and the agent used for inflammatory challenge is primarily encountered by cells facing the airspaces so is unlikely to be directly causing systemic platelet aggregation leading to subsequent pulmonary thromboembolism.

Traces from noninvasive recordings where thoracic radioactivity was measured over time in animals infused with ^{111}In-labelled platelets show that the time courses of responses to intravenous versus inhaled LPS are contrasting. Intravenous LPS at a high dose in rats cause a lung platelet recruitment response which dissipated within 30 minutes (Figure 1.4), whereas when LPS was given *via* the inhaled route as an aerosol in guinea pigs, lung platelet recruitment was sustained for over 2 hours (Figure 1.5), a time course more closely resembling that of recruitment of radiolabelled neutrophils to LPS-inflamed lungs, which was sustained beyond 30 minutes in rabbits (Jones et al., 2002).

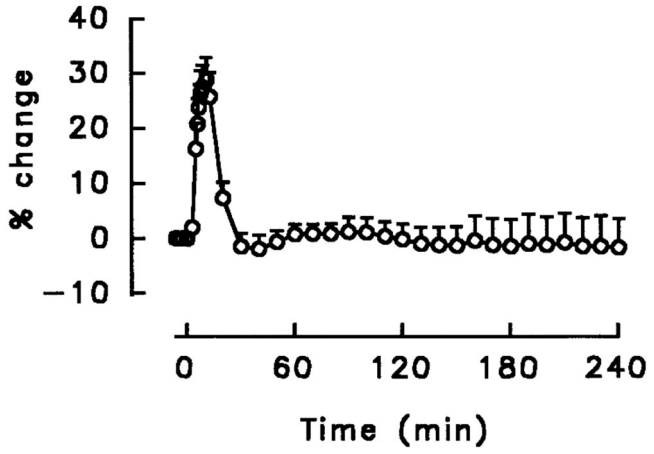

Figure 1.4: Non-invasive measurement of lung platelet recruitment following intravenous LPS injection into rats. Thoracic radioactivity over time in rats transfused with ^{111}In-labelled platelets, with 10 mg/kg of LPS given i.v. at 0 minutes. Means ± standard error, n=6. Adapted from Itoh et al., (1996) with permission from Elsevier.

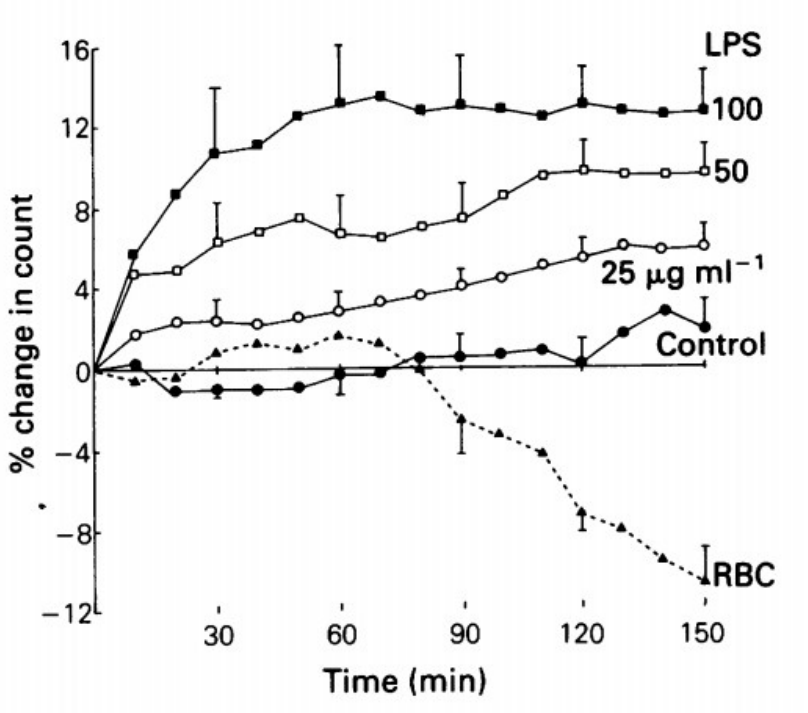

Figure 1.5: Non-invasive measurement of lung platelet recruitment following LPS inhalation in guinea pigs. Thoracic radioactivity over time in guinea pigs transfused with ^{111}In-labelled platelets, or red blood cells as a perfusion control (RBC, dashed line). At 0 minutes guinea pigs were exposed to saline aerosol (Control) or LPS aerosol at the concentrations indicated (RBC group was given LPS at 50 µg/ml. Means ± standard error, n=6-11. Reproduced from Beijer et al., (1987) with permission from Wiley-Blackwell Publishing.

Pharmacological studies investigating lung platelet recruitment following LPS inhalation have identified that in guinea pigs, treatment with platelet activating factor antagonists CV-3988 and brotizolam, the anti-coagulant and anti-inflammatory molecule heparin, the prostacyclin analogue ZK 36374, or high doses of the COX inhibitor indomethacin, might reduce inflammatory lung platelet recruitment (Beijer et al., 1987), whilst in mice this response might be decreased by treatment with high doses of aspirin (Ortiz-Muñoz et al., 2014). However, lung platelet recruitment in response to inhaled inflammatory stimuli is little-characterised when compared to the processes of platelet recruitment in haemostasis, and leukocyte recruitment in inflammation, which have both been extensively studied with the use of the wide range of imaging technologies and genetic, antibody and pharmacological interventions that are now available for use in mice. A mouse model and techniques were therefore sought for use in the study of lung platelet recruitment following LPS inhalation in mice.

1.3 Aims and objectives

1.3.1 Methods for measuring LPS-induced lung platelet recruitment

Characterising an LPS inhalation model of lung inflammaiton

As reviewed above, platelet responses to LPS *in vitro* have been widely studied, and the platelet dependence of responses to LPS-treatment has been explored in a variety of animal models, many of which showed that removal of platelets reduced the extent of inflammation or other pathological measurements (Table 1.1).

LPS models offer the advantages of relative reproducibility and rapidity of use, and are widely used as models for the study of processes which are hallmarks of the ARDS, and that also occur in COPD, such as lung neutrophil recruitment, cytokine production in the lungs, and plasma extravasation into airspaces (Matute-Bello et al., 2008). LPS inhalation is also more generally used to study the phenomonen of directed neutrophil migration into lung airspaces (Pan et al., 2015), a response which is protective in host defence against lung infections, but could also be pathophysiological when neutrophil recruitment is excessive, unresolving or unwarranted (Munford, 2008). LPS inhalation has also been used more specifically to study occupational byssinosis which is thought to be caused by inhalation of dust containing residual LPS (Rylander et al., 1981).

Previous studies have demonstrated the platelet dependence of lung neutrophil recruitment following intranasal (Kornerup et al., 2010; Pan et al., 2015) or aerosolised (Grommes et al., 2012), inhalational challenge with LPS (Table 1.1). Lung inflammation following LPS

inhalation appears to involve platelet mechanisms which contrast with those involved in haemostasis and thrombosis. For example inflammation following LPS inhalation depends on platelet P-Rex and Vav guanine nucleotide exchange factors which are dispensible for haemostasis, and in contrast to thrombotic responses show a greater dependence on signalling through the $P2Y_1$ than the $P2Y_{12}$ purinergic G-protein coupled receptor (Amison et al., 2017).

Furthermore, LPS inhalation appears to cause lung platelet recruitment in mice with platelets also migrating into airspaces, responses that are reduced when other elements of the inflammatory response are inhibited (Ortiz-Muñoz et al., 2014).

The initial aim of this project was therefore to characterise a mouse LPS inhalation model similar to those used in the previous experiments showing platelet dependence of neutrophil recruitment and lung platelet recruitment in order to enable the study of lung platelet recruitment and platelet migration into lung airspaces, as well as lung neutrophil recruitment, following inflammation originating in the lung airspaces.

Immunohistochemistry

Platelets are prevalent in the blood which perfuses all tissues, but as they are anucleate and chemical stains allow for limited discrimination of platelets in tissues[4], individual platelets can be easily overlooked in conventional histological preparations stained for example with

[4] Wright's stain allowed for association of blood platelets with megakaryocytes in cytological samples (Wright, 1906; Lee et al., 2002), but is less useful in tissue preparations, particularly when platelets are not aggregated into large thrombi, as is the case with Carstairs' stain for fibrin and platelets (Carstairs, 1965). Transmission electron microscopy methods also allow for identification of platelets but with a low throughput (Feng et al., 1998).

haematoxylin and eosin. The position and number of platelets can, however, be revealed with the use of immunohistochemistry techniques to deposit dyes or fluorophores at sites of high density of expression of epitopes highly restricted to the megakaryocyte/platelet lineage, as pioneered by Carstairs (1965). Examples of platelet-specific epitopes used in the present body of work to immunostain platelets are regions of CD41 (ITGA2B, Integrin α_{IIb}, a component of the receptor for fibrinogen and vWF) and CD42b (GP1BA, Glycoprotein Ibα, a component of the receptor complex for vWF).

Previous studies have demonstrated increased CD41 staining in inflamed lungs, but few have quantified platelets made visible using immunohistochemistry. In the present body of work, a novel approach was therefore employed combining rapid collection of mouse lung samples, snap freezing, and staining for platelet CD41 or CD42b. DAB reporters were used as they are highly sensitive and do not suffer from photobleaching, so samples are permanently stained and could be imaged using a new bright field microscope available in our laboratory. This method was quantified through the deconvolution of DAB reporter signal (Ruifrok and Johnston, 2001) with the use of automated counting methods for increased throughput, and supported by immunofluorescence staining using tiling methods which allowed for viewing high resolution images of relatively large areas of tissue (Preibisch et al., 2009).

Immunohistochemistry can also be applied to human samples, so platelets were also immunostained in samples previously generated from human *ex vivo* blood-perfused lungs exposed to LPS intrabronchially (Hamid et al., 2017), as a proof-of concept study exploring the suitability of the use of this method in human tissue.

Radiolabelling studies

With excellent depth of penetration and improving spatial resolution, platelets and other cells can be tracked throughout the body using radiolabelling and radioimaging methods, and radiolabelled autologous platelets have established clinical use for studying platelet lifespan and fate in the context of thrombocytopenia (Mathias and Welch, 1984).

Early experiments using radiolabelled platelet methods in laboratory animals permitted measurement of platelet aggregation noninvasively *in vivo* through the quantification of lung platelet aggregate trapping following intravenous injection of platelet agonists using the index of increased thoracic radioactivity (Page et al., 1982). Similar noninvasive methods have been applied to the measurement of increases in lung platelet signal following the inhalation of LPS in guinea pigs (Beijer et al., 1987) (Figure 1.5), and also following intravenous injections of LPS into rats (Itoh et al., 1996).

Platelet responses to LPS, or any other inflammatory stimuli, have not been measured non-invasively using platelet radiolabelling in mice, but the method for non-invasively measuring thromboembolism in the lungs has been scaled down for use in mice (Tymvios et al., 2008). Destructive organ biodistribution studies in mice have been carried out and have revealed increases in platelet signal in lungs of mice following intraperitoneal injection of LPS (Andonegui et al., 2005), and in mouse lungs after induction of a model of transfusion-induced acute lung injury involving inhalation of LPS followed by intravenous anti-MHCI antibody (Looney et al., 2009), but have been minimally studied following LPS inhalation alone (Looney et al., 2009).

We therefore sought to develop a method in a mouse LPS model for non-invasive measurements of thoracic platelet content as an index of lung platelet recruitment. This was combined with a more sensitive, but destructive, organ biodistribution approach to measure platelet accumulation in lungs as well as their major sites of clearance in the liver and spleen, and also in samples of bronchoalveolar lavage (BAL) in order to quantify extravascular movement of platelets into the lung airspaces.

Intravital microscopy

Intravital microscopy renders dynamic cellular processes visible in their living context. The first quantitative studies of leukocyte and platelet recruitment to blood vessel walls using intravital videomicroscopy started the research field of investigating the different mechanisms by which leukocytes and platelets are recruited from the blood to the endothelial lining (Atherton and Born, 1972, 1973a, 1973b), and a wide variety of methods for intravital imaging platelets in blood vessels are now available.

The imaging of cellular processes in lungs has been challenging relative to other tissues due to the situation of the lungs inside the ribcage and the motion of the lungs which is required for efficient ventilation. Lung imaging is important as many processes occur differently in the systemic and pulmonary vasculature – for example LPS-induced neutrophil recruitment in the pulmonary circulation does not appear to require P-selectin (Kornerup et al., 2010), whilst the same process in the liver circulation does (Klintman et al., 2004). Other vascular beds widely used for intravital microscopy studies due to their ease of access and stability for example the cremaster muscle or mesentery preparations, are not in 'barrier' tissues directly exposed to pathogenic stimuli, and do not normally become inflamed.

Advances in intact lung microscopy allowed for the discovery of the pulmonary capillaries (Malpighi, 1661), the use of a vacuum window permitted stabilised imaging of the living pulmonary microcirculation in closed-chest conditions in of dogs (Terry, 1939), and *ex vivo* fluorescent labelling of platelets allowed for the first imaging and quantification of recruitment of activated platelets to the capillaries and venules of the lungs of rabbits (Eichhorn et al., 2002). Similar technology has also allowed for the first microscopy studies of platelet recruitment to rabbit lungs following intravenous LPS infusions (Kiefmann et al., 2004, 2006).

Intravital microscopy methods have more recently been adapted and developed upon for imaging lungs of mice (Tabuchi et al., 2007; Looney et al., 2011; Ortiz-Muñoz et al., 2014; Headley et al., 2016; Lefrançais et al., 2017). Coupling the enhanced depth of penetration possible with multiphoton microscopy with the use of a mouse strain in which platelet membranes are genetically labelled with green fluorescent protein has allowed for the imaging of a complete population of endogenously labelled platelets, proplatelets and megakaryocytes in physiological quantities in living lungs (Lefrançais et al., 2017).

Using the same mouse strain and similar microscopy methods as thosed used by Lefrançais et al, (Lefrançais et al., 2017), a pilot study was carried out using intravital multiphoton microscopy to image and quantify platelet adhesion in the lungs of healthy control mice and mice treated intranasally with LPS.

1.3.2 Exploring mechanisms of LPS-induced lung platelet recruitment

Dependence of LPS-induced lung platelet recruitment on neutrophils

Both platelets and neutrophils are under consideration as targets for therapeutic interventions for inflammatory diseases. Understanding how the recruitment of both of these cell types depends upon the recruitment of the other will be important for predicting and interpreting any anti-inflammatory efficacy or side-effects that might result from interventions targeting platelet or neutrophil recruitment to lungs.

Neutrophils are amongst the earliest cellular responders to a variety of inflammatory insults, and make up the vast majority of recruited cells following LPS inhalation. In a study where the effects of platelet depletion, neutrophil depletion, and depletion of both cell types were compared head-to head, all treatments inhibited LPS-induced lung inflammation to a similar extent (Grommes et al., 2012). Several experiments in mouse models of lung inflammation suggest that lung neutrophil recruitment largely depends on the presence and function of platelets, including in LPS inhalation models (Kornerup et al., 2010; Grommes et al., 2012; Ortiz-Muñoz et al., 2014; Pan et al., 2015; Amison et al., 2017), following acid inhalation (Zarbock et al., 2006), and in response to LPS priming and anti-MHCI antibody model of transfusion-associated lung injury (Looney et al., 2009).

As lung platelet recruitment may be a key mechanism for the platelet dependence of lung neutrophil recruitment, it is of interest whether neutrophil depletion affects lung platelet recruitment following LPS inhalation. The neutrophil dependence of lung platelet recruitment following LPS inhalation has not been previously explored, but several studies have found

platelet recruitment to require neutrophils in other contexts. These at least partially neutrophil-dependent responses include platelet deposition on infarcted myocardium in dog models (Bednar et al., 1985), ischemia-induced platelet adhesion in mesenteric postcapillary venules of mice (Cooper et al., 2004), intravenous LPS-induced platelet adhesion in the cremaster muscle microcirculation (Rumbaut et al., 2006), as well as platelet recruitment to the lungs following treatment of mice with intraperitoneal LPS (Andonegui et al., 2005), and following inhaled LPS priming and intravenous anti-MHCI antibody to induce lung injury (Looney et al., 2009).

Antibody-based neutrophil depletion technologies for use in mouse models that have improved selectivity have relatively recently become available. These new neutrophil depleting antibodies target Ly6-G+ neutrophils without also depleting functionally important Ly6C+ inflammatory monocytes which were depleted together with neutrophils by earlier anti-Gr-1 antibodies used in all of the mouse models investigating neutrophil dependence of platlet recruitment listed above (Daley et al., 2008). A neutrophil depletion strategy was therefore validated and used to compare platelet response to LPS inhalation in mice depleted of neutrophils with anti-Ly6-G antibody, to neutrophil replete controls in order to test whether whether platelet depletion was neutrophil-dependent.

PSGL-1, P-selectin and lung platelet recruitment

P-selectin and PSGL-1 are attractive molecules for an investigation into platelet recruitment to inflamed lungs as P-selectin and PSGL-1 are required for platelet-leukocyte, platelet-endothelium and leukocyte-endothelium interactions. In LPS inhalation models PSGL-1 has been implicated as an important mediator of platelet-dependent lung inflammation (Kornerup

et al., 2010), and P-selectin has been suggested to mediate LPS-induced neutrophil rolling in the airway vasculature (Pan et al., 2015). Furthermore, platelet recruitment to the pulmonary circulation in rabbits during endotoxaemia showed evidence of P-selectin dependence (Kiefmann et al., 2006).

P-selectin and PSGL-1 interactions are important to investigate as these adhesion molecules are targets for drugs in development for a variety of diseases. The P-selectin inhibitor crizanlizumab recently showed efficacy in clinical trials for preventing pain crises in sickle cell disease (Ataga et al., 2017), and P-selectin also has been implicated in lung inflammation in cobra venom factor intravenous administration models (Mulligan et al., 1992), in postischaemic renal failure in mice (Singbartl et al., 2001), acid inhalation-injuced lung injury (Zarbock et al., 2006), as well as in the formation of NETs (Etulain et al., 2015).

Likewise, inhibitors of PSGL-1 function are currently in development (Kanabar et al., 2016), and blocking PSGL-1 has previously also shown efficacy in reducing inflammation in *in vivo* models of atherosclerosis (Phillips et al., 2003), caecal ligation and puncture (Asaduzzaman et al., 2009b) , anti-MHCI antibody-induced lung injury (Sreeramkumar et al., 2014). It should be noted that the anti-inflammatory effects of blocking PSGL-1 appear to extend beyond those of blocking interactions with selectins as recombinant PSGL-1, which blocks all PSGL-1 interactions, is anti-inflammatory at 1/30 of the dose required to inhibit leukocyte rolling (Hicks et al., 2003), and in a mouse caecal ligation and puncture model, the effects of PSGL-1 blockade on reducing lung neutrophil recruitment occurred in addition to the effects of following platelet depletion (Asaduzzaman et al., 2009b).

The effects of blockade of P-selectin or PSGL-1 on lung platelet recruitment and inflammation following LPS inhalation in mice were therefore investigated to clarify the involvement of these mediators in this model.

Drugs targeting platelet P2Y ADP receptors and lung platelet recruitment

Platelets sense extracellular ADP, a danger signal for cellular damage or the release of dense granules from activated platelets, through the expression of the purinergic GPCRs $P2Y_1$ and $P2Y_{12}$, as well as through the ion channel $P2X_1$.

$P2Y_{12}$ expression is relatively restricted to platelets, and antagonists of $P2Y_{12}$ possess potent antithrombotic activity which underlies the clinical success of $P2Y_{12}$ inhibitors including clopidogrel, prasugrel, cangrelor and ticagrelor in the treatment of cardiovascular diseases (Jackson and Schoenwaelder, 2003; Cattaneo, 2010).

The expression of $P2Y_1$ is less restricted to the megakaryocyte-platelet lineage than $P2Y_{12}$ – $P2Y_1$ is also expressed in the brain and the respiratory epithelium amongst other tissues – and so there has been caution around the targeting $P2Y_1$ in humans. However, antagonists with relative $P2Y_1$ selectivity have been produced and retain interest in the thrombosis field as studies in mice, rabbits and cynomolgus monkeys suggest that $P2Y_1$ inhibitors may increase bleeding risk to a lesser extent than $P2Y_{12}$ inhibitors whilst retaining an equivalent degree of anti-thrombotic activity towards ADP (Yang et al., 2014; Wong et al., 2016).

Inhibition of $P2Y_1$, but not $P2Y_{12}$, reducs lung leukocyte recruitment in both allergen challenge and LPS inhalation models, without greatly increasing bleeding time (Amison et al., 2015, 2017). Exposure of platelets to ADP concentrations insufficient to promote platelet

aggregation also enhances platelet-dependent leukocyte chemotaxis towards macrophage derived chemokine (MDC), suggestive that $P2Y_1$ inhibitors may act through reducing the ability of platelets to enhance leukocyte endothelial transmigration (Amison et al., 2015).

Other groups have also explored the dependence of lung and LPS-induced inflammation on platelet $P2Y_1$ and $P2Y_{12}$ receptors in other models involving systemic exposure to LPS, reaching a range of different conclusions. Genetic deletion of $P2Y_1$ in mice failed to prevent intraperitoneal LPS-induced pulmonary leukocyte trapping (Liverani, 2017), and in a similar model inhibition of $P2Y_{12}$ worsened LPS-induced inflammatory responses (Liverani et al., 2014). Conversely, in the mouse caecal ligation and puncture model of polymicrobial sepsis, pretreatment with the $P2Y_{12}$ inhibitor ticagrelor reduced both pulmonary neutrophil recruitment and lung oedema (Rahman et al., 2014).

In humans dosed with intravenous LPS, $P2Y_{12}$ inhibition with ticagrelor reduced levels of inflammatory cytokines and coagulation markers in one study (Thomas et al., 2015), but had no effect on either in another human trial (Schoergenhofer et al., 2016).

The effects of inhibition of platelet P2Y receptors on lung platelet recruitment in inflammation are unknown, so the effects of $P2Y_1$ and $P2Y_{12}$ inhibition on LPS-induced lung platelet recruitment in mice were investigated using the same treatments, as previously described (Amison et al., 2015, 2017).

Aspirin and lung platelet recruitment

Aspirin is an irreversible inhibitor acting through inhibitory acetylation of cyclooxygenase (COX) enzymes which convert free arachidonic acid to the unstable intermediate PGH_2, a

necessary step for the subsequent production of the bioactive mediators (TXA_2, PGD_2, PGE_2, PGF_2, PGI_2) by other downstream enzymes in cells where these are expressed (Fuster and Sweeny, 2011).

There are two known isoforms of COX, and inhibition of COX-1 is thought to mediate the clinically proven anti-platelet action of aspirin through inhibition of the production of TXA_2 by COX-1 in anucleate platelets, which have a limited ability to synthesise replacements for the irreversibly aspirin-inhibited COX enzymes (Fuster and Sweeny, 2011). Although aspirin shows some selectivity for COX-1, at higher doses it can also inhibit the other COX isoform, COX-2 (Mitchell et al., 1993). COX-2 is expressed primarily in stromal cells and leukocytes, but also in megakaryocytes and newly-formed platelets (Rocca et al., 2002), with expression constitutive in the brain but induced in other cells in inflammation (Flower, 2003). Increased prostaglandin mediator production by COX-2 is particularly important in the signalling leading to inflammation and pain, and selective inhibitors of COX-2 have clinically proven anti-inflammatory action in the treatment of inflammatory conditions (Flower, 2003).

As inhibition of COX-2 function was previously associated with anti-inflammatory effects, the observation that COX-$2^{-/-}$ mice, and mice treated with a COX-2 inhibitor, had increased lung inflammation after acid inhalation-induced lung injury was surprising (Fukunaga et al., 2005). Interestingly, lung inflammation in acid-injured mice treated with high dose aspirin was unaltered, but was still increased in mice treated with high dose aspirin and a COX-2 inhibitor (Fukunaga et al., 2005). The production of pro-resolution, anti-inflammatory lipoxins by COX-2 was identified as the cause of increased lung inflammation in the absence of COX-2. In contrast to action of reversible COX-2 inhibitors, acetylation by aspirin can alter

COX-2 function in such a way that it produces 15-*R*-hydroxyeicosatetraenoic acid from arachidonic acid, which can result in increased production of the anti-inflammatory aspirin-triggered lipoxin 15*R*-epi-lipoxin A4 in the context of COX-2 induction in LPS-induced inflammation (Kirkby et al., 2013).

Other groups have reported that aspirin treatment could reduce lung inflammation following acid-inhalation (Zarbock et al., 2006), LPS inhalation and intravenous anti-MHC-I antibody treatment (Looney et al., 2009), and LPS inhalation (Ortiz-Muñoz et al., 2014; Tilgner et al., 2016). Further experiments in LPS models identified increases in the aspirin-triggered lipoxin 15*R*-epi-lipoxin-A4 acting through formyl peptide receptors 2 and/or 3 as a pathway mediating the anti-inflamamtory effects of aspirin, rather than the assumed TXA_2 (Ortiz-Muñoz et al., 2014).

The preclinincal work described above, combined with data from several observational clinical studies (Toner et al., 2015), has led to interventional studies measuring the effects of aspirin on inflammation following inhalational exposure to LPS in *ex vivo* blood-perfused human lungs and healthy volunteers, both of which showed an anti-inflamamtory effect of aspirin (Hamid et al., 2017), as well as a clinical trial of aspirin in prevention of ARDS in at-risk intensive care patients, in which aspirin had no detected effect (Kor et al., 2016b).

As previous work has suggested that reversible COX inhibition might reduce LPS-induced lung platelet recruitment as indomethacin reduced radiolabelled platelet recruitment to lungs of guinea pigs following LPS inhalation (Beijer et al., 1987), and LPS-induced lung platelet recruitment assessed by IHC was suggested to be greatly decreased with aspirin treatment in

mice (Ortiz-Muñoz et al., 2014), we sought to investigate the effect of aspirin on lung platelet recruitment and inflammatory readouts in a mouse LPS inhalation model.

1.3.3 Summary of aims and objectives

- Establish a mouse model of LPS inhalation in which platelet responses can be observed, and use:
    - Immunohistochemistry in order to image and quantify platelets in lungs.
    - Blood microsampling in order to monitor blood platelet counts over time.
    - Radiolabelled platelet tracking in order to study the fate of platelets across the body.
    - Intravital microscopy in order to measure platelet adhesion in lungs.
- Use human lung tissue from *ex vivo* blood-perfused lung experiments with intrabronchial LPS challenge for immunostaining to assess the potential for use of platelet immunostaining in the human setting.
- Use the mouse model of LPS inhalation to explore:
    - Whether there is any evidence for inflammation-induced platelet transendothelial migration.
    - Whether platelet recruitment to lungs following LPS inhalation is dependent upon neutrophils, using neutrophil depleting antibody treatment.
    - Whether platelet recruitment to lungs following LPS inhalation is dependent upon P-selectin or PSGL-1, using blocking antibody interventions.

- Whether platelet recruitment to lungs following LPS inhalation is dependent upon purinergic signalling through $P2Y_1$ or $P2Y_{12}$, or is sensitive to aspirin treatment, using pharmacological intervention.

2 Methods

2.1 Materials

2.1.1 Reagents and equipment

Table 2.1: List of reagents used for experiments and suppliers of the reagents.

Reagent	Supplier
$^{111}InCl_3$	Mallinckrodt, UK
2,2'-azino-bis(3-ethylbenzothiazoline-6-sulphonic acid (ABTS) solution	Roche/Sigma-Aldrich, UK
2-[4-(2-hydroxyethyl)piperazin-1-yl]ethanesulfonic acid (HEPES)	Sigma-Aldrich, UK
3,3'-Diaminobenzidine tetrahydrochloride hydrate (DAB)	Sigma-Aldrich, UK
ACD (Acid-citrate dextrose) anticoagulant	Sigma-Aldrich, UK
Acid-alcohol differentiation solution	Sigma-Aldrich, UK
Adenosine diphosphate (ADP)	Sigma-Aldrich, UK
Anti-CD41 (biotinylated) [MWReg30] antibody	Abcam, UK
Anti-CD41 [K-18] antibody	Santa Cruz Biotechnology, USA
Anti-CD41 [MWReg30] antibody	Abcam, UK
Anti-CD42b [SP219] antibody	Abcam, UK
Anti-DNA (peroxidase) [MCA-33] antibody	Roche/Sigma-Aldrich, UK
Anti-GPIbα (R300) (no azide) platelet depletion antibody	Emfret, Germany
Anti-histone H3 (citrulline R2 + R8 + R17) (ab5103, ChIP grade)	Abcam, UK
Anti-Ly6-G [1A8] antibody	BioXCell, USA

Anti-neutrophil elastase (polyclonal ab68672) antibody	Abcam, UK
Anti-P-selectin (no azide) [RB40.34] antibody	Becton Dickinson (BD), USA
Anti-PSGL-1 (no azide) [4RA10] antibody	BioXCell, USA
Anti-rabbit IgG (AlexaFluor488) antibody	ThermoFisher Scientific, UK
Anti-rabbit IgG (biotinylated) antibody	Vector Laboratories, USA
Anti-rat IgG (AlexaFluor594) antibody	ThermoFisher Scientific, UK
Anti-trinitrophenol (no azide) [2A3] monoclonal rat control IgG antibody	BioXCell, USA
AR-C 66096 tetrasodium salt	Tocris, UK
Aspirin	Sigma-Aldrich, UK
Bovine Serum Albumin (BSA), heat shock fraction, >98%	Sigma-Aldrich, UK
BSA standard solution 2mg/ml	ThermoFisher Scientific, UK
Cell death detection ELISA plus kit	Roche/Sigma-Aldrich, UK
D-Glucose	Sigma-Aldrich, UK
DPX mountant	Sigma-Aldrich, UK
Dulbecco's modified Eagle's meadium (DMEM)	Gibco, ThermoFisher Scientific, UK
DuoSet ELISA kit 96 well high-binding plate	R&D Systems, UK
DuoSet ELISA kit wash buffer concentrate	R&D Systems, UK
DusoSet ELISA kit reagent diluent concentrate	R&D Systems, UK
Ethylemediaminetertraacetic acid (EDTA)	Sigma-Aldrich, UK
Fluoromount G mountant	Southern Biotech, USA
Haematoxylin	Sigma-Aldrich, UK
Hoechst 33258	Sigma-Aldrich, UK
Hydrogen peroxide (30%)	Sigma-Aldrich, UK
Industrial ethanol	Sigma-Aldrich, UK
Isocare isoflurane anaesthetic	Baxter International, USA
KCl	Sigma-Aldrich, UK

Ketamine	Sigma-Aldrich, UK
Kwik Diff differental stain	ThermoFisher Scientific, UK
L-Glutamine	Gibco, ThermoFisher Scientific, UK
LPS (O111:B4, *E. coli*, prepared by phenol extraction)	Sigma-Aldrich, UK
LPS (O55:B5, *E. coli*, prepared by phenol extraction)	Sigma-Aldrich, UK
$MgCl_2$	Sigma-Aldrich, UK
MRS2500 tetraammonium salt	Tocris, UK
Na_2HPO_4	Sigma-Aldrich, UK
NaCl	Sigma-Aldrich, UK
$NaHCO_3$	Sigma-Aldrich, UK
NH_4Cl	Sigma-Aldrich, UK
Optimal Cutting Temperature (OCT) compound	VWR International, UK
Paraformaldehyde (37%)	Sigma-Aldrich, UK
PBS tablets	ThermoFisher Scientific Oxoid, UK
PGE_1	Sigma-Aldrich, UK
RM1(E) diet	Special Diets Services, UK
Stromatol platelet counting solution	Mascia Brunelli, Italy
Total protein BCA assay kit	ThermoFisher Scientific, UK
Tris(hydroxymethly)aminomethane (tris)	Sigma-Aldrich, UK
Tri-sodium citrate	Fisher Scientific, UK
Tropolone	Sigma-Aldrich, UK
Türk's solution	Merck Millipore, USA
Tween 20	Fisher Scientific, UK
Urethane	Sigma-Aldrich, UK
Vectastain Elite ABC HRP kit (Peroxidase, standard)	Vector Laboratories, USA
Xylazine	Sigma-Aldrich, UK

Table 2.2: List of equipment used for experiments and suppliers of the equipment.

Equipment	Supplier
LSRII Flow Cytometer	Becton Dickinson (BD), USA
Model OT Cryostat	Bright Instruments, UK
Liquid blocker (PAP pen)	Cosmo Bio, Japan
Single Point Extended Area Radiation (SPEAR) detector	eV Microelectronics (now i3 electronics), USA
Single edge razor blades	Fisher Scientific, UK
Incell Analyzer 6000 microscope system	GE Healthcare, USA
Minivent ventilator	Harvard Apparatus, UK
Neubauer improved haemocytometer	Hawksley, Sigma Life Sciences, UK
DM2000 LED bright field microscope	Leica Microsystems, UK
DFC295 bright field microscope camera	Leica Microsystems, UK
Leica RM2125 RT rotary microtome,	Leica Microsystems, UK
A1R multiphoton microscope	Nikon Instruments, USA
Tender Cooker microwave pressure cooker	Nordic Ware, USA
Amvex vacuum regulator	Ohio Medical, USA
Heated stage controller	Omega Engineering, USA
Genesis haematology analyzer	Oxford Science, USA
Mai Tai DeepSee infrared laser	Spectra Physics, USA
UCS30 spectrometer	Spectrum Techniques, USA
Intravital window 90° angle post clamp	Thor Labs, USA
Small animal recovery chamber	VetTech Solutions, UK
Superfrost plus slides	VWR International, UK
Compugamma gamma counter	Wallac (now LKB

Instruments/Perkin Elmer), UK

2.1.2 Buffer solutions

Aqueous buffers were made up in ultrapure deionised water and sterile filtered at 0.2 µm where required. Phosphate buffered saline (PBS) contained 137 mM NaCl, 3 mM KCl, 8 mM Na2HPO_4 and 1.5 mM KH_2PO_4 at pH 7.3 and was prepared in deionised water from tablets (Oxoid). Sterile filtered citrate-dextrose solution (ACD) was purchased ready-made and used as an anticoagulant for blood collection.

Calcium and Magnesium-free Tyrode's solution (CFTS) consisted of 134 mM NaCl, 2.7 mM KCl, 5.55 mM D-glucose, 11.9 mM $NaHCO_3$ and 0.21 mM Na_2HPO_4. CFTS was also mixed with (ACD) (9 volumes of CFTS with 1 volume of ACD) and supplemented with 2.5 µM of the platelet activation inhibitor, PGE_1 in order to produce Tyrode's-ACD-PGE_1 (TAP) buffer.

HEPES-buffered Tyrode's solution contained 20 mM 2-[4-(2-hydroxyethyl)piperazin-1-yl]ethanesulfonic acid (HEPES), 134 mM NaCl, 2.92 mM KCl, 12 mM $NaHCO_3$, 0.34 mM Na_2HPO_4 and 1 mM $MgCl_2$ with pH adjusted to 7.4.

For enzyme-linked immunosorbent assays, concentrates in DuoSet ancillary reagent kits (R&D Systems) were used to prepare ELISA reagent diluent (1% BSA in PBS) and ELISA wash buffer (0.05% vol/vol Tween 20 in PBS). Red blood cell lysis buffer was 155 mM NH_4Cl, 12 mM $NaHCO_3$ and 0.1 mM EDTA.

2.2 Animals

2.2.1 Wild type mice used at King's College London

Mice (Female, 6-12 weeks of age) used at King's College London were of the Balb/C strain from Charles River, housed in non-barrier facilities. Animals were given unlimited access to RM1(E) diet (Special Diets Services), and water. Animal experiments were conducted following local ethical approval and in accordance with the Animals (Scientific Procedures) Act, 1986 and amended regulations of 2012. Mice were monitored at least daily during experiments and if mice showed visible signs of sickness all animals in that experiment were provided with moistened food. Terminal anaesthesia was achieved using urethane (3 g/kg delivered i.p. in PBS) with euthanasia confirmed with exsanguination or cervical dislocation.

2.2.2 PF4-cre × mTmG mice used at UCSF

For experiments at University of California, San Francisco (UCSF), all experiments were approved and conducted by experimenters with training approved by the institutional animal care and use committee. Mice were bred in specific pathogen-free facilities at UCSF. PF4-cre × mTmG mice (Lefrançais et al., 2017) were generated from from crosses of PF4-cre mice (C57BL/6-Tg(Pf4-icre)Q3Rsko/J, Jackson), in which expression of the *Pf4* gene (encoding platelet factor-4 or CXCL4) drives the expression of Cre recombinase in cells committed to the megakaryocyte lineage (Tiedt et al., 2007; Pertuy et al., 2015), and mTmG mice (*Gt(ROSA)26Sor*$^{tm4(ACTB\text{-}tdTomato,\text{-}EGFP)Luo}$/J, Jackson), in which a membrane targeted tandem dimer of tomato fluorescent protein (Tomato, mT) is constitutively expressed, with the exception of cells expressing Cre recombinase, in which the Cre/*loxP* recombination system

turns off Tomato expression and activates expression of membrane-targeted enhanced green fluorescent protein (GFP, mG) (Muzumdar et al., 2007).

PF4-cre × mTmG mice were phenotyped by assaying an unstained submandibular blood microsample for GFP and Tomato fluorescent protein positivity using a BD LSR II flow cytometer at least 2 weeks before mice were used for further experiments (Figure 2.1). Male mice at 6-12 weeks of age were used for intravital microscopy experiments due to their larger size. Terminal anaesthesia was induced with 125 mg/kg ketamine combined with 12.5 mg/kg xylazine delivered i.p. in PBS.

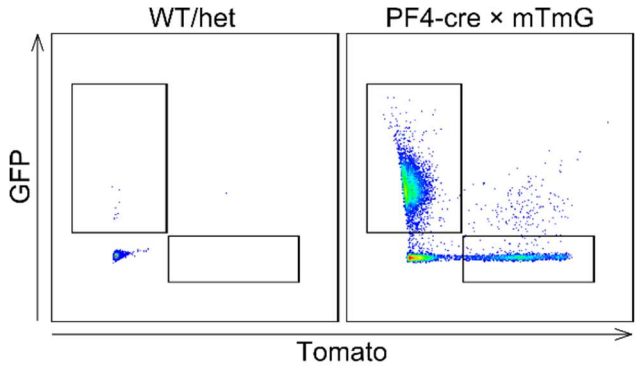

Figure 2.1: Phenotyping PF4-cre × mTmG mice. Left: flow cytometry density plot from blood sample from mouse with no *mTmG* phenotype and unknown *Pf4-cre* status, Right: density plot from sample from PF4-cre × mTmG mouse. GFP+Tomato- events are platelets or cells expressing PF4, GFP-Tomato+ events are cells with no PF4 expression, double positive events are platelet-leukocyte aggregates.

2.3 LPS challenge in mice

In order to provoke lung inflammation, mice were briefly anaesthetised with inhaled isoflurane, then challenged with LPS (from *E. coli*, O55:B5 serotype, prepared by phenol extraction), or PBS vehicle control, by intranasal delivery at 2 µl/g body weight using a 200 µl pipette tip to deposit the dose in the nostrils. Mice were held upright for 30 seconds after dosing and delivery was confirmed by audible chest crackling. This method has been shown to deliver ~55% of the prepared dose into the lower airways and lung (Southam et al., 2002; Su et al., 2004).

A dose of 5 mg/kg LPS was chosen based on the dose used previously with LPS-induced lung platelet recruitment reported (Ortiz-Muñoz et al., 2014). A lower dose of 0.05 mg/kg LPS was also tested but in preliminary studies this lower dose did not show significant lung platelet recruitment.

2.4 Immunohistochemistry studies

2.4.1 Collection of mouse lungs for histology

Mice were terminally anaesthetised, and the trachea was opened and the diaphragm was exposed and dissected along the ventral ribcage to collapse the lungs. A tracheal cannula was swiftly introduced and the lung was inflated with 0.5 ml of OCT (optical cutting temperature coumpound, VWR International) delivered over 2 seconds. The heart was then excised to stop circulation, left and right lung lobes were rapidly removed, cross-sectioned in half laterally, placed cut face down in plastic 15×15 mm moulds (VWR International), and surrounded with OCT. Samples were then snap frozen from the bottom up by placing on a lead heat sink which was cooled by partial immersion in liquid nitrogen. Samples were then stored at -80 °C until required for use.

2.4.2 Human ex vivo blood-perfused lungs

Formalin-fixed paraffin embedded human lung samples generated from the work of Hamid *et al.,* (2017) were generously provided by Dr. Cecilia O'Kane, Queen's University Belfast, and were used for experiments testing the effect of aspirin treatment on LPS intralobar instillation in isolated human lung preparations using a method adapted from that previously reported by Lee *et al.,* (2009).

Briefly, human lungs were obtained with donor consent given to International Institute for the Advancement of Medicine and local ethics board approval at Queen's University Belfast. *Ex vivo* human lung experiments were carried out at Queen's University Belfast. Lungs were free of exterior contusions, had no air leak on ventilation, and were collected under

aseptic conditions 0-60 minutes from cessation of blood circulation, and used within 48 hours of collection. Upon arrival at Queen's University Belfast, the pulmonary artery was connected to a peristaltic pump and a bronchus intubated, and the lungs suspended inside sealed acrylic container. Lungs were rewarmed by perfusion with DMEM containing L-glutamine and 5% albumin for 1 hour until at 35 °C, and then ventilated with 95% O_2 + 5% CO_2 with 10 cmH_2O continuous positive airway pressure. Normal alveolar fluid clearance (>10% concentration of protein in a 125 ml PBS + 5% albumin instillation within 1 hour) was confirmed before lungs were used.

To induce inflammation LPS (6 mg of O111:B4 from *E. coli* in 10 ml 0.9% saline + 5% albumin) was introduced into the right middle lobe or left lower lobe, and 100 ml of whole blood (treated *ex vivo* with vehicle or 24 mg aspirin 1 hour previously), from a healthy volunteer was added 1:10 to the perfusate. At 4 hours after LPS exposure, BAL was collected, and samples from the LPS-challenged lobe were fixed in formalin before routine dehydration and paraffin embedding.

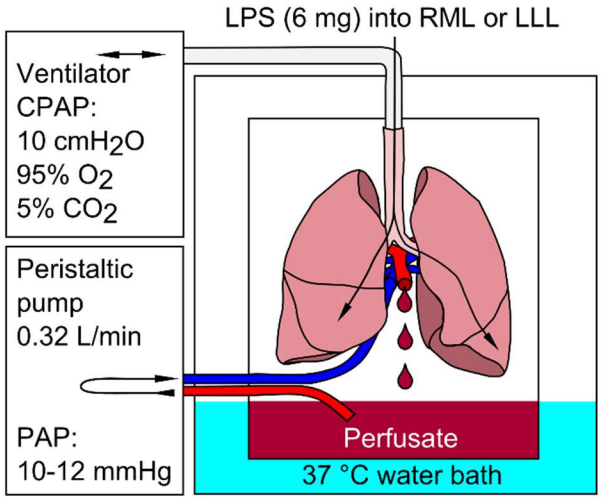

Figure 2.2: Isolated blood-perfused human lungs. Human donor lungs were ventilated with 10 cmH_2O continuous positive airway pressure (CPAP), and perfused with blood 1:10 in DMEM+L-Glutamine and 5% albumin. Pulmonary arterial pressure (PAP) was maintained at 10-12 mmHg, and blood was allowed to flow freely from the pulmonary vein into the perfusate reservoir before recirculation. LPS was instilled by intralobar instillation into either the right middle lobe or left lower lobe. Diagram based on Lee et al., (2009).

2.4.3 Frozen sections

Frozen 10 µm cross-sections of tissue (6-9 per mouse) were made using a Bright Model OT cryostat and thaw-mounted onto superfrost plus slides then air dried overnight in a fume hood.

2.4.4 Paraffin wax sections

Sections of formalin-fixed paraffin-embedded tissue (9 per human lung lobe) were sectioned at 6µm thickness using a Leica RM2125 RT rotary microtome, and mounted using a water bath onto superfrost plus slides before overnight drying in a fume hood.

2.4.5 Immunohistochemistry using DAB reporter

Dried frozen sections were immersed in 4% vol/vol paraformaldehyde in PBS and fixed for 15 minutes. Following a tap water wash, endogenous peroxidase activity was blocked by immersion in 3% vol/vol hydrogen peroxide in ethanol (99% industrial grade), which also served to bleach endogenous pigment. Slides were then washed with PBS before nonspecific binding was blocked with 1% BSA in PBS for 10 minutes. The reagent diluent for primary and secondary antibodies as well as the avidin-biotinylated HRP complex (ABC) was also 1% w/vol BSA in PBS. Primary antibodies were incubated with the sample for 2 hours at room temperature. Because future experimental plans involved giving mice depleting, blocking, or control antibodies raised in cells from rats, platelet staining methods not reliant on anti-rat IgG reporters were sought and IHC preparations tested for minimal cross-reactivity with rat antibodies. Primary antibody details are listed in Table 2.3.

Table 2.3: Antibodies used for immunohistochemistry experiments in mouse tissue.

Target	Catalogue #	Clonality	Clone	Host	Dilution factor
CD41	ab33661	Monoclonal	MWReg30	Rat	1/500
CD41 (biotin)	ab95727	Monoclonal	MWReg30	Rat	1/250
CD42b	ab183345	Monoclonal	SP219	Rabbit	1/200
Neutrophil elastase	ab68672	Polyclonal	n/a	Rabbit	1/50

Formalin-fixed paraffin embedded human lung sections were stained using similar methods, but were first dewaxed in xylenes, rehydrated, endogenous peroxides blocked as described above, and subjected to heat-induced epitope retrieval carried out with 10 mM tri-sodium citrate with 0.05% vol/vol Tween 20 at Ph 6.0, 100 °C using a microwave pressure cooker.

Slides were then cooled with tap water, then blocked with 1% BSA in PBS and then incubated with primary antibodies as described above. Antibody titrations are listed in Table 2.4.

Table 2.4: Antibodies used for immunohistochemistry experiments in human tissue.

Target	Catalogue #	Clonality	Clone	Host	Dilution factor
CD41	sc-6604	Polyclonal	K-18	Goat	1/500
CD42b	ab183345	Monoclonal	SP219	Rabbit	1/250
Neutrophil elastase	ab68672	Polyclonal	n/a	Rabbit	1/100

Following a PBS wash, samples incubated with rabbit primary antibodies were incubated with biotinylated anti-rabbit IgG (1:200, Vector), samples incubated with goat primary antibodies were incubated with biotinylated anti-sheep IgG 50% cross reactive with goat IgG (1:200, Vector). After 1 hour, sections were washed again and incubated for 1 hour with avidin and biotinylated HRP (Vector, PK1600 components A and B mixed to form ABC both at 1:200 at 30 minutes before use). For samples stained with biotinylated primary antibodies, the secondary antibody incubation step was omitted. After a final PBS wash slides were then developed in 1.2 mM DAB (3,3-diaminobenzidine tetrahydrochloride) in 0.1 M Tris buffer (pH 7.6) also containing 0.03% vol/vol hydrogen peroxide substrate for 10 minutes.

Developed slides were then rinsed in tap water, counterstained with Gill's no. 2 haematoxylin which was differentiated by 10× immersions of ~1 s duration in acid alcohol before dehydration with industrial ethanol, clearing with xylenes and coverslipping with DPX

mountant. Fidelity of staining is shown across serial sections in Figure 2.3 (mouse) and Figure 2.4 (human).

In a blinded fashion, 6× fields of 447×596 µm of the respiratory portion of lung were captured across each section, with 6 sections collected per mouse, using a 20× objective on a Leica DM 2000 LED bright field microscope with Leica DFC295 camera and Leica Application Suite acquisition software v4.4.

Separate blinded analyses were also conducted on the same microscope using a 63× objective to capture 50 image fields of 189×142 µm of fields of the respiratory portion of the lung from each mouse in order to enable the imaging of platelets which appeared outside of the pulmonary circulation in the bronchoalveolar space. These platelets which were spatially dis-associated with the pulmonary circulation were manually counted by an independent operator.

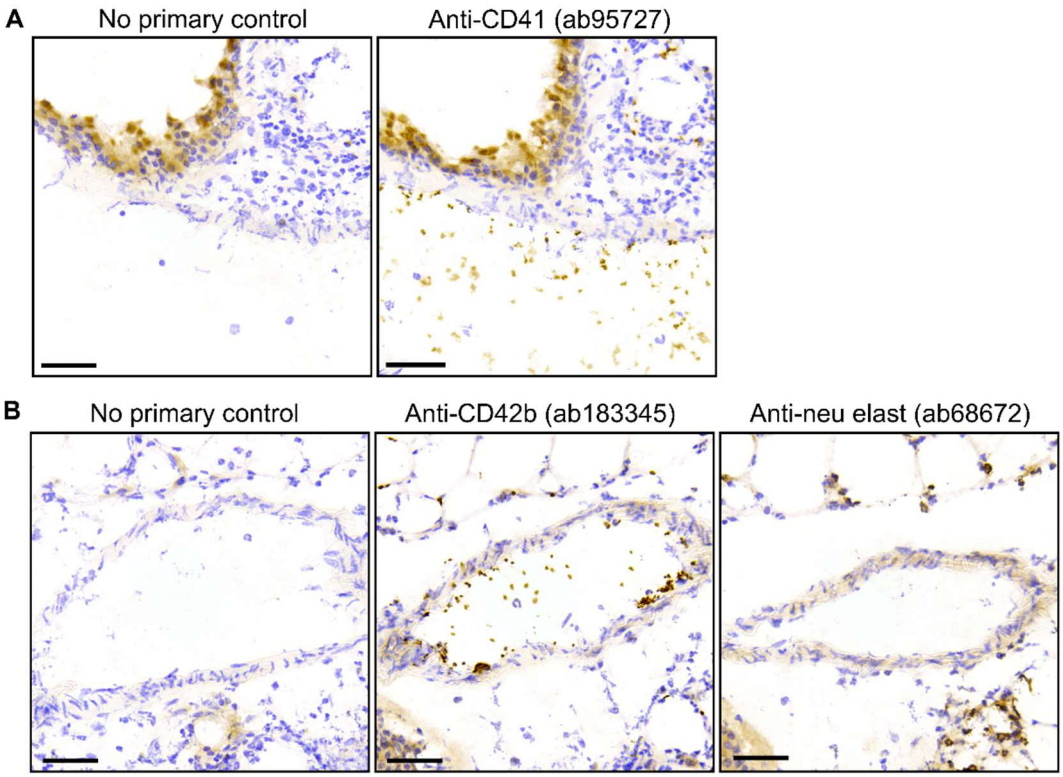

Figure 2.3: Mouse lung immunohistochemistry using DAB reporter. Serial sections from LPS-challenged mouse lungs incubated with or without primary antibodies were compared to assess fidelity of immunostaining. DAB reporter positivity in brown, haematoxylin counterstain in blue. (A) CD41 staining using biotinylated rat primary antibody. Single platelets are visible in blood vessel (bottom), false positive staining on respiratory epithelium (top left). (B) CD42b and neutrophil elastase staining using rabbit primary antibodies. CD42b+ platelets are visible in the blood vessel in centre field, neutrophil elastase positivity can be seen in the alveolar-capillary network surrounding. Scale bar = 20 µm.

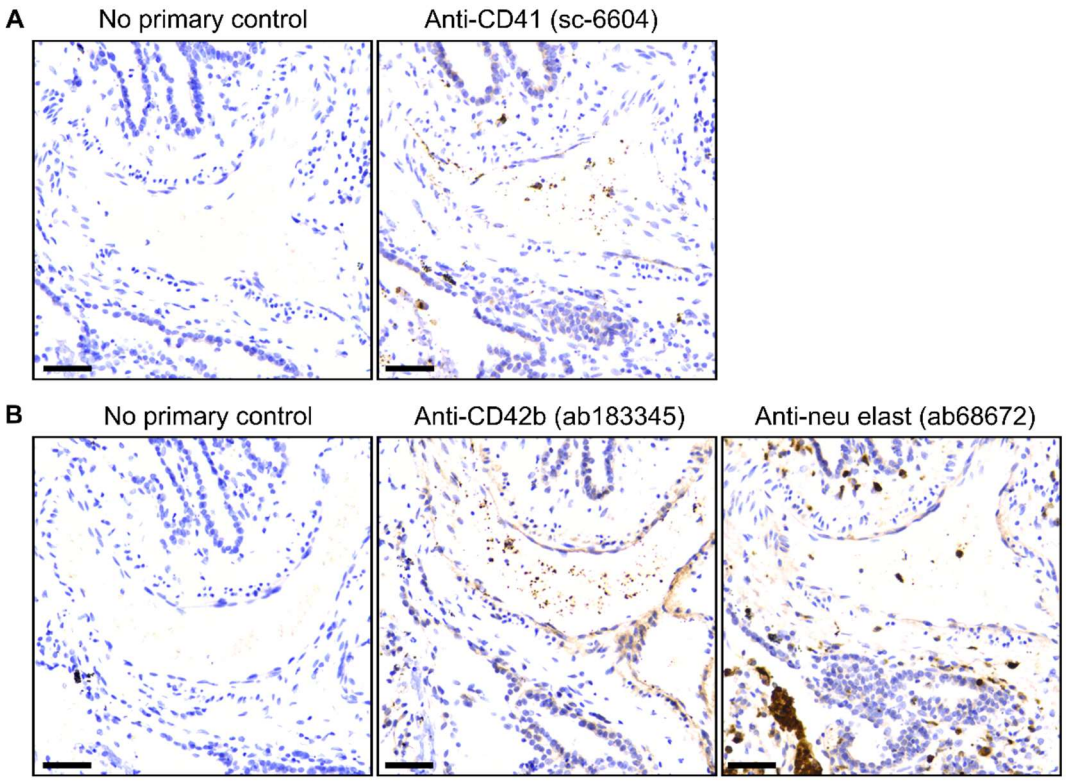

Figure 2.4: Human lung immunohistochemistry using DAB reporter. Serial sections from LPS-challenged human lungs incubated with or without primary antibodies were compared to assess fidelity of immunostaining. DAB reporter positivity in brown, haematoxylin counterstain in blue. (A) CD41 staining using goat primary antibody. CD41+ platelets are visible in blood vessel (centre). (B) CD42b and neutrophil elastase staining using rabbit primary antibodies. CD42b+ platelets are visible in the blood vessel in centre field, neutrophil elastase positivity can be seen in the blood vessel and in the neighbouring airway wall and alveolar-capillary units. Scale bar = 20 µm.

2.4.6 Immunohistochemistry using fluorescent reporters

For immunofluorescence experiments, lungs were sectioned, and sections were dried and fixed as described above. After blocking non-specific binding for 10 minutes using 1% BSA in PBS, rat anti-mouse CD41 primary antibody and rabbit anti-mouse/human neutrophil elastase primary antibody (Table 1) were coincubated with the sample in 1% BSA in PBS. Following a PBS wash, anti-mouse IgG conjugated to the fluorophore AlexaFluor 594 (1:500), anti-rabbit IgG conjugated to the fluorophore AlexaFluor 488 (1:500) and Hoechst 33258

DNA stain (1:20,000) were incubated together on the sample in 1% BSA in PBS for 1 hour before a final PBS wash. Slides were then coverslipped using Fluoromount G mountant and stored in the dark at 4°C for up to a week before imaging.

Fluorescence micrographs (Figure 2.5) were captured using an Incell Analyser 6000 system (GE Healthcare) with 20× objective, open aperture, excitation/emission wavelength filter sets for AlexaFluor 595: 561/605nm, Alexafluor 488: 488/525nm and Hoechst 33258: 405/455nm. Image fields were 665.6×665.6µm. Tiled acquisition was used with 15% overlap for stitching and both IR laser autofocus on the slide/section interface and software autofocus on the Hoechst channel to maintain focus whilst tiling across the entire section. Fidelity of staining in serial sections is shown in Figure 2.5.

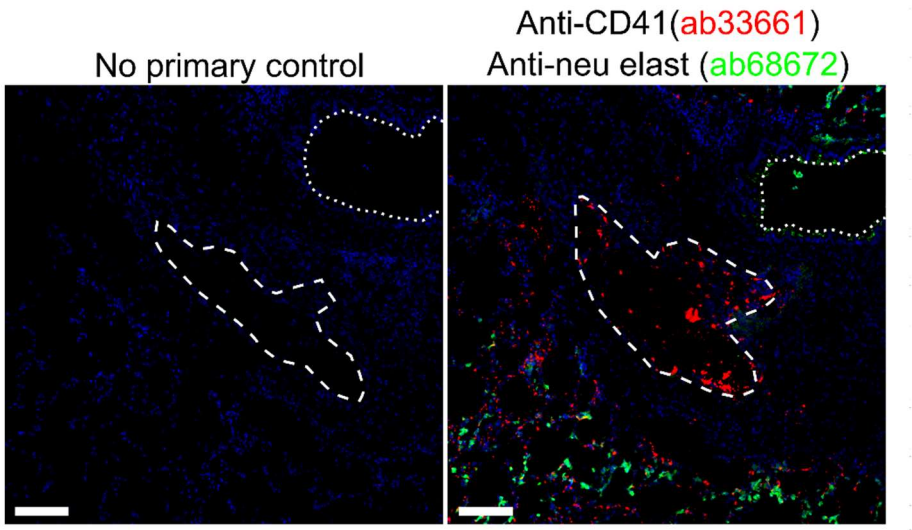

Figure 2.5: Mouse lung immunohistochemistry using fluorescent reporters. (A) Diagram showing indirect staining method used for fluorescence microscopy studies into CD41 and neutrophil elastase tissue distribution. (B) Serial sections from an inflamed lung showing a pulmonary blood vessel (centre, dashed white line for emphasis) with alveolar-capillary network (bottom left) and small airway (top right, dotted white line for emphasis). CD41 is shown as red, neutrophil elastase is in green and nuclei are shown as blue. Scale bar = 20µm.

2.4.7 Image analysis

Macros for automated platelet counting were developed using ImageJ 1.48 (National Institutes of Health).[5] The colour deconvolution plugin produced by G. Landini, University of Birmingham,[6] was used to split the brown DAB stain and blue haematoxylin stain from RGB images into separate greyscale images (Figure 2.6), as previously described (Ruifrok and Johnston, 2001), and positive staining was defined using an intensity threshold based on no primary control and positively stained sections (typically intensities >150 out of 255 on an 8 bit depth). For platelet counts a size filter was used to remove objects smaller than 0.45 μm^2.

The ImageJ particle analysis module was then used to count the number of platelets per mm^2 of section imaged as well as the percentage of sample covered by positive staining. During inflammation, neutrophil elastase is released from neutrophils, and neutrophils form bundles during transendothelial migration, so cell segmentation was not used and this antigen was quantified using only percentage of sample fields stained positive.

[5] ImageJ, NIH: https://imagej.nih.gov/ij/
[6] Colour deconvolution: http://www.mecourse.com/landinig/software/cdeconv/cdeconv.html

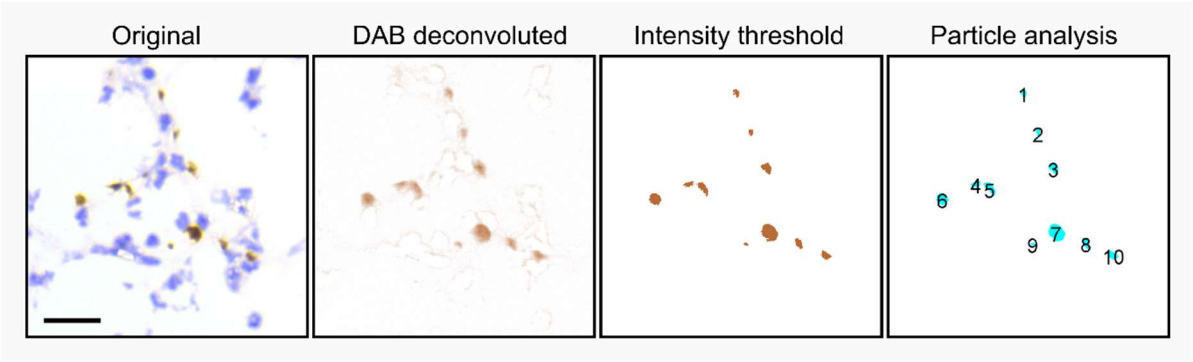

Figure 2.6: Counting platelets with ImageJ using colour deconvolution and particle analysis. Original RGB colour images with CD41 staining in brown and haematoxylin staining in blue were deconvoluted to split our the colour channels corresponding to DAB staining in a separate greyscale image. An intensity threshold was then set on the greyscale image to define areas of positivity. Particle analysis was then used to count platelet sized objects. Scale bar = 20µm.

CD41+ platelets and neutrophil elastase coverage was also quantified in fluorescence micrographs of mouse lungs using ImageJ with similar methods, although for these images colour deconvolution was not required as channels were already separate. CD41+ bodies with proplatelet morphology were counted following identification by size (>55 µm^2) and circularity (circularity = $4\pi(\frac{area}{perimeter^2})$ = <0.5, where 1.0 is a perfect circle).

For counting rarer events in lungs, such CD41+ platelets inside of airways, and cells with CD41+ cytoplasm surrounding a large nucleus,, whole lung section stitches were prepared for manual inspection using the ImageJ Grid/Collection stitching plugin produced by S. Preibisch, Max Delbrück Center (Preibisch et al., 2009)[7].

[7] Example zoomable stitched images produced using the GMap Cutter tool (Centre for Advanced Spatial Analysis, UCL, and Google Maps), used for surveying whole lung sections, are

Spatial association of platelet CD41 immunostaining with neutrophil elastase was investigated using the relate objects module of CellProfiler to make separate counts of CD41+ platelets with any overlap with neutrophil elastase staining and those that did not.[8]

2.4.8 Blood microsampling

Mice were placed in a heated chamber (37 °C) for 10 minutes before relocation to a custom-made box which exposed only the tail. A 1-2 mm cut was made with a scalpel blade across the lateral tail vein. Using a micropipette, 2 µl of blood was rapidly diluted 1:100 into stromatol solution for platelet counts, a further 2 µl diluted 1:50 in Türk's solution for leukocyte counts (both using a Neubauer improved haemocytometer), and 4 µl was taken for a blood smear stained with Kwik-Diff modified Romanowsky stain to be used for leukocyte differential counts (200 cells identified per smear).

Gentle pressure was applied to the cut until cessation of bleeding and any future serial samples were taken from alternate sides of the tail at sites further upstream of veins relative to previous cuts (towards the end of the tail, care was taken to avoid damaging the central tail artery). Manual counts were made with the experimenter blinded to identity of samples within treatment groups.

---

privately hosted at http://bit.do/PBSlung and http://bit.do/LPSlung. CD41=red, Neutrophil elastase=green, Nuclei=blue.

[8] CellProfiler cell image analysis software, Broad Institute, http://cellprofiler.org.

2.5 Radiolabelled platelet studies

2.5.1 Radiolabelling platelets with ^{111}In-tropolonate

Platelets were labelled using a technique adapted from previously reported experiments labelling mouse platelets with ^{111}In-oxine (Tymvios et al., 2008; Moore et al., 2011; Solomon et al., 2013; Smyth et al., 2015). With the number of donor mice equal to the number of recipients, blood was collected by cardiac puncture from terminally anaesthetised donor mice into a syringe containing 0.2 ml of ACD using a 26 gauge needle.

After gentle mixing, blood samples were centrifuged at 300 rcf for 3 minutes and the resulting supernatant (platelet-rich plasma, PRP) was collected. Remaining blood was then gently mixed with 0.4 ml of TAP buffer in order to prevent platelet activation, and centrifuged again at 300 rcf for 3 minutes for collection of further PRP. Pooled PRP was then centrifuged at 200 rcf for 2 minutes to sediment out any contaminating erythrocytes and leukocytes, and the purified PRP separated. Purified PRP was then centrifuged at 1500 rcf for 7 minutes, supernatant removed and the platelet pellets resuspended together in 600 µl TAP buffer for every 4 mice used. A 2 µl sample was taken for dilution in 198 µl Stromatol for platelet counts.

Pooled platelet suspensions from every batch of 4 donor mice (with a platelet density of $6.12 \pm 0.88 \times 10^8$ platelets/ml) were then added to a mixture of a volume of containing 1.8 MBq $^{111}InCl_3$ in sterile 0.9% w/vol NaCl (Mallinckrodt, UCL Hospital *via* the Radiopharmacy Department, Guy's and St Thomas' Hospitals Trust) which was mixed 5 minutes earlier with one-fifth volume of 90 mM tropolone in HEPES-buffered Tyrode's solution in order to pro-

duce lipophilic ^{111}In-(tropolone)$_3$ complexes which can penetrate cell membranes and dissociate inside cells, with cytoplasmic retention of ^{111}In, but not free tropolone, leading to the cytoplasmic accumulation of ^{111}In (Dewanjee et al., 1982). Similar labelling and chelation methods are used clinically for imaging sites of platelet sequestration and clearance in patients with idiopathic thrombocytic purpura (Cuker and Cines, 2010; McKiddie et al., 2016), and ^{111}In is retained in platelets after degranulation and aggregation (Thakur et al., 1981).

Platelets were incubated with ^{111}In at room temperature for 10 minutes and during this time, a single point extended area radiation (SPEAR) gamma detector containing a CdZnTe 5×5×5 mm^3 detector crystal, with a UCS30 spectrometer powered by USX 1.2 software was calibrated to record photon energies from decay of ^{111}In (Figure 2.7A). This gamma detector was then used to measure radioactivity of the sample during labelling. The platelet suspension was centrifuged again at 1500 rcf for 7 minutes. Radioactive supernatant was removed and the platelet pellet resuspended in a volume of CFTS equivalent to the volume of platelets plus the volume of $InCl_3$ solution and volume of tropolone solution used that day in order to measure retained radioactivity to calculate labelling efficiency ($\frac{retained\ radioactivity}{labelling\ radioactivity} \times 100 =$ 62±5%).

The volume of the platelet suspension was then adjusted to 200 µl per recipient plus 38 µl per recipient of syringe dead space allowance, and after 45 minutes of time allowed for of the biological effects of PGE_1 to diminish, recipient mice were each infused with 200 µl bolus injection of the ^{111}In-labelled platelets *via* a lateral tail vein. Assuming 100% recovery of platelets after the wash step, and accounting for syringe dead space, mice each received an estimated 2.75±0.30 $\times 10^8$ platelets labelled with 0.24±.02 MBq ^{111}In.

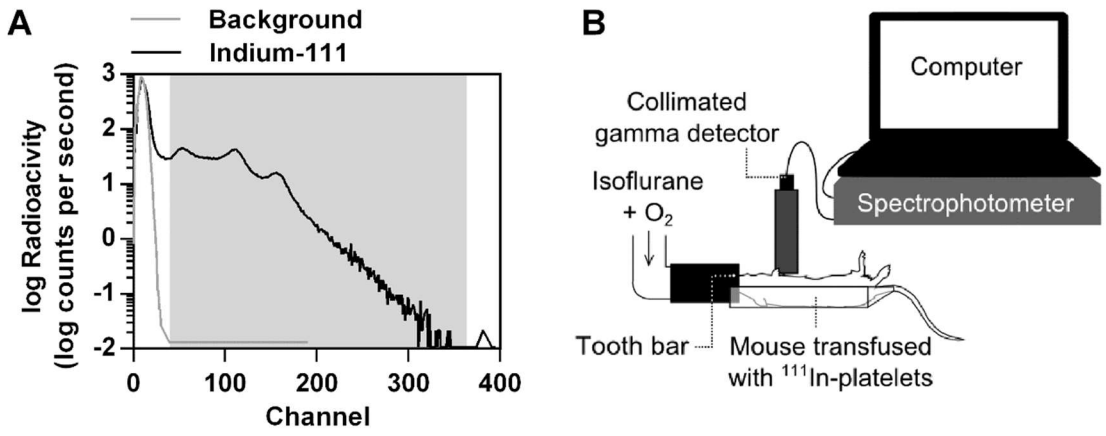

Figure 2.7: Measuring ^{111}In signal using SPEAR probes. (A) Energy spectra from background signal (grey line) and signal from ^{111}In (black line). Peaks arise from ^{111}In decay photon energies at 23, 171 and 245 keV but due to unavailability of reference radionuclides x axis units are given as uncalibrated channels (arbitrary units on a bit depth of 1024). In order to exclude background and maximise signal from ^{111}In, lower and upper energy limits were set so that only photon energies in the grey shaded region were recorded. (B) Mice transfused with ^{111}In-labelled platelets were anaesthetised using isoflurane, with repeated recordings made over the same region of thorax by clamping a gamma detector at a fixed position relative to a tooth bar and custom cradle attached to the isoflurane mask. Signal from the gamma detector was deconvoluted using a UCS30 spectrophotometer and data logged on a computer running USX software.

2.5.2 Non-invasive radiolabelled platelet tracking

After 1 hour had elapsed following injection of radiolabelled platelets, noninvasive recordings of thoracic radioactivity were made in terminally anaesthetised mice. Successful measurement of the extent of thromboembolism was confirmed by measuring responses to 4 mg/kg ADP i.v. in PBS. For experiments over 4 to 48 hours, sample recordings over 5 minutes were made under isoflurane anaesthesia using the equipment described in Figure 2.7B. These measurements were then repeated at later intervals for noninvasive monitoring of thoracic platelet content over time.

2.5.3 Platelet biodistribution studies

In order to track the fate of radiolabelled platelets, 2 µl of the radiolabelled platelet suspension was collected before intravenous injections (1% of injected dose) and stored diluted in PBS. At +4 or +48 hours after intranasal challenge, mice transfused with radiolabelled platelets were terminally anaesthetised, and 100 µl of whole blood was collected by cardiac puncture and diluted in 400 µl PBS. Bronchoalveolar lavage (BAL, 3x separate washes and recoveries of 0.5 ml PBS through a tracheal cannula, pooled) was then collected, and lung, liver and spleen were collected into scintillation vials after removal of exterior clots by rolling the organ surface on guaze.

BAL was divided into cell pellet and supernatant by centrifugation of 750 µl of neat BAL at 1500 rcf for 7 min and collection of resultant supernatant and cell pellet resuspended in 750 µl PBS in scintillation vials. In order to confirm an inflammatory response in lungs, BAL was also used to measure total leukocyte counts (50 µl BAL in 50 µl Türk's solution counted using haemocytometer), and BAL leukocyte differential counts using BAL cytospin preparations (50 µl BAL in 50 µl PBS, 113 rcf for 1 minute using Cytospin 2, ThermoFisher Scientific), stained with KwikDiff (ThermoFisher Scientific).

Blood, BAL, organ, 1% injected dose, and blank controls were then analysed in scintillation vials using a Compugamma gamma counter (LKB Wallac) to record gamma radiation emitted from each sample over 1 minute. Blood radioactivity was expressed as percentage of injected dose per ml, and BAL and organ radioactivity is expressed as percentage of injected dose recovered in BAL or per organ, divided by percentage of dose per ml of blood, as previously described (Andonegui et al., 2005; Looney et al., 2009).

2.6 Intravital microscopy

2.6.1 Preparation of mice for intravital microscopy

At 48 hours after PBS or LPS (5 mg/kg) inhalation PF4-cre × mTmG mice were terminally anaesthetised. The dorsal left ribcage was shaved and the trachea cannulated and the mouse moved onto a Mini Vent ventilator with isoflurane and oxygen supplied at 130× 250 µl breaths per minute with 2 cmH_2O of positive end expiratory pressure.

Mice were then moved onto a heated stage at 37 °C and were given 0.5 ml of PBS i.p. as fluid support. Skin over the shaved region was removed to expose the ribcage, and an approximately 1 cm long intercostal incision was carefully made to expose the ventilated left lung and allow the surface of the visceral pleura to fall away from the parietal pleura.

As previously reported (Looney et al., 2011; Headley et al., 2016), a custom-made thoracic window (Figure 2.8) was then inserted to sit between two ribs, secured onto a 90° angle post clamp attached to the stage and ~4 kPa negative pressure was applied between the visceral pleura of the lung and the inner surface of the window using an Amvex vacuum regulator in order to immobilise the lung, and to remove air from the pleural cavity.

2.6.2 Intravital multiphoton microscopy

After around 10 minutes of stabilisation, the lung was brought into focus on a customised Nikon A1R multiphoton microscope coupled with a MaiTai DeepSee infrared excitation laser tuned to 920 nm for simultaneous excitation of GFP and tomato excitation, using a 20× Nikon water immersion objective, and emission filters set for Tomato at 570-620 nm and for

GFP at 500-550 nm. Image capture was controlled using NIS Element AR software with high resolution Galvano scanning over 512×512 pixels.

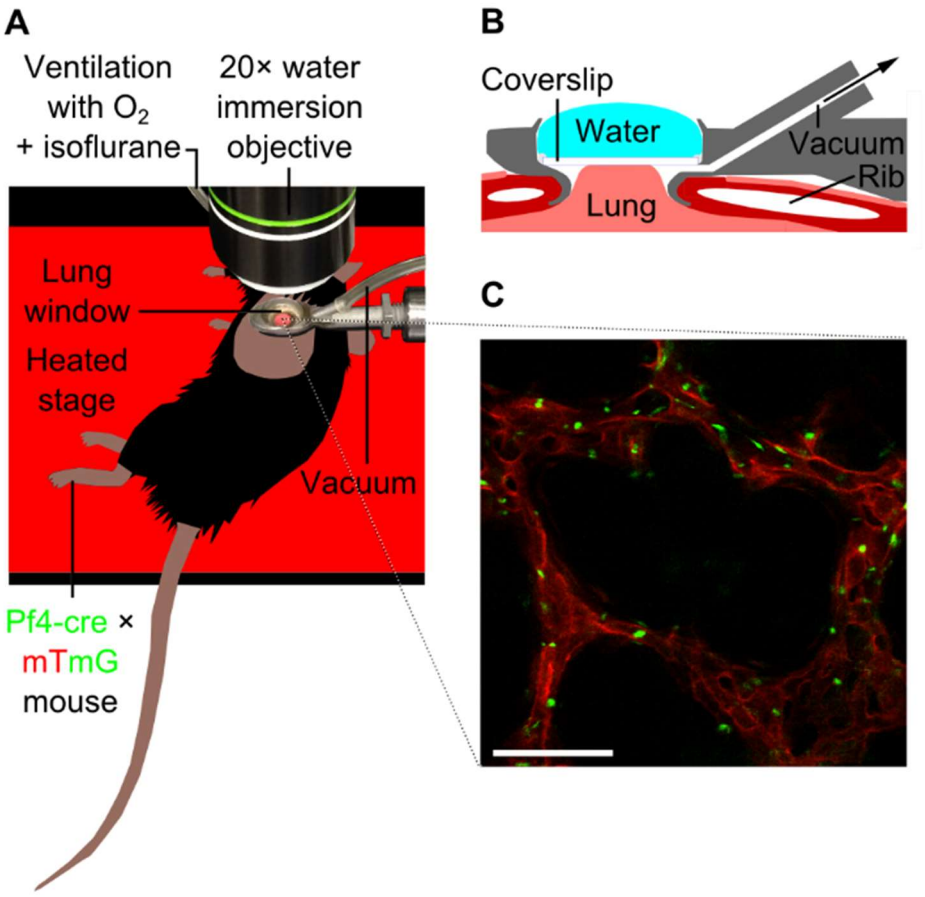

Figure 2.8: Intravital multiphon microscopy setup. (A) diagram showing positioning of Pf4 ×mTmG mouse, microscope objective and window for intravital imaging. (B) Cross section of the implanted thoracic window showing lung immobilisation method. (C) Micrograph of a field of Pf4-cre × mTmG mouse lung from the intravital multiphoton microscope showing Tomato+ lung cells (red) and GFP+ platelets (green). Scale bar = 50µm.

The internal surface of the final generation of alveoli, a densely networked capillary bed, was brought into focus and then using a Z-drive the imaging plane was moved 10 µm deeper into the lung to establish an imaging plane of at a consistent depth into the lung. Video recordings at the maximum speed possible using Galvano scanning (0.91 frames per second)

were then made in order to produce datasets where platelets adhesive in the lung microvasculature could be quantified. For each mouse, 8× videos of 230×230 µm fields with a duration of 5 minutes were sampled at different sites across the window.

In order to confirm inflammatory response in mice used for imaging, BAL was collected after sacrifice (3× washes of the same 1 ml volume of PBS with 5 mM EDTA) and leukocytes in this sample automatically counted using a haematology analyser system (Genesis).

2.6.3 Platelet adhesion tracking for analysis of intravital microscopy

Videos were analysed using NIS Elements 4.5 (Nikon). An intensity threshold, with size filters set to remove events smaller than 0.1 µm^2 in order to reduce noise, was set to binarise platelet events in each image. The NIS tracking module was then used to match events over time, tracking adhesive platelets which had a between-frame speed of less than 2 µm per second and a position in neighbouring frames less than 5 standard deviations (SD) away from between-frame positions predicted using a random motion model.[9]

[9]A video demonstrating the intravital microscopy platelet adhesion tracking method is hosted at http://bit.do/intravital

2.7 Antibody and anti-platelet drug treatments

2.7.1 Neutrophil depletion.

Neutrophil depletion was achieved with three intraperitoneal doses of 1A8 monoclonal anti-Ly6-G antibody (BioXCell BE0075-1) at 25 mg/kg in 200 µl PBS at -24, -1 and +24 hours relative to intranasal challenge with route of administration and dose based on previously reported work (Daley et al., 2008). Depleted animals were compared against animals treated with equivalent dose of control IgG (either Chrompure polyclonal rat IgG, Jackson, or monoclonal 2A3 anti-trinitrophenol, BioXCell). Clearance of neutrophils following exposure to 1A8 is mediated by macrophage/monocytes (Bruhn et al., 2016), and the 1A8 clone is selective for the Ly6-G epitope and does not deplete Ly6C+ inflammatory monocytes which are depleted with neutrophils by the [Gr-1] monoclonal antibody that has been used for neutrophil depletion in previously reported studies (Daley et al., 2008). Tail blood microsamples were made immediately before doses of antibodies were given in order to test if blood neutrophil counts were recovering before further doses of anti-Ly6-G antibody were given.

2.7.2 Blocking P-selectin and PSGL-1 function.

Mice were treated with no-azide, low-endotoxin antibodies for experimental blockade of adhesion molecule function, either anti-P-selectin monoclonal antibody (clone [RB40.34], BD Biosciences), and an anti-PSGL-1 monoclonal antibody (clone [4RA10] BioXCell), compared against clone [2A3] control rat IgG raised against trinitrophenol (BioXCell). Doses were given at 4 mg/kg i.v. in PBS at -1 and +24 hours relative to intranasal LPS challenge and with dose and frequency selected based on previously published work from our laboratory in a

mouse LPS inhalation model (Kornerup et al., 2010), and further supported by reports using other models showing efficacy at similar doses (Bosse and Vestweber, 1994; Phillips et al., 2003; Zanardo et al., 2004; Sreeramkumar et al., 2014; Biswas et al., 2015).

2.7.3 Anti-platelet drug dosing

Dosage of the purinergic antagonists used to suppress $P2Y_1$ receptor (MRS2500) or $P2Y_{12}$ receptor (AR-C 66096) function (both 3 mg/kg i.v. in 100 µl PBS at -1 and +24 hours relative to intranasal challenge) and of aspirin to inhibit cycoloxygenase activity (100 mg/kg i.p. in 200 µl 2% vol/vol DMSO in PBS at -1 and +24 hours relative to intranasal challenge) was based on those successfully used for reducing inflammatory responses or for causing increased bleeding time in similar mouse models (Ortiz-Muñoz et al., 2014; Amison et al., 2015, 2017). In order to reduce the number of mice required to carry out experiments, aspirin-treated mice also received intravenous PBS vehicle, and MRS2500 and AR-C 66096 treated mice were given 2% vol/vol DMSO in PBS vehicle i.p., with PBS and LPS vehicle control mice receiving vehicles by both routes.

2.7.4 Platelet depletion

Blood platelets were depleted by the intravenous administration of 1 mg/kg anti-GP1bα antibodies (R300, Emfret), a proprietary mixture of two monoclonal anti-GP1bα antibodies ([p0p3] and [p0p4]) which have previously been shown to cause profound platelet depletion within 1 hour of dosing lasting between 24 and 48 hours (Bergmeier et al., 2000; Nieswandt et al., 2000). Platelet depleted mice were compared to control mice receiving 1 mg/kg control

IgG (BioXCell [2A3]). Depletion over 48 hours was ensured by dosing at -1 and +24 hours relative to intranasal challenge.

2.8 Analysis of protein, NETs and red blood cell content of BAL

2.8.1 Total protein assay

Protein in supernatant from neat BAL supernatant samples (25 µl, prepared by centrifugation of whole BAL at 1500 rcf for 7 minutes) was quantified using the bicinchoninic acid (BCA) assay (Smith et al., 1985), using serial dilutions of a 2 mg/ml BSA standard in PBS as a reference according to the protocol provided by the manufacturer (ThemoFisher Scientific Pierce BCA assay kit). Samples were incubated with 200 µl of reagent diluent (reagants A:B 50:1) for 20 minutes at room temperature, then an absorbance plate reader was used to measure at 562 nm. Background values were subtracted and experimental samples were interpolated against dilutions of the BSA standard using a 4-parameter logistic curve fit.[10]

2.8.2 PF4 ELISA

Platelet factor-4 (PF4, CXCL4) was quantified using the DuoSet DY595 mouse PF4 ELISA kit (R&D Systems). For ELISA analysis, blood plasma was prepared by centrifugation of ACD-anticoagulated blood at 1500 rcf for 7 minutes for collection of plasma supernatant, BAL supernatant was collected from BAL using the same centrifugation method, and samples were stored at -80 °C.

PF4 ELISAs were carried out according to instructions on the kit. High-binding plates were coated at room temperature overnight with capture antibody, plates were washed (3

[10] Curve fitting for total protein and ELISA assays was carried out using the MyAssays Ltd 4-parameter logistic fit tool: http://www.myassays.com

times with 200 µl ELISA wash buffer), plates were blocked with addition of reagent diluent for 1 hour, washed again before addition of appropriately diluted experimental samples and recombinant PF4 standards which were incubated on plates for 2 hours. Plates were then washed again, biotinylated detection antibody added for 1 hour, followed by a further wash, addition of streptavidin-HRP for 1 hour, a final wash and development with 100 µl of the kit tetramethylbenzidine substrate solution for 20 minutes. The reaction was then stopped with 50 µl 2 N H_2SO_4 and plates were read at 450 nm with optical correction by subtracting readings at 540 nm.

2.8.3 NETs ELISA

Neutrophil extracellular traps (NETs) are highly decondensed chromatin structures released from neutrophils which contain DNA, histone proteins that are characteristically hypercitrullinated by peptidylarginine deiminase 4 to promote decondensation, and neutrophil granule contents such as neutrophil elastase and myeloperoxidase (Li et al., 2010; Hirose et al., 2014; Masuda et al., 2016).

NETs were quantified in BAL by removal of cells by centrifugation of BAL at 1500 rcf for 7 minutes in order to yield only extracellular contents of the BAL. The quantity of extracellular citrullinated histone H3-DNA complexes (NETs) in BAL supernatant samples were then quantified using an ELISA approach. Briefly, this involved coating a 96 well high-binding plate with the rabbit polyclonal anti-histone H3 (citrulline R2 + R8 + R17) at (1 in 1000) in PBS overnight, washing (3 × 200 µl washes with ELISA wash buffer), non-specific binding blocking with ELISA reagent diluent (1% BSA in PBS), washing again, and then a 2 hour capture step involving incubation of samples (diluted 1 in 2 or 1 in 4 in reagent diluent) and

a serial dilution of a biological standard containing pooled BAL supernatant from 12 mice exposed to 5 mg/kg LPS intranasally, diluted serially from a top 1 in 2 dilution in reagent diluent.

The plate was then washed again, incubated with a peroxidase-conjugated anti-DNA antibody [MCA-33] for 1 hour, washed again and then incubated for 1 hour with ABTS reporter substrate solution (from Roche Cell death detection ELISA plus kit). Oxidation of ABTS was quantified by reading the well absorbance at 405 nm at 1 hour. NETs values are expressed as relative units compared with 4-parameter logistic fitting of the pooled standard curve (1 NET unit is bioequivalent to the concentration of NETs detected in the 1× pooled standard), with background readings from a blank sample subtracted from all wells.

2.8.4 Red blood cell content of BAL

BAL red blood cell content was also measured as an index of bleeding into lung airspaces by measuring the optical density at 405 nm of the lysed BAL cell pellet in a similar manner to that previously described for measuring inflammatory bleeding into lungs (Deppermann et al., 2017). Whole BAL (125 µl) was centrifuged at 1500 rcf for 7 minutes and BAL supernatant removed to yield a BAL cell pellet. The cell pellet was resuspended in 125 µl red cell lysis buffer to selectively lyse red blood cells. Remainining cells were then pelleted by centrifugation at 1500 rcf for 7 minutes and the optical density of 100 µl of the resultant supernatant measured at 405 nm as an index of free haemoglobin concentration.

2.9 Experimental design and statistical analysis

Where feasible, randomised balanced or imbalanced latin square designs were used for blocking application of treatments within and across cages to minimise potential confounding effects of treatment order or cage. Measurements were made with the experimenter blinded to the treatment group of samples. In cases where previous knowledge from literature or pilot studies was available, power analysis was used to set sample sizes required to see an effect size considered biologically meaningful at 80% power.

Parametric statistics were used to analyse continuous numerical data where possible in order to maximise power. For each test, residuals versus predicted plots and normal probability plots were considered to determine whether data transformation was required (transformation approaches used were Y=logY, with 1 added to all Y values if zero values were present, or Y=$\sqrt{Y}$).

Simple comparisons between single independent measurements from two groups were made using two-tailed unpaired Student's t-tests or Mann-Whitney U-tests where appropriate. Depending on experimental design, single or repeated measures 1-way anlaysis of variance (ANOVA), 2-way ANOVA, or 3-way ANOVA were used to test for effects of interventions. Repeated measures analysis of covariance (ANCOVA) approaches with baseline values fit as covariates were used to analyse datasets with high baseline variability (body weight and non-invasive radiolabelled platelet tracking), as recommended by Bate and Clark (2014).

The threshold for statistical significance was set at $P<0.05$. P-values reported are from t-tests, or where necessary multiplicity-adjusted P-values (Dunnett's or Holm's adjustments where appropriate), with the exception of direct reference to ANOVA or ANCOVA main

effect results, where Fisher's F-statistic for the relevant effect is reported with the P-value in the format "F(numerator, denominator) = F-value, P-value".

Correlations were analysed using Pearson's test to derive the R^2 value describing goodness of fit, and P-values are the results of an F-test for the probability that an R^2 value as high as each R^2 value generated from experimental data would have arisen from randomly generated datasets with no correlation.

Effect sizes and variances are reported in text as group means ± standard error with relevant P-values from group comparisons. Data are graphed and reported as means ± standard error with raw or normalised individual data points plotted where sensible. Group sizes (n) are listed in figure legends.

The software packages Excel 2016 (Microsoft Office), InVivoStat 3.6 (InVivoStat), and Prism 6.0 (Graphpad) were used for tabulation, statistical analysis and graphing.

3 Results I: Measuring LPS-induced lung platelet recruitment

3.1 Immunohistochemistry and LPS model characterisation

3.1.1 Background – immunohistochemistry and LPS model characterisation

A mouse model in which lung platelet recruitment following LPS inhalation could be studied was sought. In mice, LPS from O55:B5 serotype of *E. coli* given at 5 mg/kg body weight intratracheally was previously suggested, based on increased immunostaining of platelet CD41, to cause lung platelet recruitment at 48 hours after challenge (Ortiz-Muñoz et al., 2014), with neutrophil migration into airspaces detected by 4 hours after LPS inhalation (Ortiz-Muñoz et al., 2014). Aspirin and exogenous 15-epi-lipoxin A4 treatment decreased lung neutrophil recruitment in this model (Ortiz-Muñoz et al., 2014), and in similar studies from our laboratory where mice were administered the same serotype of LPS intranasally, anti-PSGL-1 antibody treatment, platelet depletion and $P2Y_1$ receptor antagonism could also reduce lung neutrophil recruitment, suggesting that this response is both preventable and platelet-dependent (Kornerup et al., 2010; Ortiz-Muñoz et al., 2014; Pan et al., 2015; Amison et al., 2017).

The effect of LPS inhalation on the number of platelets detected in lungs using immunohistochemisty has not yet been quantified. Development of such methods would allow the use of tools available for mouse models to characterise inflammatory lung platelet recruitment responses. In order to investigate their recruitment to lungs, the quantity of platelets and neutrophil elastase was measured using immunohistochemical staining in frozen lung sections,

and platelets and neutrophils in blood were counted using microsamples from tail veins, in order to test the effect of inhalation of LPS (O55:B5, 5 mg/kg i.n.) versus PBS vehicle control at 4 and 48 hours after challenge.

LPS from E. coli (O111:B4) had also been instilled into human lungs for recently published *ex vivo* blood-perfused lung studies (Hamid et al., 2017), so platelets and neutrophil elastase were also immunostained for imaging in samples from these inflamed human lung samples kindly provided by Dr. Cecilia O'Kane, Queen's University Belfast.

3.1.2 Results – immunohistochemistry and LPS model characterisation

Effect of LPS inhalation on quantity of CD41+ platelets in the lung

Inhalation of LPS caused significant increases in the number of CD41+ platelets detected in lungs 48 hours after intranasal challenge (PBS vs. LPS: 9±4 vs. 68±14 platelets/mm^2 of lung field, P<0.001), but no difference from PBS control was detected with the earlier 4 hour time point (PBS vs. LPS: 1.1±0.5 vs. 3.8±1.2 platelets/mm^2 of lung field, P=0.392) (Figure 3.1).

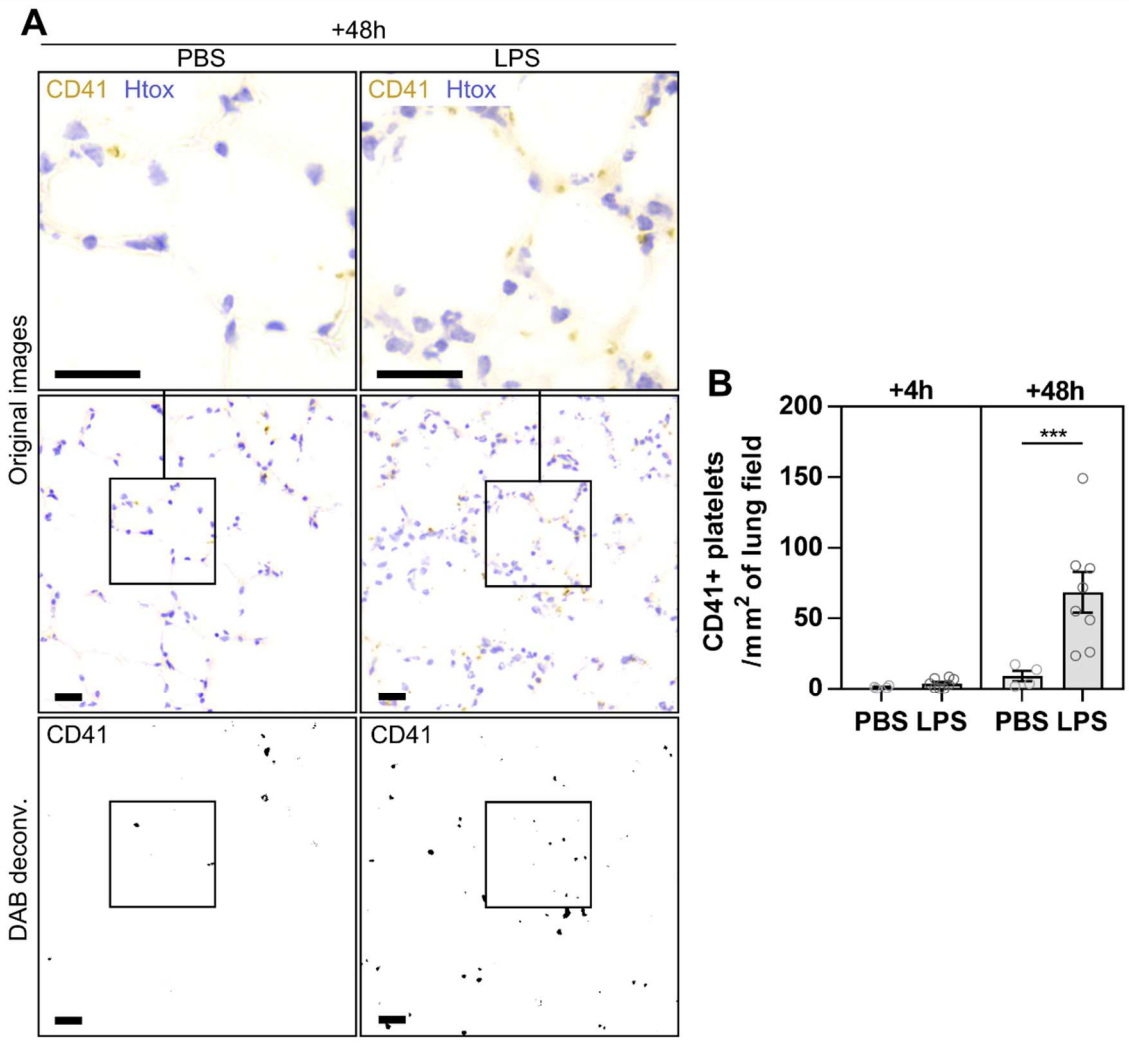

Figure 3.1: Effect of LPS inhalation on quantity of CD41+ platelets in lungs measured using bright field microscopy. Mice were administered PBS or LPS intransally, and lungs harvested at 4 hours and 48 hours. (A) CD41+ platelets were stained in 10 µm frozen lung sections using immunohistochemical methods (brown) with a haematoxylin counterstain (blue) (top and middle rows). The brown CD41 staining was deconvoluted for quantification of platelets (bottom row). Scale bar = 20 µm. (B) Results of platelet quantification. PBS groups n=4, LPS groups n=8. Two-way ANOVA with Holm's test within time points, ***=P<0.001.

Further lungs were collected at 48 hours after mice were challenged intranasally with LPS or PBS control, and stained for fluorescence microscopy analysis. LPS inhalation again increased the number of CD41+ platelets in lung fields (PBS vs. LPS: 752±106 vs. 1205±41 platelets/mm^2 of lung field in mice challenged with LPS, P=0.001) (Figure 3.2B).

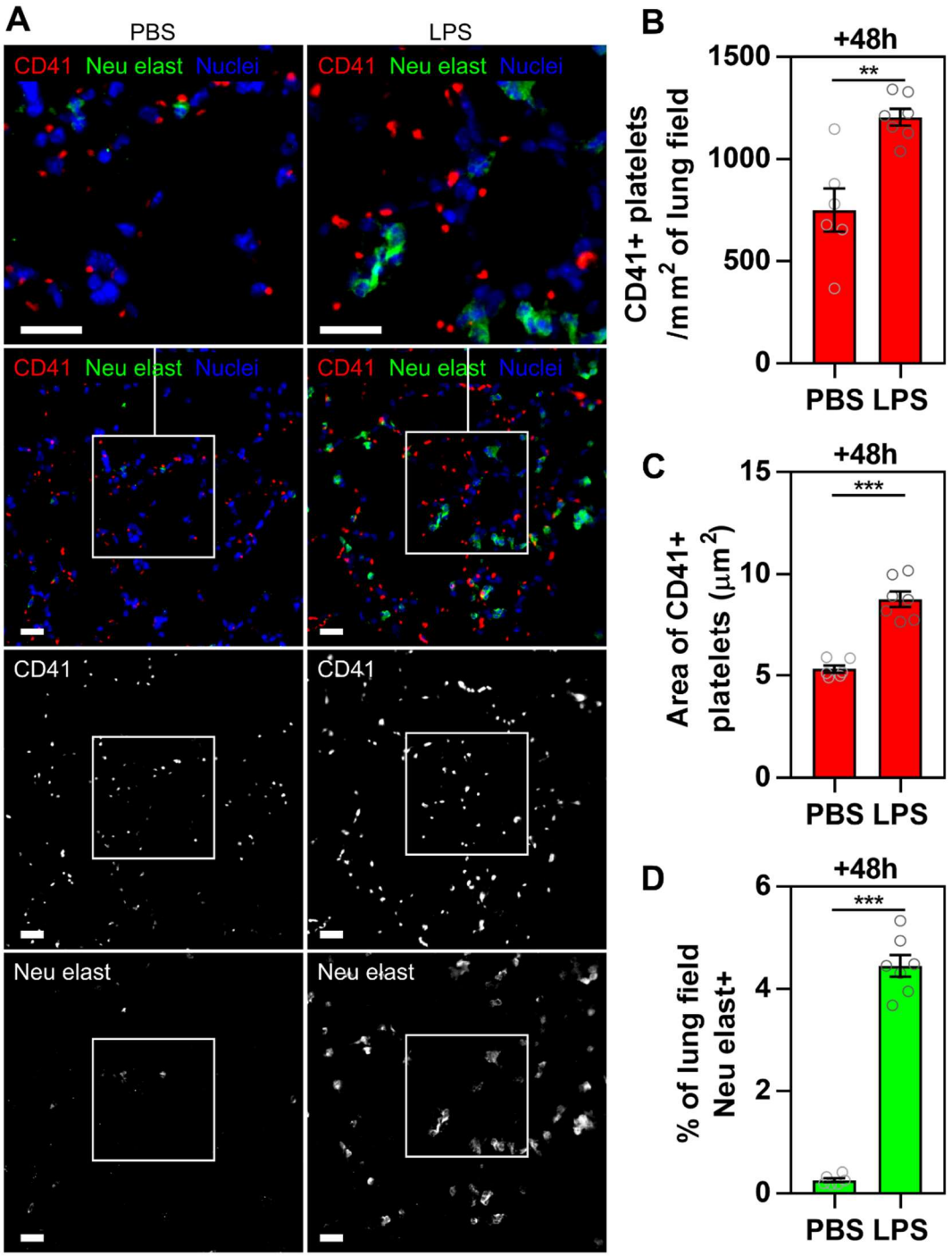

Figure 3.2: Effect of LPS inhalation on quantity of lung CD41 and neutrophil elastase detected using immunofluorescence. Mice were administered PBS or LPS intransally, and lungs harvested at 48 hours.(A) Platelet CD41 and neutrophil elastase were stained in frozen lung sections using immunofluorescence. Sample fields are shown as merges, where CD41+ platelets are in red, neutrophil elastase stainingis in green and Hoechst-stained nuclei are in blue (top two rows), as well as CD41+ events (second from bottom row), and neutrophil elastase (bottom row) shown separately, Scale bar = 20µm. (B) Quantification of number of CD41+ platelets, (C) size of CD41+ platelets and (D) neutrophil elastase staining. PBS group n=6, LPS group n=7, unpaired t-test, **=P<0.01, ***=P<0.001.

Detection of a more complete population of the platelets in lungs allowed for analysis of the size of the CD41+ platelets. LPS inhalation increased the size of platelets seen in lung sections (Area of CD41+ events detected in PBS vs. LPS lung fields: 5.3±0.2 vs. 8.8±0.4 μm^2, P=0.001), although the majority of platelets seen in LPS-challenged lungs appeared to be alone, with a minority appearing as doublets, or potentially as microthrombi or CD41+ events with the elongated morphology of proplatelets (Figure 3.2). The respiratory lung did not contain gross thrombi as can be seen following intravenous administration of platelet agonists, which occlude small blood vessels and take up areas of ~400 μm^2 in fields of respiratory lung sections (see Figure 3.5).

Dual immunofluorescence staining allowed for analysis of whether platelets were spatially associated or not spatially associated with neutrophil elastase in lung sections.[11] LPS inhalation appeared to increase both the quantity of platelets not associated with neutrophil elastase in lungs (709±105 vs. 882±43 platelets per mm^2 of lung fields, P=0.037) which remained in the majority in lungs of both PBS and LPS challenged mice, as well as the quantity of neutrophil elastase associated platelets detected in lungs (42±6 vs. 323±22 platelets per mm^2 of lung fields, P=0.003).

[11] The term "spatially associated" is used here rather than colocalised as confocal microscopy was not used to narrow the focal plane, so neutrophil elastase-associated platelets may not be in direct contact with neutrophil elastase but could therefore appear in images without direct contact. Platelets not visisbly spatially associated within this section may also be in contact with neutrophil elastase outside of the region of tisse in the section and focal plane.

Perhaps unsurprisingly given the large LPS-induced increase in extent of neutrophil elastase staining in lungs together with the LPS-induced increase in lung platelet numbers, LPS inhalation increased the percentage of platelets spatially associated with neutrophil elastase (PBS vs. LPS: 6±1 vs. 27±2 % of platelets spatially associated with neutrophils, $P<0.001$). The increase in neutrophil elastase-associated platelets did not occur to the same extent as the increase in neutrophil elastase coverage of lungs as with LPS inhalation neutrophil elastase became less densely decorated with spatially-associated platelets (PBS vs. LPS: 12467±1467 vs. 7576±624 neutrophil elastase-associated platelets per mm^2 of neutrophil elastase staining).

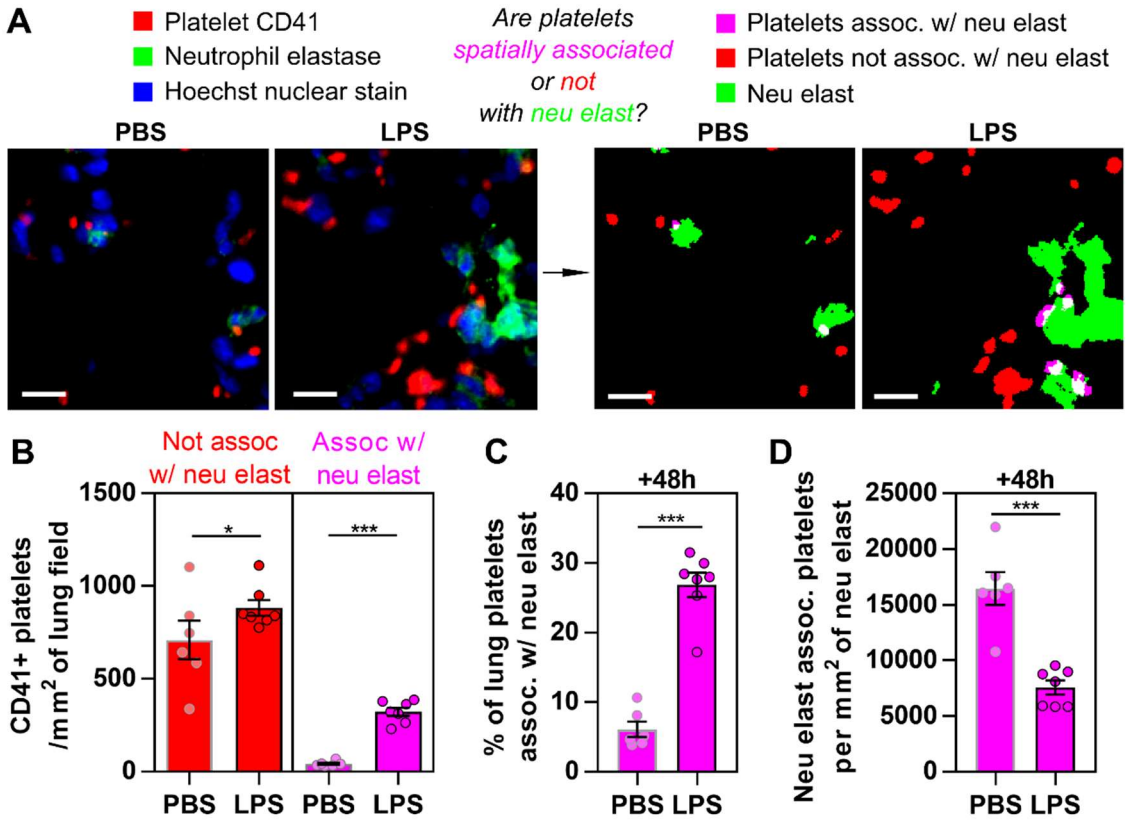

Figure 3.3: Effect of LPS inhalation on spatial association of platelets with neutrophil elastase in lungs. Mice were challenged with PBS or LPS intranasally and lungs collected after 48 hours for immunostaining platelet CD41 and neutrophil elastase. (A) CellProfiler was used to separate platelets into two populations, those not visibly associated with neutrophil elastase (red), and platelets associated with neutrophil elastase (magenta/white). Scale bars = 20 µm. (B) (C) The percentage of platelets associated with neutrophil elastase (D) The number of platelets associated with neutrophil elastase per mm^2 of neutrophil elastase staining. Mean ± standard error, 2-way ANOVA with repeated measures and Holm's test for effects of LPS inhalation, or unpaired t-test, *=P<0.05, ** = P<0.01, ***=P<0.001.

Immunofluorescence allowed for detected and segmentation of a more complete population of platelets than the bright field method using DAB reporter, and also allowed the simultaneous imaging of neutrophil elastase. Unfortunately this immunofluorescence method required the use of an anti-rat secondary antibody reporter to amplify CD41 immunostaining, which introduced interference in cell depletion and adhesion molecule blocking experiments where mice were dosed *in vivo* with antibodies raised in rats.

In order to ensure that a more complete population of lung platelets were detected, a method was developed for immunostaining CD42b using a monoclonal antibody raised in rabbits, which allowed for signal amplification with an anti-rabbit reporter antibody, revealing a more complete population of platelets, particularly in PBS control mice, with numbers more closely resembling the numbers seen with immunofluorescence than initial experiments using anti-CD41 antibody and bright-field microscopy (Figure 3.1, Figure 3.2, and Figure 3.4)

Lungs were also collected from mice 1 minute after induction of pulmonary thromboembolism with an intravenous bolus dose of collagen to demonstrate the appearance of gross thrombus formation in the lung. CD42b+ thromboemboli seen after collagen administration were much larger than platelet staining seen in lungs following inhalation of PBS or LPS (Figure 3.5).

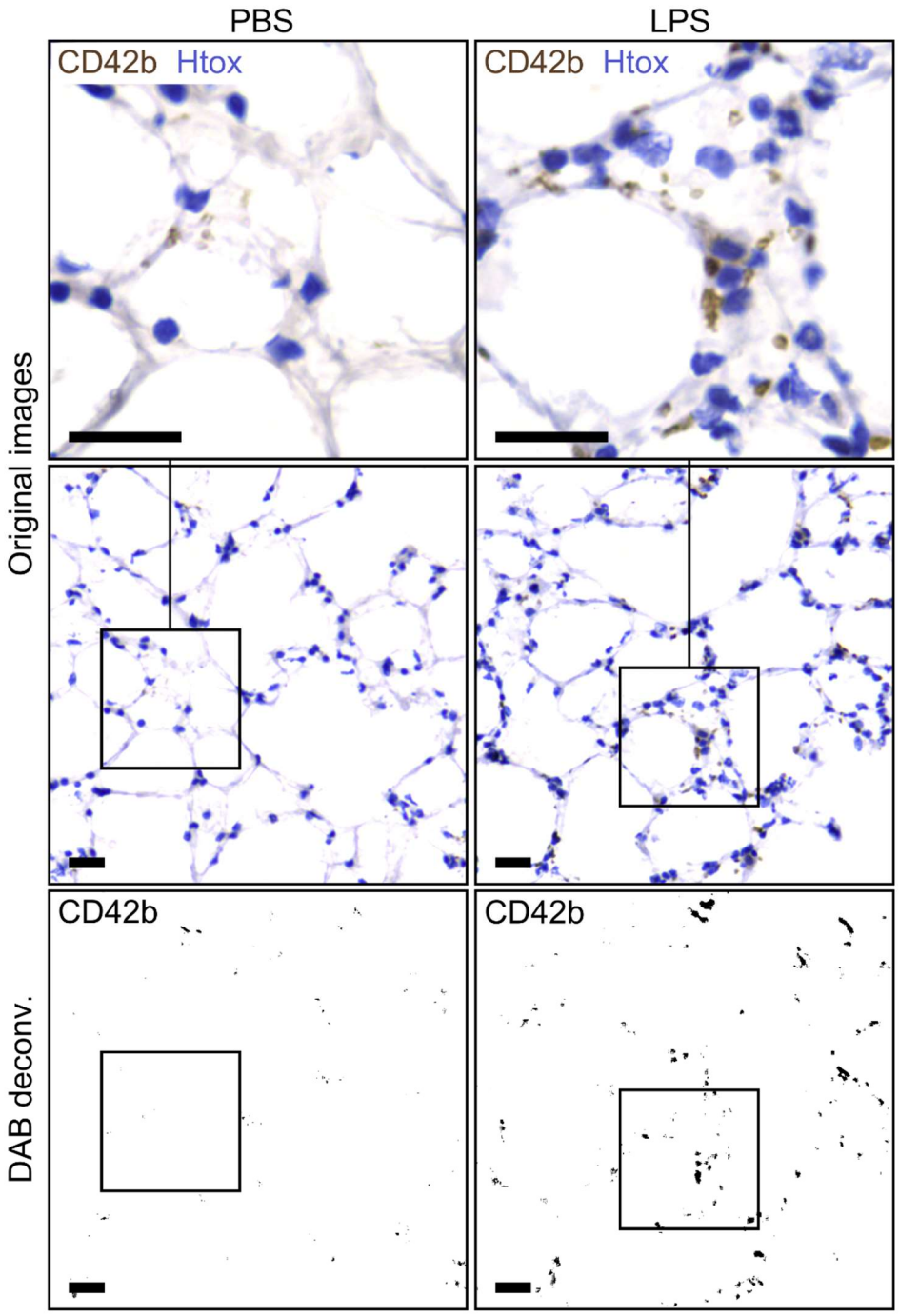

Figure 3.4: Immunostaining CD42b+ platelets in lungs. Mice were challenged with LPS or PBS control and 48 hours later lungs were collected for immunostaining platelet CD42b (brown) with haematoxylin counterstain (blue). Top and middle row: Bottom row: deconvolution of brown DAB CD42b immunostaining for quantification. Scale bars = 20µm.

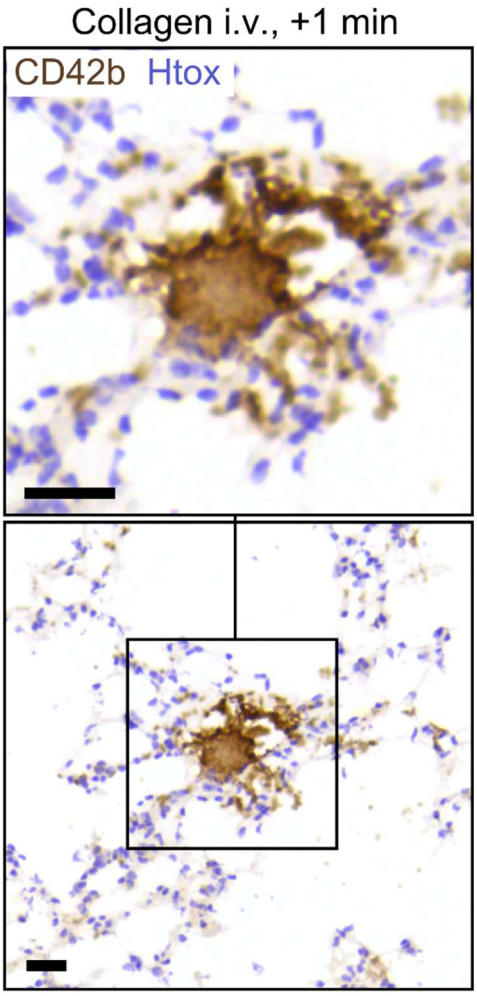

Figure 3.5: Effect of intravenous collagen on lung CD42b+ platelet staining. Mice were given collagen (bolus i.v. *via* tail vein, 50 µg/kg) in order to induce pulmonary thromboembolism. CD42b+ platelet staining (brown) and haematoxylin counterstain (blue) are shown. Scale bars = 20 µm.

Effect of LPS inhalation on blood platelet counts

In order to confirm that increases in lung section platelet content were due to lung platelet recruitment rather than just an increase in circulating blood platelet content, platelets were counted in tail blood microsamples. Inhalation of LPS caused a decrease in tail blood platelet counts at 4 hours after intransal challenge (PBS vs. LPS: 1.02±0.10 vs. 0.78±0.05 $\times 10^9$

platelets per ml of blood, P=0.025), with platelet counts then returning to levels not significantly different from PBS controls by 48 hours after intranasal challenge (PBS vs. LPS: 1.03±0.04 vs. 1.14±0.05 $\times 10^9$ platelets per ml of blood, P=0.426) (Figure 3.6). This lack of difference between blood platelet counts at 48 hours after intranasal challenge is supportive of the increased lung platelet staining resulting from lung platelet recruitment, rather than from an increase in platelets in blood perfusing the lung.

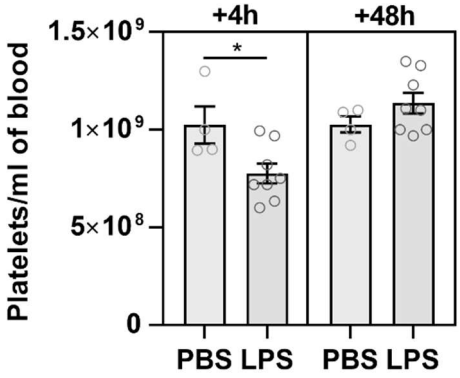

Figure 3.6: Effect of LPS inhalation on blood platelet counts. Platelets were counted by phase contrast microscopy in tail blood microsamples diluted 1 in 100 in stromatol, taken at 4 and 48 hours after intranasal administration of PBS or LPS PBS groups: n=4, LPS groups: n=8. Two-way ANOVA with Holm's test within time points, *=P<0.05.

Effect of LPS inhalation on the presence of platelets in the bronchoalveolar space

Immunofluorescence images had clear CD41+ platelet discrimination with the absence of false positive staining around airways, which allowed for identification of extravascular platelets in the airspaces of small airways. CD41+ platelets were detected in the lumen of small airways of 5 of 7 LPS-challenged mice, with no airway platelets detected in lung sections from PBS controls. The total number of airway lumen platelets was added up for each lung section analysed and divided by the total area of the lung section, and mice challenged with LPS had

0.046±0.017 airway lumen platelets/mm^2 of lung section (P=0.021 vs. PBS controls with a Mann-Whitney test) (Figure 3.7). Platelets in airway lumen were mainly associated with nuclear staining, with some extravascular platelets clearly spatially associated with neutrophil elastase (Figure 3.7).

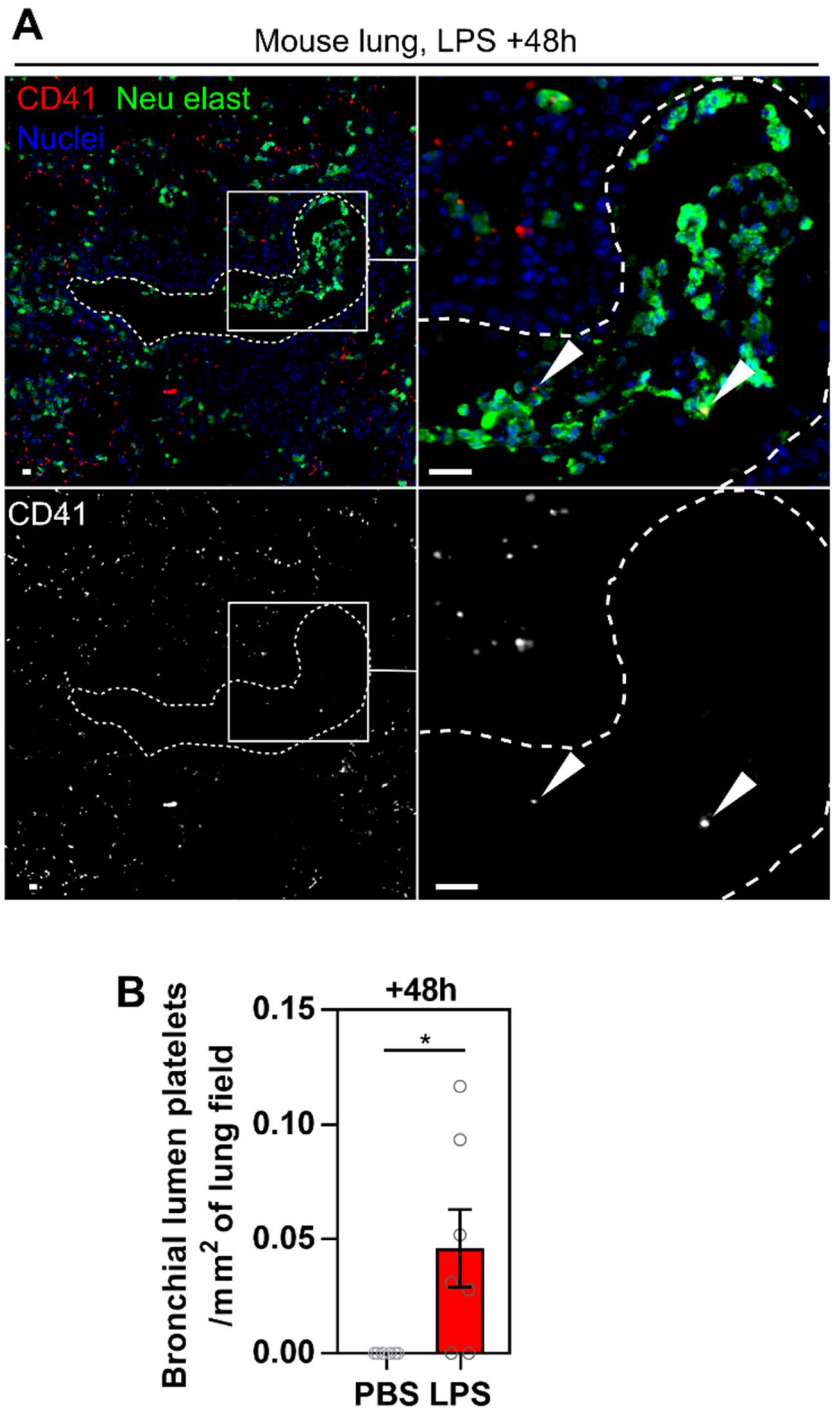

Figure 3.7: Effect of LPS inhalation on quantity of platelets inside airways. Mice were administered PBS or LPS intransally, and lungs collected at 48 hours. (A) Airways (dashed line) were identified in lung sections stained for CD41 (red), neutrophil elastase (green) and nuclei (blue) (top panels). Bottom panels: CD41 stain only. Airway lumen platelets are highlighted with arrowheads. Scale bar: 20µm. (B) The number of CD41+ platelets within airways was quantified and expressed as number per total area of sections surveyed. Mean ± standard error, comparisons are Mann-Whitney test, PBS: n=6, LPS: n=7, *=P<0.05.

Separately, images of fields of alveolar-capillary networks stained for platelet CD42b were captured with a high-power 63× objective and used for manual counting of platelets that were not visibly within alveolar capillaries or pulmonary blood vessels and so appeared extravascular in the alveolar airspaces. LPS inhalation caused a significant increase in these extravascular platelets (PBS vs. LPS: 55±5 vs. 252±65 platelets with extravascular appearance per mm^2 of lung fields, P=0.004) (Figure 3.8).

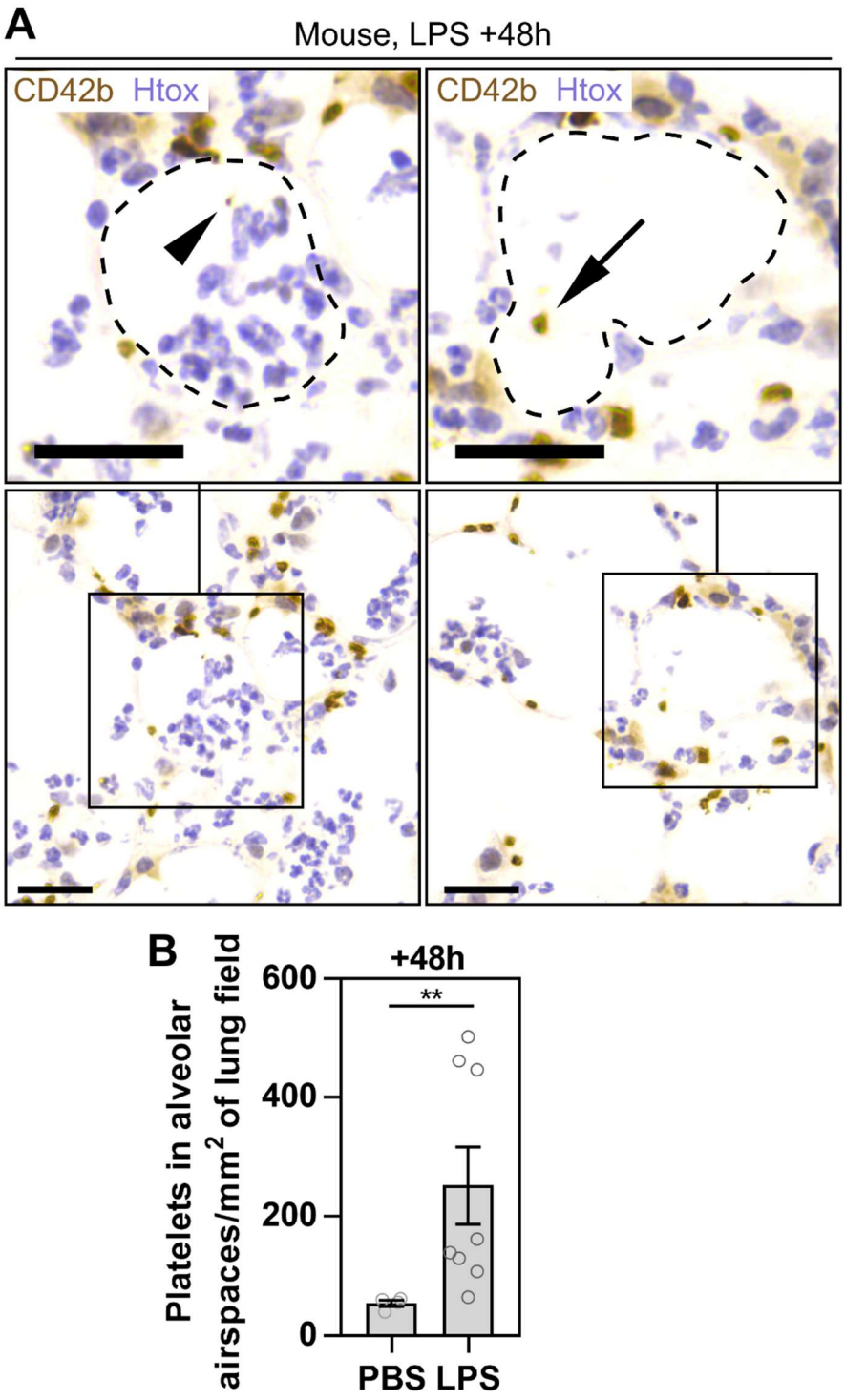

Figure 3.8: Effect of LPS inhalation on quantity of platelets appearing extravascularly in the alveolar airspaces. Mice were challenged with PBS or LPS intranasally and lungs collected 48 hours later. Lung sections immunostained for CD42b (brown) with haematoxylin counterstain (blue). (A) Platelets appearing extravascularly with intra-alveolar neutrophils (black arrowhead) and alone (black arrow) inside alveolar airspaces (dotted lines) are shown. Scale bars = 20 µm. (B) Quantification of CD42b+ platelets detected in alveolar airspaces. Mean ± standard error, comparisons are Mann-Whitney test, PBS: n=4, LPS: n=8, **=P<0.01.

Effect of LPS inhalation on lung CD41+ objects with proplatelet morphology and CD41+ cells

In addition to CD41+ platelets, CD41+ proplatelets and megakaryocytes have also been observed in mouse lungs (Zhang et al., 2013; Lefrançais et al., 2017). In order to assess the contribution of these CD41+ objects to lung platelet recruitment measurements, and in order to investigate whether LPS inhalation had a detectable effect on lung thrombopoiesis, CD41+ objects with proplatelet morphology and cells with large nuclei surrounded by CD41 positivity were quantified from immunofluorescence micrographs (Figure 3.9).

LPS inhalation increased the quantity of CD41+ objects with the large and elongated morphology of proplatelets detected in lungs (PBS vs. LPS: 1.1±0.5 vs. 7.6±1.8 CD41+ objects with proplatelet morphology per mm^2 of lung fields, P=0.010) (Figure 3.9), although these objects were a small minority (<1%) of the total number of CD41+ objects counted as platelets in sample fields of lung sections (Figure 3.2).

LPS inhalation also increased the number of CD41+ cells detected across whole lung sections which were less frequently observed than objects with proplatelet-like morphology (PBS vs. LPS: 0.01±0.01 vs. 0.06±0.01 CD41+ cells per mm^2 of lung fields, P=0.014) (Figure 3.9).

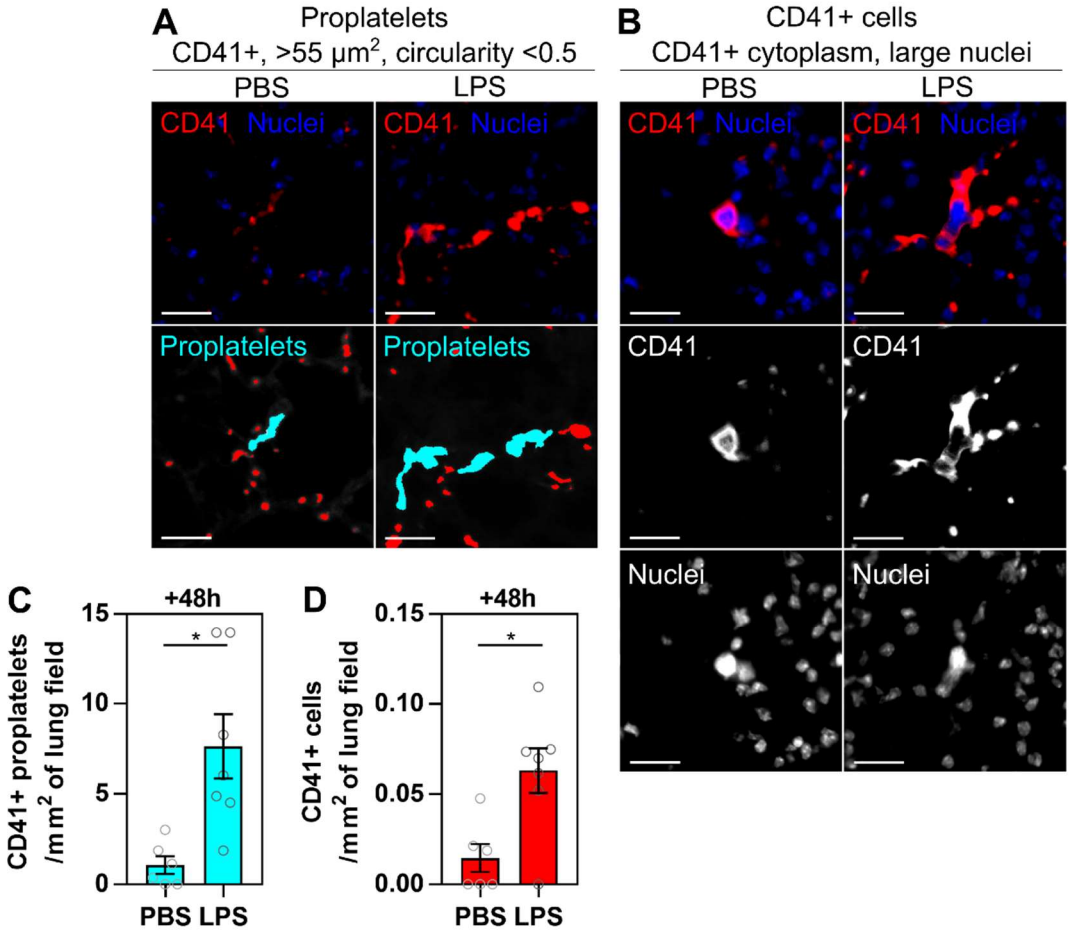

Figure 3.9: Effect of LPS inhalation on quantity of CD41+ objects wth proplatelet morphology and CD41+ cells in lungs. Mice were administered PBS or LPS intransally, and lungs collected 48 hours later. (A) CD41+ objects with proplatelet morphology (area >55 µm², circularity <0.5, cyan in lower images) in lung sections. (B) Large nuclei surrounded by CD41+ cytoplasm in lungs. Scale bars = 50 µm. (C) Quantification of proplatelet events in sampled fields and (D) quantification of CD41+ cell events across whole lung sections. Mean ± standard error, comparisons are unpaired t-test or Mann-Whitney U-test, PBS: n=6, LPS: n=7, *=P<0.05.

Effect of LPS inhalation on lung neutrophil elastase

In order to confirm the presence of neutrophilic lung inflammation following LPS challenge, neutrophil elastase was also quantified in serial lung sections relative to those used for platelet quantification.

LPS inhalation caused increased lung neutrophil elastase staining at 4 hours (PBS vs. LPS: 0.027±0.006% vs. 0.408±0.106% of lung fields covered by neutrophil elastase positivity,

P<0.001), and at 48 hours (PBS vs. LPS: 0.038±0.003% vs. 3.136±0.662% of lung fields covered by neutrophil elastase positivity, P<0.001) after LPS inhalation (Figure 3.10).

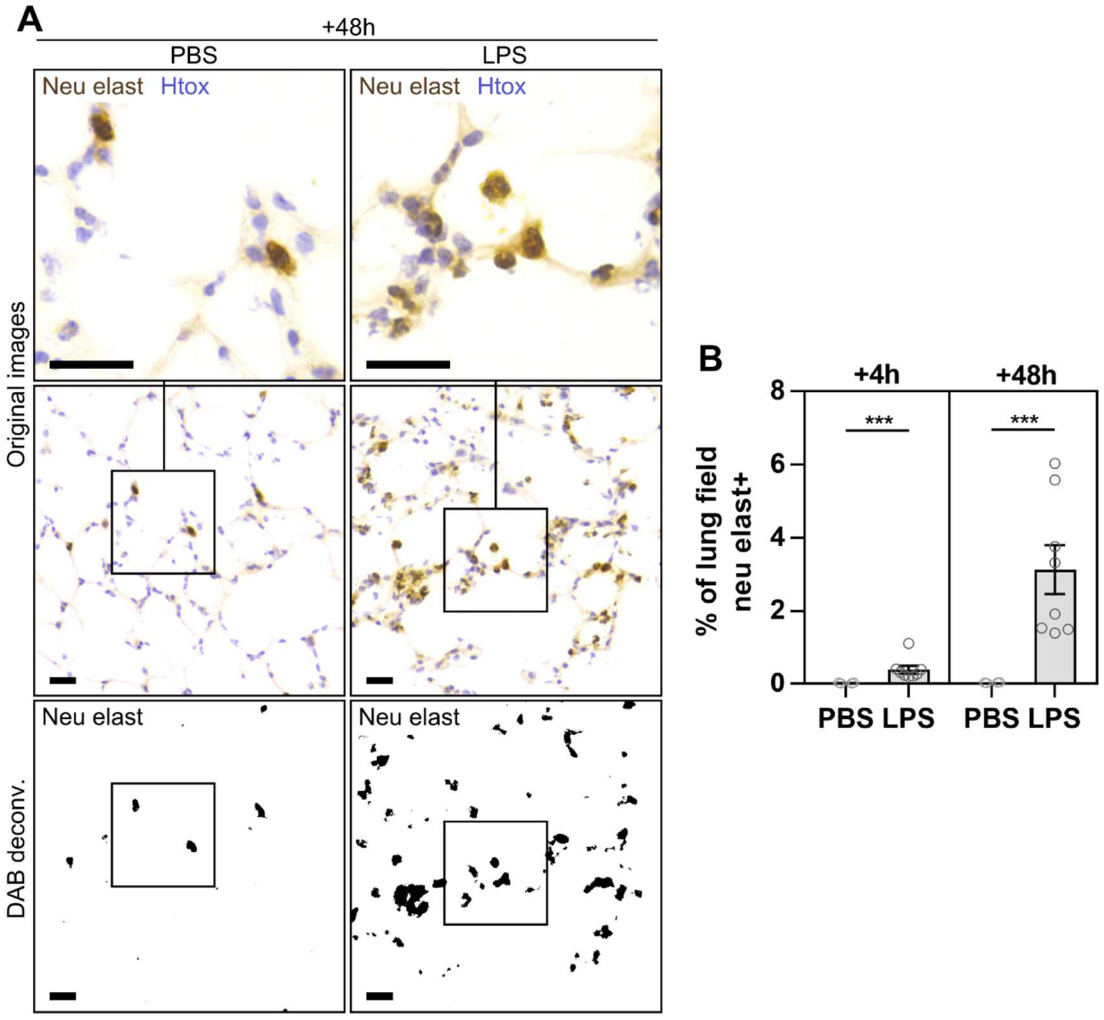

Figure 3.10: Effect of LPS inhalation on lung neutrophil elastase staining. Mice were administered PBS or LPS intransally, and lungs collected at 4 and 48 hours. (A) Neutrophil elastase was stained in 10µm frozen lung sections using immunohistochemical methods (brown) with a haematoxylin counterstain (blue) (top and middle row). The brown neutrophil elastase staining was deconvoluted for quantification of neutrophil elastase coverage of the lung fields (lower panels). Scale bar = 20µm. (B) Quantification of neutrophil elastase in fields sampled from lungs at 4 and at 48 hours after challenge. PBS groups n=4, LPS groups n=8. Two-way ANOVA with Holm's test within time points, ***=P<0.001. Lung neutrophil elastase was also quantified from lung sections prepared for immunofluorescence. At 48 hours after challenge, LPS inhalation also increased the quantity of neutrophil elastase in lungs detected using this method (PBS vs.

LPS: 0.038±0.003% vs. 3.136±0.662% of lung fields covered by neutrophil elastase positivity, P<0.001) (Figure 3.2C).

Effect of LPS inhalation on blood neutrophil counts

LPS inhalation had no detected effect on blood neutrophil counts at 4 or 48 hours after challenge (Figure 3.11), so LPS-induced increases in lung section neutrophil elastase staining represented lung neutrophil recruitment rather than an increased in circulating blood neutrophil content of the pulmonary circulation.

Although blood neutrophil counts were maintained, LPS inhalation caused a decrease in total blood leukocyte counts which was due to a decrease in blood mononuclear leukocyte counts (see appendix Figure 4.26).

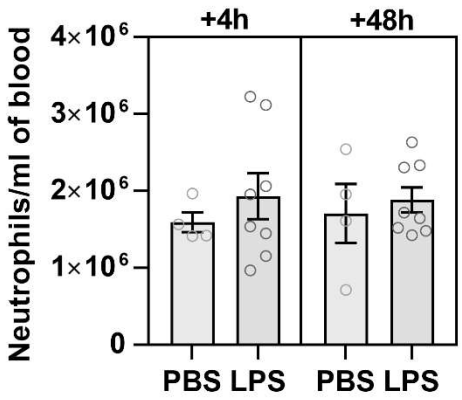

Figure 3.11: Effect of LPS inhalation on blood neutrophil counts. Mice were administered PBS or LPS intransally, and tail blood microsamples taken at 4 and 48 hours. Blood neutrophil counts were estimated from total leukoyte counts combined with blood smear differential cell counts. PBS groups: n=4, LPS groups: n=8. Two-way ANOVA with Holm's test within time points.

Effect of LPS inhalation on body weight

Body weight was monitored as an index of general health status of mice. Inhalation of LPS resulted in body weight loss detectable at 24 and 48 hours after challenge, whilst PBS

inhalation had no effect on body weight (24 hours after challenge, PBS vs. LPS: 0.0±2.1% vs. -9.0±0.8 change from baseline body weight, 48 hours after challenge, PBS vs. LPS: 0.0±2.0% vs. -13.7±1.4% change from baseline body weight) (Figure 3.12).

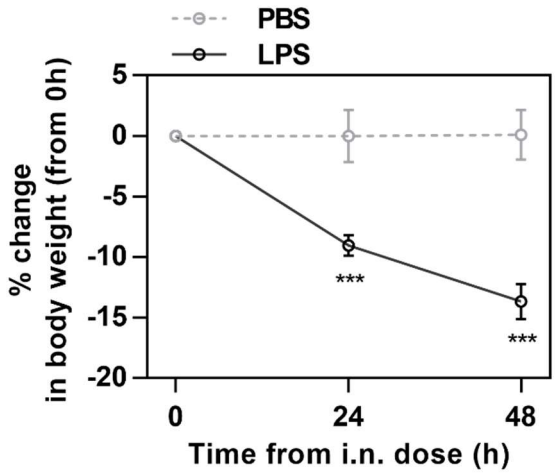

Figure 3.12: Effect of LPS inhalation on body weight. Mice were administered PBS or LPS intransally. Body weight was measured at baseline (immediately before intranasal challenge), then at 24 and 48 hours after intranasal challenge. Data are means ± standard error, PBS group: n=4, LPS group: n=8, repeated measures 2-way ANCOVA with baseline weights fit as covariates, Holm's test for LPS effect within time points, ***=P<0.001.

Immunostaining of platelets and neutrophil elastase in LPS-challenged human lungs

Human lung samples obtained from *ex vivo* blood perfused lung studies exposed to LPS *via* intrabronchial instillation in a previous study (Hamid et al., 2017), were also immunostained for CD41 or CD42b for detection of platelets as well as for neutrophil elastase content.

Platelets and neutrophil elastase were successfully stained in human lungs challenged with LPS, and platelet and neutrophil elastase staining had a similar appearance to those in mouse lungs. No overt thrombosis was seen in the microvasculature but many single platelets could be seen in CD41 and CD42b-stained sections (Figure 3.13).

Similarly to mouse lungs following LPS inhalation (Figure 3.7), inside inflamed human airways exposed to LPS, clusters of cells were seen together with fibrous bodies with extracellular haematoxylin and neutrophil elastase positivity, indicative of neutrophil extraceullar trap (NET) release (Masuda et al., 2016). These bodies in the airway lumen also contained platelets, as confirmed by immunostaining for both CD41 and CD42b in serial sections (Figure 3.14).

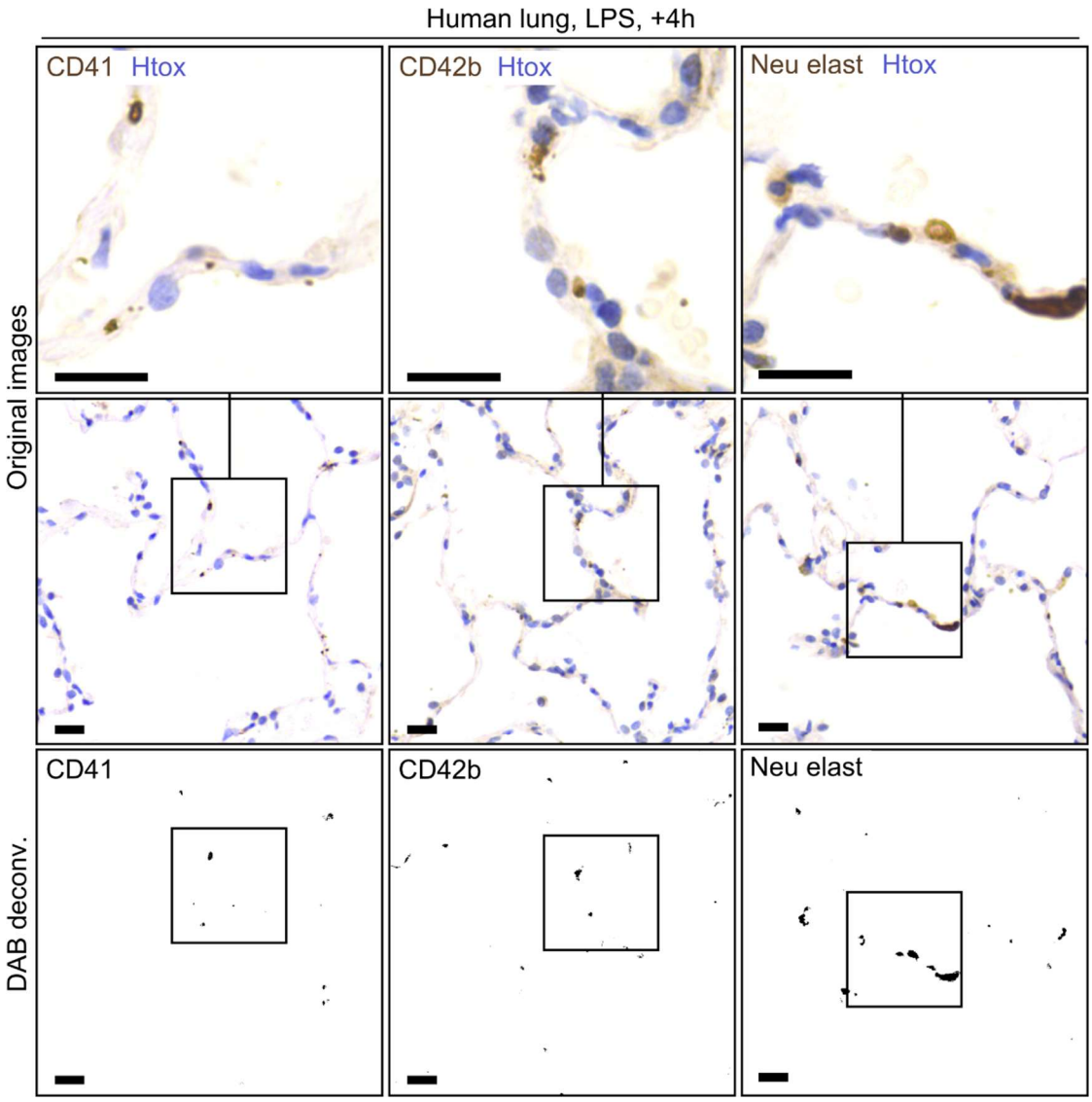

Figure 3.13: Imaging platelets and neutrophil elastase in human LPS-exposed lungs. Human lungs were perfused *ex vivo* with blood and exposed to 6 mg O111:B4 LPS *via* intrabronchial instillation. At 4 hours after LPS challenge, lung samples were collected from the LPS-challenged lobe for histological examination. Representative fields of alveolar capillary units with immunostaining (brown) for platelet CD41 (left column) platelet CD42b (centre column) and neutrophil elastase (right column) are shown with haematoxylin counterstain (blue) (top and middle rows). Output of DAB deconvolution is shown on the bottom row. Scale bar = 20µm.

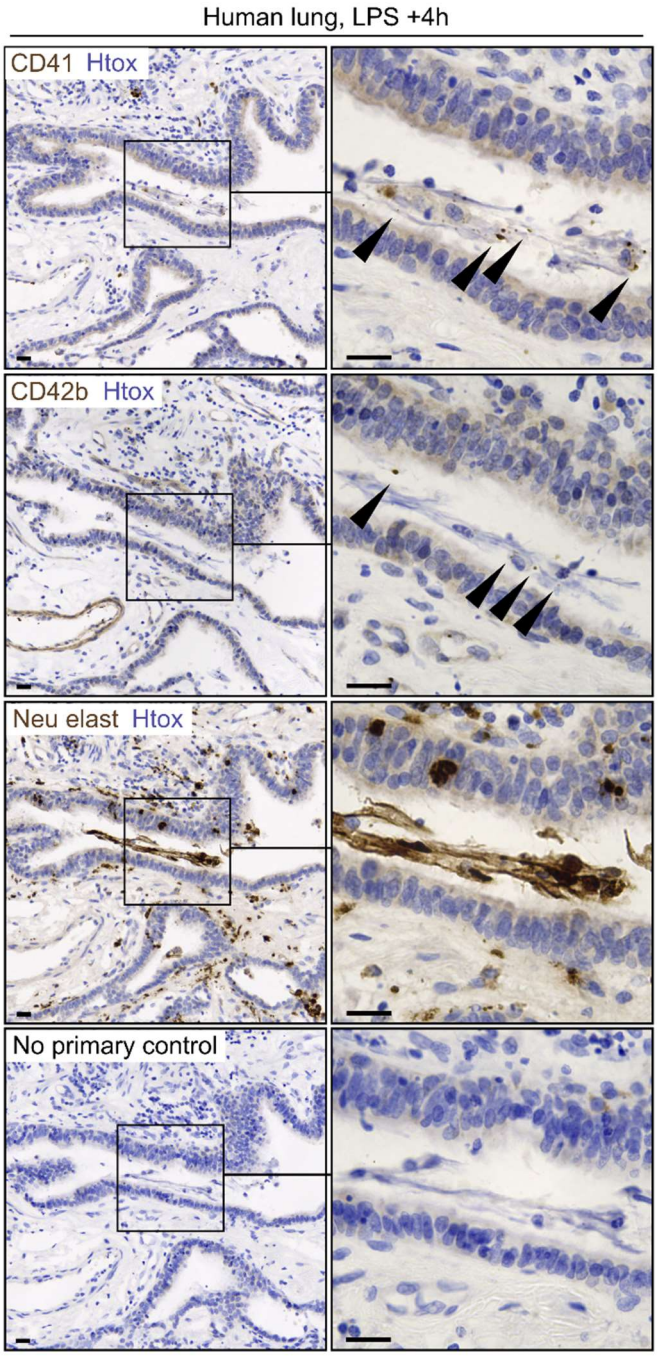

Figure 3.14: Presence of platelets in the airway lumen of human lungs challenged with LPS. Serial sections of an airway following LPS-induced inflammation are shown from top to bottom with an image collected with a 20× objective on the left and 63× objective on the right. Immunostaining (DAB reporter) is brown, haematoxylin (Htox) counterstain in blue. The airway lumen contained bodies with cellular and acellular haematoxylin staining also containing (from top to bottom) CD41+ platelets, CD42b+ platelets (highlighted with black arrowheads on 63× objective images), and neutrophil elastase positivity. Staining was absent when primary antibodies were omitted in control samples. Non-inflamed control lung samples were not available at time of writing. Representative of 3 samples. Scale bars = 20 µm.

3.1.3 Summary – immunohistochemistry and LPS model characterisation

At 48 hours after LPS inhalation, mice had increased lung platelet counts with no significant alterations in circulating blood platelet counts, demonstrating platelet recruitment to lungs. LPS inhalation caused events counted as platelets to appear larger than in control lungs, but the formation of gross thrombi as seen following aggregatory stimuli was not observed in lungs challenged with LPS. Platelets in lungs were seen in increased amounts with LPS inhalation both spatially associated, and not spatially associated with neutrophil elastase.

Lung platelet recruitment was not detected at 4 hours after LPS inhalation whilst lung neutrophil recruitment was, suggesting that lung neutrophil recruitment might precede the platelet recruitment, although blood platelet counts were decreased at this earlier time point suggesting that a platelet response to LPS had occurred at this time point.

At 48 hours after LPS inhalation, increased numbers of platelets were detected in the bronchoalveolar spaces, so it is possible that LPS inhalation may induce transendothelial platelet migration in lungs after LPS-induced inflammation, as previously observed following LPS inhalation (Ortiz-Muñoz et al., 2014), and in the context of allergic airway inflammation (Pitchford et al., 2008).

Proplatelets and megakaryocytes did not appear to make a major contribution to the increase in CD41+ objects counted as platelets in lungs, although LPS inhalation did increase the quantity of objects with proplatelet and megakaryocyte morphology detected in lungs, so lung inflammation may increase the frequency, or the duration, of lung thrombopoiesis events.

Successful immunostaining of platelets and neutrophil elastase in human lung samples suggest that immunohistochemistry methods for quantifying platelet recruitment to mouse lungs be adapted to experiments in the human tissue context, and observations of platelets in human lung airways inflamed by LPS instillation *ex vivo* are suggestive that platelet migration might occur into inflamed human airspaces, Platelets in airspaces were also observed both spatially associated with, and not spatially associated with, neutrophil elastase positive, haematoxylin-staining bodies which had the appearance characteristic of NETs (Caudrillier et al., 2012; de Buhr and von Köckritz-Blickwede, 2016).

LPS inhalation also caused body weight loss, allowing for a simple, repeated measures, non-invasive measurement of a marker of general health status following LPS inhalation. Previous studies using systemic LPS exposure have associated body weight loss with decreased water intake, decreased food intake, and muscle wastage (Braun et al., 2013; Martin et al., 2013; Harris et al., 2017).

Studying lung platelet recruitment using immunohistochemistry allows for the direct imaging of platelets in specific anatomical compartments, but necessitates the killing of experimental animals in order to collect lung samples. Many mice are therefore required in order to quantify a dynamic response using immunohistochemistry, so non-invasive methods for measuring recruitment of platelets to mouse lungs were sought.

3.2 Non-invasive radiolabelled platelet tracking

3.2.1 Background – non-invasive radiolabelled platelet tracking

Tracking thoracic radiolabelled platelet count has allowed for the non-invasive continuous study of lung platelet recruitment following LPS inhalation in guinea pigs within 2 hours of challenge with LPS aerosol (Beijer et al., 1987). Dynamic lung platelet recruitment responses can be quantified in real time noninvasively in mice following intravenous injection of agonists which cause thromboembolism in the lungs (Tymvios et al., 2008). This mouse method has been also used to investigate the effects of diesel exhaust particle inhalation on extent of thromboembolism (Solomon et al., 2013; Smyth et al., 2017), but has not been applied to measurement of lung platelet recruitment responses induced by inflammatory stimuli.

The non-invasive radiolabelled platelet tracking method was therefore adapted for testing the effect of LPS inhalation on thoracic radiolabelled platelet content as an index of lung platelet content.

3.2.2 Results – non-invasive radiolabelled platelet tracking

Effects of ADP infusions on non-invasive measurements of thoracic radiolabelled platelet content

In order to to validate the method for measuring radiolabelled platelet recruitment to lungs, ADP was injected intravenously in order to cause reversible platelet thromboembolism in the lung as previously described (Page et al., 1982; Moore and Emerson, 2012). The signal-to-noise ratio was enhanced by addition of a lead collimating tube around the detector to

maximise the detection of radiolabelled platelets in the region of the thorax containing the pulmonary circulation directly beneath the probe (Figure 3.15).

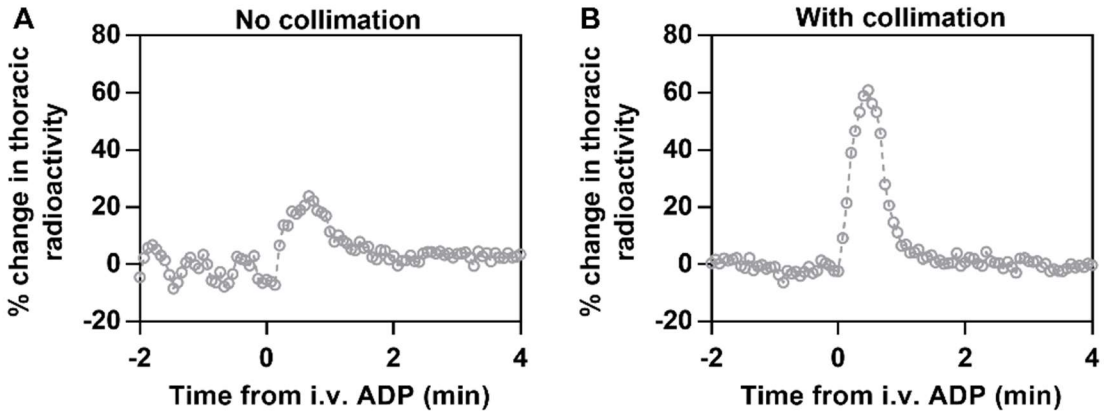

Figure 3.15: Effect of collimation of detector probe on non-invasive measurements of ADP-induced thromboembolism. (A) Single trace showing increase in thoracic radioactivity following injection of 4 mg/kg ADP i.v. into a mouse transfused 1 hour previously with ^{111}In-labelled platelets. (B) amplitude of the same response in the same mouse is increased by collimation of the gamma detector.

When responses to ADP injections were recorded using collimated probes at 48 hours after infusion of mice with ^{111}In-labelled platelets, increases in thoracic radioactivity were detected following ADP injections (Maximal percentage change in thoracic radioactivity from 5 minute baseline over the 2 minutes before ADP dose vs. 2 minutes post ADP dose: 11±3% vs. 23±4%, P=0.001, Figure 3.16B; 2 minute AUC pre ADP vs. post ADP: -45±11 vs. 224±113 arbitrary units, P=0.002, Figure 3.16C), showing that the thoracic radiation monitoring method could detect the recruitment to lungs of viable, labelled platelets at 48 hours after ^{111}In-labelled platelet infusions (Figure 3.16).

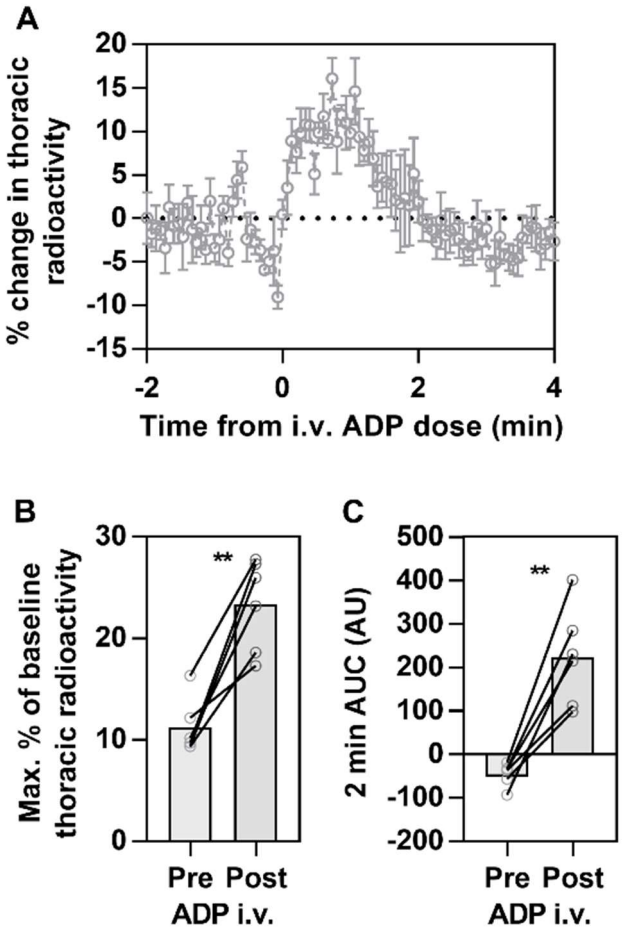

Figure 3.16: ADP-induced thromboembolism detected noninvasively 48 hours after infusion of radiolabelled platelets. (A) Responses to i.v. injections of 4 mg/kg ADP in mice infused 48 hours previously with ^{111}In-labelled platelets. Analysis of pre and post ADP signal showing (B) maximal percentage increases in time periods relative to the baseline and (C) area under the curve (AUC, arbitrary units (AU)), 2 minutes either side of the ADP injection. Data are mean ± standard error where error bars are shown, comparisons are paired t-tests, n=6, **=P<0.01.

Effects of LPS inhalation on thoracic radioabelled platelet content

In initial experiments, mice were terminally anaesthetised and transfused with platelets radiolabelled with ^{111}In-tropolonate. Baseline thoracic radioactivity levels were established for 5 minutes before intranasal treatment with LPS or PBS vehicle control with recordings of thoracic radioactivity were made during and following the intranasal challenge. No obvious

increase in thoracic platelet content was found during the time period within which it was possible to keep mice alive under terminal anaesthesia without more advanced ventilation and fluid support (1-2 hours, Figure 3.17).

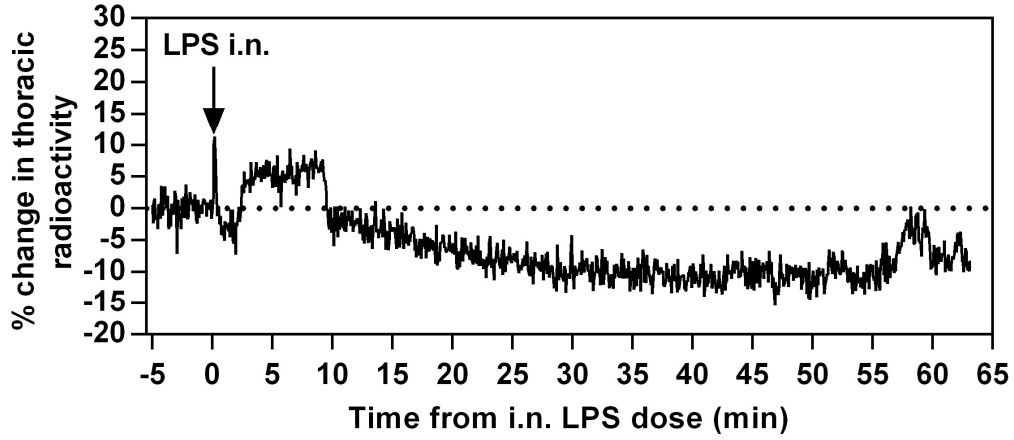

Figure 3.17: Acute effects of LPS inhalation on quantity of thoracic radiolabelled platelets. Single trace showing response to LPS inhalation in a terminally anaesthetised mouse. The mouse stopped breathing at around 60 minutes after challenge.

Two problems were identified when acute responses to LPS inhalation were recorded. Firstly, intranasal dosing in terminally anaesthetised mice caused choking and gasping not seen in other mice used for recording responses to intravenous ADP, or in other mice briefly anaesthetised for intranasal dosing, perhaps because of inhibitory effects of terminal anaesthesia on respiratory drive. Secondly, based on data from IHC experiments, radiolabelled platelet recruitment to lungs may be occurring over days rather than minutes, so maintenance of anaesthesia for continuous recordings would be technically challenging, and would have a low throughput.

The experimental set-up was therefore adapted to involve measurements of thoracic radioactivity under brief isoflurane anaesthesia over 5 minute sampling windows at baseline (immediately before intranasal challenge), and then at 2, 4, 24, and 48 hours after intranasal challenge with PBS control or LPS, with the mouse held in a fixed position relative to probes with a tooth bar and body cradle (Figure 3.18A).

Instead of an increase in thoracic radioactivity in LPS-treated mice compared to PBS controls that would be indicative of lung platelet recruitment, no significant effect of LPS inhalation was detected on thoracic radiolabelled platelet content at any of the time points at which measurements were made (ANCOVA main effect of LPS on thoracic radioactivity: $F(1,7)=3.93$, $P=0.088$) (Figure 3.18B).

Comparison with serial blood platelet counts made from tail blood microsamples in separate mice (Figure 3.18C), corroborated previous data from terminal sampling (Figure 3.6), and demonstrate that changes in the blood platelet count might be a confounding factor for simple non-invasive measurement of lung radiolabelled platelet recruitment, where probes receive signal from both the pulmonary circulation and the blood supply to the rest of the thoracic tissue below the probes, especially if decreases in the blood signal are not entirely due to recruitment to lungs.

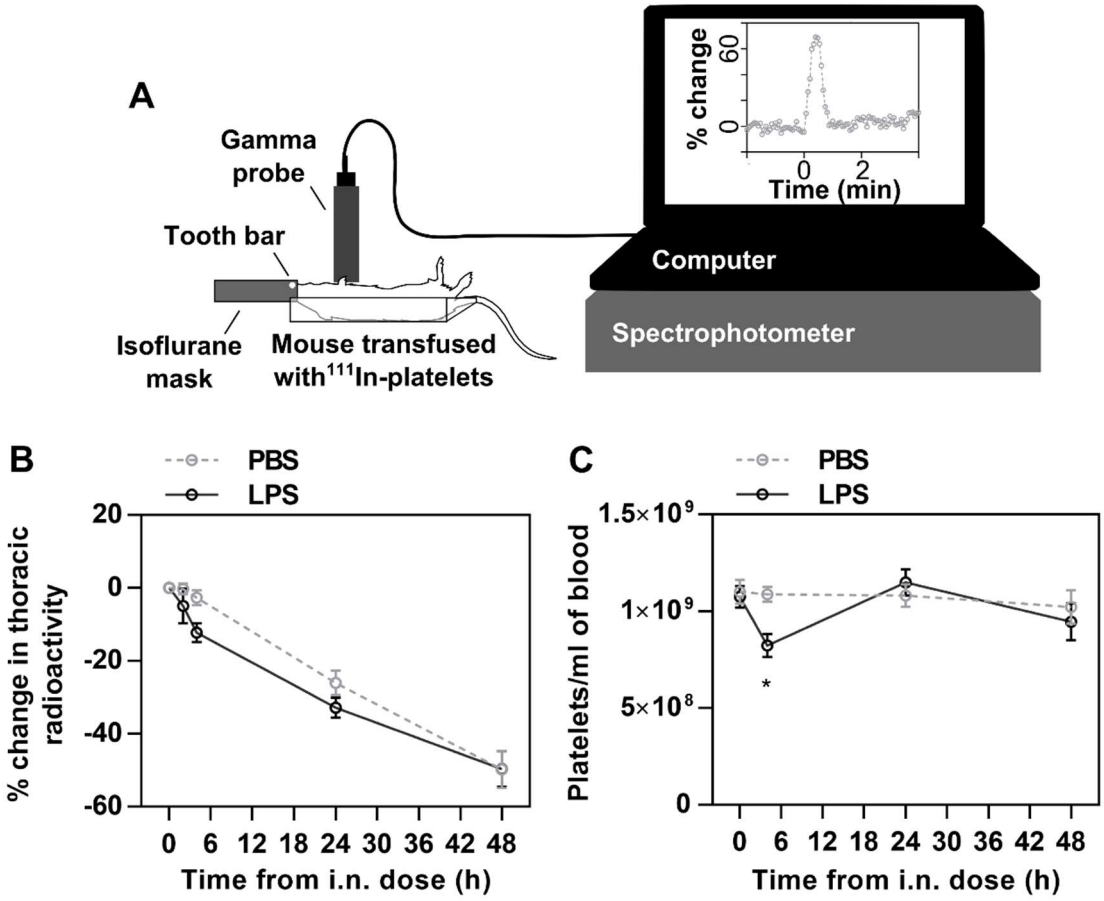

Figure 3.18: Effect of LPS inhalation on thoracic radiolabelled platelet content and blood platelet counts over 48 hours. (A) Mice were infused with ^{111}In-labelled platelets, measurements of thoracic radioactivity were made at 0, 2, 4, 24, and 48 hours after intranasal challenge with positioning of mice maintained with isoflurane anaesthesia and positioning relative to probes using a tooth bar and body cradle as shown in diagram. (B) Effect of LPS inhalation on thoracic radiolabelled platelet content over time vs. PBS controls, data shown as % change from time 0 hours) n=5. (B) In separate mice, serial blood platelet counts made from tail microsamples were conducted at 0, 4, 24, and 48 hours after PBS or LPS inhalation (n=6). Two way ANCOVA with baseline values fit as covariates, or ANOVA, with repeated measures and Holm's test for effects of LPS inhalation within time points, *=$P<0.05$.

3.2.3 Summary – non-invasive radiolabelled platelet tracking

Non-invasive radiolabelled platelet tracking through the recording of thoracic radioactivity in mice infused with ^{111}In-labelled platelets allowed for measurement of pulmonary thromboembolism following intravenous infusions of ADP but was not sensitive enough to permit measurement of LPS-induced lung platelet recruitment.

As systemic blood platelet counts were reduced, non-invasive measurements of ^{111}In-labelled platelet content in the lungs may have been confounded by decreases in the platelet content of the systemic circulation of the central veins, heart and the vessels perfusing the skin and the tissue making up the ribcage and pleura which would also be detected by the gamma probe. This problem would be overcome through use of micro SPECT imaging which would enable discrimination between positron emission events from ^{111}In-labelled platelets within the pulmonary as opposed to the systemic circulatory beds (Khalil et al., 2011).

Measuring radiolabelled platelet content of blood microsamples would also allow for the discernment of the contribution of platelets flowing in blood versus those retained within tissue. Using a gamma counter, the potential utility of this method for measuring platelet recruitment was therefore explored using terminal blood and lung samples in radiolabelled platelet biodistribution studies.

3.3 Biodistribution of radiolabelled platelets

3.3.1 Background – biodistribution of radiolabelled platelets

Previous studies have suggested that the decrease in blood platelet counts following LPS exposure might be a direct consequence of platelet recruitment to the lungs (Beijer et al., 1987; Shibazaki et al., 1999; Zhao et al., 2002). However, the lack of temporal association in changes in platelet content of the pulmonary circulation with changes in blood platelet counts at 4 hours post LPS administration (Figure 3.1 and Figure 3.6), together with no detection of increased thoracic radiolabelled content at 4 hours after LPS inhalation (Figure 3.18), suggested that the decrease in blood platelet counts might have more complex origins.

Biodistribution studies were therefore carried out in order to explore the effect of LPS inhalation on distribution of radiolabelled platelets between the blood, lung, liver, spleen and the bronchoalveolar space.

3.3.2 Results – biodistribution of radiolabelled platelets

Effect of LPS inhalation on the quantity of radiolabelled platelets in blood

LPS inhalation decreased the quantity of ^{111}In-labeled platelets recovered in blood at 4 hours after challenge (percentage of ^{111}In-labelled platelets remaining in blood, PBS vs. LPS: 78.5±2.4% vs. 50.0±4.2%, P<0.001), but not at 48 hours from challenge (percentage of ^{111}In-labelled platelets remaining in blood, PBS vs. LPS: 42.7±4.2% vs. 33.8±3.9%, P=0.18) (Figure 3.19).

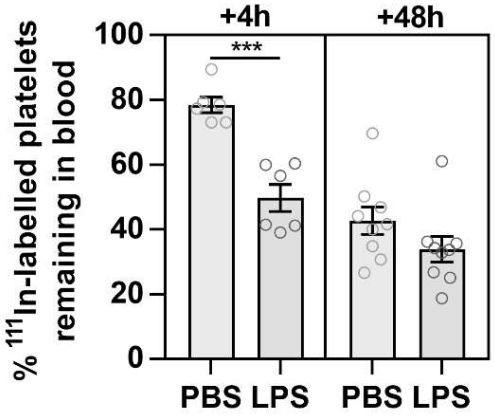

Figure 3.19: Effect of LPS inhalation on radiolabelled platelet content of blood. Mice were administered ^{111}In-labelled platelets intravenously, then PBS or LPS intranasally, and cardiac blood collected at 4 and 48 hours after intranasal challenge for measurement of platelet retention in blood. Mean ± standard error, 4 hours time point: n=6, 48 hour time point: n=9, 2-way ANOVA with Holm's test for LPS effect within time points, ***=P<0.001.

Effect of LPS inhalation on the quantity of radiolabelled platelets recruited to lungs

Lungs were collected and surface blood was removed by rolling on blotting paper. In order to account for the effect of alterations in remaining blood platelet content, a recruitment index was calculated in a similar manner to previously described radiolabelled platelet bio-distribution studies (Andonegui et al., 2005; Looney et al., 2009), by dividing the percentage of injected ^{111}In-labelled platelets in lungs with their retained blood, by the percentage of injected ^{111}In-labelled platelets remaining in the blood.

LPS inhalation had no detected effect on recruitment of ^{111}In-labelled platelets to lungs at 4 hours after challenge (PBS vs. LPS lung/blood ratios: 0.074±0.005 vs. 0.093±0.010, P=0.156), but at 48 hours after challenge LPS inhalation increased ^{111}In-labelled platelet recruitment to lungs (PBS vs. LPS lung/blood ratios: 0.090±0.005 vs. 0.122±0.008, P=0.008) (Figure 3.20).

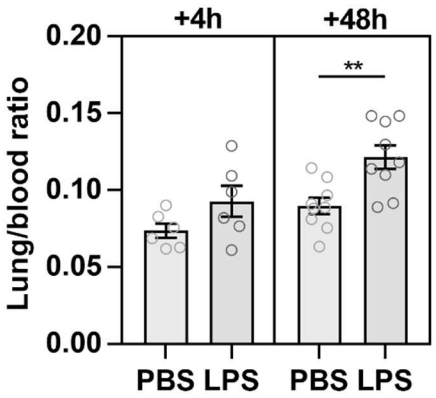

Figure 3.20: Effect of LPS inhalation on radiolabelled platelet recruitment to lungs. Mice were administered ^{111}In-labelled platelets intravenously, then PBS or LPS intranasally. Lungs and blood were collected at 4 and 48 hours after intranasal challenge. The % ^{111}In-labelled platelet radioactivity of the lungs was divided by the % of injected ^{111}In-labelled platelet radioactivity remaining in the blood to measure lung platelet recruitment. Mean ± standard error, 4 hours time point: n=6, 48 hour time point: n=9, 2-way ANOVA with Holm's test for LPS effect within time points, **=P<0.01.

Effect of LPS inhalation on the quantity of radiolabelled platelets recruited to the liver

Livers were collected in a similar manner to lungs. LPS inhalation increased the recruitment of ^{111}In-labelled platelets to the liver at 4 hours after challenge (PBS vs. LPS liver/blood ratios: 0.126±0.021 vs. 0.307±0.078, P=0.004). At 48 hours after intranasal challenge liver ^{111}In-labelled platelet recruitment was not significantly different between PBS and LPS-challenged mice (PBS vs. LPS liver/blood ratios: 0.819±0.055 vs. 1.146±0.090, P=0.087) (Figure 3.21).

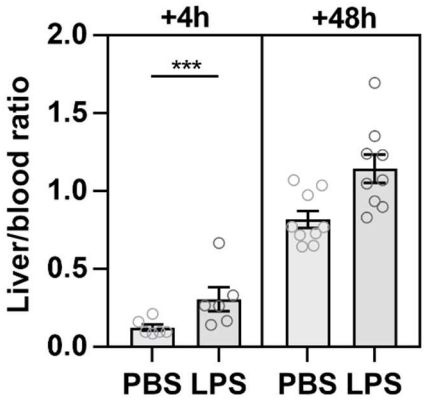

Figure 3.21: Effect of LPS inhalation on radiolabelled platelet recruitment to the liver. Mice were administered ^{111}In-labelled platelets intravenously, then PBS or LPS intranasally. Livers and blood were collected at 4 and 48 hours after intranasal challenge. The % ^{111}In-labelled platelet radioactivity of the liver was divided by the % of injected ^{111}In-labelled platelet radioactivity remaining in the blood to measure liver platelet recruitment. Mean ± standard error, 4 hours time point: n=6, 48 hour time point: n=9, 2-way ANOVA with Holm's test for LPS effect within time points, ***=P<0.001.

Effect of LPS inhalation on the quantity of radiolabelled platelets recruited to the spleen

Spleens were collected in a similar manner to lungs. LPS inhalation also increased splenic recruitment of ^{111}In-labelled platelets at 4 hours after challenge (PBS vs. LPS spleen/blood ratios: 0.162±0.024 vs. 0.297±0.059, P=0.014), but 48 hours after intranasal challenge splenic ^{111}In-labelled platelet recruitment was not significantly different between PBS and LPS-challenged mice (PBS vs. LPS spleen/blood ratios: 0.670±0.068 vs. 0.732±0.085, P=0.085) (Figure 3.22).

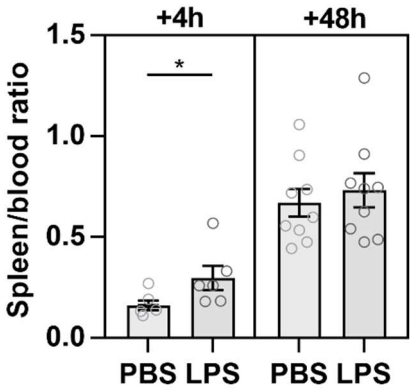

Figure 3.22: Effect of LPS inhalation on radiolabelled platelet recruitment to the spleen. Mice were administered ^{111}In-labelled platelets intravenously, then PBS or LPS intranasally. Spleens and blood were collected at 4 and 48 hours after intranasal challenge. The % ^{111}In-labelled platelet radioactivity of the spleen was divided by the % of injected ^{111}In-labelled platelet radioactivity remaining in the blood to measure spleen platelet recruitment Mean ± standard error, 4 hours time point: n=6, 48 hour time point: n=9, 2-way ANOVA with Holm's test for LPS effect within time points, *=P<0.05.

Effect of LPS inhalation on the quantity of radiolabelled platelets in BAL

As immunohistochemistry staining indicated the presence of platelets inside the bronchoalveolar airspace, the migration of radiolabelled platelets into airspaces was quantified by measurement of radioactivity in BAL.

LPS inhalation had no detectable effect on recovery of ^{111}In-labelled platelets in BAL at 4 hours after challenge (Percentage of injected ^{111}In-labelled platelets per ml of BAL, PBS vs. LPS: 0.009±0.002 vs. 0.007±0.002, P=0.520) but at 48 hours after challenge LPS inhalation increased the recovery of ^{111}In-labelled platelets in BAL (Percentage of injected ^{111}In-labelled platelets per ml of BAL, PBS vs. LPS: 0.008±0.002 vs. 0.024±0.004, P=0.003) (Figure 3.23).

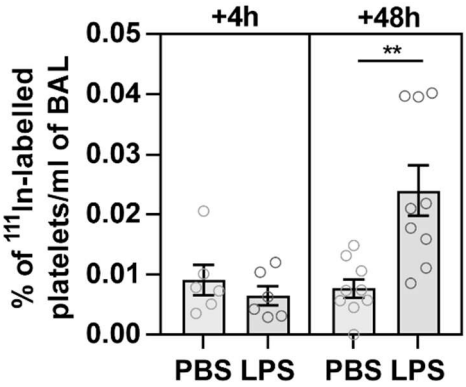

Figure 3.23: Effect of LPS inhalation on the quantity of radiolabelled platelets in BAL. Mice were administered ^{111}In-labelled platelets intravenously, then PBS or LPS intranasally. BAL fluid was collected at 4 and 48 hours after exposure and ^{111}In-platelet content quantified. Mean ± standard error, 4 hours time point: n=6, 48 hour time point: n=9, 2-way ANOVA with Holm's test for LPS effect within time points, **=P<0.01.

Effect of LPS inhalation on the quantity of neutrophils in BAL

In mice used for radiolabelled platelet studies, LPS inhalation increased the number of neutrophils detected in BAL at 4 hours after challenge (PBS vs. LPS: 5.1±2.4 $\times 10^3$ vs. 1.2±0.4 $\times 10^4$ neutrophils per ml of BAL, P=0.013), and at 48 hours after challenge (PBS vs. LPS: 3.8±2.8 $\times 10^2$ vs. 2.5±0.3 $\times 10^6$ neutrophils per ml of BAL, P=0.001), confirming successful induction of experimental lung inflammation responses to LPS at each time point in mice used for biodistribution experiments (Figure 3.24).

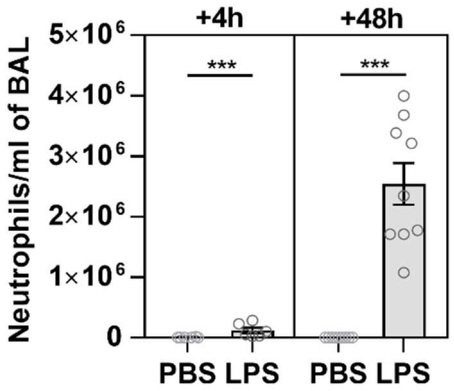

Figure 3.24: Effect of LPS inhalation on the quantity of neutrophils in BAL. LPS inhalation increased the number of neutrophils in BAL fluid at 4 and 48 hours after intranasal challenge in mice used for ^{111}In-labelled platelet studies. Mean ± standard error, 4 hours time point: n=6, 48 hour time point: n=9, 2-way ANOVA with Holm's test for LPS effect within time points, ***=P<0.001.

Effect of LPS inhalation on biodistribution of radiolabelled platelets infused 24 hours after intranasal challenge

The effect of LPS inhalation on the biodistribution of radiolabelled platelets infused 24 hours after intranasal chellenge was also measured in an attempt to decrease the effects of radiolabel decay and platelet lifespan on reducing signal over the course of a 48 hour response, and to see whether the potentially confounding factor of thrombocytopenia temporally associated with hepatic and splenic platelet accumulation at 4 hours after intranasal challenge could be circumvented by infusing radiolabelled platelets later on in the course of the inflammatory response.

As blood platelet counts returned to normal levels 24 hours after LPS inhalation (Figure 3.18), radiolabelled platelets were infused 24 hours after intranasal challenge. When samples

were collected at 48 hours after intranasal challenge, no effects of LPS inhalation were detected on the quantity of radiolabelled platelets remaining in blood (percentage of ^{111}In-labelled platelets remaining in blood, PBS vs. LPS: 60.6±6.0% vs. 49.4±5.1%, P=0.184), or on the recruitment of radiolabelled platelets to lungs (PBS vs. LPS lung/blood ratios: 0.080±0.010 vs. 0.088±0.010, P=0.448). Increased radiolabelled platelet recruitment to the liver (PBS vs. LPS liver/blood ratios: 0.280±0.017 vs. 0.449±0.032, P<0.001), and the spleen (PBS vs. LPS spleen/blood ratios: 0.316±0.035 vs. 0.418±0.023, P=0.049), was however detected in this experiment.

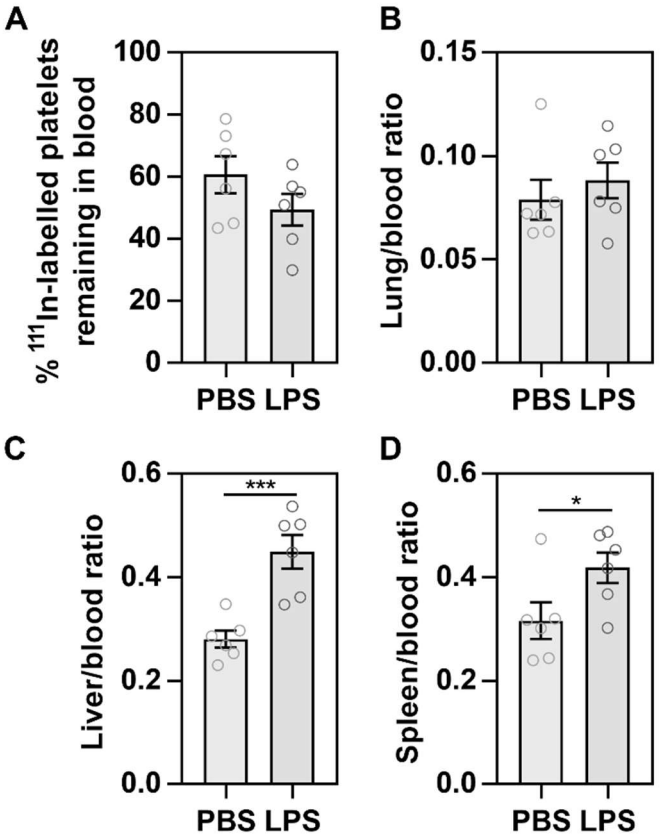

Figure 3.25: Effect of LPS inhalation on biodistribution of radiolabelled paltelets infused 24 hours after intranasal challenge. Mice were administered PBS or LPS intranasally, then ^{111}In-labelled platelets were given i.v. 24 hours after intranasal challenge. ^{111}In-platelet biodistribution measurements were made at48 hours after intranasal chellenge. (A) The percentage of ^{111}In-labelled platelets remaining in blood, as well as (B) lung, (C) liver and (D) spleen recruitment ratios were measured. Data shown as a ratio of % ^{111}In-labelled platelet radioactivity of the organ of interest, divided by the % of injected ^{111}In-labelled platelet radioactivity remaining in the blood. Means ± standard error, n=6 , unpaired t-tests, *=P<0.05, ***=P<0.001.

LPS inhalation increased total BAL radiolabelled platelet content (ANOVA main effect of LPS inhalation on percentage of injected ^{111}In-labelled platelets per ml of BAL, PBS vs. LPS: 0.005±0.001 vs. 0.009±0.001% per ml of BAL, $F(1,10)=17.07$, $P=0.002$) (Figure 3.26A).

In these experiments BAL was also centrifuged to enable the separate measurement of the cell pellet containing cells and platelets, and the BAL supernatant potentially containing

platelet microparticles, which have size and density properties which mean that they would not be pelleted by the centrifugation cycle used (Lacroix et al., 2013), or ^{111}In released from cleared platelets that had moved into the lung with plasma protein. LPS inhalation increased radiolabelled platelet content of both BAL cell pellet (Percentage of injected ^{111}In-labelled platelets per ml of BAL, PBS vs. LPS: 0.001±0.0004 vs. 0.003±0.0004, P=0.011) and BAL supernatant (Percentage of injected ^{111}In-labelled platelets per ml of BAL, PBS vs. LPS: 0.004±0.001 vs. 0.006±0.001, P=0.005) (Figure 3.26A). As a greater amount of radiolabel was detected in the supernatant of samples from both PBS and LPS-treated mice, it is possible that the majority of the ^{111}In radiolabel detected in airspaces was no longer platelet-associated at this time point.

BAL neutrophil content was also increased with inhalation of LPS (PBS vs. LPS: 4.9±4.1 $\times 10^3$ vs. 3.8±0.4 $\times 10^6$ neutrophils per ml of BAL, P=0.001) (Figure 3.26B).

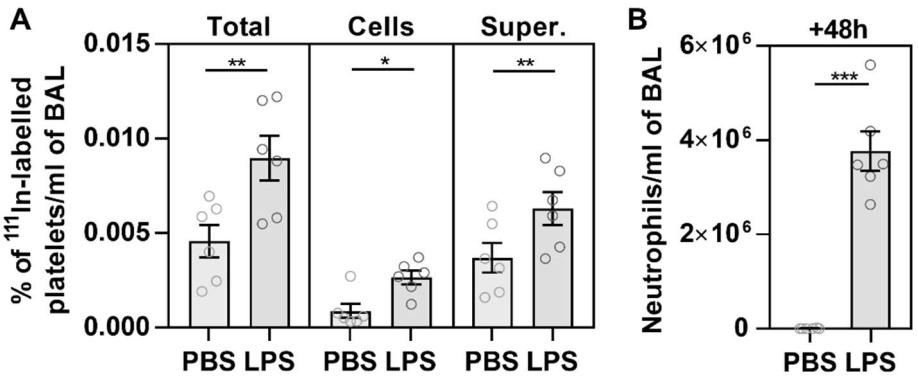

Figure 3.26: Effect of LPS inhalation on BAL platelet and neutrophil content when radiolabelled platelets were infused 24 hours after intranasal challenge. Mice were administered PBS or LPS intransally, and 24 hours afterwards, ^{111}In-labelled platelets infused intravenously. BAL fluid was collected 48 hours after LPS exposure to measure (A) ^{111}In-labelled platelet, and (B) LPS neutrophil content. Means ± standard error, n=6 , 2-way ANOVA with repeated measures or unpaired t-test, *=P<0.05, **=P<0.01, ***=P<0.001.

3.3.3 Summary – biodistribution of radiolabelled platelets

Investigations into the effects of LPS inhalation on the biodistribution of radiolabelled platelets allowed for several findings. Firstly, radiolabelled platelet recruitment data was concordant with platelet immunostaining data (Figure 3.1) in that platelet recruitment to lungs was detected at 48, but not at 4, hours after LPS challenge.

The detection of decreased retention of radiolabelled platelets in blood at 4 hours after LPS inhalation was also consistent with data from blood platelet counts.

Increased liver and spleen platelet recruitment at 4 hours after LPS inhalation provides an explanation for the decrease in blood platelet counts at this time point, and for the failure of non-invasive measurements of thoracic radioactivity to detect radiolabelled platelet recruitment to lungs. It is unclear from this dataset whether the platelets recruited to lungs are those recruited earlier to the spleen or liver or are a separate population of platelets, more advanced whole-body platelet tracking experiments may prove enlightening.

Quantification of BAL radioactivity supported data from immunohistochemistry experiments in suggesting that platelets migrate into the bronchaolveolar space following LPS inhalation, although this increase may also have been the result of increased movement of free ^{111}In radiolabel released from platelets into the bronchoalveolar space.

Limitations of studies using radiolabelled platelets include the manipulation of platelets required *ex vivo* for radiolabelling, the supraphysiological blood platelet counts imposed following platelet transfusions, and the requirement of donor mice which increases the number

of mice required for experiments. Genetically modified mice expressing fluorescent proteins restricted to platelets are available, so a method for investigating genetically labelled platelet recruitment to lungs was therefore sought.

3.4 Intravital microscopy

3.4.1 Background – intravital microscopy

The effect of LPS inhalation on lung platelet-leukocyte interactions made visible using intravital microscopy has been previously explored using genetic labelling of platelets in mice (Ortiz-Muñoz et al., 2014), but total lung platelet recruitment and the nature of lung platelet recruitment was not studied in these experiments. Platelets and megakaryocytes can now be observed more clearly at lower laser powers using multiphoton microscopy to image the lungs of mice with platelet and megakaryocyte membranes labelled with GFP (PF4-cre × mTmG mice) (Lefrançais et al., 2017).

In order to directly image the effects of LPS inhalation on platelets in the living pulmonary circulation, intravital multiphoton microscopy video recordings were made in lungs of PF4-cre × mTmG mice at 48 hours after intranasal exposure to LPS or PBS control during a two month travelling fellowship to the laboratory of Prof. Mark Looney at UCSF.

3.4.2 Results – intravital microscopy

Effects of LPS inhalation on total quantity of platelets in the lung microcirculation

Platelets could be detected in the lungs of PF4-cre × mTmG mice using intravital multiphoton microscopy. The total flux of detected platelets was measured frame-by-frame with a 0.91 frames per second acquisition rate. There was no significant effect of LPS inhalation detected on the total platelet flux detected in lung fields (PBS vs. LPS: 1,599±105 vs. 1,884±256 platelets per mm^2 of lung field/frame, P=0.223) (Figure 3.28). Single platelets

were successfully identified but this method may favour detection of slower-moving platelets as some platelets appeared blurred by motion.

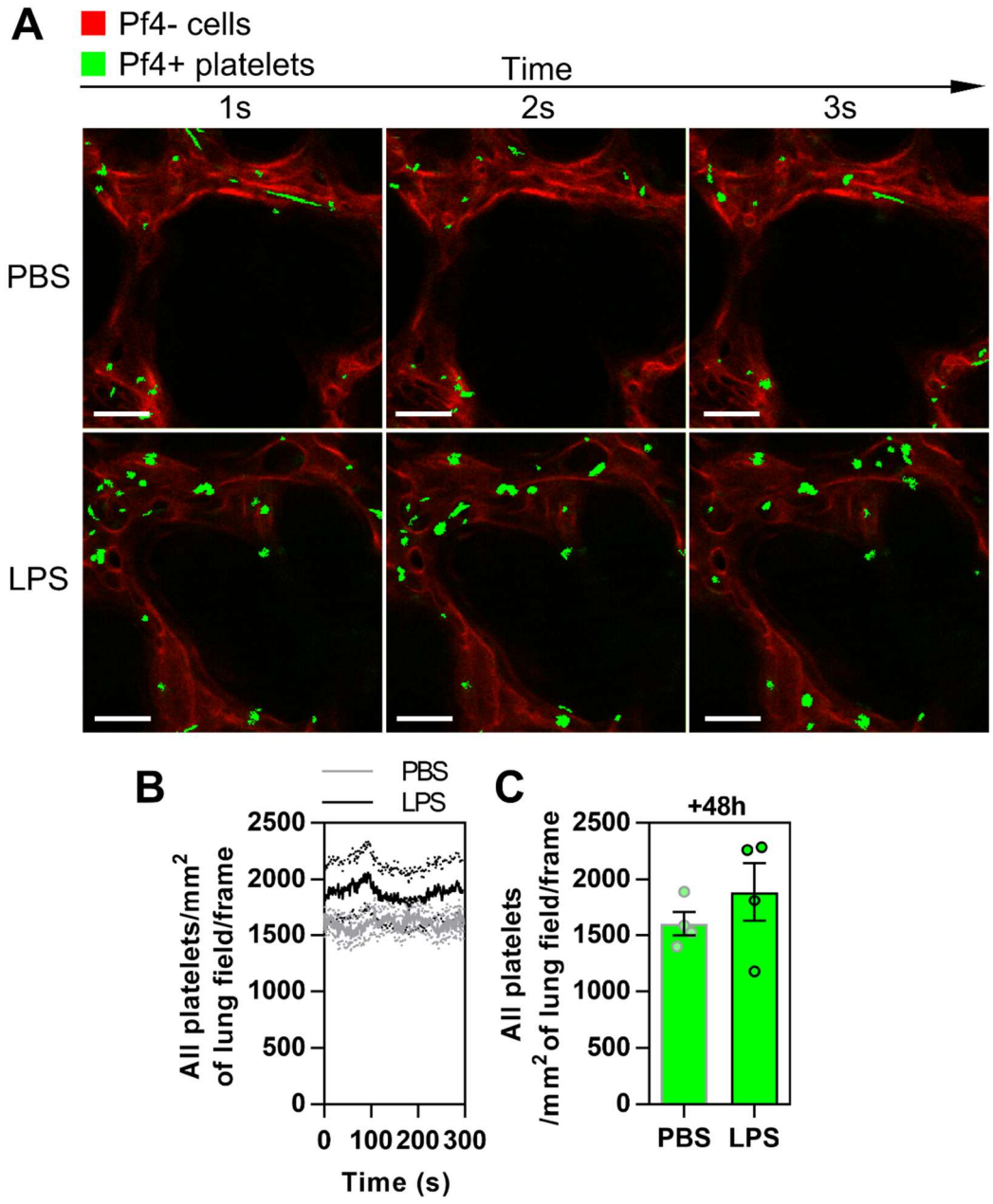

Figure 3.27: Effect of LPS inhalation on lung platelet flux. (A) Pf4+ platelets (green) and Pf4- cells (red) were imaged in lungs of PF4-cre × mTmG mice at 48 hours after PBS control (top row) or LPS inhalation (bottom row). (B,C) Quantification of total detected flux of platelets. Scale bars = 20µm. Means ± standard error, n=4.

Effects of LPS inhalation on the quantity of adhesive platelets in the lung microcirculation

In order to focus analysis on adhesive platelets, tracking software was used to isolate a population of adhesive platelets which did not move between frames too fast (velocity <2 µm per second) or too far (position <5 SD from that predicted by a random motion model), to be considered as free flowing in the blood circulation.[12] LPS inhalation increased the number of adhesive platelets detected in lungs (PBS vs. LPS: 714±59 vs. 1,050±81 adhesive platelets per mm^2 of lung field/frame, P=0.017) (Figure 3.28A,B,C). Adhesion events were largely transient, occurring over seconds, with no significant effect of LPS inhalation detected on adhesion duration (Duration of platelet adhesion events:, PBS vs. LPS: 3.2±0.3 vs. 4.5±0.5, P=0.054) (Figure 3.28D).

[12] Representative videos and a demonstration of the platelet adhesion tracking method can be seen at http://www.bit.do/intravital.

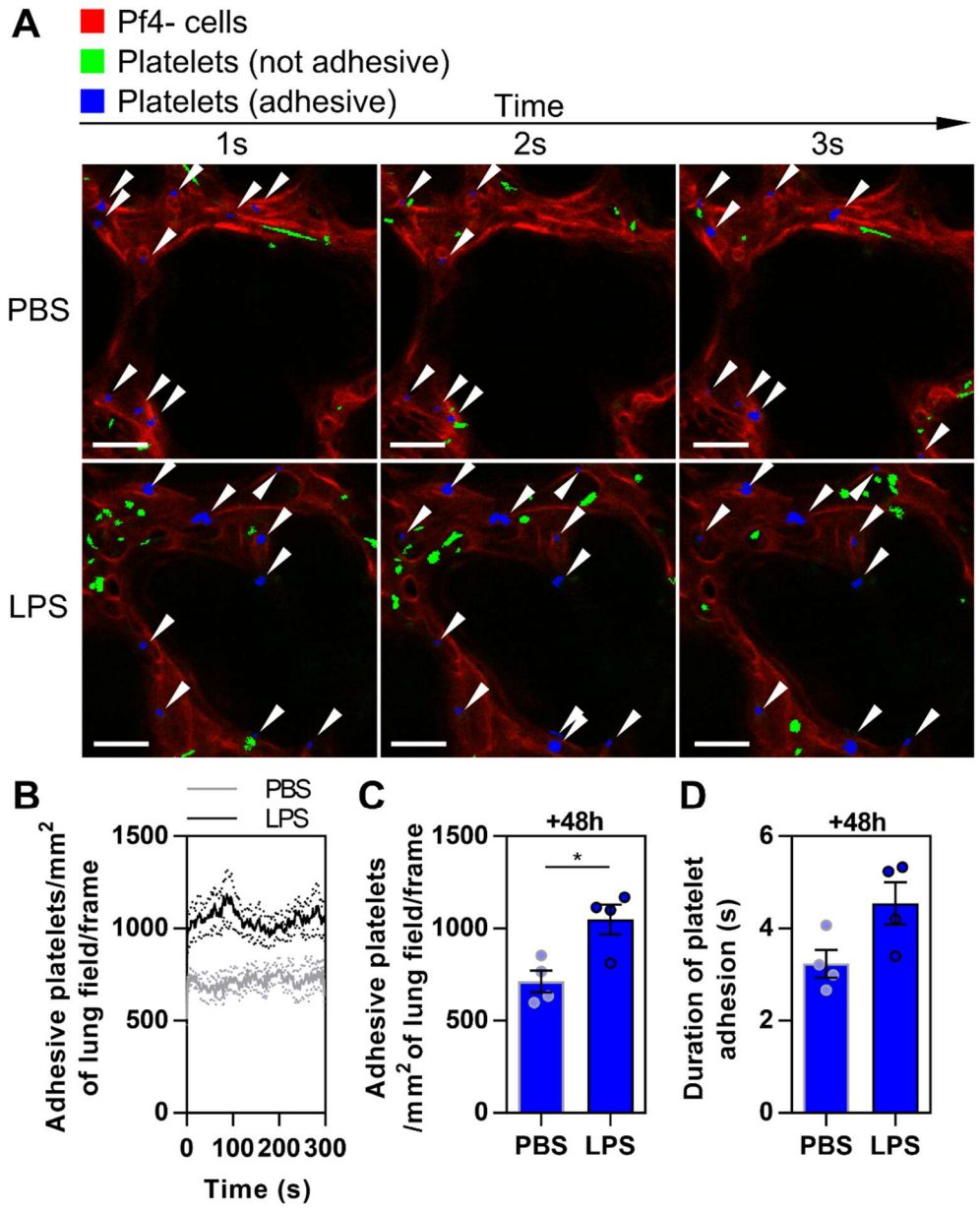

Figure 3.28: Effect of LPS inhalation on lung platelet adhesion. (A) Pf4+ platelets (green or blue) and Pf4- cells (red) were imaged in lungs of PF4-cre × mTmG mice at 48 hours after PBS control (top row) or LPS inhalation (bottom row). Adhesive platelets were tracked between frames (blue, emphasised with white arrowheads). (B,C) Quantification of adhesive platlets over time. (D) Duration of platelet adhesion event. Scale bars = 20µm. Means ± standard error, n=4, unpaired t-tests, *=P<0.05.

Effects of LPS inhalation on BAL neutrophils in mice observed with intravital microscopy

BAL was collected from mice used for intravital microscopy after imaging was completed in order to provide evidence that neutrophil recruitment had occured. LPS inhalation increased neutrophil counts in BAL (PBS vs. LPS: 0.00±0.00 vs. 2.37±1.09 $\times 10^6$ neutrophils per ml of BAL, P<0.001), confirming experimental induction of lung inflammation in these mice.

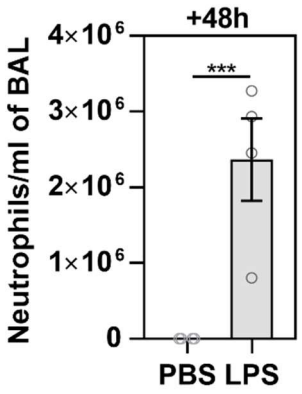

Figure 3.29: Effect of LPS inhalation on BAL neutrophil content of mice used for intravital microscopy. Mice were administered PBS or LPS intranasally, and BAL was collected after intravital microscopy at 48 hours following exposure. Means ± standard error, n=4, unpaired t-test, ***=P<0.001.

3.4.3 Summary – intravital microscopy

Intravital microscopy videos revealed that platelet recruitment to the lungs appeared to involve platelet adhesion. Similarly to lung platelet staining using immunohistochemistry, there was no apparent sign of gross thrombotic events. The adhesive platelets were not visibly attached to neutrophils, although this method did not allow for clear detection of neutrophils, and capillaries with adhesive platelets appeared perfused as platelets could be seen moving

through the vasculature of all preparations, and the majority of adhesion events occurred transiently before release back into the circulation.

3.5 Summary – methods for measuring LPS-induced lung platelet recruitment

In summary, three different methods for measuring lung platelet recruitment were successfully adapted for use with a mouse LPS inhalation model, and each enabled the characterisation of different aspects of the phenomenon of lung platelet recruitment following lung inflammation induced by LPS inhalation (Table 3.1).

Table 3.1: Aspects of lung platelet recruitment revealed by three different methods.

	Method		
	Immunohistochemistry	**Radiolabelled platelet tracking**	**Intravital microscopy**
Detected effect of LPS inhalation on platelets:	↑ platelet content of sample fields of lungs	↑ platelet recruitment to whole lung	↑ platelet adhesion in sample fields of lungs
	↑ platelet content of bronchoaveolar space		

In order to further investigate the mechanistic basis of the lung platelet recruitment response, studies were carried out to test the effects of interventions targeting neutrophils, neutrophil platelet interactions, and receptors expressed by platelets. The immunohistochemical quantification of CD42b+ platelets in lungs was chosen as the first method to use for measuring LPS-induced lung platelet recruitment in interventional studies as this method had relatively high throughput and sensitivity compared to radiolabelling studies, revealed a more complete population of lung platelets than the method for CD41 immunostaining, did not suffer from interference from administration depleting or blocking antibodies, and was readily available in our laboratory.

4 Results II: Investigations into mechanisms of LPS-induced lung platelet recruitment

4.1 Effects of treatment with neutrophil-depleting antibodies

4.1.1 Background – neutrophil depletion

Lung neutrophil recruitment following LPS inhalation can depend on the presence of platelets (Kornerup et al., 2010; Grommes et al., 2012; Pan et al., 2015), which is suggestive that platelet recruitment might precede and enable neutrophil recruitment. However, lung neutrophil recruitment was detected before lung platelet recruitment in the LPS inhalation model used in this study, and platelet interactions with neutrophils could also conceivably mediate lung platelet recruitment, as has previously been demonstrated in platelet recruitment to lungs following intraperitoneal LPS (Andonegui et al., 2005), and following priming with inhaled LPS and acute lung injury with subsequent intravenous anti-MHCI antibody treatment (Looney et al., 2009).

The neutrophil dependence of platelet recruitment following LPS inhalation in the absence of any exogenous intravascular or systemic pro-inflammatory stimulus is so far unexplored, and the method of neutrophil depletion used in previous studies investigating the neutrophil dependence of platelet responses also used depletion methods which targeted functionally important Ly6-C+ Ly6-G- inflammatory monocytes in addition to Ly6-C- Ly6-G+ neutrophils (Daley et al., 2008).

The effect of antibody treatment-mediated neutrophil depletion through selective targeting of Ly6-G on platelet recruitment induced by LPS inhalation was therefore investigated.

4.1.2 Results – neutrophil depletion

Effects of LPS inhalation and anti-Ly6-G treatment on blood neutrophil counts

Blood neutrophil counts were made from serial tail microsamples in order to confirm experimental neutrophil depletion (Figure 4.1).

Treatment with anti-Ly6-G antibody caused a profound and sustained removal of polymorphonuclear neutrophils from the systemic circulation over the course of the experiment in both PBS control mice and mice challenged with LPS. Anti-Ly6-G antibody administration caused neutrophil depletion immediately before intranasal challenge (0h) (PBS+control IgG vs. PBS+anti-Ly6-G: 1.04±0.13 vs. 0.07±0.05 $\times 10^6$ neutrophils per ml; LPS+control IgG vs. LPS+anti-Ly6-G: 8.02±0.92 vs. 2.15±1.22 $\times 10^5$ neutrophils per ml, both $P<0.001$).

Neutrophil depletion was maintained 4 hours (PBS+control IgG vs. PBS+anti-Ly6-G: 2.30±0.36 vs. 0.05±0.02 $\times 10^6$ neutrophils per ml; LPS+control IgG vs. LPS+anti-Ly6-G: 1.71±0.39 vs. 0.06±0.01 $\times 10^6$ neutrophils per ml, both $P<0.001$), 24 hours (PBS+control IgG vs. PBS+anti-Ly6-G: 9.08±1.20 vs. 0.45±0.15 $\times 10^5$ neutrophils per ml; LPS+control IgG vs. LPS+anti-Ly6-G: 1.23±0.30 vs. 0.06±0.01 $\times 10^6$ neutrophils per ml, both $P<0.001$), and 48 hours after intranasal challenge (PBS+control IgG vs. PBS+anti-Ly6-G: 1.28±0.19 vs. 0.04±0.01 $\times 10^6$ neutrophils per ml; LPS+control IgG vs. LPS+anti-Ly6-G: 2.10±0.60 vs. 0.06±0.01 $\times 10^6$ neutrophils per ml, both $P<0.001$) (Figure 4.1).

No effect of LPS inhalation on blood neutrophil counts was detected at any of the time points investigated when comparing control IgG or anti-Ly6-G-treated mice (ANOVA main effect of LPS inhalation on blood neutrophil counts $F(1,44)=0.67$, $P=0.418$, Figure 3.24).

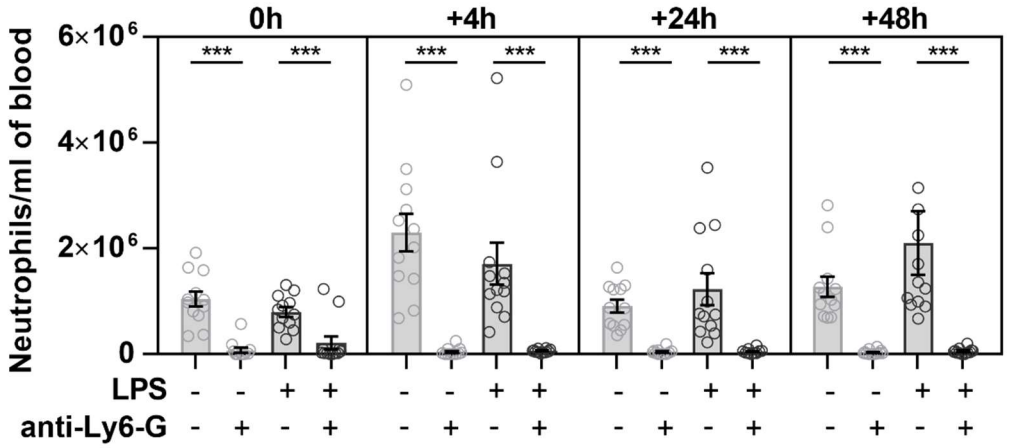

Figure 4.1: Effect of LPS inhalation and anti-Ly6-G antibody treatment on blood neutrophil counts. Mice were administered either control IgG or anti-Ly6-G antibody at -24h, -1h, and +24h in relation to intranasal administration of PBS or LPS. Serial tail blood microsamples were used to quantify blood neutrophils immediately before (0h), and at +4h, +24h, and +48h after PBS or LPS administration. One data point in the +48h LPS+control IgG group (8.25×10^6 neutrophils per ml of blood) is off the scale of the graph, but was included in the analysis. Mean ± standard error, n=12, 3-way ANOVA with repeated measures and Holm's test for LPS and anti-Ly6-G treatment effects, ***=$P<0.001$.

Blood mononuclear cell counts were unaltered with anti-Ly6-G antibody treatment, with the exception of LPS-treated mice at 4 hours after intranasal challenge, possibly due to the involvement of monocytes in neutrophil clearance, or due to a reduction in the cytokine response triggering mobilisation of inflammatory monocytes (See Appendix Figure 4.27).

Effects of LPS inhalation and neutrophil depletion on quantity of neutrophil elastase in lungs

Neutrophil depletion with anti-Ly6-G antibody treatment decreased the quantity of neutrophil elastase detected in both PBS control mice (PBS+control IgG vs. PBS+anti-Ly6-G: 0.06±0.02 vs. 0.01±0.01% of lung fields neutrophil elastase positive, P=0.001), and in mice exposed to intranasal LPS (LPS+control IgG vs. LPS+anti-Ly6-G: 7.85±2.81 vs. 1.58±0.40% of lung fields neutrophil elastase positive, P=0.003). Although the LPS-induced increase in lung neutrophil elastase staining was reduced by ~80%, the quantity of lung neutrophil elastase was increased by LPS inhalation in both control mice (P<0.001), and neutrophil depleted mice (P<0.001).

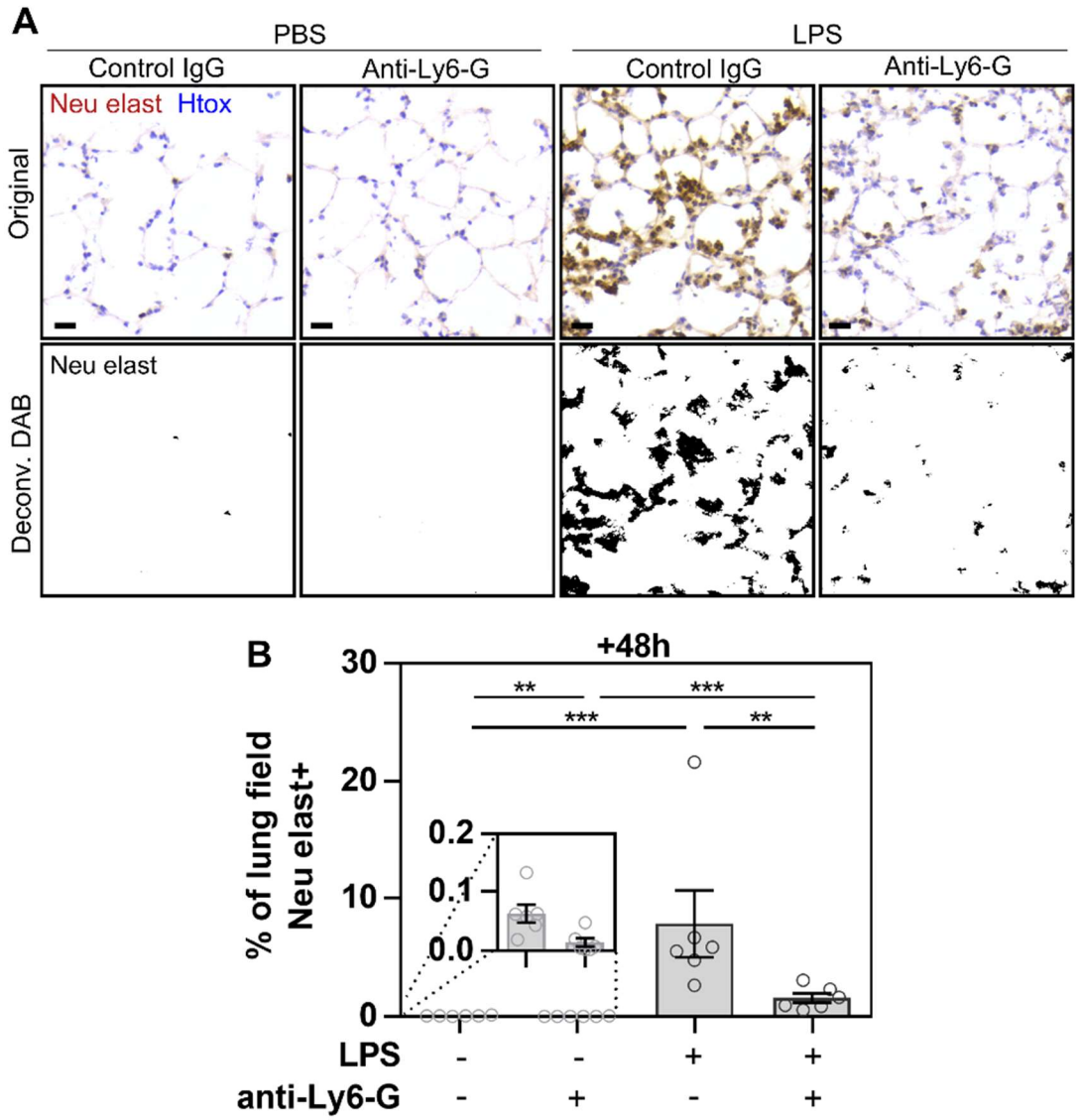

Figure 4.2: Effect of neutrophil depletion on LPS-induced increases in lung neutrophil elastase staining. Mice were administered either control IgG or anti-Ly-6G antibody at -24h, -1h, and +24h in relation to intranasal administration of PBS or LPS, and lungs were harvested at +48h and processed for immunohistochemistry (A) Neutrophil elastase was immunostained in lung sections, and in sample fields neutrophil elastase DAB reporter positivity (brown in top row) was deconvoluted (black in bottom row, from same images as top row) for image analysis. Scale bar = 20 µm. (B) Quantification of neutrophils in lung sections. Mean ± standard error, n=6, 2-way ANOVA with Holm's test for LPS and anti-Ly6-G treatment effects, **=P<0.01, ***=P<0.001.

Effects of LPS inhalation and neutrophil depletion on BAL neutrophil counts

Neutrophil depletion with anti-Ly6-G antibody treatment decreased the quantity of neutrophils in the bronchoalveolar space following intranasal LPS challenge (LPS+control IgG vs. LPS+anti-Ly6-G: 3.72±0.06 vs. 0.55±0.13 $\times 10^6$ neutrophils per ml of BAL, P<0.001), with no detected effect of anti-Ly6-G treatment on PBS control mice (PBS+control IgG vs. PBS+anti-Ly6-G: 880±553 vs. 0±0 neutrophils per ml of BAL, P=0.867) (Figure 4.3).

LPS inhalation resulted in increased BAL neutrophil counts in both control IgG-reated mice (P<0.001), and anti-Ly6-G antibody treated mice (P<0.001), indicating that neutrophil recruitment to the bronchoalveolar airspaces was still occurring in neutrophil-depleted mice, although reduced in magnitude by ~85% (Figure 4.3).

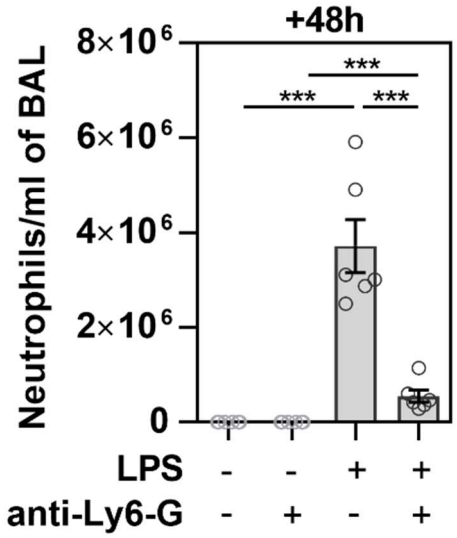

Figure 4.3: Effects of LPS inhalation and neutrophil depletion on BAL neutrophil counts. Mice were administered either control IgG or anti-Ly6-G antibody at -24h, -1h, and +24h in relation to intranasal administration of PBS or LPS, and BAL was conducted at +48h . Mean ± standard error, n=6, 2-way ANOVA with Holm's test for LPS and anti-Ly6-G treatment effects, **=P<0.01, ***=P<0.001.

The number of monocyte/macrophages recovered in BAL was not significantly altered by anti-Ly6-G antibody treatment (see Appendix Figure 4.28).

Effects of LPS inhalation and neutrophil depletion on lung CD42b+ platelet recruitment

LPS inhalation increased the number of platelets detected in lungs in both control IgG treated mice (PBS+control IgG vs. LPS+control IgG: 74±12 vs. 829±111 CD42b+ platelets per mm^2 of lung fields, $P<0.001$), and neutrophil depleted mice (PBS+anti-Ly6-G vs. LPS+anti-Ly6-G: 149±39 vs. 661±57 CD42b+ platelets per mm^2 of lung fields, $P<0.001$) (Figure 4.4).

There was no detected effect of anti-Ly6G antibody treatment on quantity of CD42b+ platelets in lung fields between mice exposed to intranasal PBS control ($P=0.173$), or between LPS-challenged mice ($P=0.527$) (Figure 4.4).

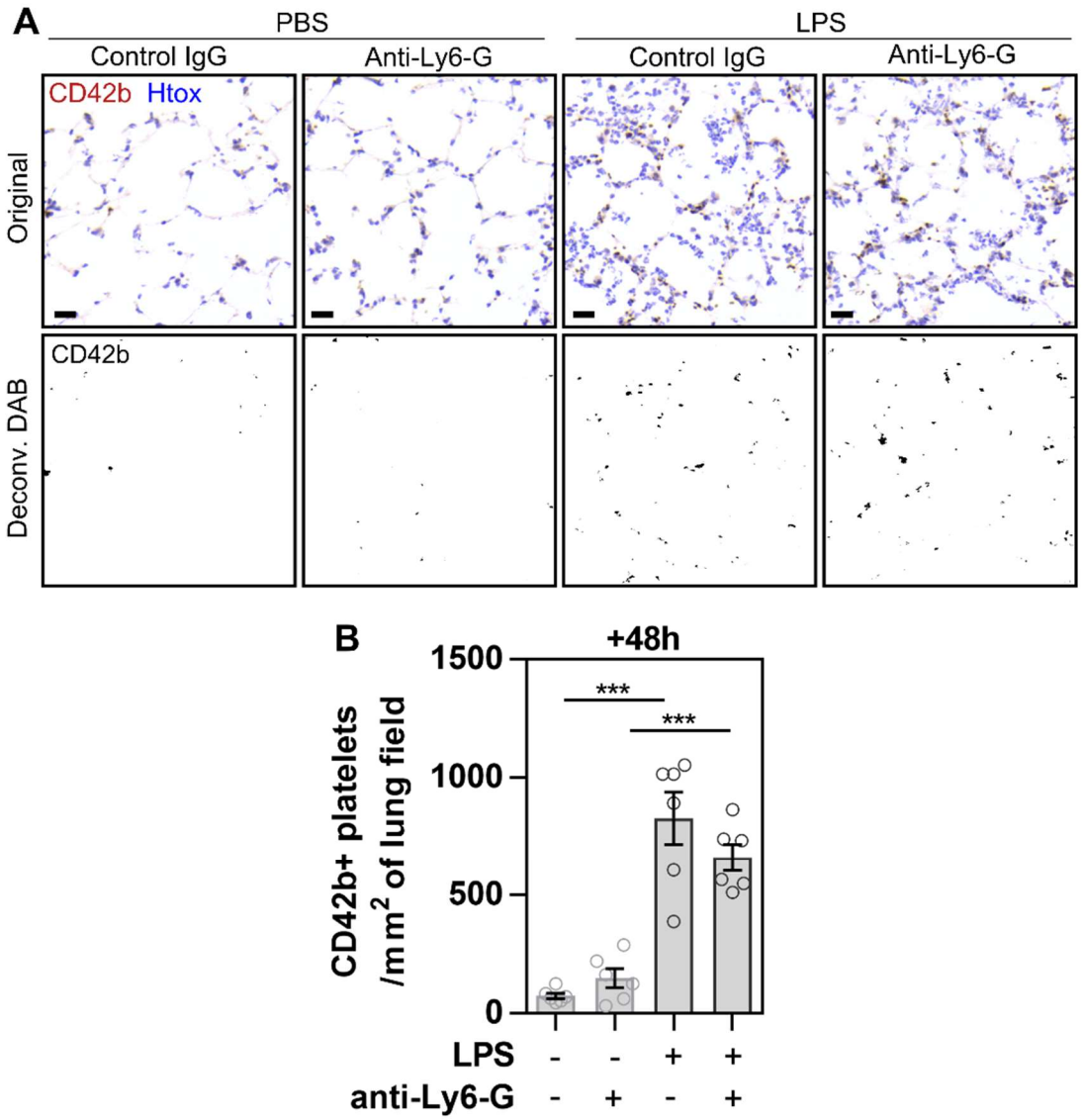

Figure 4.4: Effect of neutrophil depletion on LPS-induced increases in lung CD42b platelet staining. Mice were administered either control IgG or anti-Ly6-G antibody at -24h, -1h, and +24h in relation to intranasal administration of PBS or LPS, and lungs were collected at +48h and processed for immunohistochemistry (A) Platelet CD42b was immunostained in lung sections, and in sample fields CD42b DAB reporter positivity (brown in top row) was deconvoluted (black in bottom row, from same images as top row) for image analysis. Scale bar = 20 µm. (B) Quantification of platelets in lung sections. Mean ± standard error, n=6, 2-way ANOVA with Holm's test for LPS and anti-Ly6-G treatment effects, ***=P<0.001.

Effects of LPS inhalation and neutrophil depletion on blood platelet counts

Blood platelet counts were also made from serial tail blood microsamples, primarily to investigate the effects of neutrophil depletion on the previously observed LPS-induced decrease in blood platelet counts at 4 hours after intranasal challenge.

Both LPS inhalation and neutrophil depletion were found to have additive and temporally distinct effects towards causing decreases in blood platelet counts (Figure 4.5). There was no detected effect of anti-Ly6-G treatment immediately before intranasal challenge (0h). At 4 hours after intranasal challenge LPS inhalation reduced blood platelet counts in both control IgG-treated mice (PBS+control IgG vs. LPS+control IgG: 1.16±0.05 vs. 0.87±0.04×10^9 platelets per ml of blood, P=0.002), and neutrophil-depleted mice (PBS+anti-Ly6-G vs. LPS+anti-Ly6-G: 8.48±0.32 vs. 5.91±0.33 ×10^8 platelets per ml of blood, P<0.001). Neutrophil depletion caused further reductions in blood platelet counts in both mice challenged with PBS control (P<0.001), and LPS-challenged mice (P<0.001).

At 24 hours after intranasal challenge there was no longer a significant LPS-induced reduction in blood platelet counts in mice treated with control IgG (PBS+control IgG vs. LPS+control IgG: 1.16±0.05 vs. 0.87±0.04×10^9 platelets per ml of blood, P=0.002), but neutrophil depleted mice still had significantly lower blood platelet counts if they were challenged with LPS (PBS+anti-Ly6-G vs. LPS+anti-Ly6-G: 1.11±0.05 vs. 0.58±0.03 ×10^9 platelets per ml of blood P<0.001). The effect of neutrophil depletion on decreasing blood platelet counts remained in both PBS control mice (P<0.001), and mice challenged with LPS (P<0.001).

At 48 hours after intranasal challenge there was no detected effect of LPS inhalation in either control or depleted mice, but neutrophil depletion had reduced blood platelet counts in both PBS (PBS+control IgG vs. PBS+anti-Ly6-G: 1.18±0.07 vs. 0.89±0.05 $\times 10^9$ platelets per ml of blood P<0.001), and LPS (LPS+control IgG vs. LPS+anti-Ly6-G: 1.06±0.08 vs. 0.74±0.04 $\times 10^9$ platelets per ml of blood, P<0.001), challenged mice.

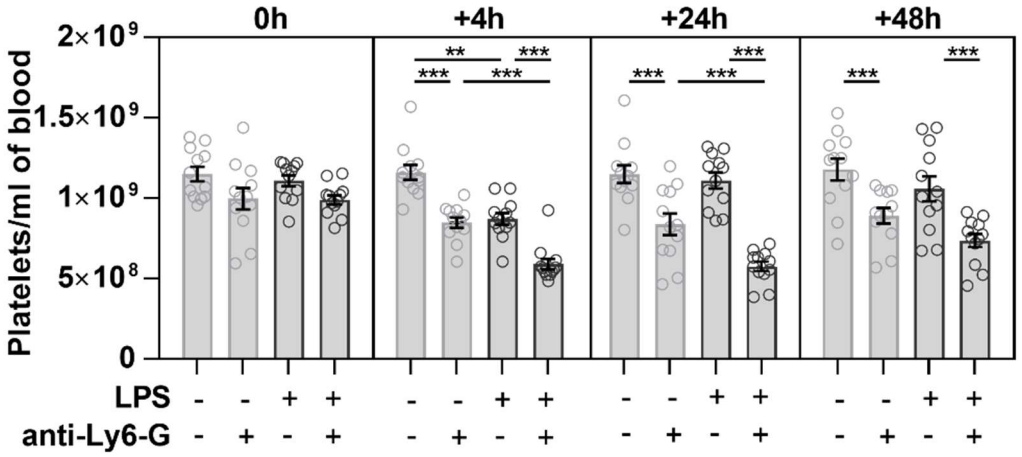

Figure 4.5: Effects of LPS inhalation and neutrophil depletion on blood platelet counts. Mice were administered either control IgG or anti-Ly6-G antibody at -24h, -1h, and +24h in relation to intranasal administration of PBS or LPS, and serial tail blood microsamples were used to quantify blood platelet counts. Mean ± standard error, n=12, 3-way ANOVA with repeated measures and Holm's test for LPS and anti-Ly6-G treatment effects, **=P<0.01, ***=P<0.001.

Effects of LPS inhalation and neutrophil depletion on the quantity of PF4 in BAL and blood plasma

The quantity of PF4 in BAL and blood plasma was measured as an index of platelet α-granule release in the lung airspaces and in systemic blood.

LPS inhalation increased the quantity of PF4 detected in BAL in both control IgG-treated mice (PBS+control IgG vs. LPS+control IgG: 13±13 vs. 134±16 pg of PF4 per ml of BAL

supernatant, P<0.001), and anti-Ly6-G antibody-treated mice (PBS+anti-Ly6-G vs. LPS+anti-Ly6-G: 5±3 vs. 160±48 pg of PF4 per ml of BAL supernatant, P<0.001). There was no detected effect of anti-Ly6-G treatment between PBS (P=0.999) or LPS-challenged mice (P=0.999) (Figure 4.6A).

LPS inhalation had no effect on the quantity of PF4 detected in blood plasma in both control IgG-treated mice (PBS+control IgG vs. LPS+control IgG: 213±55 vs. 268±34 ng of PF4 per ml of BAL supernatant, P=0.721), or in anti-Ly6-G antibody-treated mice (PBS+anti-Ly6-G vs. LPS+anti-Ly6-G: 345±54 vs. 221±64 ng of PF4 per ml of BAL supernatant, P=0.324). There was no detected effect of anti-Ly6-G treatment between PBS (P=0.324) or LPS-challenged mice (P=0.721) (Figure 4.6B).

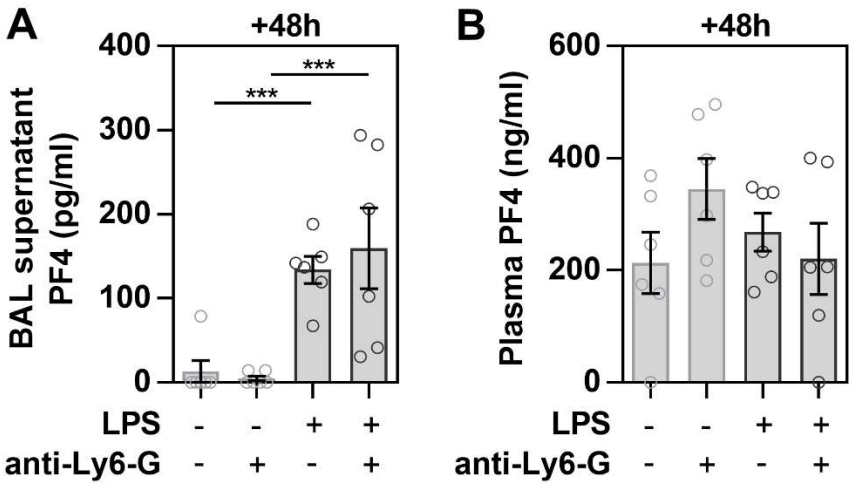

Figure 4.6: Effects of neutrophil depletion and LPS inhalation on the quantity of PF4 in BAL and plasma. Mice were administered either control IgG or anti-Ly6-G antibody at -24h, -1h, and +24h in relation to intranasal administration of PBS or LPS, and PF4 was measured by ELISA in BAL supernatant and blood plasma collected at 48 hours after intranasal challenge. Mean ± standard error, n=6, 2-way ANOVA and Holm's test for LPS and anti-Ly6-G treatment effects, ***=P<0.001.

Effects of LPS inhalation and neutrophil depletion on body weight change

Body weight was monitored over the course of the experiment as an index of general health status, starting from 24 hours before intranasal challenge at the first injection of control or dpleting antibody treatment. Both LPS inhalation and neutrophil depletion had effects on decreasing body weight (Figure 4.7). Immediately before intranasal challenge (0h, 24 hours after first antibody doses and baseline weight recordings), a small decrease in body weight change was detected in PBS controls (PBS+control IgG vs. PBS+anti-Ly6-G: 2.0±0.7 vs. -0.4±0.4% change in body weight, P=0.041), but there was no significant effect of neutrophil depletion detected between the groups of mice subsequently challenged with LPS (LPS+control IgG vs. LPS+anti-Ly6-G: 0.9±0.5 vs. -0.7±0.6% change in body weight, P=0.096).

At 24 hours after intranasal challenge an effect of LPS inhalation on decreasing body weight was detected in both control mice and neutrophil depleted mice (both $P<0.001$). Neutrophil depletion decreased body weight relative to controls in mice receiving PBS intranasally (PBS+control IgG vs. PBS+anti-Ly6-G: 2.0±0.7 vs. -0.4±0.4% change in body weight, $P=0.001$). No effect of neutrophil depletion was detected in LPS treated mice (LPS+control IgG vs. LPS+anti-Ly6-G: -10.8±0.6 vs. –11.2±1.0% change in body weight, $P=0.631$).

At 48 hours after intranasal challenge an effect of LPS inhalation on decreasing body weight was detected in both control mice and neutrophil depleted mice (both $P<0.001$). Additionally, neutrophil depletion decreased body weight relative to controls when comparing mice receiving PBS intranasally (PBS+control IgG vs. PBS+anti-Ly6-G: 0.9±0.8 vs. -1.7±0.6% change in body weight, $P=0.031$) and in mice exposed to LPS intranasally (LPS+control IgG vs. LPS+anti-Ly6-G: -16.2±0.7 vs. –18.3±0.9% change in body weight, $P=0.041$).

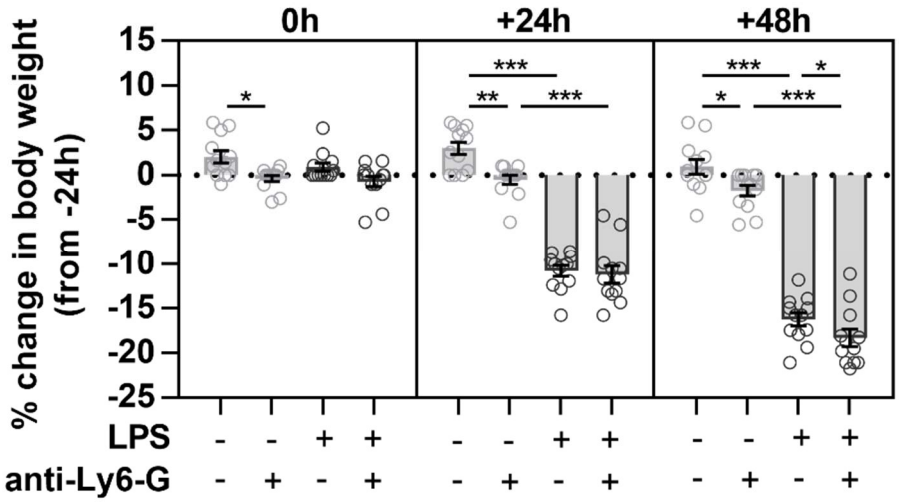

Figure 4.7: Effects of LPS inhalation and neutrophil depletion on body weight change. Mice were administered either control IgG or anti-Ly6-G antibody at -24h, -1h, and +24h in relation to intranasal administration of PBS or LPS, and mice were weighed at 0h +24h and +48h. Means ± standard error, 3-way ANCOVA with baseline values at 24 hours before intranasal challenge fit as covariates, Holm's test for within-time point LPS and anti-Ly6-G treatment effects, *=P<0.05, **=P<0.01, ***=P<0.001.

Associating lung platelet content with lung neutrophil elastase content

With the hypothesis that if increases in lung platelet content were dependent on neutrophils, lung CD42b+ platelet counts would be expected to have a positive correlation with the percentage of lung fields covered by neutrophil elastase, the quantity of CD42b+ platelets and neutrophil elastase detected in lungs of mice in LPS groups with no additional treatment shown in Figure 4.4, Figure 4.11, and Figure 4.16 were pooled for correlation analysis.

Pearson's correlation was used to test goodness of fit (R^2) and P-values are reported representing the probability of obtaining an R^2 value as high as that which was observed from experimental data from randomly selected data points as calculated with an F-test.

No evidence of positive correlation was found with raw data (R^2=0.040, P=0.371) (Figure 4.8A), or when this dataset was log transformed (R^2=0.080, P=0.202) (Figure 4.8B). As results from *in vivo* experiments and quantification of immunohistochemistry varied from batch to batch, data from the three experiments carried out at different times were normalised to the means of each individual dataset. Normalised data showed no positive correlation (R^2=0.117, P=0.119) (Figure 4.8C). and when normalised data were logarithmically transformed the line of best fit became significantly non-zero but the correlation was still only weakly positive (R^2=0.220, P=0.028) (Figure 4.8D).

Conclusions of correlation analyses were unaltered with removal of the very high neutrophil elastase value (notable in Figure 4.8A, value where % of lung field neutrophil elastase+ is >20), with the exception of normalised, log transformed data, where the R^2 value became not significantly different from that would be expected with randomly selected data points (R^2=0.144, P=0.090).

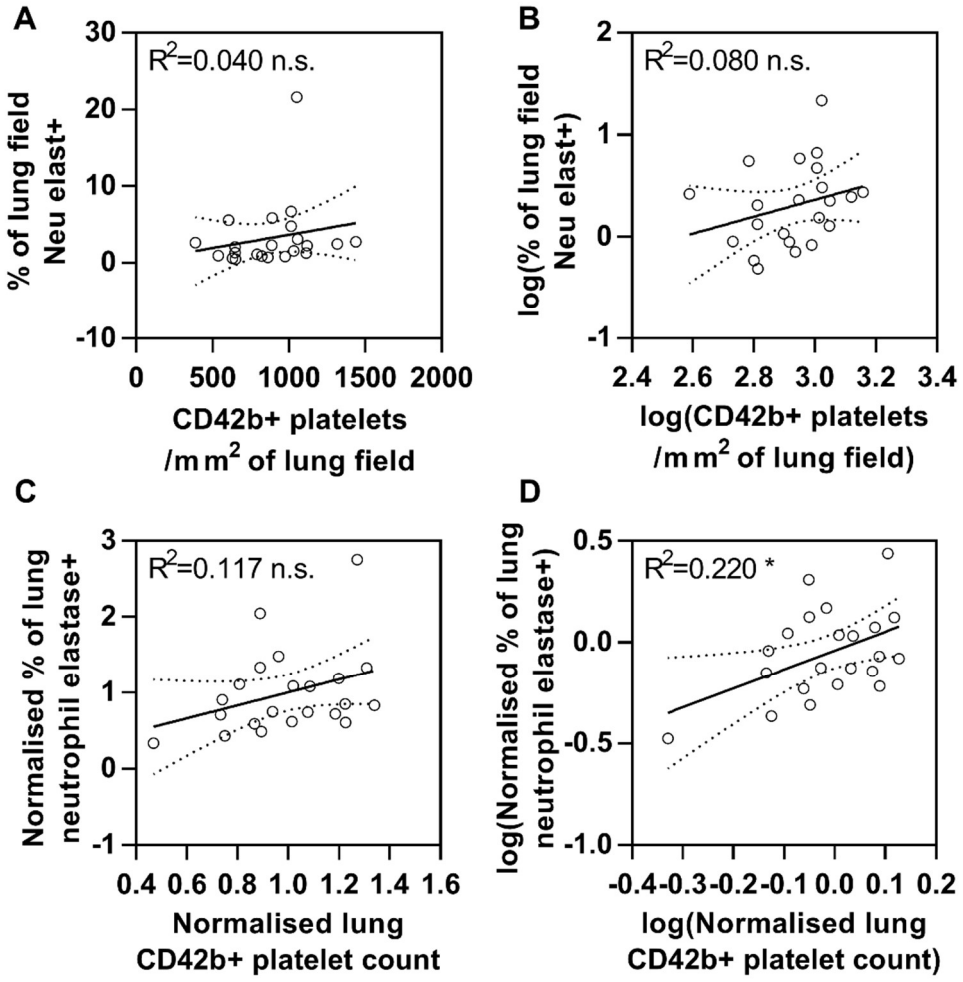

Figure 4.8: Association of lung platelet content and lung neutrophil elastase content following LPS inhalation. At 48 hours after LPS (+control IgG or vehicle) treatment, CD42b+ platelets and neutrophil elastase were quantified in lung sections (pooled data from **Figure 4.4**, **Figure 4.11**, and **Figure 4.16**). Correlations were measured using (A) raw data, (B) log transformed data, (C) data normalised to average values for the 3 separate datasets, and (D) log normalised data. Line of best fit and 95% confidence bands shown, n=22, Pearson's correlation, R^2 values and results of F-test for significantly non-zero slope are shown, * = $P<0.05$.

4.1.3 Summary – neutrophil depletion

Treatment with anti-Ly6-G antibody caused neutrophil depletion in the blood sustained over the course of the experiment, reduced LPS-induced increases in neutrophil elastase in lungs by ~80%, and reduced LPS-induced neutrophil recruitment to the bronchoalveolar space by ~85%. In contrast, neutrophil depletion had no detected effect on LPS-induced lung platelet recruitment, suggesting that neutrophils are not critical for the lung platelet recruitment response.

The fact that no effect of neutrophil depletion was detected on LPS-induced lung platelet recruitment despite decreased blood platelet counts in neutrophil depleted mice, and the observation that the quantity of neutrophil elastase and platelets in LPS-inflamed lungs displayed an absence of, or a weak, positive correlation, both lend further support to the hypotheisis that lung platelet recruitment occurred independently of neutrophils.

Furthermore, the detection of increased quantities of PF4 following LPS inhalation in BAL supernatant, but not in blood plasma, are suggestive of platelet α-granule release in the lungs, and the lack of any detected effect of neutrophil depletion on the BAL PF4 increase response is suggestive that LPS-induced platelet activation in lungs, and potentially in lung airspaces, does not show neutrophil-dependence. However, these data should be interpreted with some caution, as PF4 levels are high in plasma, and so increases in PF4 content of BAL may be a result of movement of blood plasma into airspaces, and so further methods for measuring platelet activation are required.

Although the neutrophil depletion strategy used in this model reduced LPS-induced lung neutrophil recruitment, the lung neutrophil recruitment response to LPS inhalation was not

completely prevented, so it is possible that activity of remaining neutrophils may have been sufficient to promote neutrophil-dependent responses, and neutrophil depletion may have had some adverse effects on mice as depleted mice showed increased weight loss and decreased blood platelet counts. Methods for more specifically targeting platelet-neutrophil interactions were therefore sought.

4.2 Effects of treatment with blocking antibodies against P-selectin or PSGL-1

4.2.1 Background – P-selectin or PSGL-1 blockade

The adhesion and signalling molecules P-selectin and PSGL-1 are binding partners which can mediate platelet-leukocyte, platelet-endothelial cell and leukocyte-endothelial cell interactions (Page and Pitchford, 2013), with both P-selectin and PSGL-1 expressed by platelets (Frenette et al., 2000; Pan et al., 2015). P-selectin has been implicated in the recruitment of platelets to rabbit lungs following LPS infusion into rabbits (Kiefmann et al., 2006), whilst in mice exposed to LPS *via* inhalation, blockade of PSGL-1, but not P-selectin, reduced neutrophil recruitment to BAL (Kornerup et al., 2010), whereas at an earlier time point blockade of P-selectin reduced LPS-induced neutrophil rolling and adhesion in the tracheal circulation (Pan et al., 2015).

The potential involvement of both P-selectin and PSGL-1 in both LPS-induced platelet and neutrophil recruitment to lungs offered an opportunity for finding out more about the mechanisms of lung platelet recruitment, and the relationship of lung platelet recruitment to neutrophil recruitment, so the effects of blockade of P-selectin or PSGL-1 on lung platelet recruitment and on inflammatory responses were investigated.

4.2.2 Results – P-selectin or PSGL-1 blockade

Effects of blockade of P-selectin or PSGL-1 on LPS-induced neutrophil recruitment to BAL

Intranasal challenge with LPS caused an increase in BAL neutrophil content (PBS vs. LPS+control IgG: 0.00±0.00 vs. 1.97±0.60 $\times 10^6$ neutrophils per ml of BAL, P<0.001). Similar to the results obtained by Kornerup et al., (2010), P-selectin blockade had no detected effect on BAL neutrophil content (1.61±0.45 $\times 10^6$ neutrophils per ml of BAL, P=0.283 vs. LPS+control IgG), but PSGL-1 blocking antibody treatment reduced the quantity of neutrophils present in BAL by ~51% (to 0.96±0.23 $\times 10^6$ neutrophils per ml of BAL, P<0.001 vs. LPS+ control IgG) (Figure 4.9).

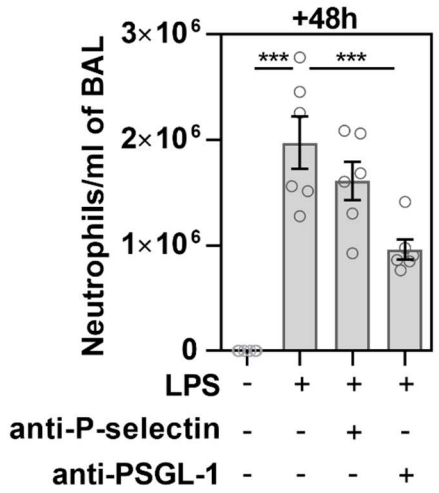

Figure 4.9: Effect of blockade of P-selectin or PSGL-1 on LPS-induced BAL neutrophil recruitment. Mice were administered either control IgG, anti-P-selectin antibody, or anti-PSGL-1 antibody at -1h, and +24h in relation to intranasal administration of PBS or LPS, and BAL was collected at +48h. Means ± standard error, n=6, one-way ANOVA with Dunnett's test for difference vs. LPS+control IgG group, ***=P<0.001.

Effect of blockade of P-selectin or PSGL-1 on LPS-induced increases in lung neutrophil elastase content

LPS inhalation increased the quantity of neutrophil elastase immunostaining detected in images of lungs (PBS+control IgG vs. LPS+control IgG: 0.18±0.03 vs. 2.07±0.27 % of lung fields neutrophil elastase positive, $P<0.001$), with neutrophil elastase staining in lungs significantly increased with anti-P-selectin blocking antibody treatment (5.45±1.37 % of lung fields neutrophil elastase positive, $P=0.049$ vs. LPS+control IgG), and no detected effect of anti-PSGL-1 blocking antibody treatment (1.67±0.23 % of lung fields neutrophil elastase positive, $P=0.758$ vs. LPS+control IgG) (Figure 4.10). Unlike quantification of BAL neutrophils quantification of neutrophil elastase in lung sections does not distinguish between intra- and extravascular neutrophils, and effects of P-selectin on blood platelet counts (see Figure 4.13) and effects of PSGL-1 on preventing successful neutrophil transendothelial and transepithelial migration

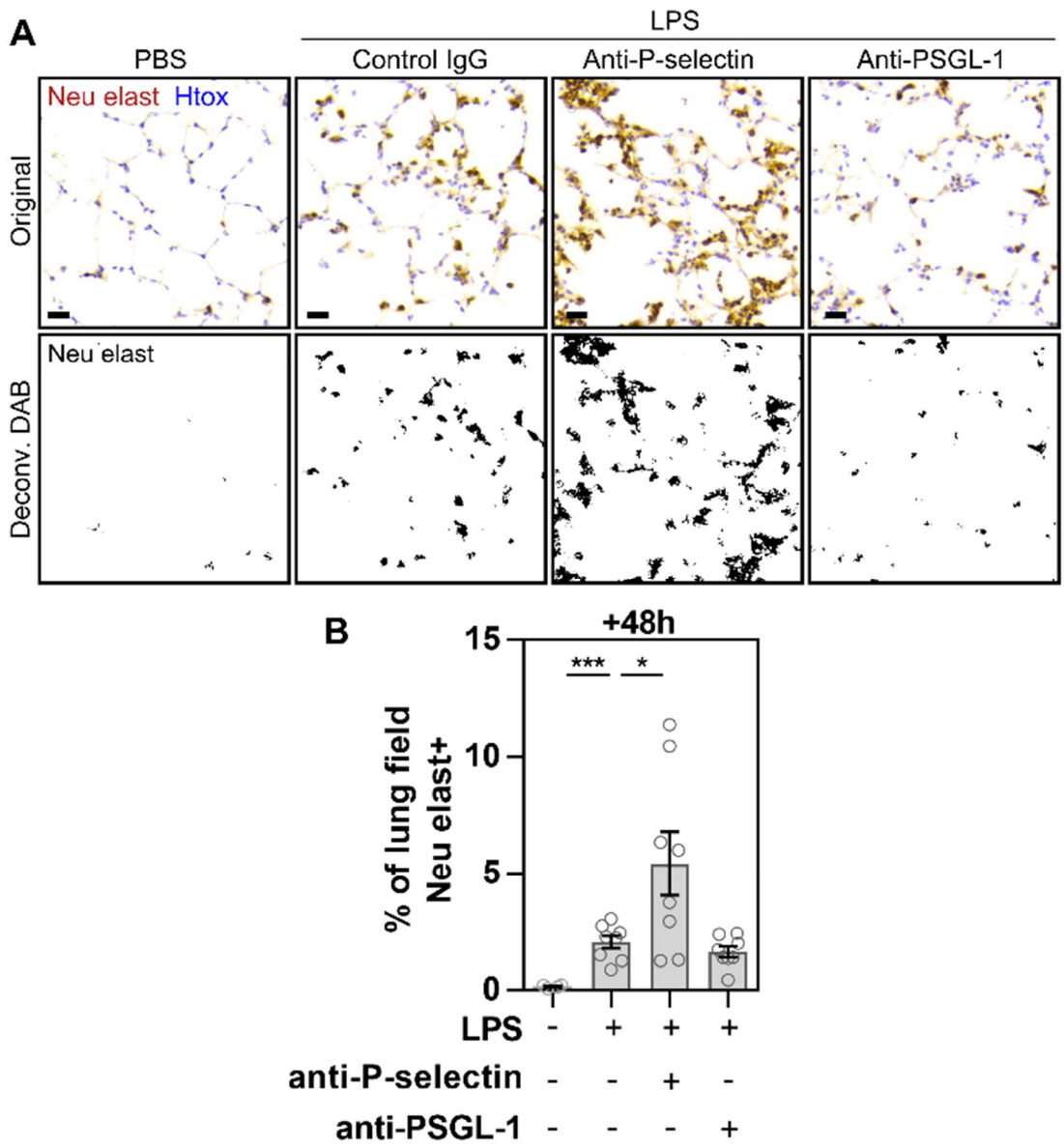

Figure 4.10: Effect of blockade of P-selectin or PSGL-1 on LPS-induced increases in lung neutrophil elastase content. Mice were administered either control IgG, anti-P-selectin antibody, or anti-PSGL-1 antibody at -1h, and +24h in relation to intranasal administration of PBS or LPS, and lungs were harvested at +48h and processed for immunohistochemistry (A) Neutrophil elastase was immunostained in lung sections, and in sample fields neutrophil elastase DAB reporter positivity (brown in top row, with haematoxylin counterstain in blue) was deconvoluted (black in bottom row, from same images as top row) for image analysis. Scale bar = 20 µm. (B) Quantification of neutrophil elastase stain in lung sections. Means ± standard error, PBS group: n=4, LPS groups: n=8, one-way ANOVA with Dunnett's test for difference vs. LPS+control IgG group, *=P<0.05, ***=P<0.001.

Effect of blockade of P-selectin or PSGL-1 on LPS-induced lung CD42b+ platelet recruitment

LPS inhalation increased the quantity of CD42b+ platelets detected in images of lungs (PBS+control IgG vs. LPS+control IgG: 581±157 vs. 1099±204 CD42b+ platelets per mm^2 of lung fields, $P<0.001$), but no effect was detected on this response of blockade of either P-selectin (1153±236 CD42b+ platelets per mm^2 of lung fields, $P=0.973$ vs. LPS+control IgG) or PSGL-1 (1022±277 CD42b+ platelets per mm^2 of lung fields, $P=0.799$ vs. LPS+control IgG) (Figure 4.11).

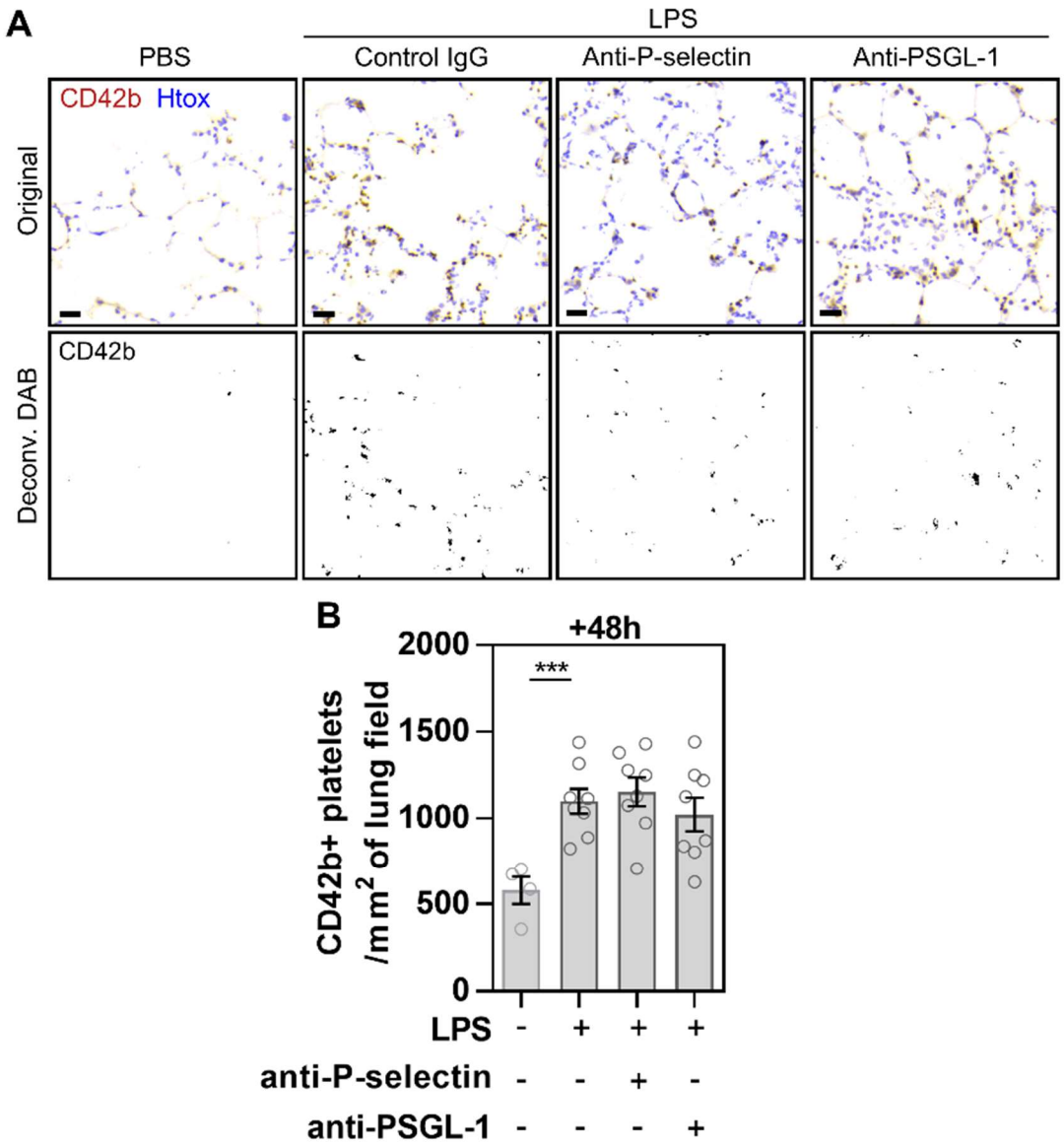

Figure 4.11: Effect of blockade of P-selectin or PSGL-1 on LPS-induced lung CD42b+ platelet recruitment. Mice were administered either control IgG, anti-P-selectin antibody, or anti-PSGL-1 antibody at -1h, and +24h in relation to intranasal administration of PBS or LPS, and lungs were collected at +48h and processed for immunohistochemistry (A) Platelet CD42b was immunostained in lung sections, and in sample fields CD42b DAB reporter positivity (brown in top row, with haematoxylin counterstain in blue) was deconvoluted (black in bottom row, from same images as top row) for image analysis. Scale bar = 20 µm. (B) Quantification of CD42b+ platelets in lung tissue. Means ± standard error, PBS group: n=4, LPS groups: n=8, one-way ANOVA with Dunnett's test for difference vs. LPS+control IgG group, ***=P<0.001.

Effect of blockade of P-selectin or PSGL-1 on the effect of LPS inhalation on blood platelet counts

Similarly to previous studies, LPS inhalation decreased blood platelet counts at 4 hours after intranasal challenge (PBS+control IgG vs. LPS+control IgG: 1.43±0.06 vs. 1.02±0.06 $\times 10^9$ platelets per ml of blood, P<0.001). Neither blockade of P-selectin (1.07±0.07 $\times 10^9$ platelets per ml of blood, P=0.868 vs. LPS+control IgG), nor PSGL-1 (1.00±0.05 $\times 10^9$ platelets per ml of blood, P=0.990 vs. LPS+control IgG), significantly altered this response (Figure 4.12).

Similarly to previous experiments, no significant effect of LPS inhalation was detected at 48 hours after intranasal challenge, and no effect of treatement with either blocking antibody was detected at this time point (Figure 4.12).

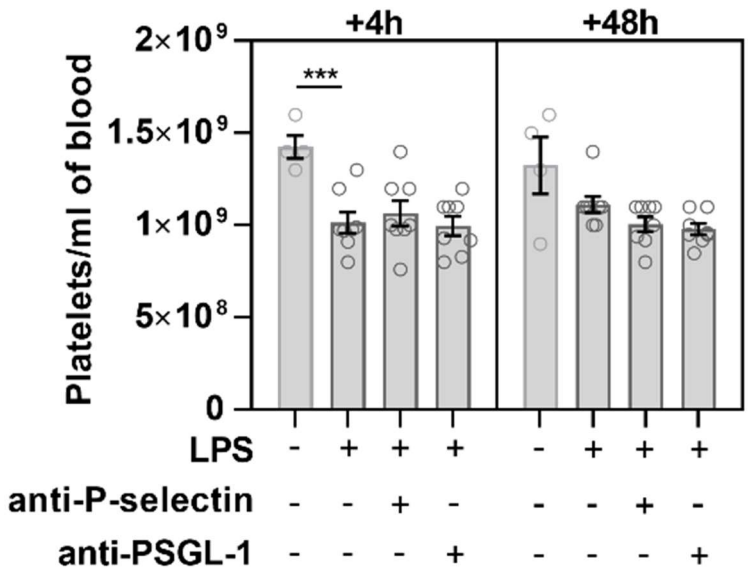

Figure 4.12: Effect of blockade of P-selectin or PSGL-1 on the effect of LPS inhalation on blood platelet counts. Mice were administered either control IgG, anti-P-selectin antibody, or anti-PSGL-1 antibody at -1h, and +24h in relation to intranasal administration of PBS or LPS,and circualting platelet counts were measured at +4h and +48h. Means ± standard error, PBS group: n=4, LPS groups: n=8, two-way ANOVA with repeated measures and Holm's test for difference vs. LPS+control IgG group, ***=P<0.001.

Effect of blockade of P-selectin or PSGL-1 and LPS inhalation on blood neutrophil counts

LPS inhalation increased the quantity of neutrophils detected in blood at 4 hours after intranasal challenge (PBS+control IgG vs. LPS+control IgG: 0.77±0.10 vs. 1.85±0.45 $\times 10^6$ neutrophils per ml of blood, P=0.035), with neither anti-P-selectin antibody treatment (2.69±0.21 $\times 10^6$ neutrophils per ml of blood, P=0.060), nor anti-PSGL-1 antibody treatment (1.55±0.15 $\times 10^6$ neutrophils per ml of blood, P=0.999), significantly altering blood neutrophil counts in the context of LPS inhalation (Figure 4.13).

At 48 hours after intranasal challenge, LPS inhalation had no detected effect on blood neutrophil counts (PBS+control IgG vs. LPS+control IgG: 1.15±0.22 vs. 1.24±0.20 $\times 10^6$

neutrophils per ml of blood, P=0.035), but in the context of LPS inhalation, treatment with P-selectin blocking antibody increased blood neutrophil counts (2.49±0.59 $\times 10^6$ neutrophils per ml of blood, P=0.018 vs. LPS+control IgG), whilst treatment with PSGL-1 blocking asntibody decreased blood neutrophil counts (0.29±0.05 $\times 10^6$ neutrophils per ml of blood, P<0.001 vs. LPS+control IgG) (Figure 4.13).

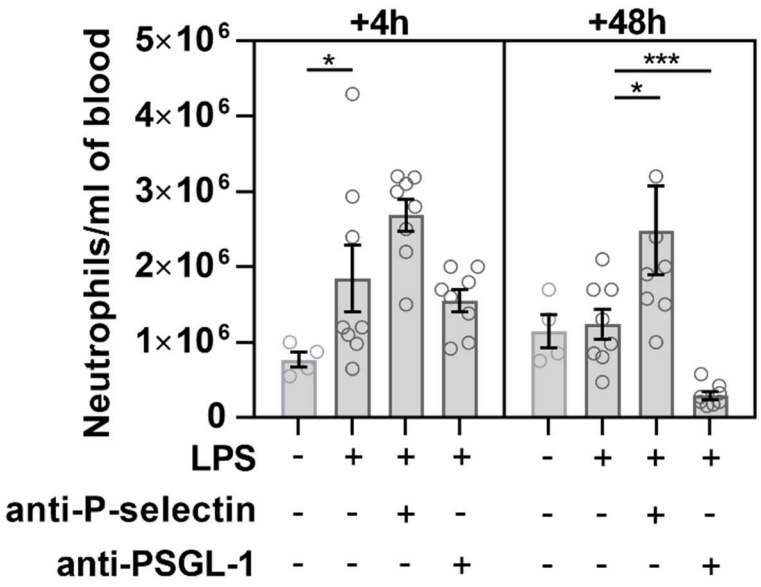

Figure 4.13: Effect of blockade of P-selectin or PSGL-1 and LPS inhalation on blood neutrophil counts. Mice were administered either control IgG, anti-P-selectin antibody, or anti-PSGL-1 antibody at -1h, and +24h in relation to intranasal administration of PBS or LPS, and circulating neutrophil counts were measured at +4h and +48h. One data point from the +48h LPS+anti-P-selectin group (6.3 $\times 10^6$ neutrophils per ml of blood) is off the scale of the graph but was included in analysis. Means ± standard error, PBS group: n=4, LPS groups: n=8, two-way ANOVA with repeated measures and Holm's test for difference vs. LPS+control IgG group, *=P<0.05; ***=P<0.001.

Effect of blockade of P-selectin or PSGL-1 on LPS-induced increases in NETs in BAL

Interactions between activated platelets and neutrophils mediated through P-selectin and PSGL-1 have been implicated in the formation of NETs (Caudrillier et al., 2012; Etulain et

al., 2015), so the effect of P-selectin or PSGL-1 blockade was investigated on the quantity of NETs recovered in BAL supernatant following LPS inhalation.

LPS inhalation increased the quantity of NETs detected in BAL (PBS+control IgG vs. LPS+control IgG: 0.10±0.02 vs. 0.95±0.08 NET units per ml of BAL, P<0.001) with neither anti-P-selectin antibody treatment (1.09±0.06 NET units per ml of BAL, P=0.689 vs LPS+control IgG), nor anti-PSGL-1 antibody treatment (0.97±0.07 $\times 10^6$ NET units per ml of BAL, P=0.997 vs LPS+control IgG), significantly altering LPS-induced increases in BAL NET content (Figure 4.14).

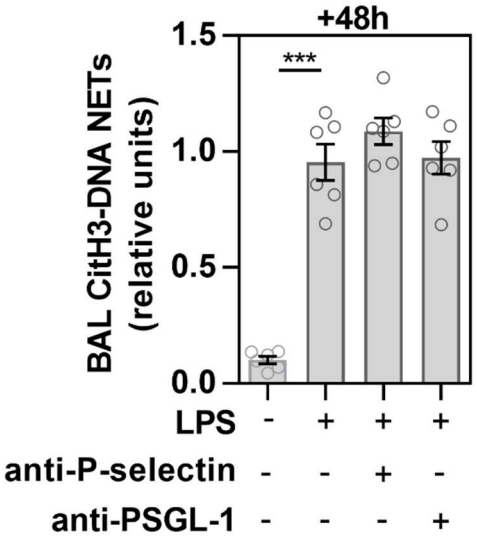

Figure 4.14: Effect of blockade of P-selectin or PSGL-1 on LPS-induced increases in quantity of NETs in BAL. Mice were administered either control IgG, anti-P-selectin antibody, or anti-PSGL-1 antibody at -1h, and +24h in relation to intranasal administration of PBS or LPS, and BAL was collected at +48h and the supernatant assayed for quantity of NETs (CitH3-DNA complexes). Means ± standard error, PBS group: n=4, LPS groups: n=8, one-way ANOVA with Dunnett's test for difference vs. LPS+control IgG group, *=P<0.05, ***=P<0.001.

Effect of blockade of P-selectin or PSGL-1 on LPS-induced body weight loss

Body weight was monitored as an index of general health status of mice. LPS inhalation caused body weight loss at 24 hours after intranasal challenge (PBS+control IgG vs. LPS+control IgG: 0.03±0.54 vs. -10.9±0.5 % change in body weight, P<0.001), with no detected effect of anti-P-selectin blocking antibody treatment (-9.3±0.5 % change in body weight, P=0.050 vs. LPS+control IgG), but a significant effect of anti-PSGL-1 blocking antibody treatment towards reducing LPS-induced weight loss (-9.2±0.4 % change in body weight, P=0.048 vs. LPS+control IgG) detected at this time point (Figure 4.15).

LPS inhalation also caused a decrease in body weight detectable at 48 hours after intranasal challenge (PBS+control IgG vs. LPS+control IgG -0.92±0.60 vs. -15.1±0.6 % change in body weight, P<0.001). At this time point there was no detected effect of anti-P-selectin blocking antibody treatment (-14.1±0.6 % change in body weight, P=0.097 vs. LPS+control IgG, but treatment with anti-PSGL-1 blocking antibody significantly reduced the extent of LPS-induced body weight loss (-11.2±0.8% change in body weight, P<0.001 vs. LPS+control IgG) (Figure 4.15).

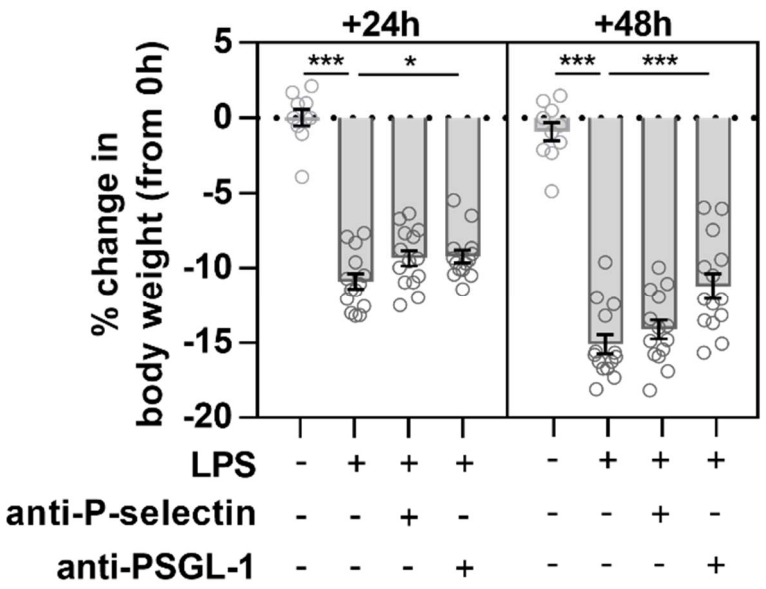

Figure 4.15: Effect of blockade of P-selectin or PSGL-1 on LPS-induced body weight loss. Mice were administered either control IgG, anti-P-selectin antibody, or anti-PSGL-1 antibody at -1h, and +24h in relation to intranasal administration of PBS or LPS, and mice were weighed at +24h and +48h as measured on change in body weight from baseline values before intranasal challenge (0h). Means ± standard error, PBS group: n=10, LPS groups: n=14, two-way ANCOVA with repeated measures and baseline weights fit as covariates, with Holm's test for difference vs. LPS+control IgG group, ***=P<0.001.

4.2.3 Summary –P-selectin or PSGL-1 blockade

Similarly to the findings of Kornerup et al., (2010), treatment with blocking antibody targeting PSGL-1, but not P-selectin, caused a reduction in neutrophil recruitment to lung airspaces. PSGL-1 blockade also reduced LPS-induced weight loss, suggesting an improvement of general health status of LPS-treated mice with PSGL-1 blocking antibody treatment.

In contrast, both the lung platelet recruitment and the decrease in blood platelet counts which followed LPS inhalation were unaffected by blockade of either P-selectin or PSGL-1, suggestive that these platelet responses to LPS occur independently of P-selectin or PSGL-1

function, although this observation is perhaps unsurprising given that neutrophil depletion studies were suggestive that these platelet responses to LPS occur independently of neutrophils.

The observation of contrasting effects of P-selectin and PSGL-1 blockade on blood neutrophil counts following LPS inhalation, with P-selectin blocking antibody treatment increasing and PSGL-1 blocking antibody treatment decreasing blood neutrophil counts, suggests that these adhesion molecules may be important in blood neutrophil homeostasis in inflammation.

Despite decreases in blood and BAL neutrophil counts, PSGL-1 blockade had no detected effect on LPS-induced increases in lung neutrophil elastase staining, a measure of all neutrophil elastase in the intravascular and extravascular spaces of the lung tissue sampled. A potential explanation for this observation is that PSGL-1 blockade does not decrease the initial recruitment of neutrophils to the pulmonary circulation but prevents successful neutrophil transendothelial and/or transepithelial migration, and perhaps also signalling to increase neutrophil production or release to maintain blood neutrophil counts. The increase in lung neutrophil elastase with P-selectin blockade may have been related to the increased blood neutrophil content.

The findings that the quantity of NETs in BAL was not affected by PSGL-1 blockade despite anti-PSGL-1 antibody treatment-induced decreases in BAL neutrophil content seem conflicting and do not support published *in vitro* data showing P-selectin and PSGL-1 blockade preventing NETosis (Etulain et al., 2015). It is possible that the neutrophils present in

the bronchoalveolar space of LPS-challenged mice receiving PSGL-1 blocking antibody may have been sufficient to produce a full NET release response in this model.

As platelet P-selectin did not appear to be an important mediator for LPS-induced lung platelet recruitment, experiments were designed to investigate the effects of platelet inhibition on lung platelet and neutrophil recruitment responses following LPS inhalation.

4.3 Effects of treatment with anti-platelet drugs

4.3.1 Background – treatment with P2Y antagonists or aspirin

Anti-platelet pharmacological interventions were identified which are of interest in the context of LPS-induced lung inflammation and lung platelet recruitment. In previous studies, treatment with antagonists targeting the $P2Y_1$ receptor, as well as treatment with aspirin to inhibit COX activity and promote aspirin-triggered lipoxin formation, have been found to have effects on lung inflammation following allergen or LPS exposure in mice (Ortiz-Muñoz et al., 2014; Tilgner et al., 2016; Amison et al., 2015; 2017), whilst $P2Y_{12}$ antagonism displayed no effect on lung inflammation following either allergen challenge or LPS inhalation (Amison et al., 2015; 2017). Treatment with antagonists of $P2Y_1$ or $P2Y_{12}$, as well as aspirin treatment, all have established anti-thrombotic action (Erlinge and Burnstock, 2008; Fuster and Sweeny, 2011), but the effects of treatment with these drugs on lung platelet recruitment in inflammation is unknown.

The effect of P2Y antagonists and aspirin treatment relative to vehicle controls was therefore investigated in the mouse LPS inhalation model. The selection of drugs and dosing regimen was based on those used in previously reported studies, using the P2Y antagonists used by Amison et al., (2015, 2017) (the $P2Y_1$ antagonist MRS2500 and the $P2Y_{12}$ antagonist AR-C66096, both at 3 mg/kg i.v.), and the aspirin treatment used by Ortiz-Munoz et al., (2014) and Tilgner et al., (2016) (100 mg/kg i.p.).

4.3.2 Results – treatment with P2Y antagonists or aspirin

Effects of anti-platelet drugs on LPS-induced lung CD42b+ platelet recruitment

LPS inhalation caused an increase in CD42b+ platelets detected in lung sections at 48 hours after challenge (PBS+vehicle vs. LPS+vehicle: 342±74 vs. 719±51 CD42b+ platelets per mm^2 of lung fields, P<0.001). There was no detected effect of $P2Y_1$ antagonist treatment (932±76 CD42b+ platelets per mm^2 of lung fields, P=0.322 vs. LPS+vehicle), $P2Y_{12}$ antagonist treatment (855±91 CD42b+ platelets per mm^2 of lung fields, P=0.756 vs. LPS+vehicle), or aspirin treatment (838±105 CD42b+ platelets per mm^2 of lung fields, P=0.903 vs. LPS+vehicle) (Figure 4.16).

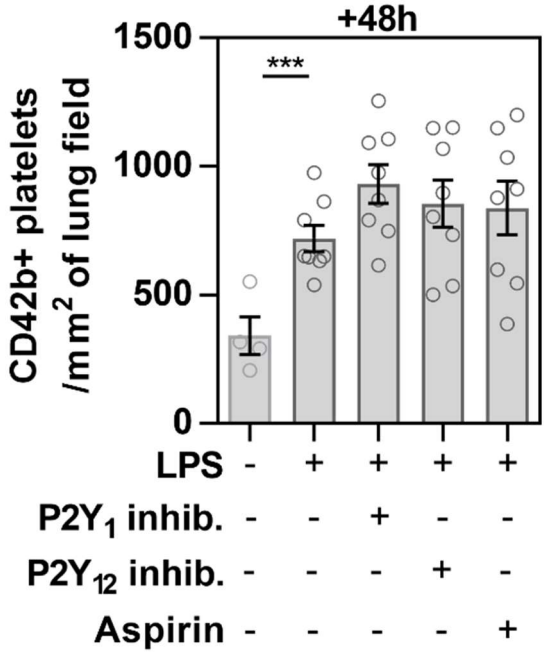

Figure 4.16: Effects of anti-platelet drugs on LPS-induced lung CD42b+ platelet recruitment. $P2Y_1$ antagonist (MRS2500, 3 mg/kg i.v.), $P2Y_{12}$ antagonist (AR-C 66096, 3 mg/kg i.v.) or aspirin (100 mg/kg i.p) treatment, or vehicle controls given at -1 hour and +24 hours relative to intranasal LPS challenge The presence of CD42b+ platelets detected in immunostained frozen lung sections was then measured after lungs were collected at +48 hours. Means ± standard error, PBS group: n=4, LPS groups: n=8, one-way ANOVA with Dunnett's test for difference vs. LPS+vehicle group, ***=P<0.001.

Effects of anti-platelet drugs on LPS-induced increases in lung neutrophil elastase content

LPS inhalation caused an increase in neutrophil elastase detected in lung sections at 48 hours after challenge (PBS+vehicle vs. LPS+vehicle: 0.07±0.01 vs. 1.00±0.18 % of lung field neutrophil elastase+, P<0.001). There was no detected effect of $P2Y_1$ antagonist treatment (1.31±0.22 % of lung field neutrophil elastase+, P=0.700 vs. LPS+vehicle), $P2Y_{12}$ antagonist treatment (1.41±0.31 % of lung field neutrophil elastase+, P=0.688 vs. LPS+vehicle), or

aspirin treatment (1.05±0.20 % of lung field neutrophil elastase+, P=0.999 vs. LPS+vehicle) (Figure 4.17).

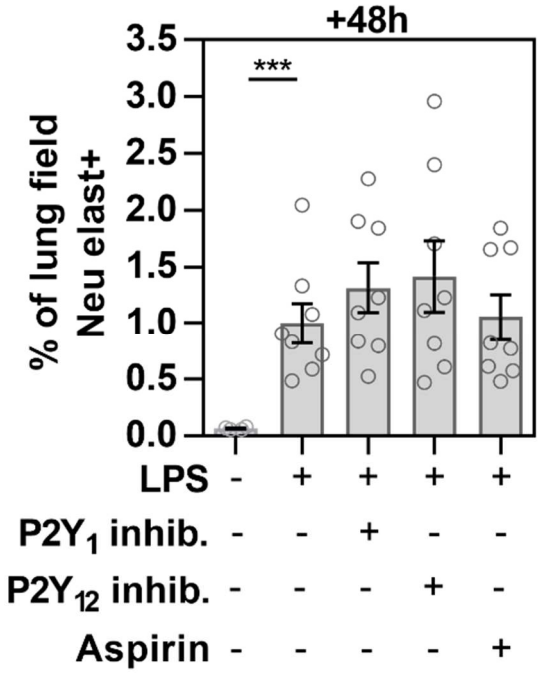

Figure 4.17: Effects of anti-platelet drugs on LPS-induced increases in lung neutrophil elastase content. $P2Y_1$ antagonist (MRS2500, 3 mg/kg i.v.), $P2Y_{12}$ antagonist (AR-C 66096, 3 mg/kg i.v.) or aspirin (100 mg/kg i.p) treatment, or vehicle controls given at -1 hour and +24 hours relative to intranasal LPS challenge The presence of neutrophil elastase detected in immunostained frozen lung sections was then measured after lungs were collected at +48 hours.Means ± standard error, PBS group: n=4, LPS groups: n=8, one-way ANOVA with Dunnett's test for difference vs. LPS+vehicle group, ***=P<0.001.

Effects of anti-platelet drugs on LPS-induced increases in BAL neutrophil content

LPS inhalation caused an increase in BAL neutrophil counts at 48 hours after challenge (PBS+vehicle vs. LPS+vehicle: 0.00±0.00 vs. 1.68±0.23 $\times 10^6$ neutrophils per ml of BAL,

P<0.001). There was no detected effect of $P2Y_1$ antagonist treatment (1.68±0.37 $\times 10^6$ neutrophils per ml of BAL, P=0.999 vs. LPS+vehicle), $P2Y_{12}$ antagonist treatment (1.62±0.28 $\times 10^6$ neutrophils per ml of BAL, P=0.999 vs. LPS+vehicle), or aspirin treatment (1.69±0.25 $\times 10^6$ neutrophils per ml of BAL, P=0.999 vs. LPS+vehicle) (Figure 4.18).

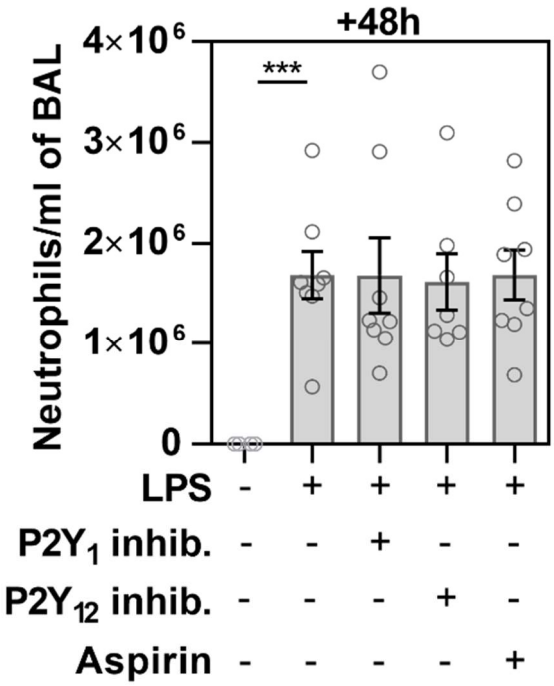

Figure 4.18: Effects of anti-platelet drugs on LPS-induced increases in BAL neutrophil content. $P2Y_1$ antagonist (MRS2500, 3 mg/kg i.v.), $P2Y_{12}$ antagonist (AR-C 66096, 3 mg/kg i.v.) or aspirin (100 mg/kg i.p) treatment, or vehicle controls given at -1 hour and +24 hours relative to intranasal LPS challenge. BAL was collected at +48h and BAL neutrophils were quantified. Means ± standard error, PBS group: n=4, LPS groups: n=8 (n=7 in LPS+$P2Y_{12}$ inhibitor group due to 1 death), one-way ANOVA with Dunnett's test for difference vs. LPS+vehicle group, ***=P<0.001.

Effects of anti-platelet drugs on LPS-induced increases in quantity of NETs in BAL

NETs were measured by CitH3-DNA complex ELISA in BAL supernatant samples in order to determine the effect of anti-platelet drug treatment on LPS-induced NET formation in lung airspaces. LPS inhalation increased quantity of NETs detected in BAL (PBS+vehicle vs. LPS+vehicle: 0.16±0.06 vs. 1.14±0.08 NET units per ml of BAL but there was no detected effect on this response of $P2Y_1$ antagonist treatment (LPS+$P2Y_1$ antagonist: 1.09±0.06 NET units per ml of BAL, P=0.999 vs. LPS+vehicle), $P2Y_{12}$ antagonist treatment (LPS+$P2Y_{12}$ antagonist: 1.15±0.10 NET units per ml of BAL, P=0.999 vs. LPS+vehicle), or aspirin treatment (LPS+aspirin: 0.94±0.12 NET units per ml of BAL, P=0.775 vs. LPS+vehicle)

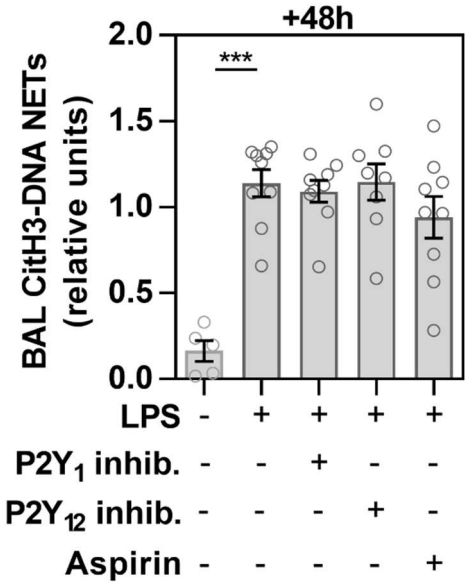

Figure 4.19: Effects of anti-platelet drugs on LPS-induced increases in BAL NETs. $P2Y_1$ antagonist (MRS2500, 3 mg/kg i.v.), $P2Y_{12}$ antagonist (AR-C 66096, 3 mg/kg i.v.) or aspirin (100 mg/kg i.p) treatment, or vehicle controls given at -1 hour and +24 hours relative to intranasal LPS challenge. BAL was collected at +48h and extracellular CitH3-DNA complexes (NETs) were quantified by ELISA. Means ± standard error, PBS group: n=4, LPS groups: n=8 (n=7 in LPS+$P2Y_{12}$ inhibitor group due to 1 death), one-way ANOVA with Dunnett's test for difference vs. LPS+vehicle group, ***=$P<0.001$.

Effects of anti-platelet drugs on LPS-induced body weight loss

Body weight was monitored over the course of experiments as an index of general health status of mice. LPS inhalation caused a decrease in body weight relative to pre-challenge baseline detected at 48 hours after challenge (PBS+vehicle vs. LPS+vehicle: -1.4±0.5 vs. -10.4±0.4 % change in body weight, $P<0.001$). At 24 hours after intranasal challenge there was no detected effect of $P2Y_1$ antagonist treatment (-11.2±0.5 % change in body weight, $P=0.999$ vs. LPS+vehicle), $P2Y_{12}$ antagonist treatment (-10.6±0.5 % change in body weight,

P=0.999 vs. LPS+vehicle), or aspirin treatment (-10.3±0.3 % change in body weight, P=0.999 vs. LPS+vehicle) (Figure 4.20).

An effect of LPS inhalation on body weight was also detected at 48 hours after challenge (PBS+vehicle vs. LPS+vehicle: -0.8±0.7 vs. -13.8±0.8 % change in body weight, P<0.001). At 48 hours after intranasal challenge there was no detected effect of $P2Y_1$ antagonsit treatment (-13.6±0.7 % change in body weight, P=0.999 vs. LPS+vehicle), $P2Y_{12}$ antagonist treatment (-13.8±0.7 % change in body weight, P=0.999 vs. LPS+vehicle), or aspirin treatment (-12.6±0.7 % change in body weight, P=0.474 vs. LPS+vehicle) (Figure 4.20).

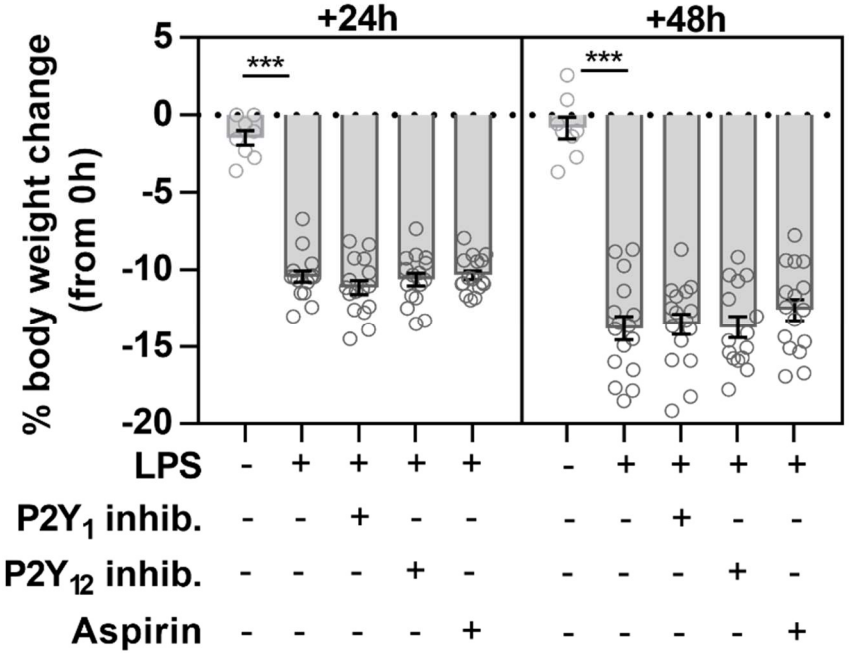

Figure 4.20: Effects of anti-platelet drugs on LPS-induced body weight loss. $P2Y_1$ antagonist (MRS2500, 3 mg/kg i.v.), $P2Y_{12}$ antagonist (AR-C 66096, 3 mg/kg i.v.) or aspirin (100 mg/kg i.p) treatment, or vehicle controls were given at -1 hour and +24 hours relative to intranasal challenge with PBS or LPS. Mice were weighed at +24h and +48h . Means ± standard error, PBS group: n=8, LPS groups: n=16 (n=15 in LPS+$P2Y_{12}$ inhibitor group due to 1 death), two-way ANCOVA with baseline weights fit as covariates and Holm's test for difference vs. LPS+vehicle group, ***=P<0.001.

4.3.3 Summary – treatment with P2Y antagonists or aspirin

In summary, no effect on LPS-induced lung platelet recruitment was seen with treatment with the $P2Y_1$ antagonist MRS2500, the $P2Y_{12}$ antagonist AR-C 66096, or the irreversible COX antagonist aspirin when drugs were administered at doses that reduced lung neutrophil recruitment (MRS2500 and aspirin) or increased bleeding time (AR-C 66096) in previously published mouse experiments (Ortiz-Muñoz et al., 2014; Amison et al., 2017). Also, none of the anti-platelet drugs tested affected LPS-induced increases in lung neutrophil elastase content, BAL neutrophil recruitment, BAL NET release or body weight loss.

As these pharmacological antagonists with anti-platelet activity showed no detectable effects on inflammatory responses, the effect of complete abrogation of platelet function using platelet-depleting antibody treatments was therefore investigated.

4.4 Effects of treatment with platelet-depleting antibodies

4.4.1 Background – platelet depletion

Previous experiments using busulphan-mediated platelet depletion (Kornerup et al., 2010), antibody-mediated platelet depletion (Grommes et al., 2012), and busulphan-mediated platelet depletion with platelet reconstitution (Pan et al., 2015), as well as studies using anti-platelet drugs (Ortiz-Muñoz et al., 2014; Amison et al., 2017), were strongly suggestive that in mice, neutrophil recruitment following LPS inhalation depends on platelets.

However, the results from the effects of anti-platelet drug treatment in the present study were not consistent with previous results in similar LPS inhalation models, and the effects of preventing LPS-induced lung platelet recruitment have not yet been explored in the model used in this report. The platelet dependence of inflammatory responses in the mouse LPS inhalation model were therefore investigated by comparing control platelet replete mice with mice depleted of platelets with anti-GPIbα antibody treatment.

4.4.2 Results – effects of platelet depletion

Effect of anti-GPIbα treatment on blood platelet counts

Anti-GP1bα antibody treatment decreased blood platelet counts made from cardiac blood samples by ~85% at 48 hours after intranasal challenge in both PBS control mice (PBS+control IgG vs. PBS+anti-GPIbα: 8.75±0.53 vs. 1.36±0.28 $\times 10^8$ platelets per ml of blood, $P<0.001$) and mice challenged with LPS-treated mice (LPS+control IgG vs. LPS+anti-GPIbα: 8.08±0.56 vs. 1.21±0.17 $\times 10^8$ platelets per ml of blood, $P<0.001$). There was no

effect of LPS inhalation on blood platelet counts between control IgG-treated groups (P=0.533), or between platelet-depleted groups (P=0.809) (Figure 4.21). Platelet quantification from CD42b immunostaining was not carried out using lungs from the platelet depletion experiment as the anti-GP1bα (CD42b) rat antibodies used for depletion interfere with CD42b rabbit antibodies resulting in false negative staining. Lungs were however collected from mice used in these experiments permitting immunostaining of platelets in these samples using alternative methods in future.

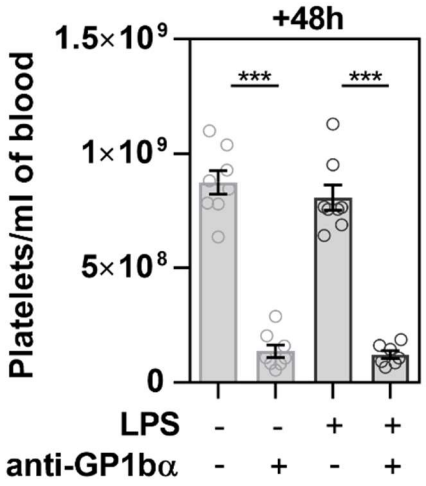

Figure 4.21: Effect of anti-GPIb α treatment on blood platelet counts. Mice were treated with anti-GPIbα antibody or control IgG (at 1 mg/kg i.v. at -1h and +24h relative to intranasal challenge) and challenged intranasally with PBS or LPS. Blood platelet counts were made from cardiac blood collected at 48 hours after intranasal challenge. Means ± standard error, n=8 (n=7 in LPS+anti-GPIbα group due to 1 death), 2-way ANOVA with Holm's test for effects of LPS and anti-GPIbα treatment, ***=P<0.001.

Effects of platelet depletion on LPS-induced BAL neutrophil recruitment

LPS inhalation increased BAL neutrophil counts in both control mice (PBS+anti-GPIbα vs. LPS+anti-GPIbα: 0.00±0.00 vs. 2.11±0.28 $\times 10^6$ neutrophils per ml of BAL, P<0.001),

and platelet-depleted mice (PBS+anti-GPIbα vs. LPS+anti-GPIbα: 0.00±0.00 vs. 2.07±0.24 $\times 10^6$ neutrophils per ml of BAL, P<0.001), and there were no detected effects of antibody-mediated platelet depletion between PBS control groups (P=0.999) or between LPS-challenged groups (P=0.999) (Figure 4.22).

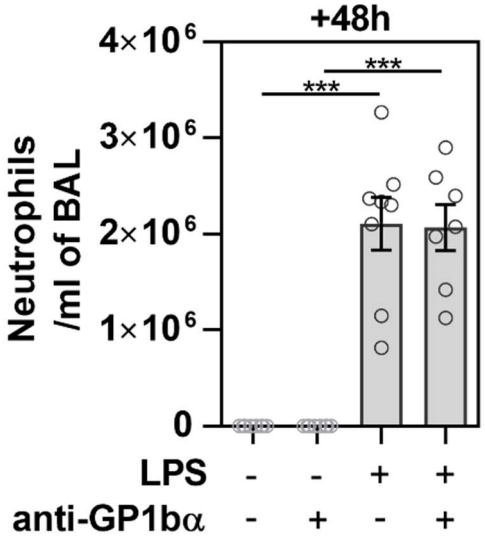

Figure 4.22: Effects of platelet depletion on LPS-induced BAL neutrophil recruitment. Mice were treated with anti-GPIbα antibody or control IgG (at 1 mg/kg i.v. at -1h and +24h relative to intranasal challenge) and challenged intranasally with PBS or LPS. BAL neutrophil counts were made from BAL collected at 48 hours after intranasal challenge. Means ± standard error, n=8 (n=7 in LPS+anti-GPIbα group due to 1 death), 2-way ANOVA with Holm's test for effects of LPS and anti-GPIbα treatment, ***=P<0.001.

Effect of platelet depletion and LPS inhalation on quantity of red blood cells in BAL

Because previous experiments had observed bleeding into lungs when LPS-induced lung inflammation was combined with thrombocytopenia (Goerge et al., 2008; Gros et al., 2015; Deppermann et al., 2017), and endothelial disruption and bleeding into airspaces might affect

measurements of neutrophil migration into airspaces, bleeding into the bronchoalveolar airspaces was quantified by measuring the index of optical density at 405 nm of a red cell-lysed and pelleted sample of BAL.

LPS inhalation had no detected effect on BAL red blood cells index in control mice (Optical density of sample in PBS+control IgG vs. LPS+control IgG: 0.05±0.01 vs. 0.10±0.03 optical density units, P=0.3115), but in platelet-depleted mice LPS inhalation caused a significant increase in the BAL red blood cell index (Optical density of sample in PBS+anti-Ly6-G 0.10±0.03 vs. 0.51±0.19, P<0.001), which was also significantly higher than in platelet replete mice challenged with intranasal LPS (P<0.001). No effect of platelet depletion was detected in PBS control mice (P=0.3115) (Figure 4.23). Bleeding into BAL was not detected in any previous experiments (Figure 4.30).

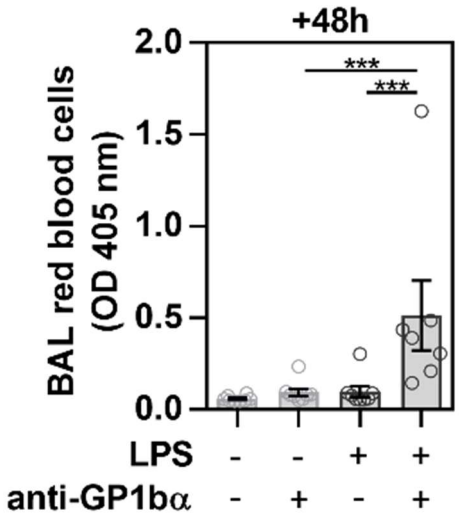

Figure 4.23: Effect of platelet depletion and LPS inhalation on quantity of red blood cells in BAL. Mice were treated with anti-GPIbα antibody or control IgG (at 1 mg/kg i.v. at -1h and +24h relative to intranasal challenge) and challenged intranasally with PBS or LPS. Bleeding into airspaces was assessed by measuring optical density at 405 nm of washed, lysed BAL cell pellet supernatant samples (100 µl). Means ± standard error, n=8 (n=7 in LPS+anti-GPIbα group due

to 1 death), 2-way ANOVA with Holm's test for effects of LPS and anti-GPIbα treatment, ***=P<0.001.

Effect of platelet depletion on quantity of NETs in BAL

NETs (extracellular complexes of citrullinated histone H3 with DNA) were quantified in BAL supernatant. Platelet depletion with anti-GPIbα antibody treatment reduced quantity of NETs in BAL (LPS+control IgG vs. LPS+anti- GPIbα: 1.06±0.06 vs. 0.57±0.11 NET units per ml of BAL, P<0.001), with no detected effect of platelet depletion on NETs in PBS control challenged mice (PBS+control IgG vs. PBS+anti- GPIbα: 0.20±0.04 vs. 0.10±0.04 NET units per ml of BAL, P=0.150). Although the quantity of NETs was reduced by ~53% with platelet depletion, LPS inhalation significantly increased BAL NET content in both platelet depleted (P<0.001), and control IgG-treated mice (P<0.001).

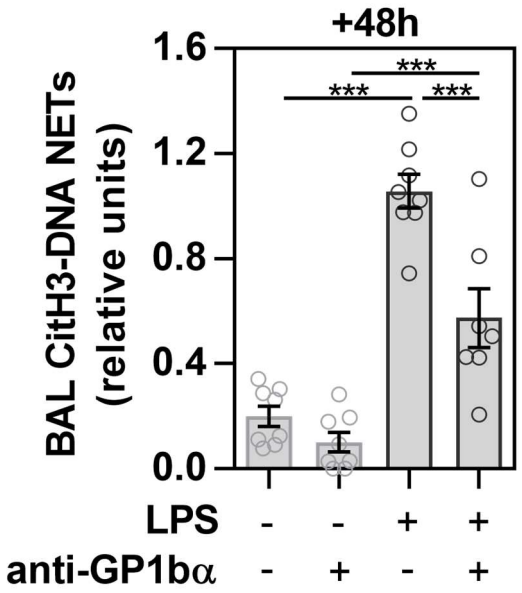

Figure 4.24: Effect of platelet depletion and LPS inhalation on quantity of NETs in BAL. Mice were treated with anti-GPIbα antibody or control IgG (at 1 mg/kg i.v. at -1h and +24h relative to intranasal challenge) and challenged intranasally with PBS or LPS. NETs (extracellular CitH3-DNA complexes) were measured in BAL supernatant samples collected at 48 hours after intranasal challenge using an ELISA method. Units are relative to a serial dilution of pooled BAL supernatant sample from 12 separate mice (1.0 NET unit). Means ± standard error, n=8 (n=7 in LPS+anti-GPIbα group due to 1 death), 2-way ANOVA with Holm's test for effects of LPS and anti-GPIbα treatment, ***=P<0.001.

Effect of platelet depletion and LPS inhalation on body weight

Body weight was monitored as an index of general health status of mice. LPS inhalation caused body weight loss in both control IgG-treated control mice (PBS+control IgG vs. LPS+control IgG: -0.8±0.5 vs. -10.6±0.4 % change in body weight, P<0.001), and platelet depleted mice (PBS+anti-GPIbα vs. LPS+ anti-GPIbα: -1.0±0.7 vs. -9.6±0.7 % change in body weight, P<0.001) detectable at 24 hours after intranasal challenge. There was no detected effect of platelet depletion between PBS control mice (P=0.999) or LPS-challenged mice (P=0.999) at 24 hours after intranasal challenge.

At 48 hours after intranasal challenge a significant decrease both control IgG-treated control mice (PBS+control IgG vs. LPS+control IgG: -0.2±0.6 vs. -14.2±0.9 % change in body weight, P<0.001), and platelet depleted mice (PBS+anti-GPIbα vs. LPS+ anti-GPIbα: -0.7±0.9 vs. -11.7±1.7 % change in body weight, P<0.001), with no detected effect of platelet depletion in PBS controls (P=0.999) or mice exposed to LPS (P=0.086) at 48 hours after intranasal challenge (Figure 4.25).

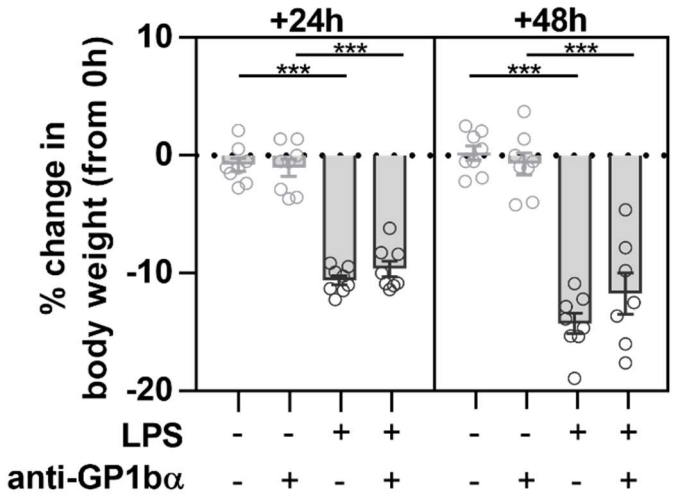

Figure 4.25: Effect of platelet depletion on the effect of LPS inhalation on body weight. Anti-GPIbα antibody treatment-induced platelet depletion had no detected effect on LPS-induced body weight loss. Means ± standard error, n=8 (n=7 in LPS+anti-GPIbα group due to 1 death), 3-way ANCOVA with repeated measures and baseline values fit as covariates, Holm's test for effects of LPS and anti-GPIbα treatment, ***=P<0.001.

4.4.3 Summary – effects of platelet depletion

In summary, platelets were successfully depleted with administration of anti-GPIbα antibodies to ~85% of control levels, but neutrophil recruitment to BAL following LPS inhalation

was not affected by platelet depletion. This observation is suggestive that a full lung neutrophil recruitment response in this model at this time point is not entirely dependent on blood platelets, which would also explain the absence of detected effects of anti-platelet drugs on LPS-induced lung neutrophil recruitement responses.

However, inflammatory bleeding into airspaces in LPS-challenged, platelet depleted mice may have confounded specific measurement of neutrophil migration into airspaces, and its is possible that remaining platelets may have been sufficient to mediate lung neutrophil recruitment as previous studies have found that platelet depletion levels of greater than 85% are required for inhibition of eosinophil recruitment to BAL following allergen challenge (Pitchford et al., 2005).

In spite of the lack of the effect of platelet depletion on neutrophil recruitment to BAL, release of NETs in BAL was reduced by ~53%, suggestive that the presence of platelets is important for release of NETs within lung airspaces. This is an interesting observation as platelets have been previously associated with formation of NETs following inflammation originating from intravascular inflammatory insult (Caudrillier et al., 2012), but not in the extravascular formation of NETs in the lung following inhaled LPS challenge.

4.5 Summary – Investigations into mechanisms of LPS-induced lung platelet recruitment

In summary, the major effects of neutrophil depletion, blocking antibody treatment, treatment with anti-platelet drugs and platelet depletion that were detected on platelet and neutrophil responses following LPS inhalation in the present body of work are summarised below (Table 4.1).

Table 4.1: Summary of effects of tested interventions on LPS-induced lung platelet recruitment and lung neutrophil inflammatory responses. ↓: Intervention decreased response measured, ↑: intervention increased response measured, no detected effect: response measured but no effect of intervention detected, blank cell: intervention effect not measured on response.

	Measurement			
Intervention	**Lung platelet recruitment**	**BAL neutrophil recruitment**	**Lung neutrophil elastase**	**BAL NETs**
Neutrophil depletion	No detected effect	↓	↓	
P-selectin blockade	No detected effect	No detected effect	↑	No detected effect
PSGL-1 blockade	No detected effect	↓	No detected effect	No detected effect
$P2Y_1$ antagonist treatment	No detected effect	No detected effect	No detected effect	No detected effect
$P2Y_{12}$ antagonist treatment	No detected effect	No detected effect	No detected effect	No detected effect
Aspirin treatment	No detected effect	No detected effect	No detected effect	No detected effect
Platelet depletion		No detected effect	No detected effect	↓

Taken together, these data are suggestive that LPS-induced lung platelet recruitment in the mouse model used at the time point tested occurs independently of neutrophils, adhesion

and signalling mediated through either PSGL-1 or P-selectin, signalling involving the $P2Y_1$ and $P2Y_{12}$ receptors, and is insensitive to aspirin treatment.

Neutrophil recruitment to the extravascular space in this model, in contrast to platelet recruitment to lungs, was reduced by PSGL-1 blocking antibody treatment, with effects on reducing the extent of LPS-induced body weight loss suggestive that PSGL-1 blockade inmproves general health status following LPS inhalation in this model.

The lack of detected effects of platelet depletion on recruitment of neutrophils to BAL suggests that the mouse model used might not be an ideal one for measuring platelet-dependent inflammatory responses, as neutrophil recruitment to lung airspaces did not show evidence of platelet dependence at the time point investigated. It is therefore still a pertinent question as to whether platelets are recruited to lungs in inflammatory scenarios where inflammation is highly dependent on platelets, and whether and through what mechanisms the platelet recruitment underlies platelet-dependence of inflammatory responses.

The effect of platelet depletion on reducing LPS-induced NET release in the lung in the model used in these studies, whilst no effects of platelet depletion were detected on the total number of neutrophils recruited to the bronchoalveolar space following LPS inhalation, also warrants further investigation.

4.6 Appendix

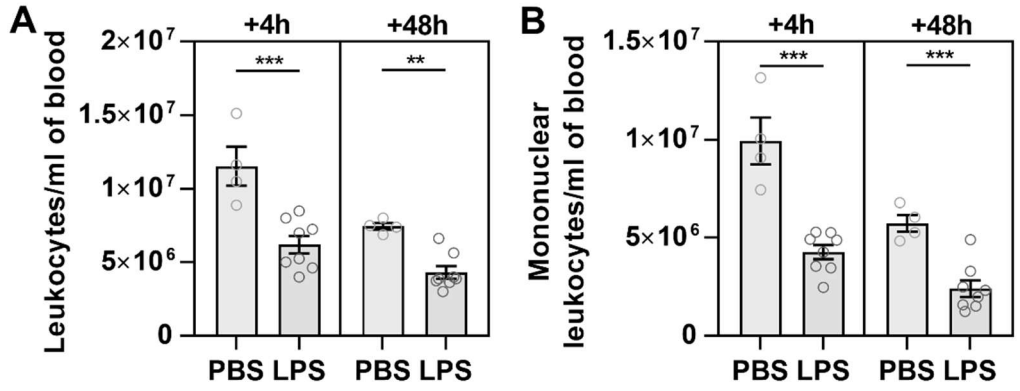

Figure 4.26: Effects of LPS inhalation on blood total leukocyte and mononuclear cell counts. Mice were administered either intranasal PBS or LPS, and tail blood samples were collected at 4 hours and 48 hours after intransal challenges. Total leukocyte counts (A) and total blood mononuclear leukocyte counts (B) were made from blood samples. Mean ± standard error, PBS groups: n=4, LPS groups: n=8, 2-way ANOVA with Holm's test for LPS effects within time points, **=P<0.01, ***=P<0.001.

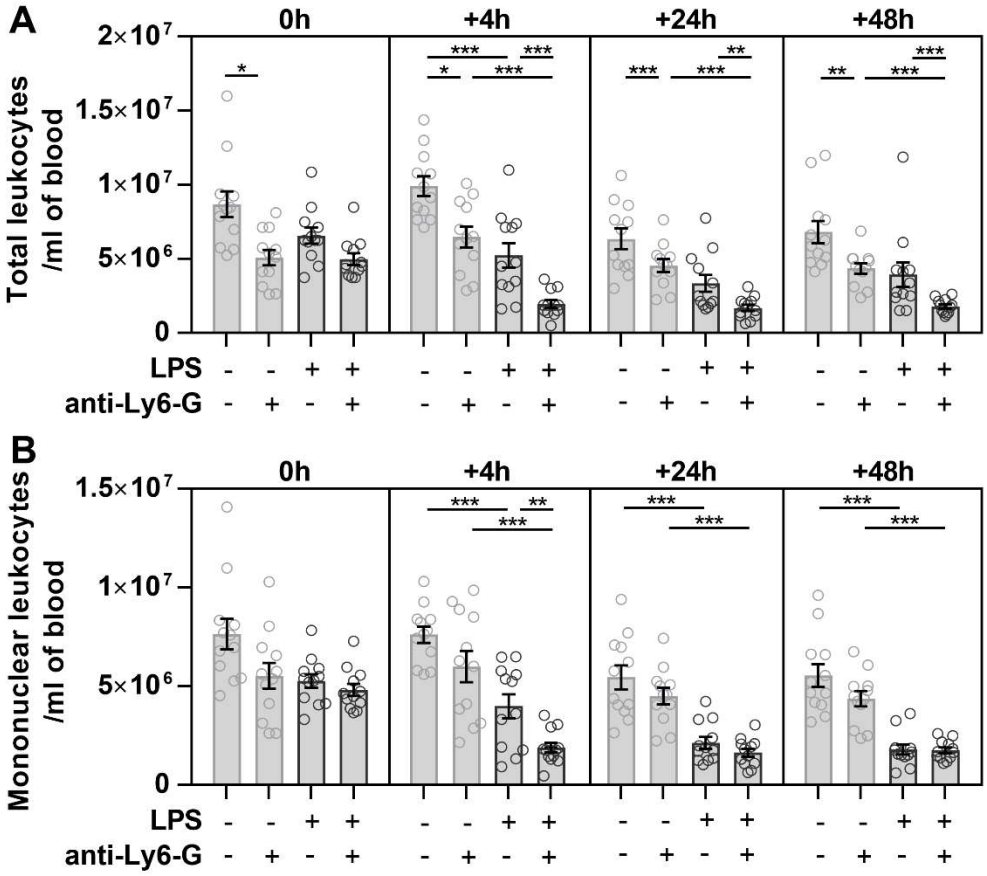

Figure 4.27: Effects of anti-Ly6-G antibody treatment and LPS inhalation on blood total leukocyte and mononuclear cell counts. Mice were administered either control IgG or anti-Ly6-G antibody at -24h, -1h, and +24h in relation to intranasal administration of PBS or LPS, and serial tail blood microsamples were used to quantify blood total leukocyte counts (A) and blood mononuclear cell counts (B). Mean ± standard error, n=12, 3-way ANOVA with repeated measures and Holm's test for LPS and anti-Ly6-G treatment effects, *=P<0.05, **=P<0.01, ***=P<0.001.

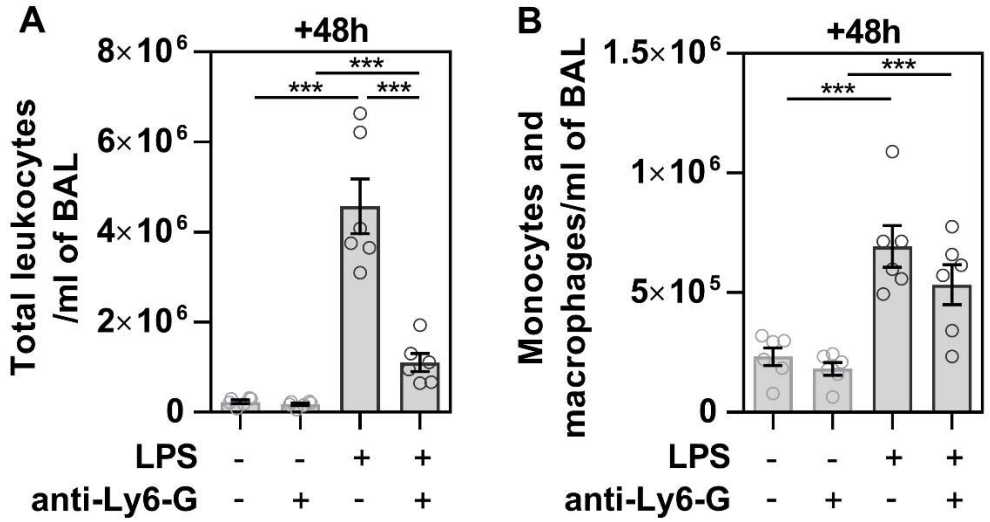

Figure 4.28: Effects of anti-Ly6-G antibody treatment and LPS inhalation on the quantity of total leukocytes and monocytes/macrophages in BAL. Mice were administered either control IgG or anti-Ly6-G antibody at -24h, -1h, and +24h in relation to intranasal administration of PBS or LPS, and BAL was collected at 48 hours after intranasal chellenges. Total leukocyte counts (A) and monocytes/macrophage counts (B) were made from BAL samples. Mean ± standard error, n=6, 2-way ANOVA with Holm's test for LPS and anti-Ly6-G treatment effects, ***=P<0.001.

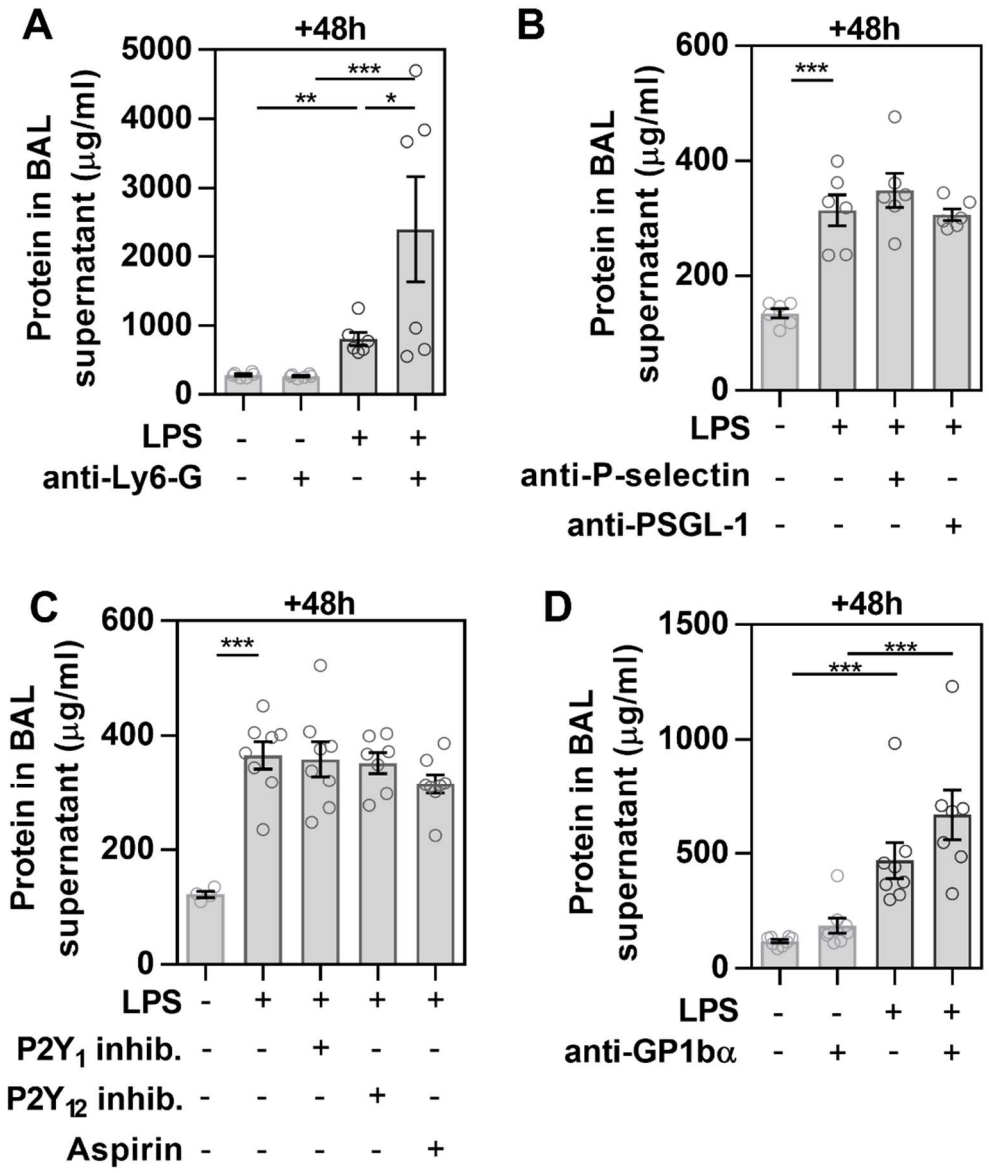

Figure 4.29: Effects of interventions on LPS-induced increases in BAL supernant protein content. Mice were challenged with PBS or LPS intranasally, treated with the various interventions tested in the present body of work, and BAL collected 48 hours later. Total protein was quantified in BAL supernatant as an index of plasma extravasation. (A) Effects of neutrophil depletion, (B) Effects of anti-P-selectin or anti-PSGL-1 blocking antibody treatment, (C) effects of treatment with the $P2Y_1$ antagonist MRS2500, the $P2Y_{12}$ antagonist AR-C 66096 or aspirin, (D) effects of platelet depletion. The increase in BAL protein with neutrophil depletion and LPS inhalation correlated with relatively high measurements of red cells in samples with high protein content and so may have been the result of bleeding into BAL. Mean ± standard error, n=4-8, one or two-way ANOVA with Holm's or Dunnett's test, *=P<0.05, **=P<0.01, ***=P<0.001.

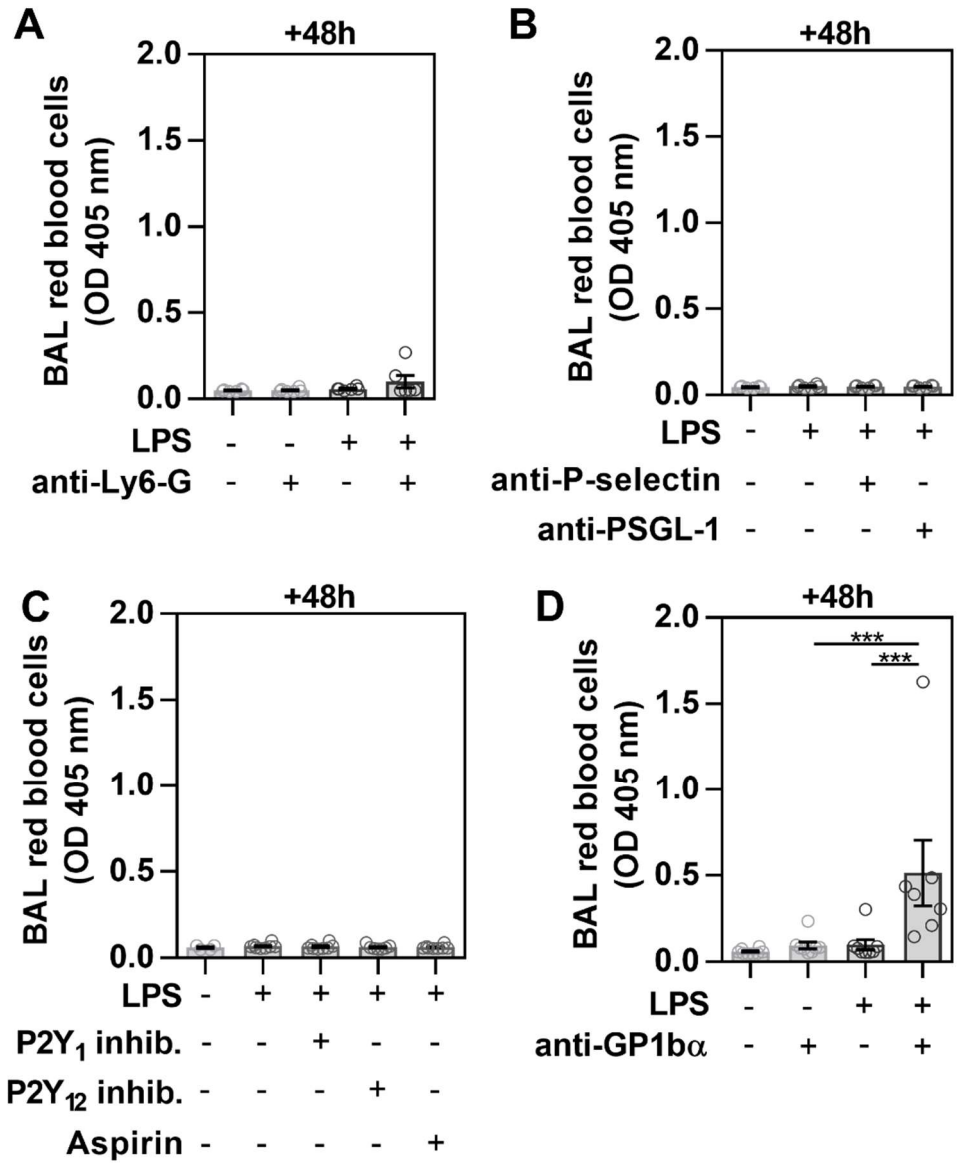

Figure 4.30: Effects of LPS inhalations and interventions on red cells in BAL. Mice were challenged with PBS or LPS intranasally, treated with the various interventions tested in the present body of work, and BAL collected 48 hours later. The optical density at 405 nm of spun, lysed and spun BAL cell samples was quantified as an index of bleeding into BAL. (A) Effects of neutrophil depletion, (B) Effects of anti-P-selectin or anti-PSGL-1 blocking antibody treatment, (C) effects of treatment with the $P2Y_1$ antagonist MRS2500, the $P2Y_{12}$ antagonist AR-C 66096 or aspirin, (D) effects of platelet depletion. Graphs are scaled to match (D) where significant bleeding was detected. Mean ± standard error, n=4-8, one or two-way ANOVA with Holm's or Dunnett's test, ***=$P<0.001$.

5 Discussion and conclusions

5.1 General discussion and future research

5.1.1 Methods for measuring platelet recruitment in inflammation

Immunohistochemistry

The immunohistochemistry methods reported here constitute a range of imaging methods allowing for imaging and relatively rapid quantification of platelets in mouse lungs, and proof-of-concept experiments showed that these methods have potential for use on human tissue samples. To be able to identify and quanitify distinct platelets *in situ* is a advance on methodologies that rely upon the detection of platelet activation markers which may become spatially disconnected from platelets (Shibazaki et al., 1996), western blots of platelet proteins which are limited by protein extraction methods (Ortiz-Muñoz et al., 2014), more qualititative observations of the extent of lung platelet staining (Looney et al., 2009; Ortiz-Muñoz et al., 2014), and the detection of platelets in tissue samples using flow cytometry which requires tissue disruption and digestion steps which may alter platelet activation status (Rafii et al., 2015).

Immunofluorescence staining also allowed for study of the spatial relationship of platelets with neutrophils in lungs, and for the counting of markers of lung thrombopoiesis. Although these studies were limited in measurements of colocalisation by the constraints of 2-dimensional epi-fluorescence microscopy (Dunn et al., 2011), these methods could be adapted to used with 3-dimensional confocal microscopy image stacks. Such 3-dimensional images could

then be used for measuring the spatial patterns of platelet activation using antibodies targeted against the high-affinity conformation of the $\alpha_{IIb}\beta_3$ integrin or membrane P-selectin in a similar fashion to flow cytometry assays of platelet activation, and to investigate whether platelets, or activated platelets, colocalise with neutrophils or other cells more or less than anticipated based on random models of platelet distribution across the pulmonary circulation, in order to provide further insights into which interactions do or do not mediate platelet recruitment to lungs.

However, it is acknowledged that these methods have the disadvantages of requiring terminaton of, or invasive sampling from the experimental subject, and of potential introduction of artifacts during sample collection and processing. Carrying out these studies in either formalin-fixed, paraffin embedded tissue or fresh, whole mount preparations made from tissue of reporter mice would minimise artifacts which are unavoidably introduced during freezing and cryosectioning of lung tissue. Quality of data could be increased and variation between groups potentially decreased by sampling from an increased number of sections from a greater number of regions across the lung, although doing so would decrease the throughput of this method.

Radiolabelled platelet tracking methods

The radiolabelled platelet studies developed for this project enabled the quantification of platelet clearance from blood and recruitment to whole livers, spleens and lungs, and platelet migration into airspaces following LPS inhalation, as well as non-invasive measurements of pulmonary thromboembolism following intravenous administration of the platelet agonist ADP. However, the non-invasive radiolabelled platelet tracking methods used in this thesis

were not sensitive enough to detect lung platelet recruitment following LPS inhalation, but the combination of blood microsampling and more advanced 3-dimensional radioimaging techniques such as single photon emission computed tomography may still enable non-invasive recordings of radiolabelled platelet recruitment to lungs following LPS inhalation (Khalil et al., 2011).

The chief disadvantages of tracking platelets through radiolabelling are the requirement of platelet manipulation *ex vivo* for radiolabelling which may alter platelet function, the partially labelled platelet pool in recipient mice with supraphysiological blood platelet counts, and the potential for changes in perfusion or blood pooling which could be mistaken for platelet recruitment.

Both immunohistochemistry, and the use of reporter mice with genetically labelled platelets for intravital microscopy, overcame the problem of only partial platelet population labelling as they allowed for imaging of more complete population of platelets, although microscopy favours larger platelets and slower platelets with the frame-rates currently possible using multiphoton intravital microscopy. A potential way to enable whole-body non-invasive imaging of platelets without requiring labelling *ex vivo* would be to use recently generated mice expressing infrared-fluorescing reporter proteins (Tran et al., 2014), for the breeding of mice with infrared reporters restricted to the megakaryocyte-platelet lineage which could be used in whole body fluorescence imaging systems to track all platelets across the body. Adapting antibody reporters developed for non-invasive imaging of conformational changes in platelet integrins associated with platelet activation, previously employed for measuring platelet activation in the brain in a murine cerebral malaria model might also allow for the first whole-

lung imaging studies of platelet activation following lung inflammation (von zur Muhlen et al., 2008). Co-administration of red cells or another perfusion control labelled with a different radionuclide allowing for spectral unmixing, as previously reported (Bureau et al., 1989), would improve radiolabelled platelet tracking studies through enabling better understanding of the contributions of variations in perfusion or blood retention to regional increases or decreases in radiolabelled platelet content.

Intravital microscopy

Intravital microscopy using PF4-cre × mTmG mice allowed for quantification of platelet adhesion within the living pulmonary circulation with the entire population of platelets labelled. Experiments comparing lungs of LPS-challenged mice with those of controls showed that LPS inhalation increased the quantity of platelet adhesion events in the circulation of living lungs, and that this adhesion did not appear to progress to aggregation, lending further support to conclusions made from measurements of LPS-induced lung platelet recruitment from immunohistochemistry and radiolabelled platelet distribution experiments which used *post mortem* tissue samples. Platelet recruitment in this manner has previously been observed in inflamed systemic venules of the mesentery, skin, and cremaster muscle (Frenette et al., 1998; Gros et al., 2015; Zuchtriegel et al., 2016), but to our knowledge this is the first automated measurement of individually counted inflammatory platelet recruitment events occurring in the pulmonary circulation.

These studies could be advanced to investigate the labelling of leukocytes in order to better detect platelet-leukocyte interactions which were not clearly visible in videos produced in this thesis, as has been previously achieved in lungs (Ortiz-Muñoz et al., 2014), and with

the simultaneous measurement of blood perfusion and oxygen saturation mapping possible in intravital preparations in order to relate platelet and cell recruitment events with deterioration in lung function over time (Tabuchi et al., 2013). Furthermore, the full time course of increases and decreases in platelet and leukocyte adhesion responses would be illuminating with respect to the primacy of platelet versus leukocyte recruitment. Another limitation of intravital multiphoton microscopy was difficulty in determining whether GFP+ events were single platelets, aggregates, or proplatelet/megakaryocyte processes. The breeding of a 'confetti' reporter mouse (Schepers et al., 2012), with a platelet lineage reporter would allow the labelling of platelets stochastically with four different fluorophores depending on their megakaryocyte of origin, and could better permit discrimination of the number of platelets incorporated into adhesion events and their motility.

Outside of the living context, the study of lungs removed from PF4-Cre × mTmG mice using confocal, multiphoton, or light-sheet microscopy might also allow for imaging of a larger area of tissue in the absence of sectioning artifacts or motion artifacts from breathing or the heartbeat, potentially allowing for clearer observation of platelets in the bronchoalveolar space.

Platelet recruitment to the liver and spleen following LPS inhalation

The increased clearance of radiolabelled platelets from the blood into the liver and spleen following LPS inhalation highlights the need for tracking cells in *in vivo* preparations with an intact systemic circulation and functioning mononuclear phagocyte system. The detection of the increased hepatic and splenic recruitment, following LPS-induced lung inflammation, but preceding lung platelet recruitment raises several questions for future research:

1. Does the liver and spleen recruitment following LPS inhalation involve permanent clearance of platelets from the bloodstream, or increased temporary sequestration through increased frequency or duration of platelet adhesion events, as previously reported following intravenous exposure to whole bacteria (Wong et al., 2013)?
2. Are the platelets recruited to lungs following LPS inhalation those that are sequestered in the liver or spleen?

Studies involving whole body radioimaging, intravital microscopy for platelet tracking in the microvasculature of the liver and spleen, and experimental mononuclear phagocyte depletion or splenectomy may provide answers to these questions. Importantly, the finding that the early thrombocytopenia shows little temporal connection to lung platelet recruitment highlights the importance of directly imaging platelets when measuring platelet recruitment to organs, as decreases in blood platelet counts have been previously used as indices of the extent of thromboembolism (Smith, 1981), and inflammatory lung platelet recruitment (Shibazaki et al., 1996).

Alterations in platelet production and clearance following LPS inhalation

Although an early decrease in blood platelet counts was detected, from 24 hours after LPS challenge blood platelet counts were returned to levels not significantly different from PBS control mice, despite evidence of platelet recruitment to lungs, liver and spleen. Megakaryocte and proplatelet events, although a minority of total CD41+ events observed in the lung, were increased with LPS inhalation suggesting that pulmonary thrombopoiesis, or pulmonary retention of megakaryocytes released into the bloodstream, might be increased in the context

of lung inflammation. Particularly with regards to previous observations that exposure to LPS one week prior to measurements alters platelet function in mice in a TLR4-independent manner (Jayachandran et al., 2007).

A more thorough analysis of the effect of LPS inhalation on the quantity of megakaryocyte release and duration of megakaryocyte-proplatelet-platelet transit time across the lungs, as well as measurements of platelet volume, reticulated 'young' platelet fraction and platelet lifespan may help to shed more light on how blood platelet counts are maintained in the context of lung inflammation.

5.1.2 Characterising mechanisms of LPS-induced lung platelet recruitment

Mechanistic insights into how platelets are recruited to lungs following LPS inhalation

The studies discussed above showed that LPS inhalation resulted in lung platelet recruitment involving increased platelet adhesion in the pulmonary circulation which did not appear to progress on to platelet aggregation.

Using the immunohistochemistry method to quantify lung platelet recruitment as well as other inflammation readouts, interventional studies enabled the identification of contrasts between the mechanisms through which neutrophils are recruited to lungs with those underlying platelet recruitment to lungs following LPS inhalation. PSGL-1 blocking antibody administration, which reduced lung neutrophil recruitement, as well as depletion of blood neutrophils to reduce lung neutrophil recruitment even further, had no detected effect on lung platlet recruitment following LPS inhalation, suggesting that platelet recruitment requires

different mechanisms to neutrophil recruitment and that neutrophils are not essential for a the optimal recruitment of platelets into the lung.

Interventional experiments also showed that both platelet and neutrophil recruitment to lungs in this model appeared to progress to similar amounts with P-selectin blocking antibody, $P2Y_1$ antagonist, $P2Y_{12}$ antagonist, or aspirin treatment, indicating that these treatments, all of which have demonstrated anti-inflammatory or anti-platelet activity in other contexts, were not active in reducing platelet or neutrophil recruitment to inflamed lungs following inhalation of LPS in the model used in this thesis.

What are the key mediators of platelet recruitment to inflamed lungs?

Experiments reported in this thesis suggest that, in the context of lung inflammation in mice following inhalation of LPS, the recruitment of platelets from the blood to the lungs does not require a full neutrophil recruitment response. Furthermore, LPS-induced lung platelet recruitment in the model used showed no significant alteration with blockade of either PSGL-1, P-selectin or with antagonists targeting $P2Y_1$, $P2Y_{12}$ or COX enzymes, suggestive that platelets did not require the function of these adhesion molecules, receptors or enzymes in order to become recruited to inflamed lungs.

However, these experiments have not identified which mediators are responsible for lung platelet recruitment following LPS inhalation. There are a number of possible experiments which may prove enlightening as to the mechanisms through which platelet recruitment to lungs in inflammation occurs.

Firstly, it would be interesting to further investigate the contribution of platelet adhesion molecules in addition to P-selectin and PSGL-1 using drug treatment, non-depleting blocking antibody interventions or knockout mouse studies. Potential platelet adhesion molecules of interest would include GP1b, $\alpha_{IIb}\beta_3$, GPVI, CLEC-2, ICAM-2, PECAM-1, which are all capable of mediating platelet adhesion and can all influence inflammatory progression to greater or lesser extents in different contexts (Diacovo et al., 1994; Woodfin et al., 2007; Varga-Szabo et al., 2008).

The importance of platelet CD40L and platelet serotonin production remains unstudied in inflammatory lung platelet recruitment whilst both mediators are important in lung inflammation responses (Dürk et al., 2013; Tian et al., 2014). Furthermore, platelet P-Rex1 and Vav1 or Vav3 GEFs, which integrate GPCR and ITAM-mediated signalling, are important for both lung neutrophil recruitment and decreases in blood platelet counts in response to LPS challenge (Pan et al., 2015), but it is unknown whether the absence of these signalling mediators alters lung platelet recruitment following LPS inhalation. Experiments in mice which have defects in platelet granule release would also be interesting to investigate whether platelet degranulation is necessary for lung platelet recruitment in inflammation (Deppermann et al., 2017).

To add to results from neutrophil depletion studies, experiments using clodronate-loaded liposomes to deplete alveolar macrophages, or blood monocytes and intravascular-facing macrophages could be used to explore whether these cell types, important for both the induction and resolution of LPS-induced inflammation (Ley et al., 2016), are important for platelet recruitment in inflammation. It would also be interesting to study the conjugation of platelets

with neutrophils, monocytes and macrophages in BAL and to investigate whether monocyte or macrophage depletion reduces platelet migration into lung airspaces.

Lastly, it is possible that inflammatory platelet recruitment may also be initiated by activation of the coagulation or complement cascades following LPS inhalation, and interventions possible in mice allow the investigation into the contributions of these systems to LPS-induced lung platelet recruitment (Shibazaki et al., 1999; Davis et al., 2016). However, it is notable that decreases in blood platelet counts were relatively small (<30%), and in a similar LPS model, bleeding times and platelet aggregation responses to ADP were not altered (Amison et al., 2017), suggestive that LPS inhalation models do not provoke a coagulation response similar to that seen in patients with disseminated intravascular coagulation. Pertinent to intravascular activation of coagulation or complement, future studies could also assess the extent to which LPS crosses into the bloodstream following LPS, and such studies may benefit from the use of human blood and the production of a humanised fibrinogen mouse, as at least in the context of human blood and O111:B4 LPS, recent studies have shown that LPS can initiate coagulation with altered fibrin mesh structure at substoichiometric concentrations, similar to mechanisms of diseases caused by prion proteins (Pretorius et al., 2016).

Differences between LPS inhalation models and detected effects of treatments

In the present body of research, the previous finding that treatment with PSGL-1 blocking antibody could reduce LPS-induced lung inflammation was reproduced (Kornerup et al., 2010). However, decreases in LPS-induced lung neutrophil recruitment were not detected with treatment with the P2Y1 antagonist MRS2500, with aspirin, or with experimental depletion of blood platelets, results that contrast with the conclusions of previously published studies

in other models of LPS inhalation in mice (Kornerup et al., 2010; Grommes et al., 2012; Ortiz-Muñoz et al., 2014; Pan et al., 2015; Tilgner et al., 2016), although it should be noted that the models used in this study and previous studies differ in several aspects, so the experiments reported in this thesis were not designed to be replication studies. Differences between models used in published studies and that used in this reported which may have lead to different resuts from studies investigating the effects of antiplatelet drug treatment or platelet depletion on LPS inhalation responses are summarised below (Table 5.1).

Table 5.1: Differences between methods used in published studies of effects of platelet depletion or anti-platelet drugs on lung inflammation response and those used in the present study. Blue shading represents difference between methodological approaches, orange represents similarity.

Mouse strain	Mouse sex	Mouse housing	LPS serotype	LPS dose	LPS route	Time point	Reference
C57Bl/6	♂	Non-barrier	*E. coli* O55:B5	1 mg/kg	i.n.	+24 hours	(Kornerup et al., 2010)
C57Bl/6	♂	Unknown	*S. enteritidis*	Unknown	Aerosolised	+4 hours	(Grommes et al., 2012)
C57Bl/6	♂	Non-barrier	*E. coli* O55:B5	0.2 mg/kg	i.n.	+4 hours	(Pan et al., 2015)
Balb/c	♂	Barrier	*E. coli* O55:B5	5 mg/kg	i.t.	+48 hours	(Ortiz-Muñoz et al., 2014)
C57Bl/6	♂	Non-barrier	*S. enteritidis*	Unknown	Aerosolised	+4 hours	(Tilgner et al., 2016)
Balb/c	♀	Non-barrier	*E. coli* O55:B5	1.25 mg/kg	i.n.	+4 hours	(Amison et al., 2017)
Balb/c	♀	Non-barrier	*E. coli* O55:B5	5 mg/kg	i.n.	+48 hours	Present study

A potentially key difference between studies is the time point at which samples were collected. In the present report samples were collected at 48 hours after LPS inhalation, whereas in the majority of other studies investigating the effects of platelet depletion or anti-platelet drugs, samples were collected earlier at 4 hours (Grommes et al., 2012; Pan et al., 2015; Tilgner et al., 2016; Amison et al., 2017), or 24 hours after LPS inhalation (Kornerup

et al., 2010). It is also notable with regards to time point of sample collection that most of the previously reported studies have involved a lesser degree of bronchoaveolar neutrophil recruitment, ~10^5 neutrophils or less, versus more than 10^6 neutrophils per ml of BAL in the present study (Kornerup et al., 2010; Grommes et al., 2012; Pan et al., 2015; Tilgner et al., 2016; Amison et al., 2017). These differences could be crucial if, over time, the inflammatory response develops such that the minority of neutrophils that are initially recruited that are independent of platelets occur sufficiently to produce a more substantial inflammatory reponse that enables a subsequent neutrophil recruitment response independently of platelets at 48 hours. Pharmacokinetics of the drugs used in the present study might provide inadequate levels of receptor antagonism over the duration of exposure despite repeated dosing, as although the same dosing strategy reduced eosinophil recruitment over four days of allergen challenge responses (Amison et al., 2015), receptor occupancy or drug efficacy may have been insufficient to prevent the more pronounced neutrophil recruitment response to LPS. In the context of platelet depletion, if haemorrhage develops over time leading to additional neutrophils entering airspaces from bleeding, as well as those that have entered the bronchoalveolar space through transendothelial migration, a later sampling time point may also show a smaller decrease in neutrophils recovered in BAL with platelet depletion.

In contrast to other published studies, Ortiz-Muñoz et al., (2014), used the same dose of LPS in the same strain of mice to cause similar levels of neutrophil recruitment (>10^6 neutrophils), and in contrast to results in the present report, found significant effects of aspirin treatment on lung inflammation (~50% reduction in BAL neutrophil recruitment), and so differences in time point and extent of inflammation are unlikely to explain the differences

the between observed effects of aspirin. A few differences between methods used in the present study and those used by Ortiz Muñoz et al., (2014) can be postulated to explain differences between reults of experiments, and may be important to investigate further.

In contrast to the model used in the present report, Ortiz Muñoz et al., (2014) used:

1. a higher quantity of DMSO in drug vehicle (15% vs 2% in the present study), which may have altered the pharmacokinetics, or may have had an additional anti-inflammatory effect as DMSO has shown anti-inflammatory properties in LPS reponses (Kelly et al., 1994; Elisia et al., 2016).
2. male mice rather than female mice, which have a number of differences in physiology including in responses to LPS (Card et al., 2006; Karp et al., 2017).
3. barrier-housed mice, which may have altered immune responses compared to more immunologically experienced non-barrier housed mice (Looney et al., 2009).
4. intratracheal rather than intranasal instillation. Intratracheal dosing may have caused a more even and consistent dispersal of LPS through the lungs than with intransasal dosing, which interventions may be more effective at targeting.

The study of all of these factors could potentially produce interesting results, as clinical investigation would be warranted if either aspirin pharmacokinetics, sex, immune experience, or distribution of inflammation could be shown to significantly alter responsiveness to aspirin in the context of lung inflammation in mice. Improving understanding the importance of these factors in animal models and in the clinic is important as effects of aspirin in reducing inflammation in models used to study ARDS (Zarbock et al., 2006; Looney et al., 2009; Ortiz-

Muñoz et al., 2014; Tilgner et al., 2016; Hamid et al., 2017), have so far not translated into efficacy in reduction of ARDS in clinical trials (Kor et al., 2016a).

Overcoming limitations of neutrophil depletion

Treatment of mice with intraperitoneal doses of anti-Ly6-G antibody depleted neutrophils from blood and consequently reduced lung neutrophil recruitment, with LPS-induced lung platelet recruitment not significantly altered, suggestive that the platelet recruitment response did not depend on neutrophils. However, neutrophil-depleted mice still had a degree of lung neutrophil recruitment, and so it remains possible that some platelet recruitment is neutrophil-dependent and the number of neutrophils present in depleted mice was sufficient to support lung platelet recruitment. A potential reason for lung neutrophil recruitment remaining in neutrophil-depleted mice might be that neutrophils were released from bone marrow and recruited to lungs before antibody and monocyte/macrophage-mediated clearance could occur (Bruhn et al., 2016). Further experiments using genetically modified mice with neutrophil deficiencies (Weber et al., 2015), and cytotoxic drugs which cause a relatively high degree of neutrophil depletion (Zuluaga et al., 2006), may be helpful to support results from anti-Ly6-G antibody-mediated neutrophil depletion experiments, as would targeting neutrophil function through either CCL2 inhibition, decreasing NETosis with PAD4 knockout or decreasing the quantity of NETs with DNAse treatment.

Decreases in body weight and blood platelet counts with administration of anti-Ly6-G antibody in both PBS control and LPS-challenged mice suggested that this highly-neutrophil selective depletion method also had some undesired adverse effects on general health status

of mice, and possibly on the production of platelets. However, all mice survived the experiment, and these adverse effects were less severe than the anaphylaxis with thrombocytopenia and increased lung neutrophil aggregate trapping reported with the intravenous administration of LPS and anti-Ly6-G antibody (Tanaka et al., 2011). In contrast, administration of anti-Ly6-G intraperitoneally reduced lung neutrophil recruitment, suggestive that intraperitoneal administration of anti-Ly6-G is a sensible method for experiments investigating the importance of neutrophils in inflammatory responses.

Reduced NETs in BAL from platelet-depleted mice without reductions in neutrophil counts

Even though the number of neutrophils recruited to the LPS-inflamed bronchoalveolar space was unaltered with platelet depletion, the finding that platelet depletion reduced the quantitiy of NETs detected in BAL was suggestive of some dependence of LPS-induced lung inflammation responses on platelets.

It is possible that this effect of platelet depletion was due to decreased interactions of neutrophils with platelets in the blood or potentially in the airspaces, and as previous *in vitro* experiments identified platelet promotion of NET release as dependent upon P-selectin function (Caudrillier et al., 2012; Etulain et al., 2015), it is of note that P-selectin blockade had no detectable effect on BAL NET content. Bleeding into lungs in platelet-depleted mice may also have led to the counting of blood neutrophils, as well as transmigrated neutrophils, in BAL, with the former possibly less disposed towards NET release, and may also have interfered with signalling that promotes NETosis.

In order to shed more light on these findings, the effects of platelet depletion at more time points over the course of the inflammatory response could be studied in order to investigate the full time course of neutrophil recruitment and NETosis in the presence and absence of platelets, and the activation status of neutrophils recruited to lung airspaces could be assessed in platlet replete and depleted mice using immunohistochemistry or flow assays. As NETs are potential mediators of pathophysiology, it would be interesting to investigate the effects of platelet depletion on changes in lung function in this model.

The observation that BAL neutrophil counts were reduced with PSGL-1 blocking antibody treatment, but the quantity of NETs detected in BAL was unaltered, seems paradoxical as the level of bronchoalveolar NETosis would be expected to be highly dependent on the number of neutrophils migrated into the bronchoalveolar space, although it is possible that the neutrophils recruited to the bronchoalveolar space in anti-PSGL-1-treated mice following LPS inhalation were sufficient in number to mount a full NET release reponse by 48 hours after challenge. The time course of lung neutrophil recruitment and NETosis, with or without PSGL-1 blockade, would also be interesting to study, as would levels of systemic cytokines, particularly KC given that PSGL-1 blockade decreased blood neutrophil counts, in order to guide investigations into how PSGL-1 blockade improves general health status of mice after LPS inhalation as indicated by reduced body weight loss.

P-selectin, PSGL-1 and inflammatory neutrophil homeostasis

The finding that P-selectin blockade increases, whilst PSGL-1 blockade decreases, blood neutrophil counts in the context of LPS inhalation suggests a role for both P-selectin and

PSGL-1 in maintaining blood neutrophil homeostasis in inflammation. Interestingly, P-selectin knockout mice have been shown to have increased blood neutrophil counts (Mayadas et al., 1993) and increased blood neutrophil lifespan (Johnson et al., 1995), whilst in contrast to blocking antibody effects reported here in the context of inflammation, PSGL-1 knockout mice displayed elevated leukocyte counts at baseline (Xia et al., 2002).

Exploring the mechanisms through which PSGL-1 blockade reduces blood neutrophil content in inflammation may reveal more about the mechanisms of the anti-inflammatory action through inhibition of PSGL-1 function and the mechanisms of inflammatory neutrophil homeostasis, both of which are incompletely understood (Basu et al., 2000; Carlow et al., 2009; Summers et al., 2010). Investigations into whether the blockade of P-selectin or PSGL-1 alter inflammatory cytokine release, neutrophil production, or neutrophil release from the bone marrow, and whether the shedding of these molecules from cells and platelets, or their mediation of cell adhesion or signalling are important in neutrophil homeostasis may therefore produce interesting results.

P-selectin or PSGL-1 blockade-induced alterations in neutrophil homeostasis in inflammation warrant further investigation as both increased neutrophil counts or neutropenia could potentially be dangerous side effects for new drugs, especially as interventions targeting P-selectin and PSGL-1 are in development and in the case of P-selectin blockade in sickle cell disease, are entering clinical usage (Kanabar et al., 2016; Ataga et al., 2017).

5.2 Conclusions

Experiments reported in this thesis showed that inhalation of LPS caused recruitment of platelets to the pulmonary microcirculation and the bronchoalveolar airspace, and demonstrate methods for quantifying these responses in mice, with immunohistochemistry and radiolabelling techniques also having potential utitility for translation into experiments in the human setting.

Interventional studies revealed that lung platelet recruitment in the mouse model appeared to occur independently of neutrophils and through different mechanisms to lung neutrophil recruitment as, in contrast to lung neutrophil recruitment, lung platelet recruitment was insensitive to treatment with an anti-PSGL-1 blocking antibody. The mouse LPS inhalation model characterised here offers a platform for the identification of which mediators are essential for lung platelet recruitment, and research into whether this response is protective or harmful.

Experiments reported here are also suggestive of alterations in platelet clearance, platelet recruitment to liver and spleen, and platelet production in the context of inflammation, and showed that P-selectin blockade increased, while PSGL-1 blockade decreased, blood neutrophil counts following LPS inhalation. These observations open up new avenues for investigation into platelet and neutrophil dynamics in the context of lung inflammation.

Hopefully, the application and further development of methods described in this report will be useful for further exploration of platelet functions in inflammation, and will aid in the development of safer and more effective drugs for use in inflammatory diseases.

6 References

Abi-Younes, S., Si-Tahar, M., and Luster, A.D. (2001). The CC chemokines MDC and TARC induce platelet activation via CCR4. Thromb. Res. *101*: 279–89.

Al-Sarraf, A.A., Christenson, J.T., and Owunwanne, A. (1988). Early and late platelet sequestration in different organs during endotoxic shock. Res. Exp. Med. *188*: 59–66.

Al-Sarraf, A.A., Owunwanne, A., and Christenson, J.T. (1989). The role of low molecular weight dextran on platelet pulmonary trapping during endotoxin-induced shock. Resuscitation *17*: 1–9.

Almqvist, P., Kuenzig, M., and Schwartz, S.I. (1983). Effect of naloxone on endotoxin-induced pulmonary platelet sequestration. Acta Chir. Scand. *149*: 23.

Amison, R.T., Arnold, S., O'Shaughnessy, B.G., Cleary, S.J., Ofoedu, J., Idzko, M., et al. (2017). Lipopolysaccharide (LPS) induced pulmonary neutrophil recruitment and platelet activation is mediated via the P2Y1 and P2Y14 receptors in mice. Pulm. Pharmacol. Ther. *45*: 62–68.

Amison, R.T., Momi, S., Morris, A., Manni, G., Keir, S., Gresele, P., et al. (2015). RhoA signaling through platelet $P2Y_1$ receptor controls leukocyte recruitment in allergic mice. J. Allergy Clin. Immunol. *135*: 528–38.

Andonegui, G., Kerfoot, S.M., McNagny, K., Ebbert, K.V.J., Patel, K.D., and Kubes, P. (2005). Platelets express functional Toll-like receptor-4. Blood *106*: 2417–2423.

André, P., Denis, C. V, Ware, J., Saffaripour, S., Hynes, R.O., Ruggeri, Z.M., et al. (2000). Platelets adhere to and translocate on von Willebrand factor presented by endothelium in stimulated veins. Blood *96*: 3322–8.

Anselmo, A., Riva, F., Gentile, S., Soldani, C., Barbagallo, M., Mazzon, C., et al. (2016). Expression and function of IL-1R8 (TIR8/SIGIRR): a regulatory member of the IL-1 receptor family in platelets. Cardiovasc. Res.

Antithrombotic Trialists' Collaboration (2002). Collaborative meta-analysis of randomised trials of antiplatelet therapy for prevention of death, myocardial infarction, and stroke in high risk patients. BMJ *324*: 71–86.

Arnoux, B., Denjean, A., Page, C.P., Nolibe, D., Morley, J., and Benveniste, J. (1988). Accumulation of Platelets and Eosinophils in Baboon Lung after Paf-acether Challenge: Inhibition by Ketotifen. Am. Rev. Respir. Dis. *137*: 855–860.

Asaduzzaman, M., Lavasani, S., Rahman, M., Zhang, S., Braun, O.Ö., Jeppsson, B., et al. (2009a). Platelets support pulmonary recruitment of neutrophils in abdominal sepsis. Crit. Care Med. *37*: 1389–1396.

Asaduzzaman, M., Rahman, M., Jeppsson, B., and Thorlacius, H. (2009b). P-selectin glycoprotein-ligand-1 regulates pulmonary recruitment of neutrophils in a platelet-independent manner in abdominal sepsis. Br. J. Pharmacol. *156*: 307–15.

Asaduzzaman, M., Zhang, S., Lavasani, S., Wang, Y., and Thorlacius, H. (2008). LFA-1 and MAC-1 mediate pulmonary recruitment of neutrophils and tissue damage in abdominal sepsis. Shock *30*: 1.

Aschoff, L. (1893). Ueber capilläre Embolie von riesenkernhaltigen Zellen. Arch. Für Pathol. Anat. Und Physiol. Und Für Klin. Med. *134*: 11–25.

Ataga, K.I., Kutlar, A., Kanter, J., Liles, D., Cancado, R., Friedrisch, J., et al. (2017). Crizanlizumab for the Prevention of Pain Crises in Sickle Cell Disease. N. Engl. J. Med. *376*: 429–439.

Atherton, A., and Born, G. V (1972). Quantitative investigations of the adhesiveness of circulating polymorphonuclear leucocytes to blood vessel walls. J. Physiol. *222*: 447–74.

Atherton, A., and Born, G. V (1973a). Proceedings: Effects of neuraminidase and N-acetyl neuraminic acid on the adhesion of circulating granulocytes and platelets in venules. J. Physiol. *234*: 66P–67P.

Atherton, A., and Born, G.V.R. (1973b). Relationship between the velocity of rolling granulocytes and that of the blood flow in venules. J. Physiol. *233*: 157–165.

Barnes, P.J. (2008). Immunology of asthma and chronic obstructive pulmonary disease. Nat. Rev. Immunol. *8*: 183–192.

Barnes, P.J. (2010). New therapies for asthma: is there any progress? Trends Pharmacol. Sci. *31*: 335–343.

Barnes, P.J., Bonini, S., Seeger, W., Belvisi, M.G., Ward, B., and Holmes, A. (2015). Barriers to new drug development in respiratory disease. Eur. Respir. J. *45*:.

Barry, B.E., and Crapo, J.D. (1985). Patterns of accumulation of platelets and neutrophils in rat lungs during exposure to 100% and 85% oxygen. Am. Rev. Respir. Dis. *132*: 548–55.

Basit, A., Reutershan, J., Morris, M.A., Solga, M., Rose, C.E., and Ley, K. (2006). ICAM-1 and LFA-1 play critical roles in LPS-induced neutrophil recruitment into the alveolar space. *291*: L200–L207.

Basu, S., Hodgson, G., Zhang, H.H., Katz, M., Quilici, C., and Dunn, A.R. (2000). 'Emergency' granulopoiesis in G-CSF-deficient mice in response to Candida albicans infection. Blood *95*: 3725–33.

Bate, S.T., and Clark, R.A. (2014). The design and statistical analysis of animal experiments (Cambridge University Press).

Bednar, M., Smith, B., Pinto, A., and Mullane, K.M. (1985). Neutrophil depletion suppresses 111In-labeled platelet accumulation in infarcted myocardium. J. Cardiovasc. Pharmacol. *7*: 906–12.

Beijer, L., Botting, J., Crook, P., Oyekan, A.O., Page, C.P., and Rylander, R. (1987). The involvement of platelet activating factor in endotoxin-induced pulmonary platelet recruitment in the guinea-pig. Br. J. Pharmacol. *92*: 803–808.

Bengtsson, T., Fryden, A., Zalavary, S., Whiss, P.A., Orselius, K., and Grenegård, M. (1999). Platelets enhance neutrophil locomotion: evidence for a role of P-selectin. Scand. J. Clin. Lab. Investig. *59*: 439–449.

Bergmeier, W., Rackebrandt, K., Schröder, W., Zirngibl, H., and Nieswandt, B. (2000). Structural and functional characterization of the mouse von Willebrand factor receptor GPIb-IX with novel monoclonal antibodies. Blood *95*: 886–93.

Berthet, J., Damien, P., Hamzeh-Cognasse, H., Arthaud, C.-A., Eyraud, M.-A., Zéni, F., et al. (2012). Human platelets can discriminate between various bacterial LPS isoforms via TLR4 signaling and differential cytokine secretion. Clin. Immunol. *145*: 189–200.

Bettex-Galland, M., and Luescher, E.F. (1959). Extraction of an actomyosin-like protein from human thrombocytes. Nature *184(Suppl 5)*: 276–7.

Bierman, H.R., Kelly, K.H., King, F.W., and Petrakis, N.L. (1951). The Pulmonary Circulation as a Source of Leucocytes and Platelets in Man. Science (80-.). *114*:.

Bigby, T.D., and Meslier, N. (1989). Transcellular lipoxygenase metabolism between monocytes and platelets. J. Immunol. *143*: 1948–54.

Biswas, A., Bruder, D., Wolf, S.A., Jeron, A., Mack, M., Heimesaat, M.M., et al. (2015). Ly6Chigh monocytes control cerebral toxoplasmosis. J. Immunol. *194*:.

Boilard, E., Nigrovic, P.A., Larabee, K., Watts, G.F.M., Coblyn, J.S., Weinblatt, M.E., et al. (2010). Platelets amplify inflammation in arthritis via collagen-dependent microparticle production. Science *327*: 580–3.

Bombeli, T., Schwartz, B.R., and Harlan, J.M. (1998). Adhesion of activated platelets to endothelial cells: evidence for a GPIIbIIIa-dependent bridging mechanism and novel roles for endothelial intercellular adhesion molecule 1 (ICAM-1), alphavbeta3 integrin, and GPIbalpha. J. Exp. Med. *187*: 329–39.

Bone, R.C., Francis, P.B., and Pierce, A.K. (1976). Intravascular coagulation associated with the adult respiratory distress syndrome. Am. J. Med. *61*: 585–589.

Boogaard, F.E. van den, Schouten, M., Stoppelaar, S.F. de, Roelofs, J.J.T.H., Brands, X., Schultz, M.J., et al. (2015). Thrombocytopenia Impairs Host Defense During Murine Streptococcus pneumoniae Pneumonia. Crit. Care Med. *43*:.

Bosse, R., and Vestweber, D. (1994). Only simultaneous blocking of the L- and P-selectin completely inhibits neutrophil migration into mouse peritoneum. Eur. J. Immunol. *24*: 3019–3024.

Boulaftali, Y., Hess, P.R., Getz, T.M., Cholka, A., Stolla, M., Mackman, N., et al. (2013). Platelet ITAM signaling is critical for vascular integrity in inflammation. J. Clin. Invest. *123*: 908–16.

Bradfield, P.F., Nourshargh, S., Aurrand-Lions, M., and Imhof, B.A. (2007). JAM Family and Related Proteins in Leukocyte Migration (Vestweber Series). Arterioscler. Thromb. Vasc. Biol. *27*: 2104–2112.

Braun, T.P., Grossberg, A.J., Krasnow, S.M., Levasseur, P.R., Szumowski, M., Zhu, X.X., et al. (2013). Cancer- and endotoxin-induced cachexia require intact glucocorticoid signaling in skeletal muscle. FASEB J. *27*: 3572–82.

Bredenberg, C.E., Taylor, G.A., and Webb, W.R. (1980). The effect of thrombocytopenia on the pulmonary and systemic hemodynamics of canine endotoxin shock. Surgery *87*: 59–68.

Brown, G.T., Narayanan, P., Li, W., Silverstein, R.L., and McIntyre, T.M. (2013). Lipopolysaccharide Stimulates Platelets through an IL-1β Autocrine Loop. J. Immunol. *191*: 5196–5203.

Bruhn, K.W., Dekitani, K., Nielsen, T.B., Pantapalangkoor, P., and Spellberg, B. (2016). Ly6G-mediated depletion of neutrophils is dependent on macrophages. Results Immunol. *6*: 5–7.

Buhr, N. de, and Köckritz-Blickwede, M. von (2016). How Neutrophil Extracellular Traps Become Visible. J. Immunol. Res. *2016*: 1–13.

Bunting, S., Gryglewski, R., Moncada, S., and Vane, J.R. (1976). Arterial walls generate from prostaglandin endoperoxides a substance (prostaglandin X) which relaxes strips of mesenteric and coeliac ateries and inhibits platelet aggregation. Prostaglandins *12*: 897–913.

Bureau, M.F., Malanchere, E., Pretolani, M., Boukili, M.A., and Vargaftig, B.B. (1989). A new method to evaluate extravascular albumin and blood cell accumulation in the lung. J. Appl. Physiol. *67*: 1479–1488.

Busse, W.W. (1998). Leukotrienes and Inflammation. Am. J. Respir. Crit. Care Med. *157*: S210–S213.

Card, J.W., Carey, M.A., Bradbury, J.A., DeGraff, L.M., Morgan, D.L., Moorman, M.P., et al. (2006). Gender differences in murine airway responsiveness and lipopolysaccharide-induced inflammation. J. Immunol. *177*: 621–30.

Carlow, D.A., Gossens, K., Naus, S., Veerman, K.M., Seo, W., and Ziltener, H.J. (2009). PSGL-1 function in immunity and steady state homeostasis. Immunol. Rev. *230*: 75–96.

Carstairs, K.C. (1965). The identification of platelets and platelet antigens in histological sections. J. Pathol. Bacteriol. *90*: 225–231.

Carvalho-Tavares, J., Hickey, M.J., Hutchison, J., Michaud, J., Sutcliffe, I.T., and Kubes, P. (2000). A role for platelets and endothelial selectins in tumor necrosis factor-alpha-induced leukocyte recruitment in the brain microvasculature. Circ. Res. *87*: 1141–8.

Cattaneo, M. (2010). New P2Y12 Inhibitors. Circulation *121*:.

Caudrillier, A., Kessenbrock, K., Gilliss, B.M., Nguyen, J.X., Marques, M.B., Monestier, M., et al. (2012). Platelets induce neutrophil extracellular traps in transfusion-related acute lung injury. J. Clin. Invest. *122*: 2661–71.

Chi, X., Zhi, L., Gelderman, M.P., and Vostal, J.G. (2012). Host Platelets and, in Part, Neutrophils Mediate Lung Accumulation of Transfused UVB-Irradiated Human Platelets in a Mouse Model of Acute Lung Injury. PLoS One *7*: e44829.

Clemetson, K.J., Clemetson, J.M., Proudfoot, A.E., Power, C.A., Baggiolini, M., and Wells, T.N. (2000). Functional expression of CCR1, CCR3, CCR4, and CXCR4 chemokine receptors on human platelets. Blood *96*: 4046–54.

Cooper, D., Russell, J., Chitman, K.D., Williams, M.C., Wolf, R.E., and Granger, D.N. (2004). Leukocyte dependence of platelet adhesion in postcapillary venules. Am. J. Physiol. Heart Circ. Physiol. *286*: H1895-900.

Cox, D., Kerrigan, S.W., and Watson, S.P. (2011). Platelets and the innate immune system: mechanisms of bacterial-induced platelet activation. J. Thromb. Haemost. *9*: 1097–1107.

Coyle, A.J., Page, C.P., Atkinson, L., Flanagan, R., and Metzger, W.J. (1990). The requirement for platelets in allergen-induced late asthmatic airway obstruction: eosinophil infiltration and heightened airway responsiveness in allergic rabbits. Am. J. Respir. Crit. Care Med. *142*: 587–593.

Cuker, A., and Cines, D.B. (2010). Evidence-Based Mini-Review: Is indium-labeled autologous platelet scanning predictive of response to splenectomy in patients with chronic immune thrombocytopenia? Hematology *2010*: 385–386.

Czapiga, M., Gao, J.L., Kirk, A., and Lekstrom-Himes, J. (2005). Human platelets exhibit chemotaxis using functional N-formyl peptide receptors. Exp. Hematol. *33*: 73–84.

Daley, J.M., Thomay, A.A., Connolly, M.D., Reichner, J.S., and Albina, J.E. (2008). Use of Ly6G-specific monoclonal antibody to deplete neutrophils in mice. J. Leukoc. Biol. *83*: 64–70.

Dall, L., Miller, T., Herndon, B., Diez, I., and Dew, M. (1998). Platelet depletion and severity of streptococcal endocarditis. Can. J. Infect. Dis. *9*: 359–66.

Davì, G., and Patrono, C. (2007). Platelet Activation and Atherothrombosis. N. Engl. J. Med. *357*: 2482–2494.

Davis, R.P., Miller-Dorey, S., and Jenne, C.N. (2016). Platelets and coagulation in infection. Clin. Transl. Immunol. *5*: e89.

Deppermann, C., Kraft, P., Volz, J., Schuhmann, M.K., Beck, S., Wolf, K., et al. (2017). Platelet secretion is crucial to prevent bleeding in the ischemic brain but not in the inflamed skin or lung in mice. Blood *129*: 1702–1706.

Dewanjee, M.K., Rao, S.A., Rosemark, J.A., Chowdhury, S., and Didisheim, P. (1982). Indium-111 tropolone, a new tracer for platelet labeling. Radiology *145*: 149–153.

Diacovo, T.G., deFougerolles, A.R., Bainton, D.F., and Springer, T.A. (1994). A functional integrin ligand on the surface of platelets: intercellular adhesion molecule-2. J. Clin. Invest. *94*: 1243–1251.

Diacovo, T.G., Puri, K.D., Warnock, R.A., Springer, T.A., and Andrian, U.H. von (1996a). Platelet-mediated lymphocyte delivery to high endothelial venules. Science *273*: 252–5.

Diacovo, T.G., Roth, S.J., Buccola, J.M., Bainton, D.F., and Springer, T.A. (1996b). Neutrophil rolling, arrest, and transmigration across activated, surface-adherent platelets via sequential action of P-selectin and the beta 2-integrin CD11b/CD18. Blood *88*: 146–57.

Dicuio, M., Pomara, G., Cuttano, M.G., Vesely, S., Travaglini, F., Cuzzocrea, D.E., et al. (2003). Penile Mondor's disease after intensive masturbation in a 31-and a 33-year-old man. Thromb. Haemost. *90*: 155–6.

Doerschuk, C.M., Downey, G.P., Doherty, D.E., English, D., Gie, R.P., Ohgami, M., et al. (1990). Leukocyte and platelet margination within microvasculature of rabbit lungs. J. Appl. Physiol. *68*: 1956–61.

Drago, L., Bortolin, M., Vassena, C., Taschieri, S., and Fabbro, M. Del (2013). Antimicrobial activity of pure platelet-rich plasma against microorganisms isolated from oral cavity. BMC Microbiol. *13*: 47.

Duerschmied, D., Suidan, G.L., Demers, M., Herr, N., Carbo, C., Brill, A., et al. (2013). Platelet serotonin promotes the recruitment of neutrophils to sites of acute inflammation in mice. Blood *121*: 1008–1015.

Dunn, K.W., Kamocka, M.M., and McDonald, J.H. (2011). A practical guide to evaluating colocalization in biological microscopy. Am. J. Physiol. Cell Physiol. *300*: C723-42.

Durham, S.K., Horan, M.A., Brouwer, A., Barelds, R.J., and Knook, D.L. (1989). Platelet participation in the increased severity of endotoxin-induced pulmonary injury in aged rats. J. Pathol. *157*: 339–345.

Dürk, T., Duerschmied, D., Müller, T., Grimm, M., Reuter, S., Vieira, R.P., et al. (2013). Production of serotonin by tryptophan hydroxylase 1 and release via platelets contribute to allergic airway inflammation. Am. J. Respir. Crit. Care Med. *187*: 476–485.

Edenius, C., Heidvall, K., and Lindgren, J.A. (1988). Novel transcellular interaction: conversion of granulocyte-derived leukotriene A4 to cysteinyl-containing leukotrienes by human platelets. Eur. J. Biochem. *178*: 81–6.

Eichhorn, M., Ney, L., Massberg, S., and Goetz, A. (2002). Platelet Kinetics in the Pulmonary Microcirculation in vivo Assessed by Intravital Microscopy Platelet Kinetics in the Pulmonary Microcirculation. J Vasc Res *3939*:.

Elisia, I., Nakamura, H., Lam, V., Hofs, E., Cederberg, R., Cait, J., et al. (2016). DMSO Represses Inflammatory Cytokine Production from Human Blood Cells and Reduces Autoimmune Arthritis. PLoS One *11*: e0152538.

Engelmann, B., and Massberg, S. (2013). Thrombosis as an intravascular effector of innate immunity. Nat. Rev. Immunol. *13*: 34–45.

Erlinge, D., and Burnstock, G. (2008). P2 receptors in cardiovascular regulation and disease. Purinergic Signal. *4*: 1–20.

Etulain, J., Martinod, K., Wong, S.L., Cifuni, S.M., Schattner, M., and Wagner, D.D. (2015). P-selectin promotes neutrophil extracellular trap formation in mice. Blood *126*: 242–6.

Feng, D., Nagy, J.A., Pyne, K., Dvorak, H.F., and Dvorak, A.M. (1998). Platelets Exit Venules by a Transcellular Pathway at Sites of F–Met Peptide–Induced Acute Inflammation in Guinea Pigs. Int. Arch. Allergy Immunol. *116*: 188–195.

Fernandes, M., Irulegui, I., Deane, M.P., and Ruiz, R. de C. (1992). Trypanosoma cruzi: course of infection in platelets-depleted mice. Rev. Inst. Med. Trop. Sao Paulo *34*: 9–13.

Fitzgerald, J.R., Foster, T.J., and Cox, D. (2006). The interaction of bacterial pathogens with platelets. Nat. Rev. Microbiol. *4*: 445–57.

Flower, R.J. (2003). The development of COX2 inhibitors. Nat. Rev. Drug Discov. *2*: 179–191.

Folco, G., and Murphy, R.C. (2006). Eicosanoid Transcellular Biosynthesis: From Cell-Cell Interactions to in Vivo Tissue Responses. Pharmacol. Rev. *58*: 375–388.

Franciosi, L.G., Diamant, Z., Banner, K.H., Zuiker, R., Morelli, N., Kamerling, I.M.C., et al. (2013). Efficacy and safety of RPL554, a dual PDE3 and PDE4 inhibitor, in healthy volunteers and in patients with asthma or chronic obstructive pulmonary disease: findings from four clinical trials. Lancet Respir. Med. *1*: 714–727.

Frenette, P.S., Denis, C. V, Weiss, L., Jurk, K., Subbarao, S., Kehrel, B., et al. (2000). P-Selectin glycoprotein ligand 1 (PSGL-1) is expressed on platelets and can mediate platelet–endothelial interactions in vivo. J. Exp. Med. *191*: 1413–1422.

Frenette, P.S., Moyna, C., Hartwell, D.W., Lowe, J.B., Hynes, R.O., and Wagner, D.D. (1998). Platelet-endothelial interactions in inflamed mesenteric venules. Blood *91*: 1318–24.

Frydman, G.H., Le, A., Ellett, F., Jorgensen, J., Fox, J.G., Tompkins, R.G., et al. (2017). Technical Advance: Changes in neutrophil migration patterns upon contact with platelets in a microfluidic assay. J. Leukoc. Biol. *101*: 797–806.

Fukunaga, K., Kohli, P., Bonnans, C., Fredenburgh, L.E., and Levy, B.D. (2005). Cyclooxygenase 2 Plays a Pivotal Role in the Resolution of Acute Lung Injury. J. Immunol. *174*:.

Fuster, V., and Sweeny, J.M. (2011). Aspirin. Circulation *123*:.

Garraud, O., and Cognasse, F. (2015). Are Platelets Cells? And if Yes, are They Immune Cells? Front. Immunol. *6*: 70.

Gawaz, M., Dickfeld, T., Bogner, C., Fateh-Moghadam, S., and Neumann, F.J. (1997). Platelet function in septic multiple organ dysfunction syndrome. Intensive Care Med. *23*: 379–85.

Gawaz, M., Fateh-Moghadam, S., Pilz, G., Gurland, H., and Werdan, K. (1995). Platelet activation and interaction with leucocytes in patients with sepsis or multiple organ failure. Eur. J. Clin. Invest. *25*: 843–851.

Gawaz, M., and Vogel, S. (2013). Platelets in tissue repair: control of apoptosis and interactions with regenerative cells. Blood *122*:.

Goerge, T., Ho-Tin-Noe, B., Carbo, C., Benarafa, C., Remold-O'Donnell, E., Zhao, B.-Q.Q., et al. (2008). Inflammation induces hemorrhage in thrombocytopenia. Blood *111*: 4958–4964.

Gramaglia, I., Velez, J., Combes, V., Grau, G.E.R., Wree, M., and Heyde, H.C. van der (2017). Platelets activate a pathogenic response to blood-stage Plasmodium infection but not a protective immune response. Blood *129*:.

Gresele, P., Dottorini, M., Selli, M.L., Canino, S., Todisco, T., Romano, S., et al. (1993). Altered platelet function associated with the bronchial hyperresponsiveness accompanying nocturnal asthma. J. Allergy Clin. Immunol. *91*: 894–902.

Grommes, J., Alard, J.E., Drechsler, M., Wantha, S., Mörgelin, M., Kuebler, W.M., et al. (2012). Disruption of platelet-derived chemokine heteromers prevents neutrophil extravasation in acute lung injury. Am. J. Respir. Crit. Care Med. *185*: 628–636.

Gros, A., Syvannarath, V., Lamrani, L., Ollivier, V., Loyau, S., Goerge, T., et al. (2015). Single platelets seal neutrophil-induced vascular breaches via GPVI during immune-complex-mediated inflammation in mice. Blood *126*: 1017–26.

Hamad, O.A., Nilsson, P.H., Wouters, D., Lambris, J.D., Ekdahl, K.N., and Nilsson, B. (2010). Complement Component C3 Binds to Activated Normal Platelets without Preceding Proteolytic Activation and Promotes Binding to Complement Receptor 1. J. Immunol. *184*: 2686–2692.

Hamid, U., Krasnodembskaya, A., Fitzgerald, M., Shyamsundar, M., Kissenpfennig, A., Scott, C., et al. (2017). Aspirin reduces lipopolysaccharide-induced pulmonary inflammation in human models of ARDS. Thorax thoraxjnl-2016-208571.

Hamzeh-Cognasse, H., Damien, P., Chabert, A., Pozzetto, B., Cognasse, F., and Garraud, O. (2015). Platelets and infections - complex interactions with bacteria. Front. Immunol. *6*: 82.

Hara, T., Shimizu, K., Ogawa, F., Yanaba, K., Iwata, Y., Muroi, E., et al. (2010). Platelets Control Leukocyte Recruitment in a Murine Model of Cutaneous Arthus Reaction. Am. J. Pathol. *176*: 259–269.

Harris, R.A., Bajo, M., Bell, R.L., Blednov, Y.A., Varodayan, F.P., Truitt, J.M., et al. (2017). Genetic and Pharmacologic Manipulation of TLR4 Has Minimal Impact on Ethanol Consumption in Rodents. J. Neurosci. *37*: 1139–1155.

Haselmayer, P., Grosse-Hovest, L., Landenberg, P. von, Schild, H., and Radsak, M.P. (2007). TREM-1 ligand expression on platelets enhances neutrophil activation. Blood *110*: 1029–1035.

Headley, M.B., Bins, A., Nip, A., Roberts, E.W., Looney, M.R., Gerard, A., et al. (2016). Visualization of immediate immune responses to pioneer metastatic cells in the lung. Nature *531*: 513–517.

Hechtman, H.B., Lonergan, E.A., Staunton, H.P., Dennis, R.C., and Shepro, D. (1978). Pulmonary entrapment of platelets during acute respiratory failure. Surgery *83*: 277–83.

Henn, V., Slupsky, J.R., Gräfe, M., Anagnostopoulos, I., Förster, R., Müller-Berghaus, G., et al. (1998). CD40 ligand on activated platelets triggers an inflammatory reaction of endothelial cells. Nature *391*: 591–4.

Herzog, B.H., Fu, J., Wilson, S.J., Hess, P.R., Sen, A., McDaniel, J.M., et al. (2013). Podoplanin maintains high endothelial venule integrity by interacting with platelet CLEC-2. Nature *502*: 105–9.

Heyde, H.C. van der, Gramaglia, I., Sun, G., and Woods, C. (2005). Platelet depletion by anti-CD41 (αIIb) mAb injection early but not late in the course of disease protects against Plasmodium berghei pathogenesis by altering the levels of pathogenic cytokines. Blood *105*:.

Hickey, M.P., Kuligowski, A.R., Kitching, M.J., Kuligowski, M.P., Kitching, A.R., and Hickey, M.J. (2006). Rolling Platelet-Derived P-Selectin in the Absence of Glomerulus: A Critical Role for Leukocyte Recruitment to the Inflamed Leukocyte Recruitment to the Inflamed Glomerulus: A Critical Role for Platelet-Derived P-Selectin in the Absence of Rolling. J Immunol Ref. 6991–6999.

Hicks, A.E.R., Nolan, S.L., Ridger, V.C., Hellewell, P.G., and Norman, K.E. (2003). Recombinant P-selectin glycoprotein ligand–1 directly inhibits leukocyte rolling by all 3 selectins in vivo: complete inhibition of rolling is not required for anti-inflammatory effect. Blood *101*:.

Hidalgo, A., Chang, J., Jang, J.-E., Peired, A.J., Chiang, E.Y., and Frenette, P.S. (2009). Heterotypic interactions enabled by polarized neutrophil microdomains mediate thromboinflammatory injury. Nat. Med. *15*: 384–391.

Hirose, T., Hamaguchi, S., Matsumoto, N., Irisawa, T., Seki, M., Tasaki, O., et al. (2014). Presence of Neutrophil Extracellular Traps and Citrullinated Histone H3 in the Bloodstream of Critically Ill Patients. PLoS One *9*: e111755.

Ho-Tin-Noé, B., Demers, M., and Wagner, D.D. (2011). How platelets safeguard vascular integrity. J. Thromb. Haemost. *9 Suppl 1*: 56–65.

Howell, W.H., and Donahue, D.D. (1937). The production of blood platelets in the lungs. J. Exp. Med. *65*: 177–203.

Inwald, D.P., McDowall, A., Peters, M.J., Callard, R.E., and Klein, N.J. (2003). CD40 is constitutively expressed on platelets and provides a novel mechanism for platelet activation. Circ. Res. *92*: 1041–8.

Iribarren, C., Tolstykh, I. V., Miller, M.K., Sobel, E., and Eisner, M.D. (2012). Adult Asthma and Risk of Coronary Heart Disease, Cerebrovascular Disease, and Heart Failure: A Prospective Study of 2 Matched Cohorts. Am. J. Epidemiol. *176*: 1014–1024.

Issekutz, A.C., Ripley, M., and Jackson, J.R. (1983). Role of neutrophils in the deposition of platelets during acute inflammation. Lab. Invest. *49*: 716–724.

Itoh, H., Cicala, C., Douglas, G.J., and Page, C.P. (1996). Platelet accumulation induced by bacterial endotoxin in rats. Thromb. Res. *83*: 405–419.

Jackson, S.P., and Schoenwaelder, S.M. (2003). Antiplatelet therapy: in search of the 'magic bullet'. Nat. Rev. Drug Discov. *2*: 775–789.

Janeway, C.A., and Medzhitov, R. (2002). Innate immune recognition. Annu. Rev. Immunol. *20*: 197–216.

Jayachandran, M., Brunn, G.J., Karnicki, K., Miller, R.S., Owen, W.G., and Miller, V.M. (2007). In vivo effects of lipopolysaccharide and TLR4 on platelet production and activity: implications for thrombotic risk. J. Appl. Physiol. *102*: 429–33.

Johnson, R.C., Mayadas, T.N., Frenette, P.S., Mebius, R.E., Subramaniam, M., Lacasce, A., et al. (1995). Blood cell dynamics in P-selectin-deficient mice. Blood *86*: 1106–14.

Jones, H., Paul, W., and Page, C.P. (2002). A new model for the continuous monitoring of polymorphonuclear leukocyte trapping in the pulmonary vasculature of the rabbit. J. Pharmacol. Toxicol. Methods *48*: 21–9.

Joseph, M., Gounni, A.S., Kusnierz, J.P., Vorng, H., Sarfati, M., Kinet, J.P., et al. (1997). Expression and functions of the high-affinity IgE receptor on human platelets and megakaryocyte precursors. Eur. J. Immunol. *27*: 2212–8.

Kanabar, V., Tedaldi, L., Jiang, J., Nie, X., Panina, I., Descroix, K., et al. (2016). Base-modified UDP-sugars reduce cell surface levels of P-selectin glycoprotein 1 (PSGL-1) on IL-1β-stimulated human monocytes. Glycobiology *26*: 1059–1071.

Karim, S., Habib, A., Lévy-Toledano, S., and Maclouf, J. (1996). Cyclooxygenase-1 and -2 of endothelial cells utilize exogenous or endogenous arachidonic acid for transcellular production of thromboxane. J. Biol. Chem. *271*: 12042–8.

Karp, N.A., Mason, J., Beaudet, A.L., Benjamini, Y., Bower, L., Braun, R.E., et al. (2017). Prevalence of sexual dimorphism in mammalian phenotypic traits. Nat. Commun. *8*: 15475.

Kelly, K.A., Hill, M.R., Youkhana, K., Wanker, F., and Gimble, J.M. (1994). Dimethyl sulfoxide modulates NF-kappa B and cytokine activation in lipopolysaccharide-treated murine macrophages. Infect. Immun. *62*: 3122–8.

Khalil, M.M., Tremoleda, J.L., Bayomy, T.B., and Gsell, W. (2011). Molecular SPECT Imaging: An Overview. Int. J. Mol. Imaging *2011*: 796025.

Kiefmann, R., Heckel, K., Schenkat, S., Dörger, M., and Goetz, A.E. (2006). Role of p-selectin in platelet sequestration in pulmonary capillaries during endotoxemia. J. Vasc. Res. *43*: 473–481.

Kiefmann, R., Heckel, K., Schenkat, S., Dörger, M., Wesierska-Gadek, J., and Goetz, A.E. (2004). Platelet-endothelial cell interaction in pulmonary micro-circulation: the role of PARS. Thromb. Haemost. *91*: 761.

Kien, M., Hechtman, H., and Shepro, D. (1971). Platelet-microvasculature interaction during one passage through the dog lung. Microvasc. Res. *3*: 209–10.

Kile, B.T. (2014). The role of apoptosis in megakaryocytes and platelets. Br. J. Haematol. *165*: 217–226.

Kirkby, N.S., Chan, M. V, Lundberg, M.H., Massey, K.A., Edmands, W.M.B., Mackenzie, L.S., et al. (2013). Aspirin-triggered 15-epi-lipoxin A 4 predicts cyclooxygenase-2 in the lungs of LPS-treated mice but not in the circulation: implications for a clinical test. FASEB J *27*: 3938–46.

Klintman, D., Li, X., and Thorlacius, H. (2004). Important role of P-selectin for leukocyte recruitment, hepatocellular injury, and apoptosis in endotoxemic mice. Clin. Diagn. Lab. Immunol. *11*: 56–62.

Kor, D.J., Carter, R.E., Park, P.K., Festic, E., Banner-Goodspeed, V.M., Hinds, R., et al. (2016a). Effect of Aspirin on Development of ARDS in At-Risk Patients Presenting to the Emergency Department. JAMA *315*: 2406.

Kor, D.J., Carter, R.E., Park, P.K., Festic, E., Banner-Goodspeed, V.M., Hinds, R., et al. (2016b). Effect of Aspirin on Development of ARDS in At-Risk Patients Presenting to the Emergency Department. JAMA *315*: 2406.

Kornerup, K.N., Salmon, G.P., Pitchford, S.C., Liu, W.L., and Page, C.P. (2010). Circulating platelet-neutrophil complexes are important for subsequent neutrophil activation and migration. J. Appl. Physiol. *109*: 758–767.

Kowal, K., Pampuch, A., Kowal-Bielecka, O., DuBuske, L.M., and Bodzenta-?ukaszyk, A. (2006). Platelet activation in allergic asthma patients during allergen challenge with Dermatophagoides pteronyssinus. Clin. Exp. Allergy *36*: 426–432.

Kraemer, B.F., Borst, O., Gehring, E.M., Schoenberger, T., Urban, B., Ninci, E., et al. (2010). PI3 kinase-dependent stimulation of platelet migration by stromal cell-derived factor 1 (SDF-1). J. Mol. Med. *88*: 1277–1288.

Kraemer, B.F., Campbell, R.A., Schwertz, H., Cody, M.J., Franks, Z., Tolley, N.D., et al. (2011a). Novel Anti-bacterial Activities of β-defensin 1 in Human Platelets: Suppression of Pathogen Growth and Signaling of Neutrophil Extracellular Trap Formation. PLoS Pathog. *7*: e1002355.

Kraemer, B.F., Schmidt, C., Urban, B., Bigalke, B., Schwanitz, L., Koch, M., et al. (2011b). High shear flow induces migration of adherent human platelets. Platelets *22*: 415–421.

Kuckleburg, C.J., Yates, C.M., Kalia, N., Zhao, Y., Nash, G.B., Watson, S.P., et al. (2011). Endothelial cell-borne platelet bridges selectively recruit monocytes in human and mouse models of vascular inflammation. Cardiovasc. Res. *91*: 134–41.

Kuligowski, M.P., Kitching, A.R., and Hickey, M.J. (2006). Leukocyte Recruitment to the Inflamed Glomerulus: A Critical Role for Platelet-Derived P-Selectin in the Absence of Rolling. J. Immunol. *176*:.

Labelle, M., Begum, S., and Hynes, R.O. (2014). Platelets guide the formation of early metastatic niches. Proc. Natl. Acad. Sci. U. S. A. *111*: E3053-61.

Lacroix, R., Judicone, C., Mooberry, M., Boucekine, M., Key, N.S., Dignat-George, F., et al. (2013). Standardization of pre-analytical variables in plasma microparticle determination: results of the International Society on Thrombosis and Haemostasis SSC Collaborative workshop. J. Thromb. Haemost.

Laidlaw, T.M., Kidder, M.S., Bhattacharyya, N., Xing, W., Shen, S., Milne, G.L., et al. (2012). Cysteinyl leukotriene overproduction in aspirin-exacerbated respiratory disease is driven by platelet-adherent leukocytes. Blood *119*: 3790–3798.

Lam, F.W., Burns, A.R., Smith, C.W., and Rumbaut, R.E. (2011). Platelets enhance neutrophil transendothelial migration via P-selectin glycoprotein ligand-1. Am. J. Physiol. Heart Circ. Physiol. *300*: H468-75.

Langer, H.F., Choi, E.Y., Zhou, H., Schleicher, R., Chung, K.-J., Tang, Z., et al. (2012). Platelets Contribute to the Pathogenesis of Experimental Autoimmune Encephalomyelitis. Circ. Res. *110*: 1202–1210.

Lapchak, P.H., Kannan, L., Ioannou, A., Rani, P., Karian, P., Dalle Lucca, J.J., et al. (2012). Platelets orchestrate remote tissue damage after mesenteric ischemia-reperfusion. Am. J. Physiol. - Gastrointest. Liver Physiol. *302*:.

Lê, V.B., Schneider, J.G., Boergeling, Y., Berri, F., Ducatez, M., Guerin, J.-L., et al. (2015). Platelet Activation and Aggregation Promote Lung Inflammation and Influenza Virus Pathogenesis. Am. J. Respir. Crit. Care Med. *191*: 804–819.

Lee, J.W., Fang, X., Gupta, N., Serikov, V., and Matthay, M.A. (2009). Allogeneic human mesenchymal stem cells for treatment of E. coli endotoxin-induced acute lung injury in the ex vivo perfused human lung. Proc. Natl. Acad. Sci. *106*: 16357–16362.

Lee, R.E., Young, R.H., and Castleman, B. (2002). James Homer Wright: a biography of the enigmatic creator of the Wright stain on the occasion of its centennial. Am. J. Surg. Pathol. *26*: 88–96.

Leeksma, C.H., and Cohen, J.A. (1955). Determination of the life of human blood platelets using labelled diisopropylfluorophosphanate. Nature *175*: 552–3.

Lefrançais, E., Ortiz-Muñoz, G., Caudrillier, A., Mallavia, B., Liu, F., Sayah, D.M., et al. (2017). The lung is a site of platelet biogenesis and a reservoir for haematopoietic progenitors. Nature *544*: 105–109.

Lellouch-Tubiana, A., Lefort, J., Pirotzky, E., Vargaftig, B.B., and Pfister, A. (1985). Ultrastructural evidence for extravascular platelet recruitment in the lung upon intravenous injection of platelet-activating factor (PAF-acether) to guinea-pigs. Br. J. Exp. Pathol. *66*: 345.

Lellouch-Tubiana, A., Lefort, J., Simon, M.-T., Pfister, A., and Vargaftig, B.B. (1988). Eosinophil recruitment into guinea pig lungs after PAF-acether and allergen administration: modulation by prostacyclin, platelet depletion, and selective antagonists. Am. Rev. Respir. Dis. *137*: 948–954.

Levaditi, C. (1901). Sur l'état de la cytase dans le plasma des animaux normaux et des organismes vaccinés contre le vibrion cholérique. Ann Inst Pasteur *15*: 894–927.

Ley, K., Laudanna, C., Cybulsky, M.I., and Nourshargh, S. (2007). Getting to the site of inflammation: the leukocyte adhesion cascade updated. Nat. Rev. Immunol. *7*: 678–689.

Ley, K., Pramod, A.B., Croft, M., Ravichandran, K.S., and Ting, J.P. (2016). How Mouse Macrophages Sense What Is Going On. Front. Immunol. *7*: 204.

Li, J.L., Zarbock, A., and Hidalgo, A. (2017). Platelets as autonomous drones for hemostatic and immune surveillance. J. Exp. Med.

Li, P., Li, M., Lindberg, M.R., Kennett, M.J., Xiong, N., and Wang, Y. (2010). PAD4 is essential for antibacterial innate immunity mediated by neutrophil extracellular traps. J. Exp. Med. *207*: 1853–1862.

Liu, T., Laidlaw, T.M., Katz, H.R., and Boyce, J.A. (2013). Prostaglandin E2 deficiency causes a phenotype of aspirin sensitivity that depends on platelets and cysteinyl leukotrienes. Proc. Natl. Acad. Sci. U. S. A. *110*: 16987–92.

Liverani, E. (2017). Lung injury during LPS-induced inflammation occurs independently of the receptor P2Y1. Purinergic Signal. *13*: 119–125.

Liverani, E., Rico, M.C., Yaratha, L., Tsygankov, A.Y., Kilpatrick, L.E., and Kunapuli, S.P. (2014). LPS-induced systemic inflammation is more severe in P2Y12 null mice. J. Leukoc. Biol. *95*: 313–23.

Ljungqvist, U., Bergentz, S.-E., and Lewis, D.H. (1971). The Distribution of Platelets, Fibrin and Erythrocytes in Various Organs following Experimental Trauma. Eur. Surg. Res. *3*: 293–300.

Looney, M.R., Nguyen, J.X., Hu, Y., Ziffle, J.A. Van, Lowell, C.A., and Matthay, M.A. (2009). Platelet depletion and aspirin treatment protect mice in a two-event model of transfusion-related acute lung injury. J. Clin. Invest. *119*: 3450.

Looney, M.R., Thornton, E.E., Sen, D., Lamm, W.J., Glenny, R.W., and Krummel, M.F. (2011). Stabilized imaging of immune surveillance in the mouse lung. Nat. Methods *8*: 91–6.

Lopes-Pires, M.E., Casarin, A.L., Pereira-Cunha, F.G., Lorand-Metze, I., Antunes, E., and Marcondes, S. (2012). Lipopolysaccharide treatment reduces rat platelet aggregation independent of intracellular reactive-oxygen species generation. Platelets *23*: 195–201.

Lowenhaupt, R.W. (1978). Human platelet chemotaxis: requirement for plasma factor (s) and the role of collagen. Am. J. Physiol. Circ. Physiol. *235*: H23–H28.

Lowenhaupt, R.W., Silberstein, E.B., Sperling, M.I., and Mayfield, G. (1982). A quantitative method to measure human platelet chemotaxis using indium- 111-oxine-labeled gel-filtered platelets. Blood *60*: 1345–1352.

Ludwig, R.J., Schultz, J.E., Boehncke, W.-H., Podda, M., Tandi, C., Krombach, F., et al. (2004). Activated, not resting, platelets increase leukocyte rolling in murine skin utilizing a distinct set of adhesion molecules. J. Invest. Dermatol. *122*: 830–6.

Lussana, F., Marco, F. Di, Terraneo, S., Parati, M., Razzari, C., Scavone, M., et al. (2015). Effect of prasugrel in patients with asthma: results of PRINA, a randomized, double-blind, placebo-controlled, cross-over study. J. Thromb. Haemost. *13*: 136–141.

Maclay, J.D., McAllister, D.A., Johnston, S., Raftis, J., McGuinnes, C., Deans, A., et al. (2011). Increased platelet activation in patients with stable and acute exacerbation of COPD. Thorax *66*: 769–774.

Maclouf, J.A., and Murphy, R.C. (1988). Transcellular metabolism of neutrophil-derived leukotriene A4 by human platelets. A potential cellular source of leukotriene C4. J. Biol. Chem. *263*: 174–181.

Malhotra, R., Priest, R., Foster, M.R., and Bird, M.I. (1998). P-selectin binds to bacterial lipopolysaccharide. Eur. J. Immunol. *28*: 983–988.

Malpighi, M. (1661). De pulmonibus. Philos. Trans. R. Soc.

Mann, K.G., Butenas, S., and Brummel, K. (2003). The dynamics of thrombin formation. Arterioscler. Thromb. Vasc. Biol. *23*: 17–25.

Martin, S.A., Pence, B.D., Greene, R.M., Johnson, S.J., Dantzer, R., Kelley, K.W., et al. (2013). Effects of voluntary wheel running on LPS-induced sickness behavior in aged mice. Brain. Behav. Immun. *29*: 113–23.

Massberg, S., Enders, G., Leiderer, R., Eisenmenger, S., Vestweber, D., Krombach, F., et al. (1998). Platelet-Endothelial Cell Interactions During Ischemia/Reperfusion: The Role of P-Selectin. Blood *92*:.

Masuda, S., Nakazawa, D., Shida, H., Miyoshi, A., Kusunoki, Y., Tomaru, U., et al. (2016). NETosis markers: Quest for specific, objective, and quantitative markers. Clin. Chim. Acta *459*: 89–93.

Matera, C., Falzarano, C., Berrino, L., and Rossi, F. (1992). Effects of tetanus toxin, Salmonella typhimurium porin, and bacterial lipopolysaccharide on platelet aggregation. J. Med. *23*: 327–38.

Mathers, C.D., and Loncar, D. (2006). Projections of global mortality and burden of disease from 2002 to 2030. PLoS Med. *3*: e442.

Mathias, C.J., and Welch, M.J. (1984). Radiolabeling of platelets. Semin. Nucl. Med. *14*: 118–127.

Matute-Bello, G., Frevert, C.W., and Martin, T.R. (2008). Animal models of acute lung injury. *295*: L379–L399.

Maugeri, N., Campana, L., Gavina, M., Covino, C., Metrio, M. De, Panciroli, C., et al. (2014). Activated platelets present high mobility group box 1 to neutrophils, inducing autophagy and promoting the extrusion of neutrophil extracellular traps. J. Thromb. Haemost. *12*: 2074–88.

Mayadas, T.N., Johnson, R.C., Rayburn, H., Hynes, R.O., and Wagner, D.D. (1993). Leukocyte rolling and extravasation are severely compromised in P selectin-deficient mice. Cell *74*: 541–554.

McDonald, J.W., Ali, M., Morgan, E., Townsend, E.R., and Cooper, J.D. (1983). Thromboxane synthesis by sources other than platelets in association with complement-induced pulmonary leukostasis and pulmonary hypertension in sheep. Circ. Res. *52*:.

McKiddie, F.I., Watson, H.G., Graham, D., Phillips, J., and Staff, R.T. (2016). The impact of cell labelling technique on the retention of indium-labelled platelet imaging for idiopathic thrombocytopenic purpura. Nucl. Med. Commun. *37*: 215–216.

Menter, D.G., Tucker, S.C., Kopetz, S., Sood, A.K., Crissman, J.D., and Honn, K. V (2014). Platelets and cancer: a casual or causal relationship: revisited. Cancer Metastasis Rev. *33*: 231–69.

Metzger, W.J., Sjoerdsma, K., Richerson, H.B., Moseley, P., Zavala, D., Monick, M., et al. (1987). Platelets in bronchoalveolar lavage from asthmatic patients and allergic rabbits with allergen-induced late phase responses. Agents Actions. Suppl. *21*: 151–159.

Middleton, E.A., Weyrich, A.S., and Zimmerman, G.A. (2016). Platelets in Pulmonary Immune Responses and Inflammatory Lung Diseases. Physiol. Rev. *96*: 1211–59.

Mitchell, J.A., Akarasereenont, P., Thiemermann, C., Flower, R.J., and Vane, J.R. (1993). Selectivity of nonsteroidal antiinflammatory drugs as inhibitors of constitutive and inducible cyclooxygenase. Proc. Natl. Acad. Sci. U. S. A. *90*: 11693–7.

Miyashita, T., Ahmed, A.K., Nakanuma, S., Okamoto, K., Sakai, S., Kinoshita, J., et al. (2016). A Three-phase Approach for the Early Identification of Acute Lung Injury Induced by Severe Sepsis. In Vivo (Brooklyn). *30*: 341–349.

Miyashita, T., Tajima, H., Makino, I., Nakagawara, H., Kitagawa, H., Fushida, S., et al. (2015). Metastasis-promoting role of extravasated platelet activation in tumor. J. Surg. Res. *193*: 289–294.

Montrucchio, G., Bosco, O., Sorbo, L. Del, Fascio Pecetto, P., Lupia, E., Goffi, A., et al. (2003). Mechanisms of the priming effect of low doses of lipopoly-saccharides on leukocyte-dependent platelet aggregation in whole blood. Thromb. Haemost. *90*: 872–81.

Montuschi, P., and Peters-Golden, M.L. (2010). Leukotriene modifiers for asthma treatment. Clin. Exp. Allergy *40*: 1732–1741.

Moore, C., and Emerson, M. (2012). Assessment of Platelet Aggregation Responses In Vivo in the Mouse. In Methods in Molecular Biology (Clifton, N.J.), pp 21–28.

Moore, C., Sanz-Rosa, D., and Emerson, M. (2011). Distinct role and location of the endothelial isoform of nitric oxide synthase in regulating platelet aggregation in males and females in vivo. Eur. J. Pharmacol. *651*: 152–8.

Mulligan, M.S., Polley, M.J., Bayer, R.J., Nunn, M.F., Paulson, J.C., and Ward, P.A. (1992). Neutrophil-dependent acute lung injury. Requirement for P-selectin (GMP-140). J. Clin. Invest. *90*: 1600.

Munford, R.S. (2008). Sensing gram-negative bacterial lipopolysaccharides: a human disease determinant? Infect. Immun. *76*: 454–65.

Mushtaq, Y. (2014). The COPD pipeline. Nat. Rev. Drug Discov. *13*: 253–254.

Muzumdar, M.D., Tasic, B., Miyamichi, K., Li, L., and Luo, L. (2007). A global double-fluorescent Cre reporter mouse. Genesis *45*: 593–605.

Myrvold, H.E., and Brandberg, A. (1977). Microembolism in experimental septic shock. Distribution of platelets and fibrinogen after intravenous injection of disintegrated Pseudomonas bacteria to dogs. Eur. Surg. Res. Eur. Chir. Forschung. Rech. Chir. Eur. *9*: 34–47.

Myrvold, H.E., and Lewis, D.H. (1977). Platelets, fibrinogen, and pulmonary haemodynamics in early experimental septic shock. Circ. Shock *4*: 201–9.

Nachman, R.L., and Rafii, S. (2008). Platelets, Petechiae, and Preservation of the Vascular Wall. N. Engl. J. Med. *359*: 1261–1270.

Nachman, R.L., and Weksler, B. (1972). The platelet as an inflammatory cell. Ann. N. Y. Acad. Sci. *201*: 131–137.

Nakano, T., Miyamoto, K., Aida, A., Saito, S., Nishimura, M., and Kawakami, Y. (1995). Effects of platelet depletion on PMA-induced acute lung injury in awake sheep. Respir. Physiol. *101*: 207–17.

Nieswandt, B., Bergmeier, W., Rackebrandt, K., Gessner, J.E., and Zirngibl, H. (2000). Identification of critical antigen-specific mechanisms in the development of immune thrombocytopenic purpura in mice. Blood *96*: 2520–7.

Nocella, C., Carnevale, R., Bartimoccia, S., Novo, M., Cangemi, R., Pastori, D., et al. (2017). Lipopolysaccharide as trigger of platelet aggregation via eicosanoid over-production. Thromb. Haemost. *117*:.

Nowak, J., and FitzGerald, G.A. (1989). Redirection of prostaglandin endoperoxide metabolism at the platelet-vascular interface in man. J. Clin. Invest. *83*: 380–385.

Nystrom, M.L., Barradas, M.A., and Mikhailidis, D.P. (1993). No effect of endotoxin on platelet aggregation. Platelets *4*: 343.

Ortiz-Muñoz, G., Mallavia, B., Bins, A., Headley, M., Krummel, M.F., and Looney, M.R. (2014). Aspirin-triggered 15-epi-lipoxin A4 regulates neutrophil-platelet aggregation and attenuates acute lung injury in mice. Blood *124*: 2625–34.

Ostermann, G., Weber, K.S.C., Zernecke, A., Schröder, A., and Weber, C. (2002). JAM-1 is a ligand of the β2 integrin LFA-1 involved in transendothelial migration of leukocytes. Nat. Immunol. *3*: 151–158.

Page, C., and Pitchford, S. (2013). Neutrophil and platelet complexes and their relevance to neutrophil recruitment and activation. Int. Immunopharmacol. *17*: 1176–84.

Page, C.P. (1988). The involvement of platelets in non-thrombotic processes. Trends Pharmacol. Sci. *9*: 66–71.

Page, C.P. (1989). Platelets as inflammatory cells. Immunopharmacology *17*: 51.

Page, C.P., Paul, W., and Morley, J. (1982). An in vivo model for studying platelet aggregation and disaggregation. Thromb. Haemost. *47*: 210–213.

Pan, D., Amison, R.T., Riffo-vasquez, Y., Spina, D., Cleary, S.J., Wakelam, M.J., et al. (2015). P-Rex and Vav Rac-GEFs in platelets control leukocyte recruitment to sites of in fl ammation. Blood *125*: 1146–1159.

Paulus, J.M. (1975). Platelet size in man. Blood *46*: 321–36.

Peerschke, E.I.B., Murphy, T.K., and Ghebrehiwet, B. (2003). Activation-dependent surface expression of gC1qR/p33 on human blood platelets. Thromb. Haemost. *89*: 331–9.

Pertuy, F., Aguilar, A., Strassel, C., Eckly, A., Freund, J.-N., Duluc, I., et al. (2015). Broader expression of the mouse platelet factor 4-cre transgene beyond the megakaryocyte lineage. J. Thromb. Haemost. *13*: 115–125.

Phillips, J.W., Barringhaus, K.G., Sanders, J.M., Hesselbacher, S.E., Czarnik, A.C., Manka, D., et al. (2003). Single injection of P-selectin or P-selectin glycoprotein ligand-1 monoclonal antibody blocks neointima formation after arterial injury in apolipoprotein E-deficient mice. Circulation *107*: 2244–2249.

Pitchford, S., Pan, D., and Welch, H.C.E. (2017). Platelets in neutrophil recruitment to sites of inflammation. Curr. Opin. Hematol. *24*: 23–31.

Pitchford, S.C. (2007). Novel uses for anti-platelet agents as anti-inflammatory drugs. Br. J. Pharmacol. *152*: 987–1002.

Pitchford, S.C. (2009). Novel uses for anti-platelet agents as anti-inflammatory drugs. Br. J. Pharmacol. *152*: 987–1002.

Pitchford, S.C., Momi, S., Baglioni, S., Casali, L., Giannini, S., Rossi, R., et al. (2008). Allergen induces the migration of platelets to lung tissue in allergic asthma. Am. J. Respir. Crit. Care Med. *177*: 604–612.

Pitchford, S.C., Momi, S., Giannini, S., Casali, L., Spina, D., Page, C.P., et al. (2005). Platelet P-selectin is required for pulmonary eosinophil and lymphocyte recruitment in a murine model of allergic inflammation. Blood *105*: 2074–2081.

Pitchford, S.C., and Page, C.P. (2006). Platelet activation in asthma: integral to the inflammatory response. Clin. Exp. Allergy *36*: 399–401.

Pitchford, S.C., Riffo-Vasquez, Y., Sousa, A., Momi, S., Gresele, P., Spina, D., et al. (2004). Platelets are necessary for airway wall remodeling in a murine model of chronic allergic inflammation. Blood *103*: 639–647.

Pitchford, S.C., Yano, H., Lever, R., Riffo-Vasquez, Y., Ciferri, S., Rose, M.J., et al. (2003). Platelets are essential for leukocyte recruitment in allergic inflammation. J. Allergy Clin. Immunol. *112*: 109–118.

Plaza, V., Casals, F., Alonso, A., and Picado, C. (1992). Platelet kinetics in asthmatic patients with and without aspirin intolerance. Thorax *47*: 533–536.

Polack, B., Delolme, F., and Peyron, F. (1997). Protective role of platelets in chronic (Balb/C) and acute (CBA/J) Plasmodium berghei murine malaria. Haemostasis *27*: 278–85.

Polanowska-Grabowska, R., Wallace, K., Field, J.J., Chen, L., Marshall, M.A., Figler, R., et al. (2010). P-Selectin-Mediated Platelet-Neutrophil Aggregate Formation Activates Neutrophils in Mouse and Human Sickle Cell Disease. Arterioscler. Thromb. Vasc. Biol. *30*: 2392–2399.

Preibisch, S., Saalfeld, S., and Tomancak, P. (2009). Globally optimal stitching of tiled 3D microscopic image acquisitions. Bioinformatics *25*: 1463–5.

Pretorius, E., Mbotwe, S., Bester, J., Robinson, C.J., and Kell, D.B. (2016). Acute induction of anomalous and amyloidogenic blood clotting by molecular amplification of highly substoichiometric levels of bacterial lipopolysaccharide. J. R. Soc. Interface *13*:.

Rafii, S., Cao, Z., Lis, R., Siempos, I.I., Chavez, D., Shido, K., et al. (2015). Platelet-derived SDF-1 primes the pulmonary capillary vascular niche to drive lung alveolar regeneration. Nat. Cell Biol. *17*: 123–36.

Rahman, M., Gustafsson, D., Wang, Y., Thorlacius, H., and Braun, O.Ö. (2014). Ticagrelor reduces neutrophil recruitment and lung damage in abdominal sepsis. Platelets *25*: 257–263.

Rahman, M., Zhang, S., Chew, M., Ersson, A., Jeppsson, B., and Thorlacius, H. (2009). Platelet-Derived CD40L (CD154) Mediates Neutrophil Upregulation of Mac-1 and Recruitment in Septic Lung Injury. Ann. Surg. *250*: 783–790.

Riffo-Vasquez, Y., Somani, A., Man, F., Amison, R., Pitchford, S., and Page, C.P. (2016). A Non-Anticoagulant Fraction of Heparin Inhibits Leukocyte Diapedesis into the Lung by an Effect on Platelets. Am. J. Respir. Cell Mol. Biol. *55*: 554–563.

Rocca, B., Secchiero, P., Ciabattoni, G., Ranelletti, F.O., Catani, L., Guidotti, L., et al. (2002). Cyclooxygenase-2 expression is induced during human megakaryopoiesis and characterizes newly formed platelets. Proc. Natl. Acad. Sci. U. S. A. *99*: 7634–9.

Rostagno, C., Prisco, D., Boddi, M., and Poggesi, L. (1991). Evidence for local platelet activation in pulmonary vessels in patients with pulmonary hypertension secondary to chronic obstructive pulmonary disease. Eur. Respir. J. *4*: 147–151.

Ruifrok, A.C., and Johnston, D.A. (2001). Quantification of histochemical staining by color deconvolution. Anal. Quant. Cytol. Histol. *23*: 291–9.

Rumbaut, R.E., Bellera, R. V, Randhawa, J.K., Shrimpton, C.N., Dasgupta, S.K., Dong, J.-F., et al. (2006). Endotoxin enhances microvascular thrombosis in mouse cremaster venules via a TLR4-dependent, neutrophil-independent mechanism. Am. J. Physiol. Heart Circ. Physiol. *290*: H1671-9.

Rylander, R., Neymer, B., Schleifer, K., Haferkamp, O., Rietschel, T., and Weckesser, J. (1981). Bacterial Toxins and Etiology of Byssinosis. Chest *79*: 34S–38S.

Salter, J.W., Krieglstein, C.F., Issekutz, A.C., and Granger, D.N. (2001). Platelets modulate ischemia/reperfusion-induced leukocyte recruitment in the mesenteric circulation. Am. J. Physiol. Gastrointest. Liver Physiol. *281*: G1432-9.

Sanjar, S., Aoki, S., Kristersson, A., Smith, D., and Morley, J. (1990). Antigen challenge induces pulmonary airway eosinophil accumulation and airway hyperreactivity in sensitized guinea-pigs: the effect of anti-asthma drugs. Br. J. Pharmacol. *99*: 679–86.

Santoso, S., Sachs, U.J.H., Kroll, H., Linder, M., Ruf, A., Preissner, K.T., et al. (2002). The junctional adhesion molecule 3 (JAM-3) on human platelets is a counterreceptor for the leukocyte integrin Mac-1. J. Exp. Med. *196*: 679–91.

Schepers, A.G., Snippert, H.J., Stange, D.E., Born, M. van den, Es, J.H. van, Wetering, M. van de, et al. (2012). Lineage Tracing Reveals Lgr5+ Stem Cell Activity in Mouse Intestinal Adenomas. Science (80-.). *337*:.

Schmidt, E.-M., Kraemer, B.F., Borst, O., Münzer, P., Schoenberger, T., Schmidt, C., et al. (2012). SGK1 sensitivity of platelet migration. Cell. Physiol. Biochem. *30*: 259–268.

Schmitt, A., Guichard, J., Massé, J.M., Debili, N., and Cramer, E.M. (2001). Of mice and men: comparison of the ultrastructure of megakaryocytes and platelets. Exp. Hematol. *29*: 1295–1302.

Schoergenhofer, C., Schwameis, M., Hobl, E.-L., Ay, C., Key, N.S., Derhaschnig, U., et al. (2016). Potent irreversible P2Y12 inhibition does not reduce LPS-induced coagulation activation in a randomized, double-blind, placebo-controlled trial. Clin. Sci. *130*: 433–440.

Schrottmaier, W.C., Kral, J.B., Zeitlinger, M., Salzmann, M., Jilma, B., and Assinger, A. (2016). Platelet activation at the onset of human endotoxemia is undetectable in vivo. Platelets *27*: 479–83.

Semple, J.W., Italiano, J.E., and Freedman, J. (2011). Platelets and the immune continuum. Nat. Rev. Immunol. *11*: 264–274.

Sender, R., Fuchs, S., and Milo, R. (2016). Revised estimates for the number of human and bacteria cells in the body. bioRxiv.

Serhan, C.N., Chiang, N., Dalli, J., and Levy, B.D. (2014). Lipid mediators in the resolution of inflammation. Cold Spring Harb. Perspect. Biol. *7*: a016311.

Shashkin, P.N., Brown, G.T., Ghosh, A., Marathe, G.K., and McIntyre, T.M. (2008). Lipopolysaccharide Is a Direct Agonist for Platelet RNA Splicing. J. Immunol. *181*: 3495–3502.

Shibazaki, M., Kawabata, Y., Yokochi, T., Nishida, A., Takada, H., and Endo, Y. (1999). Complement-Dependent Accumulation and Degradation of Platelets in the Lung and Liver Induced by Injection of Lipopolysaccharides. Infect. Immun. *67*: 5186–5191.

Shibazaki, M., Nakamura, M., and Endo, Y. (1996). Biphasic, organ-specific, and strain-specific accumulation of platelets induced in mice by a lipopolysaccharide from Escherichia coli and its possible involvement in shock. Infect. Immun. *64*: 5290–4.

Siegel, R.L., Miller, K.D., and Jemal, A. (2015). Cancer statistics, 2015. CA. Cancer J. Clin. *65*: 5–29.

Silver, L.L. (2011). Challenges of antibacterial discovery. Clin. Microbiol. Rev. *24*: 71–109.

Sin, D.D. (2014). The devastating power of platelets in COPD exacerbations: can aspirin save lives in COPD? Thorax thoraxjnl-2014.

Singbartl, K., Forlow, S.B., and Ley, K. (2001). Platelet, but not endothelial, P-selectin is critical for neutrophil-mediated acute postischemic renal failure. FASEB J. *15*: 2337–44.

Smith, G.M. (1981). A study of intravascular platelet aggregation by continuous platelet counting. Trends Pharmacol. Sci. *2*: 105–107.

Smith, P.K., Krohn, R.I., Hermanson, G.T., Mallia, A.K., Gartner, F.H., Provenzano, M.D., et al. (1985). Measurement of protein using bicinchoninic acid. Anal. Biochem. *150*: 76–85.

Smyth, E., Solomon, A., Birrell, M.A., Smallwood, M.J., Winyard, P.G., Tetley, T.D., et al. (2017). Influence of inflammation and nitric oxide upon platelet aggregation following deposition of diesel exhaust particles in the airways. Br. J. Pharmacol. *174*: 2130–2139.

Smyth, E., Solomon, A., Vydyanath, A., Luther, P.K., Pitchford, S., Tetley, T.D., et al. (2015). Induction and enhancement of platelet aggregation *in vitro* and *in vivo* by model polystyrene nanoparticles. Nanotoxicology *9*: 356–364.

Snapper, J.R., Hinson, J.M., Hutchison, A.A., Lefferts, P.L., Ogletree, M.L., Brigham, K.L., et al. (1984). Effects of platelet depletion on the unanesthetized sheep's pulmonary response to endotoxemia. J. Clin. Invest. *74*: 1782–91.

Solomon, A., Smyth, E., Mitha, N., Pitchford, S., Vydyanath, A., Luther, P.K., et al. (2013). Induction of platelet aggregation after a direct physical interaction with diesel exhaust particles. J. Thromb. Haemost. *11*: 325–334.

Southam, D.S., Dolovich, M., O'Byrne, P.M., and Inman, M.D. (2002). Distribution of intranasal instillations in mice: effects of volume, time, body position, and anesthesia. *282*: L833–L839.

Sreeramkumar, V., Adrover, J.M., Ballesteros, I., Cuartero, M.I., Rossaint, J., Bilbao, I., et al. (2014). Neutrophils scan for activated platelets to initiate inflammation. Science *346*: 1234–8.

Stadtmann, A., Germena, G., Block, H., Boras, M., Rossaint, J., Sundd, P., et al. (2013). The PSGL-1-L-selectin signaling complex regulates neutrophil adhesion under flow. J. Exp. Med. *210*: 2171–80.

Stein, M., and Thomas, D.P. (1967). Role of platelets in the acute pulmonary responses to endotoxin. J. Appl. Physiol. *23*: 47–52.

Stoppelaar, S.F. de, 't Veer, C. van, Claushuis, T.A.M., Albersen, B.J.A., Roelofs, J.J.T.H., and Poll, T. van der (2014). Thrombocytopenia impairs host defense in gram-negative pneumonia derived sepsis. Blood.

Stoppelaar, S.F. de, Claushuis, T.A.M., Jansen, M.P.B., Hou, B., Roelofs, J.J.T.H., 't Veer, C. van, et al. (2015). The role of platelet MyD88 in host response during gram-negative sepsis. J. Thromb. Haemost. *13*: 1709–1720.

Su, X., Looney, M., Robriquet, L., Fang, X., and Matthay, M.A. (2004). Direct visual instillation as a method for efficient delivery of fluid into the distal airspaces of anesthetized mice. Exp. Lung Res. *30*: 479–93.

Sullivan, P.J., Jafar, Z.H., Harbinson, P.L., Restrick, L.J., Costello, J.F., and Page, C.P. (2000). Platelet dynamics following allergen challenge in allergic asthmatics. Respiration *67*: 514–517.

Summers, C., Rankin, S.M., Condliffe, A.M., Singh, N., Peters, A.M., and Chilvers, E.R. (2010). Neutrophil kinetics in health and disease. Trends Immunol. *31*: 318–24.

Summers, C., Singh, N.R., Worpole, L., Simmonds, R., Babar, J., Condliffe, A.M., et al. (2016). Incidence and recognition of acute respiratory distress syndrome in a UK intensive care unit. Thorax *71*: 1050–1051.

Tabuchi, A., Mertens, M., Kuppe, H., Pries, A.R., and Kuebler, W.M. (2007). Intravital microscopy of the murine pulmonary microcirculation. J. Appl. Physiol. *104*: 338–346.

Tabuchi, A., Styp-Rekowska, B., Slutsky, A.S., Wagner, P.D., Pries, A.R., and Kuebler, W.M. (2013). Precapillary Oxygenation Contributes Relevantly to Gas Exchange in the Intact Lung. Am. J. Respir. Crit. Care Med. *188*: 474–481.

Takeda, T., Unno, H., Morita, H., Futamura, K., Emi-Sugie, M., Arae, K., et al. (2016). Platelets constitutively express IL-33 protein and modulate eosinophilic airway inflammation. J. Allergy Clin. Immunol. *138*: 1395–1403.e6.

Tamagawa-Mineoka, R., Katoh, N., and Kishimoto, S. (2009). Platelets play important roles in the late phase of the immediate hypersensitivity reaction. J. Allergy Clin. Immunol. *123*: 581–587.e9.

Tamagawa-Mineoka, R., Katoh, N., Ueda, E., Takenaka, H., Kita, M., and Kishimoto, S. (2007). The role of platelets in leukocyte recruitment in chronic contact hypersensitivity induced by repeated elicitation. Am. J. Pathol. *170*: 2019–29.

Tanaka, Y., Nagai, Y., Kuroishi, T., Endo, Y., and Sugawara, S. (2011). Stimulation of Ly-6G on neutrophils in LPS-primed mice induces platelet-activating factor (PAF)-mediated anaphylaxis-like shock. J. Leukoc. Biol. *91*: 485–494.

Taytard, A., Guenard, H., Vuillemin, L., Bouvot, J.L., Vergeret, J., Ducassou, D., et al. (1986). Platelet kinetics in stable atopic asthmatic patients. Am. Rev. Respir. Dis. *134*: 983.

Terry, R.J. (1939). A thoracic window for observation of the lung in a living animal. Science (80-.). *90*: 43–44.

Thakur, M.L., Walsh, L., Malech, H.L., and Gottschalk, A. (1981). Indium-111-labeled human platelets: improved method, efficacy, and evaluation. J. Nucl. Med. *22*: 381–5.

Thomas, M.R., Outteridge, S.N., Ajjan, R.A., Phoenix, F., Sangha, G.K., Faulkner, R.E., et al. (2015). Platelet P2Y12 Inhibitors Reduce Systemic Inflammation and Its Prothrombotic Effects in an Experimental Human Model. Arterioscler. Thromb. Vasc. Biol. *35*: 2562–70.

Tian, J., Zhu, T., Liu, J., Guo, Z., and Cao, X. (2014). Platelets promote allergic asthma through the expression of CD154. Cell. Mol. Immunol. *12*: 1–8.

Tiedt, R., Schomber, T., Hao-Shen, H., and Skoda, R.C. (2007). Pf4-Cre transgenic mice allow the generation of lineage-restricted gene knockouts for studying megakaryocyte and platelet function in vivo. Blood *109*: 1503–6.

Tilgner, J., Trotha, K.T. von, Gombert, A., Jacobs, M.J., Drechsler, M., Döring, Y., et al. (2016). Aspirin, but Not Tirofiban Displays Protective Effects in Endotoxin Induced Lung Injury. PLoS One *11*: e0161218.

Tinoco, R., Carrette, F., Barraza, M.L., Otero, D.C., Magaña, J., Bosenberg, M.W., et al. (2016). PSGL-1 Is an Immune Checkpoint Regulator that Promotes T Cell Exhaustion. Immunity *44*: 1190–1203.

Tocantins, L.M. (1938). The mammalian blood platelet in health and disease. Medicine (Baltimore). *17*: 155–258.

Toner, P., McAuley, D.F., and Shyamsundar, M. (2015). Aspirin as a potential treatment in sepsis or acute respiratory distress syndrome. Crit. Care *19*: 374.

Tran, M.T.N., Tanaka, J., Hamada, M., Sugiyama, Y., Sakaguchi, S., Nakamura, M., et al. (2014). In Vivo image Analysis Using iRFP Transgenic Mice. Exp. Anim. *63*: 311–319.

Trowbridge, E.A., Martin, J.F., Slate, D.N., Kishk, Y.T., Warren, C.W., Harley, P.J., et al. (1984). The origin of platelet count and volume. Clin. Phys. Physiol. Meas. *5*: 145–170.

Tymvios, C., Jones, S., Moore, C., Pitchford, S.C., Page, C.P., and Emerson, M. (2008). Real-time measurement of non-lethal platelet thromboembolic responses in the anaesthetized mouse. Thromb. Haemost. *99*: 435–440.

Valone, F.H., Austen, K.F., and Goetzl, E.J. (1974). Modulation of the Random Migration of Human Platelets. J. Clin. Invest. *54*: 1100–1106.

Varga-Szabo, D., Pleines, I., and Nieswandt, B. (2008). Cell Adhesion Mechanisms in Platelets. Arterioscler. Thromb. Vasc. Biol. *28*: 403–412.

Verschoor, A., Neuenhahn, M., Navarini, A.A., Graef, P., Plaumann, A., Seidlmeier, A., et al. (2011). A platelet-mediated system for shuttling blood-borne bacteria to CD8α+ dendritic cells depends on glycoprotein GPIb and complement C3. Nat. Immunol. *12*: 1194–1201.

Versteeg, H.H., Heemskerk, J.W.M., Levi, M., and Reitsma, P.H. (2013). New Fundamentals in Hemostasis. Physiol. Rev. *93*: 327–358.

Vesconi, S., Rossi, G.P., Pesenti, A., Fumagalli, R., and Gattinoni, L. (1988). Pulmonary microthrombosis in severe adult respiratory distress syndrome. Crit. Care Med. *16*: 111–113.

Vincent, D., Lefort, J., Chatelet, F., Bureau, M.F., Dry, J., and Vargaftig, B.B. (1993). Intratracheal E. coli lipopolysaccharide induces platelet-dependent bronchial hyperreactivity. J. Appl. Physiol. *74*: 1027–1038.

Walker, R., and Casey, L. (1985). Endotoxin interactions with platelets. In Handbook of Endotoxin, L. Berry, ed. pp 225–243.

Wang, T., Liu, Z., Wang, Z., Duan, M., Li, G., Wang, S., et al. (2014). Thrombocytopenia Is Associated with Acute Respiratory Distress Syndrome Mortality: An International Study. PLoS One *9*: e94124.

Watts, T., Barigou, M., and Nash, G.B. (2013). Comparative rheology of the adhesion of platelets and leukocytes from flowing blood: why are platelets so small? Am. J. Physiol. Heart Circ. Physiol. *304*: H1483-94.

Weber, F.C., Németh, T., Csepregi, J.Z., Dudeck, A., Roers, A., Ozsvári, B., et al. (2015). Neutrophils are required for both the sensitization and elicitation phase of contact hypersensitivity. J. Exp. Med. *212*:.

Weber, K.S.C., Alon, R., and Klickstein, L.B. (2004). Sialylation of ICAM-2 on platelets impairs adhesion of leukocytes via LFA-1 and DC-SIGN. Inflammation *28*: 177–88.

Weissmüller, T., Campbell, E.L., Rosenberger, P., Scully, M., Beck, P.L., Furuta, G.T., et al. (2008). PMNs facilitate translocation of platelets across human and mouse epithelium and together alter fluid homeostasis via epithelial cell–expressed ecto-NTPDases. J. Clin. Invest. *118*: 3682–3692.

White, J.G. (2005). Platelets are covercytes, not phagocytes: uptake of bacteria involves channels of the open canalicular system. Platelets *16*: 121–31.

White, J.G. (2006). Why human platelets fail to kill bacteria. Platelets *17*: 191–200.

Whyte, C.S., Swieringa, F., Mastenbroek, T.G., Lionikiene, A.S., Lancé, M.D., Meijden, P.E.J. van der, et al. (2015). Plasminogen associates with phosphatidylserine-exposing platelets and contributes to thrombus lysis under flow. Blood *125*:.

Wong, C.H.Y., Jenne, C.N., Petri, B., Chrobok, N.L., and Kubes, P. (2013). Nucleation of platelets with blood-borne pathogens on Kupffer cells precedes other innate immunity and contributes to bacterial clearance. Nat. Immunol. *14*: 785–92.

Wong, P.C., Watson, C., and Crain, E.J. (2016). The P2Y1 receptor antagonist MRS2500 prevents carotid artery thrombosis in cynomolgus monkeys. J. Thromb. Thrombolysis *41*: 514–521.

Woodfin, A., Voisin, M.-B., and Nourshargh, S. (2007). PECAM-1: a multi-functional molecule in inflammation and vascular biology. Arterioscler. Thromb. Vasc. Biol. *27*: 2514–2523.

Wright, J.H. (1906). The Origin and Nature of the Blood Plates. Bost. Med. Surg. J. *154*: 643–645.

Wuescher, L.M., Takashima, A., and Worth, R.G. (2015). A novel conditional platelet depletion mouse model reveals the importance of platelets in protection against Staphylococcus aureus bacteremia. J. Thromb. Haemost. *13*: 303–13.

Xia, L., Sperandio, M., Yago, T., McDaniel, J.M., Cummings, R.D., Pearson-White, S., et al. (2002). P-selectin glycoprotein ligand-1-deficient mice have impaired leukocyte tethering to E-selectin under flow. J. Clin. Invest. *109*: 939–50.

Xiang, B., Zhang, G., Guo, L., Li, X.-A., Morris, A.J., Daugherty, A., et al. (2013). Platelets protect from septic shock by inhibiting macrophage-dependent inflammation via the cyclooxygenase 1 signalling pathway. Nat Commun *4*: 2657.

Xu, W., Cardenes, N., Corey, C., Erzurum, S.C., and Shiva, S. (2015). Platelets from Asthmatic Individuals Show Less Reliance on Glycolysis. PLoS One *10*: e0132007.

Yadav, H., and Kor, D.J. (2015). Platelets in the pathogenesis of acute respiratory distress syndrome. Am. J. Physiol. Lung Cell. Mol. Physiol. *309*: L915-23.

Yang, W., Wang, Y., Lai, A., Qiao, J.X., Wang, T.C., Hua, J., et al. (2014). Discovery of 4-Aryl-7-Hydroxyindoline-Based P2Y $_1$ Antagonists as Novel Antiplatelet Agents. J. Med. Chem. *57*: 6150–6164.

Yeaman, M.R. (2014). Platelets: at the nexus of antimicrobial defence. Nat Rev Micro *12*: 426–437.

Yoshida, A., Ohba, M., Wu, X., Sasano, T., Nakamura, M., and Endo, Y. (2002). Accumulation of platelets in the lung and liver and their degranulation following antigen-challenge in sensitized mice. Br. J. Pharmacol. *137*: 146–152.

Zanardo, R.C.O., Bonder, C.S., Hwang, J.M., Andonegui, G., Liu, L., Vestweber, D., et al. (2004). A down-regulatable E-selectin ligand is functionally important for PSGL-1–independent leukocyte–endothelial cell interactions. Blood *104*:.

Zarbock, A., and Ley, K. (2009). The role of platelets in acute lung injury (ALI). Front. Biosci. a J. Virtual Libr. *14*: 150.

Zarbock, A., Singbartl, K., and Ley, K. (2006). Complete reversal of acid-induced acute lung injury by blocking of platelet-neutrophil aggregation. J. Clin. Invest. *116*: 3211.

Zhang, L., Urtz, N., Gaertner, F., Legate, K.R., Petzold, T., Lorenz, M., et al. (2013). Sphingosine kinase 2 (Sphk2) regulates platelet biogenesis by providing intracellular sphingosine 1-phosphate (S1P). Blood *122*: 791–802.

Zhao, L., Ohtaki, Y., Yamaguchi, K., Matsushita, M., Fujita, T., Yokochi, T., et al. (2002). LPS-induced platelet response and rapid shock in mice: contribution of O-antigen region of LPS and involvement of the lectin pathway of the complement system. Blood *100*: 3233–3239.

Zuchtriegel, G., Uhl, B., Puhr-Westerheide, D., Pörnbacher, M., Lauber, K., Krombach, F., et al. (2016). Platelets Guide Leukocytes to Their Sites of Extravasation. PLOS Biol. *14*: e1002459.

Zuluaga, A.F., Salazar, B.E., Rodriguez, C.A., Zapata, A.X., Agudelo, M., and Vesga, O. (2006). Neutropenia induced in outbred mice by a simplified low-dose cyclophosphamide regimen: characterization and applicability to diverse experimental models of infectious diseases. BMC Infect. Dis. *6*: 55.

zur Muhlen, C. von, Sibson, N.R., Peter, K., Campbell, S.J., Wilainam, P., Grau, G.E., et al. (2008). A contrast agent recognizing activated platelets reveals murine cerebral malaria pathology undetectable by conventional MRI. J. Clin. Invest. *118*: 1198–207.